

Green Chemistry

Cutting-edge research for a greener sustainable future

www.rsc.org/greenchem

Volume 8 | Number 9 | September 2006 | Pages 753–840



Downloaded on 07 November 2010
Published on 01 September 2006 on <http://pubs.rsc.org> | doi:10.1039/B611615A

ISSN 1463-9262

RSC Publishing

Abbott *et al.*
Cationic functionalisation of cellulose

Phair
Green chemistry for sustainable cement
production and use

Carrillo *et al.*
Zinc catalysed ester solvolysis

Liu *et al.*
Reductive degradation of TBBPA in
aqueous medium



1463-9262 (2006) 8:9;1-5

Specialised searching



The graphical abstracting services at the RSC are an indispensable tool to help you search the literature. Focussing on specific areas of research they review key primary journals for novel and interesting chemistry.

requires specialised tools



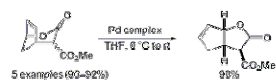
Methods in Organic Synthesis provides information on reaction schemes, new reactions and new methods. Topics include functional group changes, the introduction of chiral centres, and enzyme and biological transformations.

Methods in Organic Synthesis, "Microsoft Internet Explorer"
 Address http://www.rsc.org/Publishing/CurrentAwareness/MOS/CurrentAwareness/...
 RSC Publishing
 Search | Clear Enter search text
 Search all fields
 RSC Publishing
 Search information on:
 Select a subject
 Select a reaction type
 Select a title
 Select a product
 Select a reagent
 Select a product

59453 Tandem radical rearrangement/Pd-catalysed translocation of bicyclo[2.2.2]octanes. An efficient access to the oxa-triquinane core structure
 J.-H. Liao; N. Maulide; B. Augustyns; I. E. Marko
 Org. Biomol. Chem., 2006, 4(8), 1464-1467

The online database has excellent functionality. Search by: authors, products, reaction, reactants and reagents.

With Methods in Organic Synthesis you can find exactly what you need. Search results include diagrams of reaction schemes. Also available as a print bulletin.



Registered charity Number 207890

For more information visit

RSC Publishing

www.rsc.org/databases

Green Chemistry

Cutting-edge research for a greener sustainable future

www.rsc.org/greenchem

RSC Publishing is a not-for-profit publisher and a division of the Royal Society of Chemistry. Any surplus made is used to support charitable activities aimed at advancing the chemical sciences. Full details are available from www.rsc.org

IN THIS ISSUE

ISSN 1463-9262 CODEN GRCHFJ 8(9) 753-840 (2006)



Cover

By using green cement chemistry various mineral waste forms may be transformed into everyday concrete structures, such as this bridge. Image copyright iStockphotos, from *Green Chem.*, 2006, 8(9), 763.

CHEMICAL TECHNOLOGY

T33

Chemical Technology highlights the latest applications and technological aspects of research across the chemical sciences.

Chemical Technology

September 2006/Volume 3/Issue 9

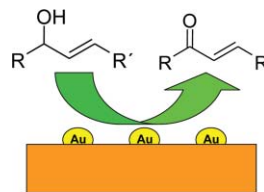
www.rsc.org/chemicaltechnology

HIGHLIGHT

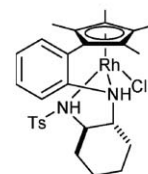
761

Highlights

Markus Hölscher reviews some of the recent literature in green chemistry.



Up to 90 % selectivities under solvent-less conditions



Asymmetric transfer hydrogenation of ketones in aqueous solution

EDITORIAL STAFF

Editor

Sarah Ruthven

News writer

Markus Hölscher

Publishing assistant

Emma Hacking

Team leader, serials production

Stephen Wilkes

Technical editor

Edward Morgan

Administration coordinator

Sonya Spring

Editorial secretaries

Lynne Braybrook, Jill Segev, Julie Thompson

Publisher

Emma Wilson

Green Chemistry (print: ISSN 1463-9262; electronic: ISSN 1463-9270) is published 12 times a year by the Royal Society of Chemistry, Thomas Graham House, Science Park, Milton Road, Cambridge, UK CB4 0WF.

All orders, with cheques made payable to the Royal Society of Chemistry, should be sent to RSC Distribution Services, c/o Portland Customer Services, Commerce Way, Colchester, Essex, UK CO2 8HP. Tel +44 (0) 1206 226050; E-mail sales@rscdistribution.org

2006 Annual (print + electronic) subscription price: £859; US\$1571. 2006 Annual (electronic) subscription price: £773; US\$1414. Customers in Canada will be subject to a surcharge to cover GST. Customers in the EU subscribing to the electronic version only will be charged VAT.

If you take an institutional subscription to any RSC journal you are entitled to free, site-wide web access to that journal. You can arrange access via Internet Protocol (IP) address at www.rsc.org/ip. Customers should make payments by cheque in sterling payable on a UK clearing bank or in US dollars payable on a US clearing bank. Periodicals postage paid at Rahway, NJ, USA and at additional mailing offices. Airfreight and mailing in the USA by Mercury Airfreight International Ltd., 365 Blair Road, Avenel, NJ 07001, USA.

US Postmaster: send address changes to Green Chemistry, c/o Mercury Airfreight International Ltd., 365 Blair Road, Avenel, NJ 07001. All despatches outside the UK by Consolidated Airfreight.

PRINTED IN THE UK

Advertisement sales: Tel +44 (0) 1223 432246; Fax +44 (0) 1223 426017; E-mail advertising@rsc.org

Green Chemistry

Cutting-edge research for a greener sustainable future

www.rsc.org/greenchem

Green Chemistry focuses on cutting-edge research that attempts to reduce the environmental impact of the chemical enterprise by developing a technology base that is inherently non-toxic to living things and the environment.

EDITORIAL BOARD

Chair

Professor Martyn Poliakoff,
Department of Chemistry
University of Nottingham,
Nottingham, UK
E-mail martyn.poliakoff@nottingham.ac.uk

Scientific editor

Professor Walter Leitner,
RWTH-Aachen, Germany
E-mail leitner@itmc.rwth-aachen.de

Members

Professor Joan Brennecke,
University of Notre Dame, USA

Dr Janet Scott, Centre for Green
Chemistry, Monash University,
Australia

Dr A Michael Warhurst,
University of Massachusetts,
USA
E-mail michael-warhurst@uml.edu

Professor Tom Welton,
Imperial College, UK
E-mail t.welton@ic.ac.uk

Professor Roshan Jachuck,
Clarkson University, USA
E-mail rjachuck@clarkson.edu

Dr Paul Anastas, Green Chemistry
Institute, USA
E-mail p_anastas@acs.org

Professor Buxing Han, Chinese
Academy of Sciences
E-mail hanbx@iccas.ac.cn

Associate editors

Professor C. J. Li, McGill
University, Canada
E-mail cj.li@mcgill.ca

Professor Kyoko Nozaki
Kyoto University, Japan
E-mail nozaki@chembio-tu-tokyo.ac.jp

INTERNATIONAL ADVISORY EDITORIAL BOARD

James Clark, York, UK
Avelino Corma, Universidad
Politécnica de Valencia, Spain
Mark Harmer, DuPont Central
R&D, USA

Herbert Hugl, Lanxess Fine
Chemicals, Germany
Makato Misono, Kogakuin
University, Japan
Colin Raston,
University of Western Australia,
Australia

Robin D. Rogers, Centre for Green
Manufacturing, USA
Kenneth Seddon, Queen's
University, Belfast, UK
Roger Sheldon, Delft University of
Technology, The Netherlands
Gary Sheldrake, Queen's
University, Belfast, UK
Pietro Tundo, Università ca
Foscari di Venezia, Italy
Tracy Williamson, Environmental
Protection Agency, USA

INFORMATION FOR AUTHORS

Full details of how to submit material for publication in Green Chemistry are given in the Instructions for Authors (available from <http://www.rsc.org/authors>). Submissions should be sent via ReSource: <http://www.rsc.org/resource>.

Authors may reproduce/republish portions of their published contribution without seeking permission from the RSC, provided that any such republication is accompanied by an acknowledgement in the form: (Original citation) – Reproduced by permission of the Royal Society of Chemistry.

© The Royal Society of Chemistry 2006. Apart from fair dealing for the purposes of research or private study for non-commercial purposes, or criticism or review, as permitted under the Copyright, Designs and Patents Act 1988 and the Copyright and Related Rights Regulations 2003, this publication may only be reproduced, stored or transmitted, in any form or by any means, with the prior permission in writing of the Publishers or in the case of reprographic reproduction in accordance with the terms of

licences issued by the Copyright Licensing Agency in the UK. US copyright law is applicable to users in the USA.

The Royal Society of Chemistry takes reasonable care in the preparation of this publication but does not accept liability for the consequences of any errors or omissions.

Ⓢ The paper used in this publication meets the requirements of ANSI/NISO Z39.48-1992 (Permanence of Paper).

Royal Society of Chemistry: Registered Charity No. 207890

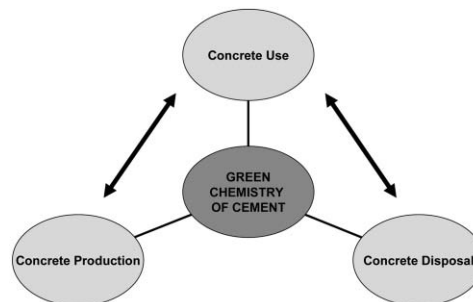
TUTORIAL REVIEW

763

Green chemistry for sustainable cement production and use

John W. Phair

The present work introduces industrial ecology and the principles of green chemistry as a means of driving the research, development and commercial attractiveness of alternative and sustainable cements.



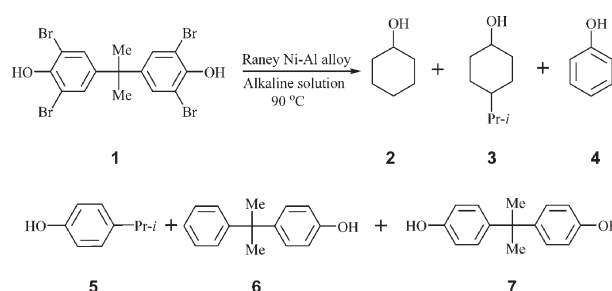
COMMUNICATIONS

781

Reductive degradation of tetrabromobisphenol A (TBBPA) in aqueous medium

Guo-Bin Liu,* Lu Dai, Xiang Gao, Miao-Kui Li and Thies Thiemann

Reductive degradation of tetrabromobisphenol A (TBBPA), a ubiquitous persistent organic pollutant, was performed in aqueous medium using Raney Ni–Al alloy.



784

Cationic functionalisation of cellulose using a choline based ionic liquid analogue

Andrew P. Abbott,* Thomas J. Bell, Sandeep Handa and Barry Stoddart

Cellulose can be produced with cationic functionalities in a chlorcholine chloride urea eutectic. The material produced has a high surface substitution and exhibits a good capacity for anionic dye adsorption.

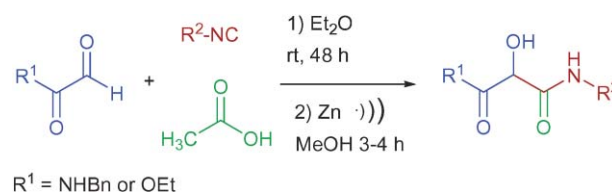


787

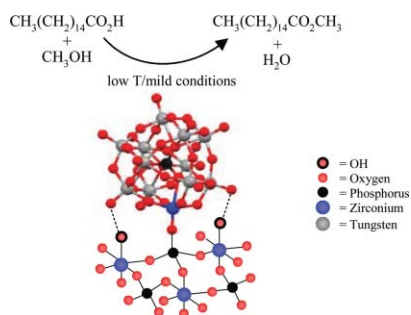
Zinc catalysed ester solvolysis. Application to the synthesis of tartronic acid derivatives

Rosa M. Carrillo, Ana G. Neo,* Lucía López-García, Stefano Marcaccini and Carlos F. Marcos*

A novel synthesis of hydroxyglycine retropeptidic derivatives was achieved through a Passerini 3-component reaction of glyoxyl amides or esters, followed by an unprecedented environmentally benign zinc catalysed solvolysis.



790

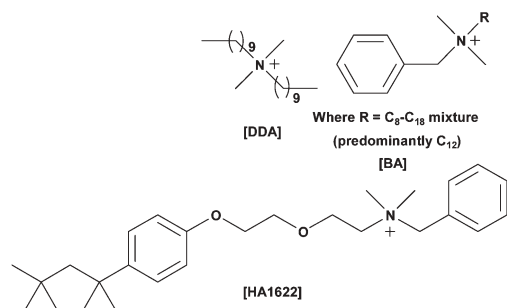


Zirconium phosphate supported tungsten oxide solid acid catalysts for the esterification of palmitic acid

Katabathini Narasimha Rao,* Adapa Sridhar, Adam F. Lee, Stewart J. Tavener, Nigel A. Young and Karen Wilson*

Tungstate-doped mesoporous zirconium phosphates exhibit high catalytic activity towards palmitic acid esterification, and are promising materials for applications in biodiesel synthesis.

798



Long alkyl chain quaternary ammonium-based ionic liquids and potential applications

Juliusz Pernak,* Marcin Smiglak, Scott T. Griffin, Whitney L. Hough, Timothy B. Wilson, Anna Pernak, Jadwiga Zabielska-Matejuk, Andrzej Fojutowski, Kazimierz Kita and Robin D. Rogers*

We present a new group of air- and moisture-stable, hydrophobic ammonium-based ionic liquids, their properties, toxicological studies and potential applications as wood preservatives, anti-bacterial, and anti-fungal agents.

807

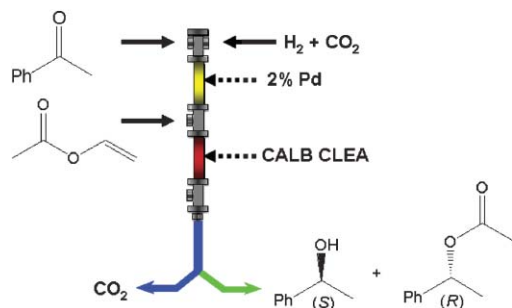


Liquid polymers as solvents for catalytic reductions

David J. Heldebrant, Heather N. Witt, Sarah M. Walsh, Taryn Ellis, Japheth Rauscher and Philip G. Jessop*

Liquid polymers can serve as environmentally benign reaction media. Several polymers are compared in terms of environmental risk, solvent polarity, and performance as solvents for catalytic reductions, catalyst recycling, and catalyst protection from air.

816



Continuous kinetic resolution catalysed by cross-linked enzyme aggregates, 'CLEAs', in supercritical CO₂

Helen R. Hobbs, Betti Kondor, Phil Stephenson, Roger A. Sheldon, Neil R. Thomas and Martyn Poliakov*

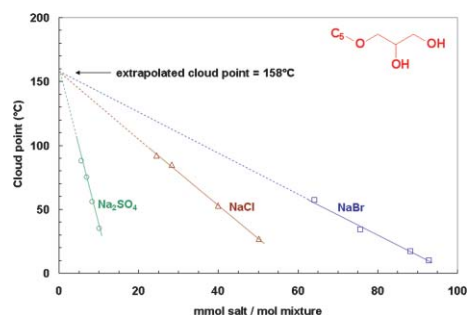
Metal-catalysed hydrogenation combined with enzymatic resolution (*Candida antarctica* lipase B in the form of Novozym 435 and CLEA) in supercritical carbon dioxide is reported. Reactions are performed in series in a continuous flow reactor with potential economic advantage since re-pressurization of solvent is avoided.

822

Short chain glycerol 1-monoethers—a new class of green solvo-surfactants

Sébastien Queste, Pierre Bauduin, Didier Touraud, Werner Kunz and Jean-Marie Aubry*

Short chain glycerol 1-monoethers $C_i\text{Gly}_1$ ($4 \leq i \leq 6$) were prepared and studied in aqueous solution with regard to surface activity, self-aggregation and clouding induced by various salts of the Hofmeister series.

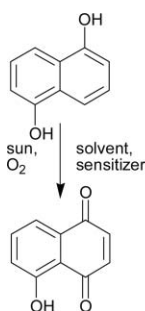


831

Green photochemistry: solar-chemical synthesis of Juglone with medium concentrated sunlight

Michael Oelgemöller,* Niall Healy, Lamark de Oliveira, Christian Jung and Jochen Mattay

This article describes photooxygenations of 1,5-dihydroxynaphthalene with soluble and solid-supported sensitizers and moderately concentrated sunlight. Moderate to good yields up to 79% of 5-hydroxy-1,4-naphthoquinone (Juglone) were achieved on multiple gram-scales after just 4 h of illumination.



835

A facile, environmentally benign sulfonamide synthesis in water

Xiaohu Deng* and Neelakandha S. Mani

A facile, environmentally benign synthesis of sulfonamides under dynamic pH control in aqueous media is described. Isolation of products involves only filtration after acidification. Excellent yields and purity were obtained without further purification.



AUTHOR INDEX

Abbott, Andrew P., 784
 Aubry, Jean-Marie, 822
 Bauduin, Pierre, 822
 Bell, Thomas J., 784
 Carrillo, Rosa M., 787
 Dai, Lu, 781
 Deng, Xiaohu, 835
 de Oliveira, Lamark, 831
 Ellis, Taryn, 807
 Fojutowski, Andrzej, 798
 Gao, Xiang, 781
 Griffin, Scott T., 798
 Handa, Sandeep, 784
 Healy, Niall, 831
 Heldebrant, David J., 807

Hobbs, Helen R., 816
 Hough, Whitney L., 798
 Jessop, Philip G., 807
 Jung, Christian, 831
 Kita, Kazimierz, 798
 Kondor, Betti, 816
 Kunz, Werner, 822
 Lee, Adam F., 790
 Li, Miao-Kui, 781
 Liu, Guo-Bin, 781
 López-García, Lucía, 787
 Mani, Neelakandha S., 835
 Marcaccini, Stefano, 787
 Marcos, Carlos F., 787
 Mattay, Jochen, 831

Neo, Ana G., 787
 Oelgemöller, Michael, 831
 Pernak, Anna, 798
 Pernak, Juliusz, 798
 Phair, John W., 763
 Poliakoff, Martyn, 816
 Queste, Sébastien, 822
 Rao, Katabathini Narasimha,
 790
 Rauscher, Japheth, 807
 Rogers, Robin D., 798
 Sheldon, Roger A., 816
 Smiglak, Marcin, 798
 Sridhar, Adapa, 790
 Stephenson, Phil, 816

Stoddart, Barry, 784
 Tavener, Stewart J., 790
 Thiemann, Thies, 781
 Thomas, Neil R., 816
 Touraud, Didier, 822
 Walsh, Sarah M., 807
 Wilson, Karen, 790
 Wilson, Timothy B., 798
 Witt, Heather N., 807
 Young, Nigel A., 790
 Zabielska-Matejuk, Jadwiga,
 798

FREE E-MAIL ALERTS AND RSS FEEDS


Contents lists in advance of publication are available on the web *via* www.rsc.org/greenchem - or take advantage of our free e-mail alerting service (www.rsc.org/ej_alert) to receive notification each time a new list becomes available.

RSS Try our RSS feeds for up-to-the-minute news of the latest research. By setting up RSS feeds, preferably using feed reader software, you can be alerted to the latest Advance Articles published on the RSC web site. Visit www.rsc.org/publishing/technology/rss.asp for details.

ADVANCE ARTICLES AND ELECTRONIC JOURNAL

Free site-wide access to Advance Articles and the electronic form of this journal is provided with a full-rate institutional subscription. See www.rsc.org/ejs for more information.

* Indicates the author for correspondence: see article for details.

 Electronic supplementary information (ESI) is available *via* the online article (see <http://www.rsc.org/esi> for general information about ESI).

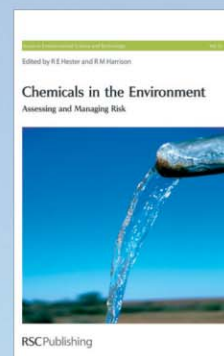
Chemicals in the Environment Assessing and Managing Risk

By R M Harrison

Chemicals in the Environment addresses important environmental issues relating to all aspects of risk management and regulation including;

- Current legislation on risk management of chemical products
- Scientific and technical issues
- Evaluating the risk of chemicals to humans and the environment
- Issues on evaluating metals in the environment
- Modelling the behaviour of organic chemicals

Ideal for industry, academia and government organisations - particularly those in environmental chemistry sectors.



Hardcover | 2006 | xvi +158 pages | £45.00 | RSC member price £29.25 | ISBN-10: 0 85404 206 7 | ISBN-13: 978 0 85404 206 7

Registered Charity No. 207890

RSCPublishing

www.rsc.org/books/2067

Highlights

DOI: 10.1039/b610851m

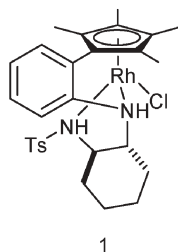
Markus Hölscher reviews some of the recent literature in green chemistry.

How does industry make drug candidate molecules?

Although industry and academia very often co-operate in many different areas of chemistry, in most cases it is not clear to the university research staff how industry decides on synthesis routes and which transformations are playing major roles. Clearly no industrial firm can open its lab-journals to the general public, but it would still be interesting to learn how industrial chemistry is composed. In a remarkable survey by Carey, Laffan, Thomson and Williams, who are R&D scientists with three major pharmaceutical players (GlaxoSmithKline, AstraZeneca and Pfizer, respectively), what happens inside industry laboratories is outlined, with a focus on chemical transformations.¹ The authors choose to outline the tool-box of how to make drug molecules from the point of view of synthesis. As an example, and with regard to chirality, it is interesting to learn that in a molecule data set containing compounds with 135 chiral centres (69 chiral drug syntheses), in 27 of the chiral molecules the chirality resided in the starting materials purchased, while for 30 molecules chirality was generated during syntheses. Looking at it from the point of distribution of chiral centres, 74% of these were “purchased”, while 38% were generated by resolution, and only 14% by asymmetric syntheses. Other topics covered are substituted aromatic starting materials, heterocycle occurrence and formation, protections and deprotections, acylation, heteroatom alkylations and arylations, oxidations, reductions, C–C bond forming reactions, and quite a few more. As far as environmental issues are concerned, novel technologies such as ionic liquids and supercritical fluids have had, as yet, little impact on industrial production.

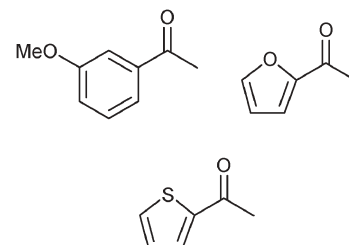
Asymmetric transfer hydrogenation of ketones in aqueous solution

One of the possibilities to generate enantiomerically pure secondary alcohols is the asymmetric transfer hydrogenation of ketones. As this method was shown to work nicely with many substrates, research efforts have been intensified over the past few years, and have resulted in the development of different classes of ligands and catalysts. Very recently Wills *et al.* from the University of Warwick developed rhodium catalyst **1** which contains a newly designed ligand.²



The authors found **1** to efficiently and selectively catalyse the reaction of a large variety of ketones to the corresponding alcohols when formic acid–triethylamine was used as reaction medium. Conversions were as high as 100% in many cases, with ee values ranging mostly in the 95 to 99% area. However, more important is the fact that the same catalyst works equally well in a mixture of water and sodium formate, generating again the secondary alcohols with conversions of 100% for most of the substrates tested, while ee values remained very high (96–98%). A variety of substrates was tested, some of them being shown below.

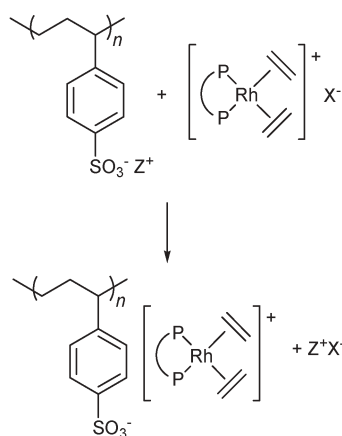
Interestingly the substrate to catalyst ratio could be increased from an initial 200 to 1000, and even to 10 000. The reactions then required longer reaction times, but the enantioselectivity did not decrease.



Immobilization of asymmetric hydrogenation catalysts on ion-exchange resins

One of the most important issues in large scale synthesis of fine chemicals using transition metal catalysts is catalyst recycling. There are different approaches to the problem, such as modification of heterogeneous catalysts with chiral auxiliaries or heterogenization and immobilization of homogeneous transition metal catalysts, to name only a few. Ion-exchange resins and the corresponding ion-exchanged based catalysts have been shown in the past few years to meet many of the desired criteria, such as thermal and mechanical stability, reliable quality, inexpensiveness, chemical resistance, easy preparation and handling. General catalyst preparation, as shown graphically below, is achieved by reacting a cationic metal complex with an anionic resin, which anchors the metal complex to the support and generates the active catalyst material.

Much effort was put into the creation of asymmetric rhodium hydrogenation catalysts and, as the available data has grown considerably in the past years, Barbaro from the National Research Council, Florence assembled the latest developments in the field very recently, and showed that this type of catalyst material has reached an elaborated state.³ Inexpensive and commercially available supports can be employed. Ligands do not need to be derivatised chirally and the immobilized catalysts can be easily prepared and handled.



Gold nanoparticles as chemoselective catalysts for the oxidation of allylic alcohols

The oxidation of alcohols is an important tool in organic chemistry. As the classic procedure requires stoichiometric amounts of oxidants or halo-oxoacids, a

more sustainable route is highly desirable. Ideally the reaction should be carried out with molecular oxygen as oxidant and with no solvent. The catalyst should only oxidize one defined group in high selectivity and conversion. Other oxidizable functional groups should not be oxidized. For allylic alcohols this is quite a challenge, which explains the high amount of research effort that is being undertaken. Gold nanoparticles formed on ceria seem to be very promising catalyst candidates, as Corma *et al.* from the University of Valencia very recently reported.⁴ Au–CeO₂ gave high conversion in oxidations with molecular oxygen, and isomerizations to other products was low or zero. Pd and Pd/Au catalysts, which were also tested, in many cases also did not isomerize the desired product, but were less selective or gave lower conversions. As an example, one of the test substrates—cinnamyl alcohol—was oxidized using Au–CeO₂

with a metal to substrate ratio of 20, yielding 99% conversion with 99% selectivity and no isomerization. Pd–apatite-, Au–Pd–CeO₂- and Au–Pd/TiO₂-catalysts also gave no isomerization; however, with the same metal to substrate ratio either conversions were lower (74, 99, 95%, respectively) or the selectivity went down (63, 93, 70%, respectively). Recycling experiments proved Au–CeO₂ to be a reusable catalyst for allylic alcohol oxidation without solvent.

References

- 1 J. S. Carey, D. Laffan, C. Thomson and M. T. Williams, *Org. Biomol. Chem.*, 2006, **4**, 2337–2347.
- 2 D. S. Matharu, D. J. Morris, G. J. Clarkson and M. Wills, *Chem. Commun.*, 2006, 3232–3234.
- 3 P. Barbaro, *Chem.–Eur. J.*, 2006, **12**, 5666–5675.
- 4 A. Abad, C. Almeda, A. Corma and H. Garcia, *Chem. Commun.*, 2006, 3178–3180.

Green chemistry for sustainable cement production and use

John W. Phair

Received 17th March 2006, Accepted 26th June 2006

First published as an Advance Article on the web 12th July 2006

DOI: 10.1039/b603997a

Concrete is in desperate need of revitalisation in the 21st century due to growing durability, maintenance and environmental concerns. Improving the cement within concrete is an essential part of addressing these concerns. While Portland cement manufacture and use can still undergo slight environmental improvements, great opportunities lie in the utilisation of cements based on alternative compositions, binding-phases and green chemistry. This allows cement to be synthesised from a variety of materials including recycled resources and mineral wastes, which reduces the energy demands during production. The present work introduces industrial ecology and the principles of green chemistry as a means of driving the research, development and commercial attractiveness of alternative and sustainable cements. Three promising alternative cements are reviewed (alkali-activated cements, magnesia cements and sulfoaluminate cements) and compared to blended ordinary Portland cements in terms of their chemistry and properties. Emphasis is given to the material properties, durability, performance and applications of the “greener” alternative cements. It is clear that alternative cements have considerable potential in terms of environmental, engineering and economic properties.

1. Introduction—the need for more sustainable, durable cement

Ordinary Portland cement (OPC) has dominated concrete construction for the past 150 years with the production rate rising from 10 million tonnes (tonne = metric ton = 1000 kg) in 1900 to 1500 million tonnes in 2000.¹ It has now plainly established itself as a commodity material and the mainstay of the construction industry.² However, much of the OPC-based concrete used in the construction of US infrastructure during the 1950's and 1960's has deteriorated to the point that extensive repair and replacement is required³ (see Fig. 1–3 for

examples). These rehabilitation problems and resulting costs could have been avoided by utilising a more durable material

Office of Infrastructure Research and Development, Federal Highway Administration, McLean, Virginia 22101, U.S.A.
E-mail: jwphair@yahoo.com



John W. Phair

John W. Phair (Ph.D B.Sc(Hons) LLB) completed his Ph.D in the Department of Chemical Engineering at the University of Melbourne in 2002 where he examined the microstructure and properties of fly-ash based geopolymers. Following his Ph.D, John was awarded a National Research Council Research Associateship to investigate the mechanisms, microstructure and products of the alkali-silica reaction (ASR) in cement. He undertook this work with Dr R. A. Livingston at the Turner-Fairbank Highway Research Center (TFHRC) in McLean, VA, USA.



Fig. 1 Crumbling façade of the Memorial Stadium at the University of California, Berkeley. Photo courtesy of Liz Mangelsdorf, San Francisco Chronicle, 2004; http://www.sfgate.com/c/pictures/2004/09/09/sp_calstadiumfacade.jpg.



Fig. 2 Crumbling section of highway I-670, courtesy of the Ohio Department of Transportation (ODOT).

in the first place.^{4,5} According to the recent 2005 report card by the American Society of Civil Engineers (ASCE), the state of America's infrastructure has reached alarmingly unacceptable levels which threaten our very lifestyle and standard of living. The average grade for America's infrastructure was D (Poor), requiring an estimated US\$1.6 trillion over the next 5 years just to return the infrastructure systems back to a serviceable condition. The fact that US\$9.4 billion a year for 20 years is required to eliminate the deficiencies in the nation's ~600,000 bridges, suggests serious systemic problems exist in the construction industry (for examples, see Fig. 4 and 5). Society is slowly coming to realise that initial predictions of cement durability may have been excessive and that concrete buildings or structures that last for only 50–70 years may not be cost effective.

With energy, resource and infrastructure demands growing in the foreseeable future, a sustainable concrete that is more durable and costs less to maintain, is becoming increasingly desirable.⁶ If the world population doubles within the century, growth in the use and production of concrete will be equally



Fig. 3 The middle of Samuelson Road in Portage, Ind., has a pothole the size of a person's head. © American Consulting Inc. Photo by Sean Porter; <http://www.asce.org/reportcard/2005/assets/gallery/2-head.jpg>.



Fig. 4 The aging Rockefeller Road Bridge in Cleveland, Ohio, is one of many decaying bridges over the rail corridor. © Cuyahoga County Engineer's Office, Photo by Robert C. Klaiber, Jr., P.E., PS.; <http://www.asce.org/reportcard/2005/assets/gallery/3-bridge.jpg>.

dramatic and put excessive demand on our natural resources and ecological well-being, unless more sustainable concrete is used (see Fig. 6). Clearly, a fundamental shift is required in the perception, production and use of concrete. Four main paradigms in the production and use of concrete that are badly in need of reassessment include:⁷

1. That the benefits of high-speed construction exceed those of slower construction which utilise resources, energy and materials more conservatively and produce concretes of longer service lifetime.
2. That high-early strength concrete is more durable and useful than slow-early strength concrete which matures over a longer time.
3. That simplistic changes to OPC-based concrete mixing (e.g. water to cement ratio) are sufficient to improve the durability.



Fig. 5 As of 2003, 27.1% of the nation's bridges (160,570) were structurally deficient or functionally obsolete, an improvement from 28.5% in 2000. © Carl J. Lehman, Photo by Carl J. Lehman, P.E., F.ASCE; <http://www.asce.org/reportcard/2005/assets/gallery/6-under.jpg>.

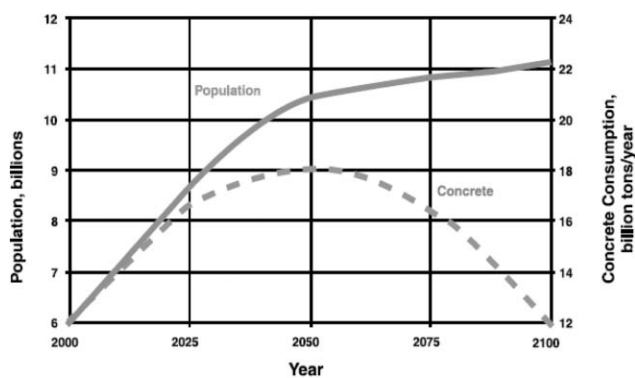


Fig. 6 Forecast of future population growth and sustainable concrete consumption.¹⁵⁶

4. That composition-based standard mix specifications should remain the dominant code for the construction industry rather than performance-based specifications.

Challenging these paradigms paves the way for innovation within the industry and point toward alternative cement binders as means of achieving the environmental and durability standards of the 21st century. Traditionally, cement has low margins for generating profits, which often are only achieved by high-production turnover. Superior material performance or lifetime are generally dismissed as insufficient justifications to invest in the development and utilisation of alternative cements. However, if all true costs (including environmental) of cement production and use are included in the equation, then alternative cements are viewed far more favourably.

The purpose of this paper is not only to review the methods for determining the true costs, environmental impact and performance of cement, but to identify the concepts and theoretical basis behind them. Industrial ecology and its tools (*e.g.* life cycle analysis) are central to this task and provide the motivating basis for research and innovation in the design and assessment of superior alternative cements to OPC. Basic strategies in ecological cement innovation are defined and illustrated, with direct reference to the chemical processing of cement. Three promising alternative cements, namely alkali-activated cements, magnesia cements and sulfoaluminate cements, will be described as case studies for innovation and compared to conventional OPC-blended cements. Not only will the basic chemical properties, microstructure and production of these cements be discussed, but their engineering performance and environmental position relative to Portland cement will be assessed.

2. Background to portland cement

2.1 Cement manufacture and utilisation

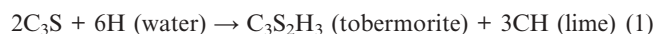
Cement is a vital ingredient to the building and construction industries since it forms the glue that holds concrete together. Although cement comprises only 10–15% of the mass of concrete, this minor constituent plays a significant role in determining the cost of concrete, its environmental impact, and the properties of both the fresh and hardened concrete paste.⁸ In particular, Portland cement has become the

Table 1 Typical engineering properties of OPC-based structural concrete¹⁵⁷

Compressive strength	35 MPa
Flexural strength	6 MPa
Tensile strength	3 MPa
Modulus of elasticity	28 GPa
Poisson's ratio	0.18
Tensile strain at failure	0.001
Coefficient of thermal expansion	$10 \times 10^{-6} \text{ } ^\circ\text{C}^{-1}$
Ultimate shrinkage strain	0.5–0.1%
Density—normal	2300 kg m^{-3}
Lightweight	1800 kg m^{-3}

centrepiece of the modern construction industry with annual global production totalling more than 5 billion tonnes ($\sim 400 \text{ L}$ per person).⁴ This is nearly ten times its nearest rivals, wood or brick. Of the varieties of cement available, Portland cement has become by far the most popular due to its low cost (~ 0.025 US dollars per kg) and ease of application. It now constitutes 95% of the cement produced annually in the U.S.

Portland cement is essentially finely ground calcium silicate minerals that are hydraulically active. The main component of Portland cement, referred to as clinker, is manufactured by mixing limestone (calcium source), sand (silica source) with small amounts of bauxite (aluminium source) and iron ore in a rotary kiln before heating to $\sim 1480 \text{ } ^\circ\text{C}$. The raw materials used in this process such as limestone, marble and chalk for calcium or clay, sand and shale for silica are readily available but preferred in virgin form. Gypsum is combined with clinker as a sulfur/calcium source at about 5% weight to form Portland cement proper. Portland cement is rich in $\text{C}_3\text{S}^\dagger$ and C_2S phases with smaller amounts of C_3A and C_4AF . C_3S and C_2S contribute 70–80% of clinker by weight. Upon hydration, both C_3S and C_2S combine with water to form CSH, the colloidal gel that binds the cement particles together, and calcium hydroxide (lime). This can be represented by a typical reaction for the formation of tobermorite, an ordered phase related to the CSH gel:



The solid mass of hydrated Portland cement paste consists primarily of CSH(50–60%), CH(20–25%) and calcium sulfoaluminate compounds (15–20%). Overall, this results in a durable and resistant artificial “stone”, suitable for myriad applications. The main advantages of concretes based on OPC include the fact that they are castable, non-flammable, fabricated on-site and relatively cheap.⁹ The typical engineering properties of OPC-based structural concrete are provided in Table 1.

2.2 The durability crisis

Experience has established that OPC-based concrete is not a material of endless durability due to the increasingly common occurrence of structural and material degradation throughout the world. The main reasons given to explain the poor

[†] Please note the cement notation used throughout the manuscript, where C = CaO, S = SiO₂, A = Al₂O₃, M = MgO, K = K₂O, N = Na₂O, $\bar{\text{S}}$ = SO₃, $\bar{\text{C}}$ = CO₂, H = H₂O

durability of OPC-based concretes are its brittleness, high permeability, low tensile strength, low ductility, volume instability (shrinkage), weak resistance to acid and reasonably low strength to weight ratio.^{10,11} Furthermore, over the past four to five decades, OPC composition has been altered from a C₃S/C₂S ratio of 1.2 to 3.0. While this has resulted in higher strengths at early ages, it is accompanied by higher heats of hydration and less strength development after 28 days. The benefits of this mix-design to durability are therefore becoming more questionable.

In general terms, most of the degradation problems of Portland cement are a direct consequence of its chemistry and microstructure, which is composed of compounds (CSH, CH, CA, CF and calcium sulfoaluminates) that do not occur as natural minerals. Consequently, these compounds are susceptible to degradation in certain environments. For instance, the presence of significant quantities of calcium hydroxide (CH) in Portland cement is a major shortcoming since calcium is highly mobile and reactive, which can lead to deficiencies in durability when in excess. CH and CSH are prone to sulfate attack by forming gypsum in the presence of sodium disulfate, or ettringite (*i.e.* sulfate attack). Sulfate attack is highly deleterious to the concrete structure and along with alkali-aggregate expansion reactions, freeze-thaw cycles, corrosion, *etc.*, constitute a long list of chemical degradation problems suffered by OPC concrete. The major shortcoming of CSH is that it is thermodynamically unstable, and has an underlying tendency to revert to silica gel and calcium carbonate in the natural environment. In an aggressive environment, the kinetics of this process are much faster. Furthermore, the colloidal structure of CSH—a 2-dimensional chain or layered molecular structure¹²—is not as strong a bonding network as that which could be achieved from a 3-dimensional hierarchical structure to maintain material integrity. Thus, having a nano/micro-structure that is discontinuous and inhomogeneous in 3 dimensions, restricts material performance and durability.

The degradative effects of chemical processes typically serve to restrict the inherent physical properties of the material, such as its tensile strength, toughness or crack resistance on impact, or permeability to fluids (particularly in aggressive environments). While structural reinforcements and admixtures can overcome a lot of these deficiencies, alternative cements offer a new approach and capabilities to solving durability and structural performance problems at the microstructural and chemical levels.

2.3 Environmental problems

Major environmental impacts associated with Portland cement include the energy required for production and transportation of clinker, the emission of greenhouse gases either directly or indirectly during manufacture, and the impact of mining, resource depletion and waste generation. Considerable energy and materials may also be consumed during the repair and rehabilitation of degraded structures. Environmental problems range from local, site-specific issues associated with mining and processing of raw materials (eg. dust, tailings, contamination *etc.*), to regional (eg. acid rain, groundwater



Fig. 7 Increasing occurrence of extreme weather patterns will increase the demand for more durable concrete. http://nandotimes.nandomedia.com/ips_rich_content/989-debris.jpg.

contamination *etc.*) and finally global (such as CO₂ and NO_x emission) scales.¹³ The most serious environmental problems are global as they are the most difficult to combat. With a burgeoning world population, it is expected that cement use in developing nations will grow dramatically over the next 50 years. This places heavy strains on the means of production and, in order to satisfy these demands, is forcing industry to re-evaluate its processes and methods of manufacture. Furthermore, since climate change is forecast to increase in the future with weather patterns becoming more extreme, the likelihood of infrastructure damage will also increase, as will the demand for more durable concrete (see Fig. 7).

3. Industrial ecology of cement

Industrial ecology may be defined as the study of combined human industrial activities and their environmental impact.¹⁴ It is a systems approach that focuses upon the interaction of industrial processes and the ecological system(s) of which they are a part.¹⁵ Unlike traditional ecological science, however, it has prescriptive tendencies. That is, it attempts to promote anthropocentric notions of sustainable development and ecological sustenance, incorporating value judgments such as the 'precautionary principle'. In practical terms, it seeks to optimise industrial activities and limit their ecological impact to a level which natural systems can be expected to sustain.¹⁶ Industrial ecology considers environmental impacts on a global scale and is not necessarily restricted to local problems.¹⁷

Industrial ecology is an emergent field and, therefore, is developing a variety of tools to assess and predict ecological sustainability by evaluating the environmental impact of a particular material or industrial process. Some of the tools and concepts already being used in the industrial ecological assessment of cement include system dynamics models,¹⁸ materials flow analysis,¹⁹ energy (or embodied energy) analysis,^{20,21} and the general principles of sustainable science and engineering.²² Fig. 8 illustrates how the system dynamics model can be used to assess the various inter-relationships and their effects on the ecological sustainability of cement. One of

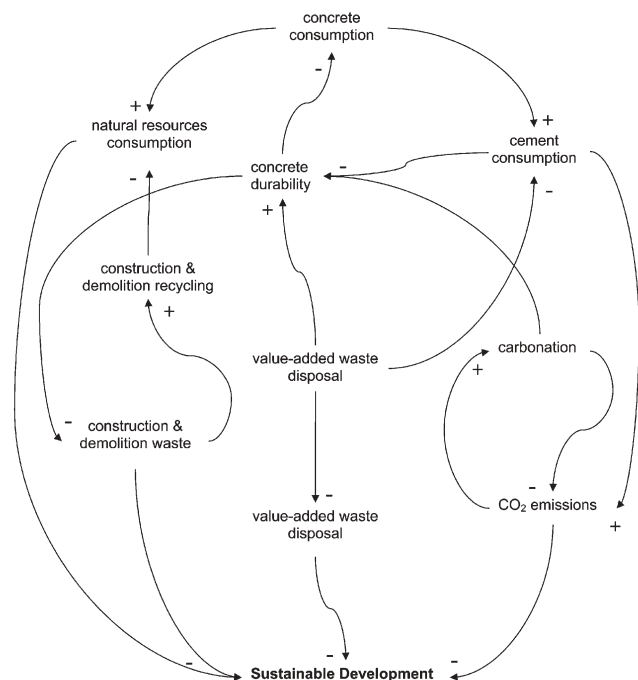


Fig. 8 Causal loop diagram of a systems dynamic model used for assessing the various relationships and their influence on the industrial ecology of cement. Here, the arrowhead indicates the direction of variable dependency while the sign (+ or -) of the arrow depicts whether it is positive or negative feedback.¹⁸

the more popular tools to quantify the environmental impact of cement is a Life Cycle Assessment (LCA), which can quantify the material and energy flow (input/output) between the product and the environment.²³ Life cycle assessment of cement typically covers the raw materials, manufacture, products, construction, utilisation and residual materials, and the various transformations they undergo.²⁴ It then assesses the relative effects they have on specific ecological parameters such as greenhouse gas emissions, depletion of the ozone layer in the stratosphere, the formation of photo-oxidants (smog), acidification of soils through acid rain and eutrophication (excessive release of nutrients into surface water).²⁵ When

LCA's are conducted on cement and compared to other construction materials (such as brick, wood and steel *etc.*), cement generally has superior performance for the cost, with significantly less severe environmental consequences with large volume use.²⁶ Its environmental consequences, such as greenhouse gas emissions, however, can still be greatly improved.¹³ For instance, cement compares favorably to other construction materials such as metals (*e.g.* steel, aluminium), wood, glass and plastics/oil in terms of production emissions per tonne of material (see Table 2).⁴ Wood production was demonstrated to emit the least gaseous airborne material followed closely by OPC concrete. This amount, alternatively, can be greatly reduced for concretes based on secondary (or value-added, waste) materials.²⁷ In addition, concrete generally exhibits more favorable characteristics in terms of production costs, energy consumption and strength than other building materials (see Table 3).²⁸ However, the variable strength properties, performance and durability of the different building materials must also be taken into this account during this assessment, as not all perform well in specific tests. Table 4 provides a comparison of the energy requirements for typical construction materials in combination with their various physical properties.

A variety of LCA tools exist for use in the cement industry but their capabilities vary depending on the intended user (*e.g.* process engineers, environmental managers, product designers, in addition to planners, architects and builders) as well as the type of LCA being performed and the volume of primary data required for the analysis. A recent examination of the various types of LCA tools determined that those which complied with the ISO 14040 series of LCA standards, contain high quality databases, make a full life cycle impact assessment and allow the marketplace to evaluate the environmental performance of final products may be useful for the cement industry.⁶ In particular the following LCA tools have been favoured: GaBi 3v2 (IKP Uni. Stuttgart/PE, Germany), LCAIT 4.0 (Cjalmer Ind,[CIT], Sweden), NIRE LCA2 (NIRE, Japan), SimaPro 4.0 (Pre Consultants, Netherlands), TEAM 3.0 (Ecobilan/Ecobalance/PWC, Europe/USA), although significant room for improvement remains.

Table 2 Production emissions of building materials⁴

Building material	CO ₂ /kg t ⁻¹	CO/kg t ⁻¹	SO ₂ /kg t ⁻¹	NO _x /kg t ⁻¹	CH/kg t ⁻¹	Dust/kg t ⁻¹
Wood	124	1.2	—	—	0.1	0.5
Concrete	147	—	0.2	0.6	—	0.1
Glass	2100	—	2.7	9.3	—	1.6
Oil and plastic	6000	—	5.0	5.0	—	1.0
Metals	3000	—	3.0	5.0	—	0.5

Table 3 Comparison between strength, production cost, energy consumption, and SO₂ emissions of building materials²⁸

Properties	Steel	Glass	Brick	Sand/lime brick	Timber	Reinforced concrete
Strength/MPa	240	30	7.5	7.5	14	13.5
Cost per m ³ (index)	100	47	3.4	2.3	5.8	2.0
Cost/strength	0.42	1.57	0.45	0.13	0.41	0.15
Energy/GJ m ⁻³	236	56	11	4.9	2.4	6.3
Energy/strength	0.98	1.87	1.48	1.65	0.17	0.47
SO ₂ /kg/m ⁻³	14	3.2	1.8	0.4	—	1.0
SO ₂ /strength	0.06	0.11	0.24	0.05	—	0.07

Table 4 Typical properties of construction materials^{13,26,158}

Material	Density/ kg m ⁻³	Tensile strength/MPa	Elastic modulus/GPa	Co-efficient of thermal expansion/10 ⁻⁶ °C ⁻¹	Thermal conductivity / W m ⁻¹ K ⁻¹	Energy requirement/ GJ m ⁻³
Aluminium—pure	2800	100	70	23	220	360
Aluminium—alloy	2800	300	70	23	125	360
Steel—mild	7800	300	210	12	50	300
Steel—high strength	7800	1000	210	11	45	—
Glass	2500	60	65	6	3	50
Wood—soft	350	50	5.5	—	0.2–0.6	—
Wood—hard	700	100	10	—	0.2–0.6	—
Plastic (polystyrene)	1000	~ 50	~ 3	72	0.1	—
Rock (granite)	2600	~ 20	~ 50	7–9	3	—
Concrete	2300	3	~ 25	10	3	3.4

To date, no LCA study has quantitatively investigated the complete material, energy and lifetime balance of alternative cements compared to that of Portland cement. While efforts have been made to compare the CO₂ emitted from raw materials during the manufacture of alternative cement compounds, this forms only one of the inputs required for a complete LCA analysis.²⁹ Future LCA studies should include not only the raw material inputs and output in terms of energy consumption, source materials *etc.*, but also consider the durability of the material and the potential energy and material costs associated with replacement and recycling.²⁴ It would also be useful to relate the LCA back to the basic chemistry of the binding phase in order to optimise mix composition and processing of the cement both environmentally and economically. Fig. 9 displays the cycle of material flow in the production and use of Portland cement. As seen in Fig. 9, the cycle is incomplete because the carbonated hydration products cannot be regenerated to form the starting material. This leaves Portland cement at a distinct disadvantage when compared to other cements such as magnesia and

alkali-activated cements, which may be regenerated from the final product, hence closing the material cycle. The ability of a cement to undergo carbonation while hardening is a way of closing the carbon cycle in the production, use and disposal of cement, but this must not occur at the expense of performance or durability of the hardened material.³⁰

After completing quantitative LCAs of the cementitious material, the next step is to design an industrial relationship that can further close the loop on any residual gaps in the material life cycle, by including any potential input/outputs from other relevant industries. Such a relationship is referred to as an industrial symbiosis.³¹ A classic example of an industrial symbiosis is the Kalundborg industrial park in Denmark, in which there is an inter-connected system of material and energy exchange between an oil refinery, a power plant, a pharmaceutical factory as well as a cement manufacturing plant.³² Numerous other examples of co-operative industrial parks are appearing throughout the world illustrating the potential benefits of cement plant symbioses with other plants, such as the Cajati industrial park in Brazil.⁶ Recent research has demonstrated that the use of geographical information systems (GIS) for designation of industrial ecosystems can reduce costs associated with transporting resources from one facility to another.

Three major stages in the industrial ecology of cement will now be discussed in greater detail.

3.1 Sustainable cement production

Sustainable cement production largely depends on the amount of non-renewable energy used and gaseous emissions. Energy is required at various stages during the production of cement, such as the quarrying, opencut mining and transportation of the basic raw materials and the processing and formation of cement clinker from raw materials. For example, the overall process of Portland cement manufacture requires approximately 4–6 GJ per tonne, although this is dependent on the particular plant size and method of processing (dry or wet).³³ At the moment, various methods are being trialled which may reduce the energy requirements.³⁴ They include the utilisation of energy-efficient plants, machinery and alternative fuel sources for manufacture, including a broad range of combustible solid and liquid wastes.^{35,36} This incurs costs advantages³⁷ as well as reducing greenhouse gas emissions.³⁸ Utilisation of alternative raw materials may also reduce energy requirements. Fly ash, for example, is already in a powdered,

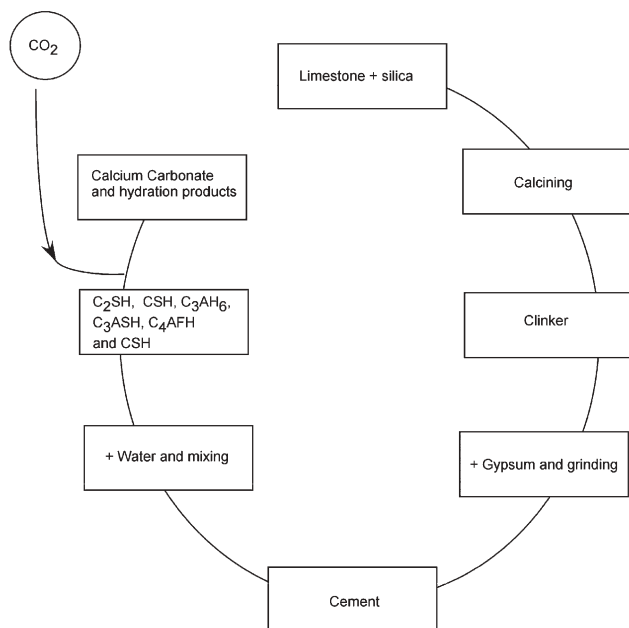


Fig. 9 Incomplete cycle of material flow in the production and use of Portland cement.¹

Table 5 The quantities of CO₂ generated from the conversion of raw materials into OPC compared to alternative cement compounds²⁹

Cement compound	Raw materials used	Quantity of CO ₂ generated (g of raw material per g of CO ₂)	Quantity of CO ₂ generated (g of raw material per ml of CO ₂)
M (magnesia, periclase)	Magnesite	1.092	3.91
C (calcia, quicklime)	Limestone	0.785	2.63
C ₃ S (alite)	Limestone + silica	0.578	1.80
β-C ₃ S (belite)	Limestone + silica	0.511	1.70
C ₃ A (tricalcium aluminate)	Limestone + alumina	0.489	1.50
C ₄ AF (calcium aluminoferrite)	As above + iron oxide	0.362	1.29
NS (sodium metasilicate)	Soda + silica	0.361	—
CA (monocalcium aluminate)	Limestone + alumina	0.279	0.83
C ₄ A ₃ S (calcium sulfoaluminate)	As above + anhydrite	0.216	0.56

pozzolanic and reactive form, and using this material can reduce both cost and energy demands of cement manufacture. Reducing the lime and alite (C₃S) content in cement clinker also lowers the energy requirements for calcining.

A major consequence of energy use is the production of greenhouse gases (GHGs), which include CO₂, NO_x, sulfur and dust. In addition, the chemical reaction of Portland cement clinker formation itself greatly influences the formation of GHG. For example, approximately 1 tonne of CO₂ is produced for every 1 tonne of Portland cement clinker manufactured:



The net result is that at least 1.5 tonnes of CO₂ are emitted for every one tonne of clinker manufactured, starting from 1.7 tonnes of raw materials.¹³ The quantities of CO₂ generated from the conversion of raw materials into OPC compared to alternative cement compounds are presented in Table 5 with only the formation of magnesia and calcia emitting more CO₂ than the formation of Portland cement clinker. Therefore, reducing energy requirements for the manufacture of cement and utilising a chemical reaction for cement formation that does not yield excessive amounts of CO₂ as a by-product will reduce global CO₂ and greenhouse gas production. Presently, CO₂ emissions from cement production in the U.S. account for up to 7% of the nation's total output,³³ and account for over half of the total U.S. CO₂ emissions from industrial processes, according to Table 6. Global estimates of carbon dioxide emissions from the manufacturing of Portland cement are much higher, with some reaching as high as 10% of the total emissions.³⁹

Reduction in the energy requirements for producing cement is usually accompanied by a reduction in greenhouse gas emissions if the energy is derived from non-renewable sources. The removal of CO₂ from flue gases (*e.g.* geosequestration) may prove practical for reducing greenhouse gas emissions. In order to develop system optimisation over the longer term, the tools of industrial ecology and sustainability planning,⁴⁰ such as Exergy, will become increasingly useful for determining the conditions under which solid waste transformations consume minimum energy.⁴¹ Furthermore, since limited ecological improvements (such as energy-saving technical upgrades to plants and utilisation of non-carbonate CaO source) can still be made to Portland cement producing plants, the greatest scope for reducing the environmental impact of cement lies in

utilising alternative cements. Future long term studies must consider the energy costs and emissions generated during repair, rehabilitation, replacement or disposal of cement in addition to production.

3.2 Cement as waste management

Industrialised societies are increasingly producing more waste, mostly associated with mineral processing, energy production, individual consumption and disposal of non-renewable resources.⁴² Table 7 provides an estimate of the annual quantities of various types of solid waste generated in the United States. These wastes are slowly accumulating in enormous quantities to the extent that 'giga-scale disposal' (*e.g.* fly ash, slag and phosphate) has become a common phenomenon.⁴³

The typical approach to managing large-scale waste has been to dispose of the material either in landfills, in the ocean or by incineration.⁴⁴ Such an approach is becoming less socially, environmentally and practically acceptable. Crude disposal of wastes is being traded for more rational and

Table 6 2002 U.S. carbon dioxide emissions from industrial processes¹⁵⁹

Source	Million tonnes of CO ₂
Cement Manufacture	
Clinker Production	42.0
Masonry Cement	0.1
Cement Kiln Dust	0.8
<i>Cement Subtotal</i>	43.0
Other Industrial	
<i>Limestone Consumption</i>	
Lime Manufacture	14.1
Iron Smelting	0.9
Steelmaking	0.5
Copper Smelting	0.1
Glass Manufacture	0.1
Flue Gas Desulfurisation	1.4
Dolomite Manufacture	0.3
<i>Limestone Subtotal</i>	17.4
Soda Ash Manufacture	3.5
<i>Soda Ash Consumption</i>	
Glass Manufacture	0.1
Flue Gas Desulfurisation	0.1
Sodium Silicate	0.2
Sodium Tripolyphosphate	0.1
<i>Soda Ash Subtotal</i>	0.5
Carbon Dioxide Manufacture	1.4
Aluminium Manufacture	4.0
<i>Other Industrial Subtotal</i>	26.7
Total	69.7

Table 7 Estimate of the annual quantities of various types of solid waste generated in the United States¹⁶⁰

Type of work	Annual quantities (millions of tonnes)
Agricultural	Unknown
Construction/demolition	28.1
Household (hazardous)	0.27
Industrial (non-hazardous, dry basis)	390
Industrial hazardous	178
Mining	1270
Municipal Solid Waste	177.6
Municipal sludge (dry basis)	7.7
Municipal combustion ash	2.1

sustainable resource use by encouraging integrated waste management options.⁴⁵ This includes waste prevention, reducing the quantity and toxicity of waste, composting, incinerating with energy recovery, recycling, re-use and resource conservation.^{46,47} Resource conservation is a key method in the reduction of wastes. This can be achieved in various ways—by reducing consumption, improving primary extraction processes, fabrication/manufacturing design, and improving product life and energy recovery.⁴⁸ A type of integrative waste management strategy that is attracting greater interest for the management of materials is to close the loop of production and consumption.^{23,49,50} This will involve substituting waste for useful products and thereby improve environmental quality within a framework of economic accountability.⁵ Conceptually, cement is evolving from a non-renewable resource-based material, to a value-added material *i.e.*, one which adds benefit to waste materials of low immediate value which are generally of environmental concern.⁵¹ This conceptual evolution is characterised in Table 8, and has been noted by other authors, such as Aitcin who has suggested that with developing socioeconomic and environmental needs, the cement industry will move away from being solely Portland cement clinker-based, to be a more general hydraulic binder industry.² Thus, cement will be customised for specific applications and the process designed so as to minimize waste and greenhouse gas emissions.⁵²

Utilisation of cement to close the loop on many waste products not necessarily associated with the manufacture of cement, is the essence of an industrial symbiosis.⁵³ Ever since coal fly ash was first recognised in the US as a valuable source of raw material and/or pozzolan for concrete in 1937 by

R.E. Davis, industrial wastes have found a purpose in cement.⁴⁴ It was initially proposed that fly ash could replace up to 20 to 50% of the Portland cement in a given mix.⁴⁴ Today, 30% of all fly ash generated is recycled for use as filler or pozzolan in concrete,⁴³ transforming early prophecies of its use into reality.

The majority of global industrial processes relied upon daily cannot be dramatically altered or halted and will continue to produce waste. Thus, even if these industrial processes are environmentally managed to produce the minimum impact, accumulation of waste will always be an issue, unless it can be recycled for use as feedstock for an alternative industrial process, such as concrete manufacture. An immense range of wastes is amenable for use in concrete, and so long as they are in solid form and are not too hazardous or require special treatment, their exact composition can vary. Fig. 10 provides an illustration of the materials which may be recycled in cement and concrete. Potentially these can include solid discards, recycled concrete and cement,^{50,54} sludges, wastewater and residuals such as combustion ashes and mine tailings.⁵⁵ Agriculture, mining and construction industries, commerce, households and energy-related activities are all sources of solid wastes, with the mining and agriculture industries contributing 90% of the waste while industrial, municipal and utility sectors only account for 10%.⁵⁶ Industrial process wastes that are most suitable for re-utilisation in concrete include sludges, combustion ashes, discarded concrete, slags, kiln dust, foundry sand and other inorganic residues.^{57,58} Mining wastes that are attractive for recycling in concrete include a variety of tailings, brines, slags (copper, phosphorous, blast furnace, steel) and residues resulting from the processing of materials. Agricultural waste that is readily biodegradable is less suitable for incorporation in concrete, but it may be added as admixture if its degradation is controllable. There is increasing impetus to combine the properties of admixtures in the waste materials so as to reduce admixture cost.⁴⁴ With such a wide variety of waste materials being used today, it is becoming much easier to find a waste substitute for an admixture, which can do the same job equally well if not better.

3.3 Sustainable cement use

Apart from recycling and conservative resource application, sustainable cement use critically depends upon the ultimate

Table 8 The evolving paradigm of cement¹⁶¹

Traditional perspective of cement	Innovative perspective of cement
Cement as a resource	Value-added materials as cement
Commodity material	Information and technology dependent material
Forms monolithic materials	Forms composites, ceramics, advanced materials, coatings, and specialty engineered products
Used mostly for structural material	Can also be used for functional materials
Produced by large-volume, continuous process	Produced by large and small-scale, batch processes
Processing plants dedicated to a single product	Processing plants designed for flexibility in production
Price and availability as competitive basis	Quality, long-term performance, environmental and ecological sustainability as competitive basis
Resource-oriented research	Processing-oriented research
Environmental resources abundant	Environmental resources limited
Research performed by single principle investigators	Research performed by multidisciplinary, collaborative research teams
Self-sufficient economy, limited vulnerabilities	Interdependent, global economy, many potential vulnerabilities

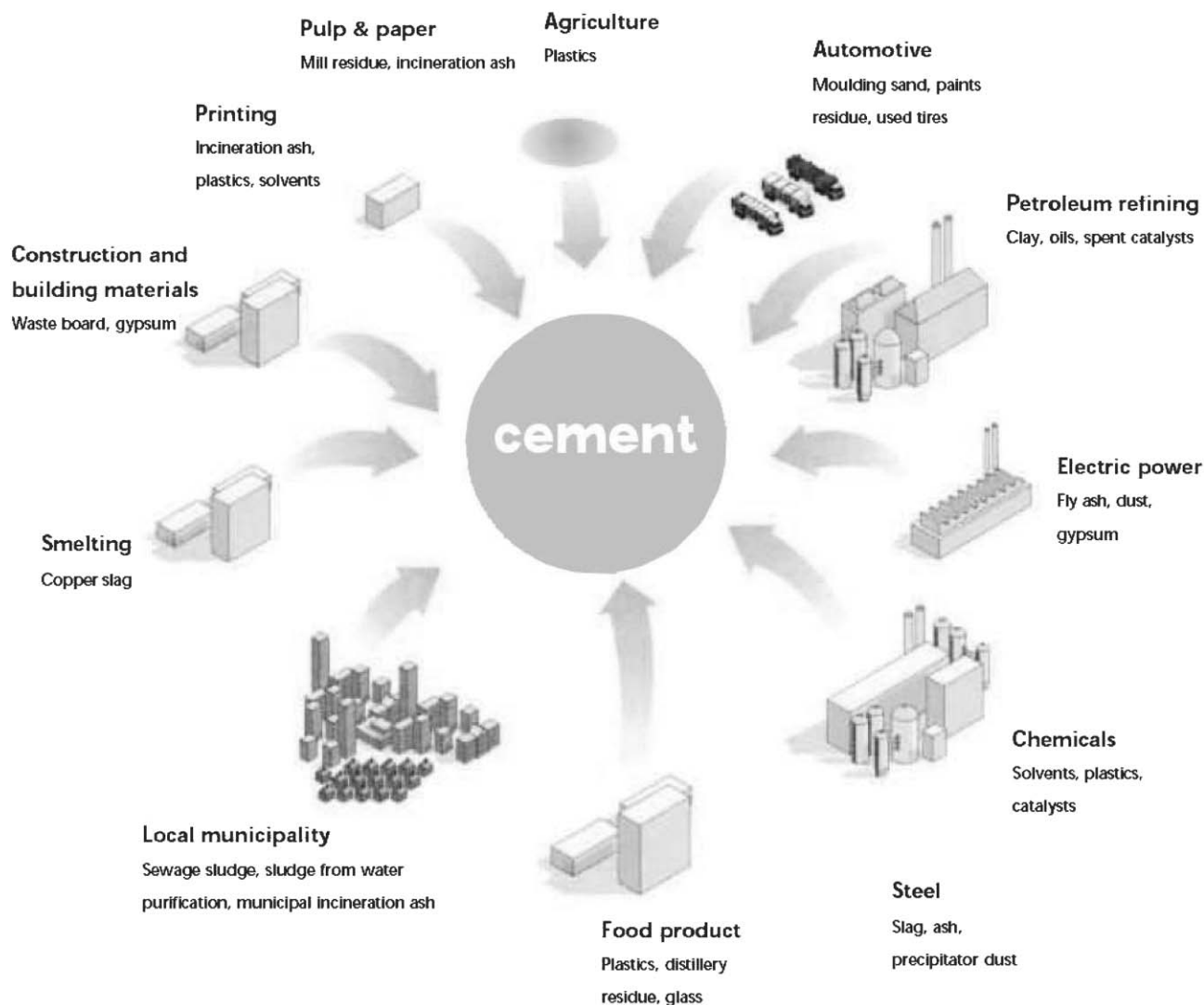


Fig. 10 Diagram of materials which can be recycled in concrete.¹⁵⁵

durability and lifetime of the cement. Ensuring that cement is used for the specific application for which it was designed is central to maximising the lifetime of a hardened cement. Designing cements to be more durable for a specific application requires consideration of a range of physical and material parameters which include:⁵⁹

(1) Pore refinement—reducing or minimising the porosity of the hardened cement.

(2) Reduced permeability—often achieved by very low porosity.

(3) Chemical resistance—achieved by limiting ion (*e.g.* Cl^- , SO_4^{2-}) penetration and transport throughout the material and forming highly insoluble cement pastes. The depletion or sequestration of any potentially harmful ions (*e.g.* alkalis) may also be necessary.

(4) Low heat of hydration (for Portland cements).

(5) Low water–binder ratio (for Portland cements).

(6) Better control of or resilience to high thermal gradients.

(7) Microstructural strength development due to crystallisation, long-term hydration, carbonation, pozzolanic or zeolitic reactions coupled with high early strength.

(8) High workability and control of slump loss.

(9) Low bleeding and plastic shrinkage.

OPC is reaching its performance limits for these various properties, so further improvements to durability based on these properties are restricted. However, these properties have been vastly under-examined in alternative binders for improved durability, and thus considerable opportunities remain for their optimisation. Alternative binders also have additional individual properties (*e.g.* extrudability) that are yet to be optimised and may indirectly affect the durability of the cement by facilitating the use of new processing, mixing and setting techniques.

4. Green chemistry for cement design

To achieve sustainable cement production, increasingly opinion suggests that conscious and pro-active earth systems engineering and management (ESEM) is the best approach. ESEM is a responsible means of limiting and controlling the impact of human activities on natural systems through full comprehension of scientific and technological domains, in

addition to the social domains of culture, politics and institutional dynamics associated with cement.⁶⁰ While the current review predominantly considers the scientific and technological aspects of ESEM, the commoditisation and institutions which control the development within the industry must not be ignored.

Nonetheless, ESEM encourages the scientific and technological design of cement and concrete materials from first principles. By considering the building blocks of cement and concrete in fundamental terms—the chemistry of the raw materials, their processing, binding phase, material properties, performance and use, in addition to the chemistry of the wastes generated—provides a comprehensive basis for environmental improvement. The role of green chemistry in optimising the three major stages in the industrial ecology of cement is illustrated in Fig. 11. By considering the environmental impact of the cement at each stage of its life cycle, green chemistry seeks cement compositions with the greatest likelihood of ecological sustainability. Therefore, factors such as atomic composition (presence of oxy anions, alkali or transition metal cations, metal oxides, pH *etc.*), atomic structure (*e.g.* crystalline *vs.* amorphous), long range structure (*e.g.* 2-dimensional *vs.* 3-dimensional network) and the range of physico-chemical properties associated with the binding phase (*e.g.* morphology, solubility, thermodynamics/kinetics of hydration, strength development, bond strength, chemical stability, durability *etc.*) are of central concern to cement throughout its complete life cycle.

A vital step in developing green chemistry for cement design is to expand the concept of cement beyond Portland cement and its standard constituent phases (*e.g.* CSH, CH, AFt [ettringite], AFm [monosulfate] and iron hydrate phases). This is necessary to encourage the development, identification and trial of new binding phases and composite materials.

Debunking the idea that cement is a low-technology or ‘solved’ problem is equally vital to ignite greater interest in its research and development. While low-tech solutions will invariably be more competitive in the long-run, that does exclude utilising better understood, high-tech materials and processes for their development. It may be useful to consider cements as ‘chemically bonded-ceramics’, a term which has previously been used to describe designer high-tech cements, emphasising a higher level of scientific order than usually appreciated.⁶¹ This name stems from the fact that strength formation occurs through chemical reactions at ambient temperatures as opposed to high temperature densification for traditional ceramics. Such a definition can cover a variety of potentially useful chemical systems that differ significantly by molecular composition, nanostructure, hydrating mechanism and hardening properties.⁶² Having defined the basic binding chemistry phase of a “green” cement of potential interest, the practical properties such as its workability as a fresh paste, its ability to include other materials, and its final material performance, durability, and recyclability must then be assessed.

Green chemistry encourages innovation in the methods and technology for cement processing so that they may be transferable to different regions and adaptable to local supplies of raw materials for the manufacture of a desired product. Development and implementation of non-destructive evaluation (NDE) techniques based on a variety of physical phenomena such as electrical, electromagnetic, wave propagation *etc.* will play a central role in modernising the processing, manufacture and in-service monitoring of cements in the future.^{63–65} This may involve either *in-situ/ex-situ* or contact/non-contact sensors to relate measurable quantities to final material properties. For example, online XRD mineral phase analyzers⁶⁶ are a new technique for characterising the green-body and powder inputs that are vital to improve the

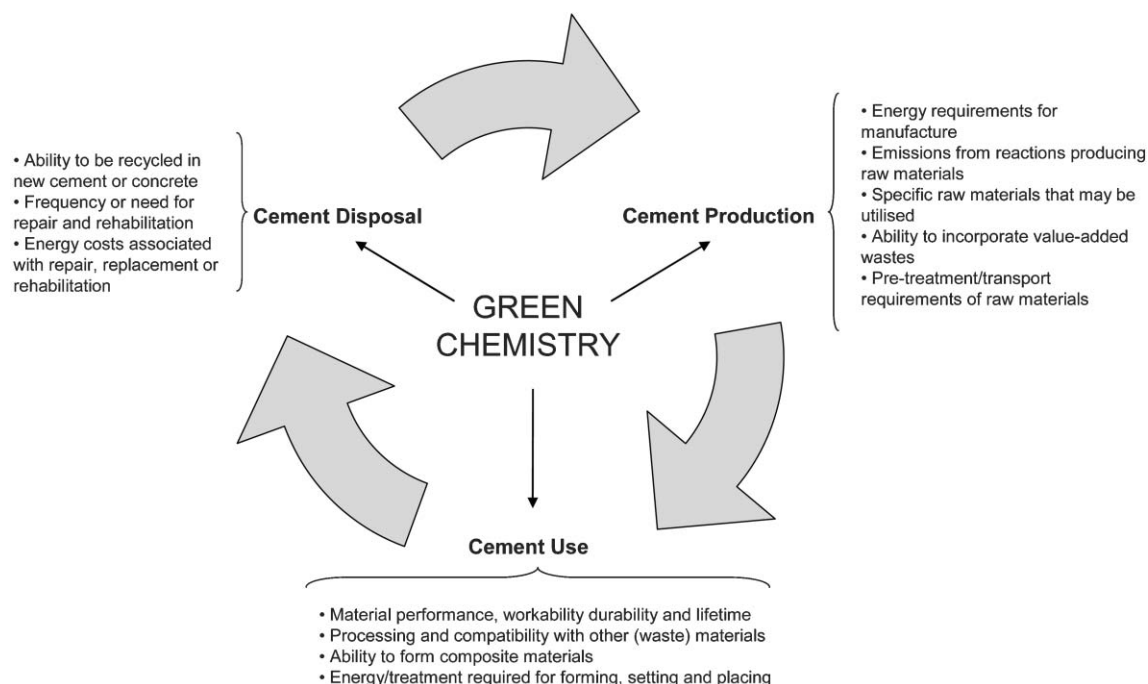


Fig. 11 The inter-relationship of green chemistry with the life cycle of cement.

automation of feedback control typically observed in the processing of highly heterogeneous waste materials.

More precise characterisation of the microstructure cements, utilising powerful techniques such as small angle neutron scattering (SANS),^{67–70} quasi-elastic neutron scattering (QENS),⁷¹ positron annihilation spectroscopy (PALS), nuclear resonance reaction analysis^{72,73} and nuclear magnetic resonance (NMR) spectroscopy,^{74–76} are critical for providing new insights into cement structure at the atomic and nano scales, and developing cement design through green chemistry. Other techniques such as Brillouin scattering⁷⁷, scanning acoustic microscopy (SAM)⁷⁸ and impedance measurements^{79–81} have also been found useful for characterising the bulk material properties of cement phases as a function of their microstructure, however, their utilisation so far has only scratched the surface of their potential.

While significant advances in the modelling of OPC material microstructure have been achieved, such as digital image-based models,^{82–85} their application to green chemistry for alternative cement design has been limited to date. The development of computer models to depict various properties of the cement microstructure over various length scales as it evolves, including the effects of additives, particle size, particle composition *etc.*, will play a critical role in the processing and design of alternative cements in the future. In addition, models which specifically characterise the transport,⁸⁶ mechanical^{87–89} or deformation⁹⁰ properties of cement and concrete under environmental conditions are very useful for determining the bulk performance properties but, to date, have seen little application for cements other than Portland cement.

Green chemistry also plays an important role in facilitating the industrial symbiosis of cement plants through co-operation and joint ventures with other major industrial branches such as steel, coal and energy generation. Such industries can supply waste as feedstock for cement or concrete production in addition to all known chemical, physical and compositional information of the material so that mix consistency can be achieved. This will go along way to reducing the problems associated with unknown variables in the processing of waste feedstock and ensure efficient quality control of the final concrete product.

Ultimately, if alternative cements designed utilising green chemistry are to be accepted by the market, greater confidence in the materials has to be achieved. This may be achieved through better monitoring of in-service performance through remote, real-time, long-term instrumentation that allows complete monitoring and feedback. In addition, the provision of licenses for prospective users to test the materials and the establishment of national and international specifications and standards governing the production, composition and utilisation of the materials, would be of considerable assistance. Less emphasis should be placed on building codes with prescriptive compositional based criteria. This will allow users to define the best material they can manufacture out of the resources they have available to them as opposed to only relying on restricted compositions to manufacture a material. As the amount of technical data describing the performance, durability and industrial ecology of alternative cements increases, their attractiveness and utilisation will grow.

5. Examples of alternative cements

5.1 Alkali-activated cements

Alkali-activated cements comprise a large family of cements characterised by a significant content of aluminosilicate bonding phase. Alkali activation is the process whereby cement particles are initiated to react after the addition of alkali in the early mixing stages. This essentially ‘activates’ the release of certain chemical constituents that form the new binding phase, as well as preparing the particle surface for bonding. Nominally, this is mainly aluminium but also includes alkali metals, Fe and Si. First reports of alkali-activated cements stem back to Glukhosvky in the 1940’s.⁹¹ Numerous types of alkali-activated cements exist today under a variety of names, but the basic principle still applies. Krivenko classified the various types of alkali-activated cements based on slight compositional differences, such as:⁹² geocements, alkali-activated slag,⁹³ fly ash,⁹⁴ Portland and aluminate cements.

Of these various forms, Geopolymer[®],^{95,96} a type of geocement with a supposed greater network of inorganic polymers, has attracted considerable commercial attention. It has already been commercially exploited as ‘Pyrament’ in the USA⁹⁷ and as ‘F’ cement in Finland. However, an inability to maintain a consistent mix limited the success of the Pyrament despite its high promise.⁹⁸ While Geopolymer was initially used to describe a mineral inorganic polymer in the form of a mouldable resin or hard and strong ceramic upon curing at high temperature,^{99,100} the chemical composition and structure in cements has been so diverse that no well recognized scientific meaning has been established. Firstly, Geopolymer is not a polymer, as a chemist would understand such a molecular entity to be. The use of the word in pure chemical terms is best left to geochemists to categorize geologically derived organic resins,¹⁰¹ amorphous organic matter,¹⁰² macromolecules¹⁰³ or asphaltens¹⁰⁴ as geopolymers. Second, the 3-dimensional Al–Si network is not infinite and homogeneously space filling, as one would expect for a glass or polymeric monolithic solid. Even for hydrothermally cured Geopolymer, there is ample evidence to suggest that full dissolution of metakaolin (calcined kaolin) does not occur.¹⁰⁵ As a consequence, “geopolymers” is an umbrella term that describes a wide variety of composite materials with limited restrictions on their composition and Al–Si content.¹⁰⁶

It is probably a slight oversimplification to consider geopolymers as mere pozzolanic cements,²⁹ since the possibility of strength development, through low hydrate formation, lower porosity and using aluminosilicates as the dominate bonding phase, are sufficient reasons to distinguish it from other pozzolanic reactions. Notwithstanding the significant problems in nomenclature, alkali-activated cements enjoy the potential of enormous environmental benefit since a host of waste¹⁰⁷ and virgin¹⁰⁶ materials can be used as significant feedstock including fly ashes, slags, alkaline sludges (*e.g.* red mud)¹⁰⁸ and other materials which are not necessarily pozzolanic.¹⁰⁹ In essence, the alkali silicate acts as glue that binds particulates together to form a hardened dispersion or chemically bonded ceramic. The setting process in geopolymers is much faster than observed for OPC, and the initial

generation of strength does not rely on the same mechanism of hydration as for OPC. While hydration mechanisms do yield greater strengths in the materials with time, these occur over different time-scales than for OPC. A significant drawback of geopolymers is the need for curing at elevated temperatures (>30 °C) if appreciable strength development is to be attained.

Increasing the curing temperature may also reduce the extent of amorphous order within the glue. Thus, geopolymeric cements can vary from the ordinary mix of Davidovits, based on metakaolin or kaolin utilising high concentrations of silicates or aluminates as vital components.^{110,111} Aside from their application as a high performance cement, geopolymers hold a range of niche applications such as racing car parts, waste immobilisation,^{112–114} thermal,¹¹⁵ roof tiles, tooling materials and decorated ceramics, but their cost remains a major drawback for application as a commodity material.⁹⁶ In addition, the lack of international standards, processing know-how, field data and generally under-developed characterisation techniques, are holding the growth of alkali-activated cements back.

The greatest advantage of alkali-activated cements is the aluminosilicate binding phase, which is extremely durable in an aggressive environment and mechanically strong. In fact, ancient concretes owe their resilience to the presence of alkaline aluminosilicate hydrates (*e.g.* calcite, analcimes and zeolites) of both crystalline and amorphous forms.¹¹⁶ Table 9 provides a comparison of the relative solubilities of the typical phases found in an alkali-activated cement compared to those found in OPC, with the phases found in alkali-activated cements generally more insoluble. Geopolymeric cements reported with lower porosity than Portland cements result in a microstructure that is more heat resistant, fire resistant and has superior thermal expansion, cracking and swelling properties compared to Portland cement.^{99,117} Specific mechanical properties that are advantageous for geopolymers to be used as a cement include the fact that they exhibit a hard (4–7 on the Mohs Scale) and smooth surface and can be moulded or extruded to a high degree of precision.

Numerous technical improvements and innovations must still be made to improve the market acceptability and

utilisation of alkali-activated cements. For instance, the process of alkali activation is highly sensitive to the mineralogy of the mineral source being activated. Low-calcium fly ash, a material commonly used for alkali activation, should be assessed for reactivity before being used to determine the amount of alkali required *etc.* and produce a final product with consistent properties. New tests are being developed to assess the reactivity to alkali, such as the Chatterjee test,^{31,118} as well as assessing the mechanism of alkali activation of fly ash by using an EDTA/TEA/NaOH mixture. Existence of such tests is vital to ensure and develop quality controls within the manufacturing process. When utilising waste or secondary materials in cement manufacture, maintaining a material source with consistent and controllable chemical and physical properties is a major obstacle to the manufacture of cement with consistent properties. For alkali-activated cements, this challenge is slightly greater given the fact that it is not readily apparent how a material will react in the presence of alkali given basic mineralogical information. Sometimes, the presence of organics or other impurities may interfere with the process, so it is necessary to develop useful test procedures prior to the synthesis of the final cement.

Critics of alkali-activated cements contend that the presence of excess alkali in these systems generally bring about an increase in the susceptibility of these materials to alkali aggregate reactions. However, research has demonstrated that the presence of excess alkali does not greatly enhance the occurrence of alkali aggregate reactions and, in fact, it has been demonstrated to mitigate the phenomenon.^{119–121} Furthermore, the requirement of larger amounts of alkali activator may also result in large energy consumptions or CO₂ generation effectively reducing the environmental advantages associated with alkali-activated cements. Utilisation of activated cements, such as fly ash-based geopolymers which require high alkaline content for activation (*e.g.* strong base, solution [OH⁻] > 0.1 M), has considerable complications during their manufacture and may result in potential harmful alkali runoff or efflorescence in the final product unless the excess alkali is tied up by a chemical or physical mechanism. Considerable opportunity exists to develop alkali-sequestering

Table 9 Comparative solubility data for phases within alkali-activated slag cements and Portland cements⁹²

Cement Type	Mineral Phase	Stoichiometric Formula	Solubility/kg m ⁻³	
Alkali-activated Cement	CSH(B)	5CaO SiO ₂ nH ₂ O	0.05	
	Xonotlite	6CaO 6SiO ₂ nH ₂ O	0.035	
	Riversideite	5CaO 6SiO ₂ 3H ₂ O	0.05	
	Plombierite	5CaO 6SiO ₂ 10.5H ₂ O	0.05	
	Gyrolite	2CaO 3SiO ₂ 2.5 H ₂ O	0.051	
	Calcite	CaCO ₃	0.014	
	Hydrogarnet	3 CaO Al ₂ O ₃ 1.5SiO ₃ 3H ₂ O	0.02	
	Na–Ca hydrosilicate	(Na, Ca) SiO ₄ nH ₂ O	0.05	
	Thomsonite	(Na, Ca) SiO ₄ Al ₂ O ₃ 6H ₂ O	0.05	
	Hydronepheline	Na ₂ O Al ₂ O ₃ 2SiO ₂ 2H ₂ O	0.02	
	Natrolite	Na ₂ O Al ₂ O ₃ 3SiO ₂ 2H ₂ O	0.02	
	Analcime	Na ₂ O Al ₂ O ₃ 3SiO ₂ 2H ₂ O	0.02	
	Portland Cement	Calcium Hydroxide	Ca(OH) ₂	1.3
		C ₂ SH ₂	2CaO SiO ₂ nH ₂ O	1.4
		CSH(B)	5CaO SiO ₂ nH ₂ O	0.05
Tetracalcium hydroaluminate		4CaO Al ₂ O ₃ 13H ₂ O	1.08	
Tricalcium hydroaluminate		3CaO Al ₂ O ₃ 6H ₂ O	0.56	
Hydrosulfoaluminate		3CaO Al ₂ O ₃ 3CaSO ₄ 31H ₂ O	high	

additives for improving the durability of a mix, with limited results to date.^{122,123} Alternatively, alkali-activated cements utilising less corrosive activators, such as Na_2CO_3 , $\text{Ca}(\text{OH})_2$ or $\text{SiO}_2:\text{Na}_2\text{O}$, with high moduli *etc.*, are growing in popularity. While the activation potential of these salts is somewhat reduced, the possibility of combining mechanical activation in the initial processing stage may be able to achieve comparable results to activation based on highly alkaline activators. Furthermore, while the main strength forming reactions that result in the hardening of OPC over extended periods of time have been well documented, considerably more work is required to detail the effect of the heat of solution and longer setting times on strength development within alkali-activated cements.

5.2 Magnesia cements

Magnesia cements are a range of cements based on magnesium oxide (MgO) as the key reactive ingredient. The first type of magnesia cement was developed by Frenchman Stanislas Sorel in 1867 and is now referred to as Sorel, magnesite or magnesium oxychloride cement.¹²⁴ Sorel cement was produced initially by the combination of magnesium oxide with concentrated aqueous magnesium chloride. This results in a hardened cement paste consisting of four main bonding phases: $2\text{Mg}(\text{OH})_2 \cdot \text{MgCl}_2 \cdot 4\text{H}_2\text{O}$, $3\text{Mg}(\text{OH})_2 \cdot \text{MgCl}_2 \cdot 8\text{H}_2\text{O}$, $5\text{Mg}(\text{OH})_2 \cdot \text{MgCl}_2 \cdot 5\text{H}_2\text{O}$ and $9\text{Mg}(\text{OH})_2 \cdot \text{MgCl}_2 \cdot \text{H}_2\text{O}$.¹²⁵ It was soon discovered, however, that the magnesium oxychloride phases are not stable after prolonged exposure to water, and will leach out in the form of magnesium chloride or magnesium hydroxide. As a consequence, Sorel cement has found limited application in the building and construction industry despite demonstrating other properties that are far superior to those of Portland cement. For instance, it has high fire resistance, low thermal conductivity, high abrasion resistance, high transverse and crushing strengths and does not require wet curing.¹²⁵ Various additives are being investigated to improve its water resistance although no spectacular discovery in this area has been made yet.

With time, a variety of other magnesia cements have been developed based on permutations of magnesium oxide as the binding phase with varying levels of success. Magnesium oxysulfate cements, formed by the reaction of a magnesium sulfate solution with magnesium oxide, have similar properties to magnesium oxychloride cements.¹²⁶ Again, they have good binding properties and combine well with a variety of inorganic and organic aggregates such as sand, marble flour, gravel, saw dust and wood flour to produce a cement with high early strength. Poor weathering resistance, however, is again the main drawback for this type of cement.

Another analogue is magnesia phosphate cements, which can be synthesised by reacting magnesium oxide with a soluble phosphate (*e.g.* ammonium phosphate).^{127,128} In essence, this is an acid–base reaction between the phosphate acid and the magnesium oxide to form an initial gel that crystallises into an insoluble phosphate, mostly in the form of magnesium ammonium phosphate hexahydrate ($\text{NH}_4\text{MgPO}_4 \cdot 6\text{H}_2\text{O}$).¹²⁹ Magnesia phosphate cements are characterised by very high early strength and rapid setting, which makes them useful as a rapid patching mortar. It can also bind well to a wide variety

of aggregates and substrates. Unlike magnesium oxychloride and oxysulfate cements, this cement has good water and freeze-thaw resistance and is, therefore, amenable to a wide variety of applications.⁶² A major drawback, however, is the expensiveness of phosphate, which confines its application to niche areas.¹³⁰

More promising magnesia cements that have recently attracted considerable interest from industry have been magnesium carbonate or magnesite cements.¹³¹ The bonding phase for these cements includes magnesium hydroxide and magnesium carbonate. In the presence of accelerating additives (such as KNO_3 , $\text{Fe}_2\text{SO}_4 \cdot x\text{H}_2\text{O}$, CaCl_2 *etc.*) magnesium oxide will undergo hydration to form magnesium hydroxide, or brucite, which is considerably less soluble than portlandite ($\text{Ca}(\text{OH})_2$), the calcium analogue.¹²⁴ Brucite can then react in the presence of sufficient carbon dioxide and a calcium source to form magnesite, hydromagnesite and calcium magnesium carbonate or dolomite ($\text{CaMg}(\text{CO}_3)_2$). These carbonates add strength to the binding phase, and in being relatively insoluble and fibrous in structure, have the ability to form a better network nanostructure than observed for calcium carbonates. The presence of the accelerator also serves to increase the setting time making the long-term strength gains comparable to that of Portland cement.¹³¹

Typically, magnesia carbonate cements can be formed when magnesia is in the presence of considerable quantities of waste materials or traditional pozzolans, provided sufficient brucite, carbon dioxide and accelerators are present.¹³¹ Such waste materials include fly ash, slag, silica fume, silica flour, mine tailings, sewerage ash *etc.* The possibility also exists for adding magnesium oxide to ordinary Portland cement, yielding more durable composite cement.^{132,133} This may be achieved by promoting the reaction of portlandite with pozzolans, thereby allowing brucite to replace it and sequester excess alkali. This is an advantageous scenario since brucite is some 100–1000 times less soluble than portlandite. ($\text{Ca}(\text{OH})_2$ $K_{\text{SP}} = 5.5 \times 10^{-6}$, $\text{Mg}(\text{OH})_2$ $K_{\text{SP}} = 1.8 \times 10^{-11}$ at 25 °C).

The main environmental advantage associated with magnesia carbonate cements is that the starting material, magnesia, is readily obtained from the calcining of magnesite. The process of magnesite decomposition occurs at temperatures around 400 °C less than that of limestone so it requires considerably less energy to manufacture. However, according to Table 5, the reaction for formation of magnesia results in the emission of considerable amounts of CO_2 , which slightly offsets the gains achieved in the lower energy requirements for processing magnesia. Nevertheless, the carbonation reaction resulting in the formation of the main bonding phase from magnesia can consume atmospheric CO_2 . This suggests that such cements could in fact act as carbon sinks, acting to favorably reduce greenhouse gas emissions. However, this reaction is slow since it is diffusion controlled, so the useful lifetime of the cement would probably be exceeded before complete carbonation could occur. Theoretically, since magnesium carbonate is the main binding phase, these cements are also readily recyclable. As opposed to Portland cements, which cannot be easily reheated to regenerate the original starting materials (calcium carbonate and clinker, see Fig. 9), the formation of magnesia from the magnesium carbonates should be much easier.

The utilisation of secondary materials such as fly ash and slag is routine in the cement industry but it is the chemistry of the bonding phases that is more important. Significantly, magnesium hydroxide is less alkaline than calcium hydroxide and, therefore, has a considerable reduction in potential problems later on. It has been reported that the addition of the accelerator allows the cement to overcome many of the problems associated with magnesia oxychloride cements.¹³¹ As a result, magnesium carbonate cements exhibit greater resistance to acids and are a less corrosive substrate that is stable in moist environments.

While magnesia carbonate cements are still in the developmental stages, there are a few downsides. For instance, despite the fact that filler materials such as industrial by-products are reasonably cheap and inexpensive to obtain, acquiring magnesium carbonate is generally more expensive than calcium carbonate and harder to find. With increasing demand, however, it is possible that the prices could dramatically drop. The technology, to some civil engineers, may also be regarded as unproven. A range of concerns still surround the material such as the load-bearing performance, long-term dimensional stability, freeze-thaw resistance, creep under load as well as a host of basic characteristics such as heat output during hydration, porosity/permeability relationships and fire resistance. However, magnesia carbonates and OPC/magnesia carbonate composite cements are the most likely large-scale magnesia cement alternatives to Portland cement.

5.3 Sulfoaluminate cements

Sulfoaluminate or ettringite cements are a type of high alumina cement that first came to prominence in the 1970s. To form calcium sulfoaluminate clinker, limestone, bauxite and gypsum are mixed and heat fired in rotary calcining kiln. Commercial sulfoaluminate clinkers developed by the Chinese predominantly consist of $C_4A_3\bar{S}$ (55–75%) (also known as Klein's compound) and α - C_2S (15–25%). The remaining phases present are $C_{12}A_7$, C_4AF and CaO , but $C_2A\bar{S}$ and $C\bar{S}$ are considered deleterious and, therefore, undesirable. Belite (C_2S)-rich sulfoaluminate cements are preferred to alite (C_3S)-rich, since belite-based cements can be formed at around 1200 °C, as opposed to 1400 °C for the alite cements. This equates to an energy savings of ~20% during manufacture¹³⁴ and, according to Table 5, results in less CO_2 being generated from the reaction of formation of C_2S compared to C_3S . Belite-based sulfoaluminate cements are also preferred for certain performance reasons, since cements containing larger quantities of C_2S than C_3S are less permeable as well as being more resistant to chemical attacks and smaller drying shrinkage. On the other hand, large proportions of C_2S do reduce the rate of strength evolution and setting point but the presence of calcium sulfate and calcium sulfoaluminate more than compensate for this deficiency.

Sulfoaluminate cements may be defined by the compositional system of $CaO-Al_2O_3-SiO_2-Fe_2O_3-SO_3$. Strength and material performance rely heavily on the specific composition and phases present. The bonding phases within sulfoaluminate cements consist predominantly of ettringite, monocalcium sulfo-aluminate hydrate, ferrite and alumina gel. Calcium

aluminates such as C_3AH_6 and C_4AH_{13} have been observed in some instances. To date, studies on the durability of these cements have been promising.¹³⁵

Typically, sulfoaluminate cements are used where rapid setting, early strength or shrinkage compensation is required. They also have the advantage that their long-term strength and durability can exceed that of Portland cement. These cements have seen widespread and high volume use as bridge decks, airport runways, patching roadways *etc.* where rapid setting is required. Approximately 81,000 tonnes were produced in 1996 in the US alone, but it has been used even more in Japan and China to construct bridges and buildings. Production now exceeds 10^6 tonnes per year.¹³⁶ However, rapid setting and expansive cements are inappropriate for certain building engineering applications. Since the hydration of belite-sulfoaluminate cements at ambient temperatures leads to the formation of ettringite as the major phase, the cements may be susceptible to degradative problems associated with carbonation,¹³⁷ delayed ettringite formation as well as thaumasite attack.¹³⁸ So if the setting time is to be properly regulated, special activators must be added to reduce the setting rate.¹³⁹ Further research is ongoing in this area to widen the potential use of sulfoaluminate cements. Supersulfated slag cement is an example of a cement that has used ettringite in combination with CSH as the main binding phase to a relative degree of success.¹⁴⁰ Supersulfated slag cements consist mostly of granulated blast-furnace slag, gypsum or anhydrite with a small amount of lime or Portland cement to catalyse the chemical reaction. Although, they exhibit slow strength development and may undergo deleterious carbonation reactions, they still have significant application potential.²⁹

Significant environmental advantages exist in using sulfoaluminate cements. According to Table 5, the calcium sulfoaluminate clinker ($C_4A_3\bar{S}$) generates the least amount of CO_2 per g of raw material as by-product of its reaction of formation. This makes it extremely attractive. Furthermore, the calcining of the raw materials for clinker formation occurs at temperatures (1160–1200 °C) much lower than those used for firing Portland cement clinker (1450 °C). Another environmental advantage of the manufacturing process of belite-rich sulfoaluminate clinkers is that it can utilise industrial by-products with high sulfate content. For example, fluidised bed combustor (FBC) fly ash,¹⁴¹ blast furnace slag, low-calcium fly ash¹⁴² or flue gas desulfurisation (FGD) sludge can be utilised to manufacture belite-rich sulfoaluminate clinkers, whereas they could not be used in the manufacture of Portland cement clinker, which limits the SO_3 content to 3.5% dry weight. Energy savings also occur in the grinding of the clinker compared to Portland cement, since the low firing temperatures result in a clinker, which is generally softer. Another advantage of calcium sulfoaluminate cements is that it can use gypsum to form hydration products which have not undergone any heat treatment in a kiln. This results in a considerable energy saving.

Utilisation of sulfoaluminate cements in both China and Japan is now becoming so widespread that they may almost be referred to as a commodity material, particularly in China. In Europe and North America, its utilisation has largely been

Table 10 Chemical oxide content of the different cement types

Cement type	CaO/%	Al ₂ O ₃ %	SiO ₂ %	Ca(OH) ₂ in hydrated cement	Significant additional component
Portland	62–66	4–6	20–22	high	—
Blended OPC	42–61	5–10	21–30	medium	—
Sulfoaluminate	35–45	25–40	3–12	low	sulfate
Alkali-activated	10–42	10–20	30–60	low	alkalis

restricted to high early strength, self-stressing or shrinkage applications. Sulfoaluminate cements could potentially become a major large-scale alternative to Portland cement, however their classification has largely been restricted to certain geographic regions with different climatic and economic conditions. As for alkali-activated cements, a significant disadvantage of sulfoaluminate cements has been the confusing nomenclature and lack of international consensus as to standards and names.

5.4 Blended OPC-based cements

Blended Portland cements or pozzolanic cements refer to hydraulic cement that consists of a homogeneous mixture of a Portland cement and replacement material.^{143,144} Blended cements are generally produced by grinding the replacement material in the presence of Portland cement clinker, by blending the replacement material and Portland cement during mix proportioning or by a combination of both.¹¹ In essence, blended cements maintain a similar CSH bonding phase to plain Portland cement. Replacement pozzolan material can be either naturally derived or waste material (silica- or aluminosilicate-rich) that reacts with calcium hydroxide to form calcium silicate hydrate.¹⁴⁵ Popular pozzolans used today include reactive silicates and aluminosilicates, such as fly ash, slag, silica fume and metakaolin of either a crystalline or amorphous structure. The *pozzolanic* reactions may be summarised as follows:¹⁴⁶



The specific composition of the final product of these reactions is highly dependent on the nature of the pozzolans,

reaction conditions and other contaminants present, and may result in the formation of mixed phases. Generally, however, CSH is the main bonding phase along with smaller amounts of CH, ettringite, aluminosulfate and iron hydrate phases. Lime is required to initiate the reaction, which may come directly from a lime source or Portland cement clinker. The advantages of utilising blended concrete is that there is a lower heat of hydration, improvement in the workability of the fresh paste and the ability of the replacement material to chemically combine with the lime and alkalis liberated from the Portland cement during the hardening period.¹⁴⁷ As a result, blended concretes may often be more resistant to chemical effects associated with the alkali-aggregate reaction.¹⁴⁸ However, compared to other types of cements, blended OPC cements still retain a significantly high CaO oxide content (present as Ca(OH)₂, see Table 10), which may restrict its application in certain aggressive environments. Furthermore, a blended concrete may be weaker at early ages, although the ultimate strength is not reduced.¹⁴⁹

It has been emphasised that the pozzolanic reaction can be extended to involve not just silica, but also iron oxide and alumina reacting with lime.¹⁴⁵ Pozzolanic reactions can be monitored by the consumption of calcium hydroxide, and may be enhanced by the presence of alkali, which promotes the dissolution of many amorphous highly insoluble aluminosilicate pozzolans.^{150,151} Portland cement can be successfully replaced with pozzolans today, for example in ASTM blended cement types I–V (ASTM C595–98 and AASHTO M240–94) or using ASTM C 1157–98(a). In most instances specifying up to 70% pozzolan in the cement is the limit, but there have been few instances of 100% replacement with pozzolan. See Table 11 for a comparison of U.S. and European standard specifications for blended and composite cements.

Table 11 U.S. and European standard specifications for blended and composite cements⁵²

Standard	Name	Portland cement content	Blended minerals
ASTM C595	Portland blast furnace slag	30–75%	Granulated blast furnace slag
	Slag-modified Portland cement	>75%	Granulated blast furnace slag
	Portland pozzolan cement	60–85%	Pozzolan
	Pozzolan modified Portland cement	<30%	Pozzolan
EN 197	Slag cement	<30%	Granulated blast furnace slag
	CEM I Portland cement	95–100%	Minor additional constituents
	CEM II ^a	65–94%	Blast furnace slag, silica fume, pozzolans (natural or calcined), fly ash, burnt shale, limestone
	CEM III ^b blast furnace cement	5–64	Blast furnace slag
	CEM IV ^c pozzolanic cement	45–89	Silica fume, pozzolans, fly ash
	CEM V ^d composite cement	20–64	Blast furnace slag, pozzolans, fly ash

^a Includes subclassification depending on type of blended mineral. ^b Includes subclassification depending on content of slag: 36–65, 66–80, 81–95%. ^c Includes subclassification depending on content of pozzolans (silica fume + pozzolans + fly ash): 11–35, 36–55%. ^d Includes subclassification depending on content of blended minerals (blast furnace slag + pozzolans + fly ash): 36–60, 62–80%.

Pozzolanic replacement of cement is advantageous since it reduces the amount of alkalis and therefore the permeability of the material.¹⁵² As a consequence of reducing the amount of CH in hydrated cement paste, the cement product is less permeable and therefore less susceptible to the various forms of sulfate attack. Disadvantages of pozzolanic replacement include the fact that their use is also restricted by the poor, or lack of, reaction with clay and dust particles, long maturation times, requirement of both coarse and fine aggregates for good bonding and minimum curing temperatures.¹¹

An example of new blended cements that have been competitive in the cement market include Cemstar[®], as developed by Texas Industries, Inc. (TXS). In the manufacturing of Cemstar, up to 33% of cement clinker is replaced with steel slag, which considerably reduces the energy costs associated with firing the clinker. High strength cement named Vicon, which is produced by adding a siliceous admixture during grinding, is another example of a new cement with low clinker content.¹⁵² Taiheyo Cement Corporation in Japan is another company that is successfully manufacturing environmentally benign cements—referred to as Eco-cements. Instead of just incorporating traditional Pozzolans into cement, Taiheyo is going the next step by utilising a wide variety of industrial and municipal waste sources after incineration, then treating the ash so it may be used as a pozzolan.¹⁵³

Slag cements, in particular, are highly attractive compared to Portland cement due to their higher long term strength, greater resistance to seawater corrosion, better density than OPC, lower heat of hydration than OPC (less cracking), higher resistance to chloride diffusion and sulfate attack. In addition, slag improves the workability of fresh cement, suppresses ASR, reduces efflorescence and lowers porosity and diffusion. Production of one tonne of ground granulated blast furnace slag (GGBFS) emits 70 kg of CO₂ as opposed to the 970 kg produced during the manufacture of OPC.¹⁵⁴

6. Conclusion

This review article has examined the relationship between green chemistry and sustainable cement production and use. It has highlighted energy requirements, greenhouse gas emissions and durability considerations as major drivers for improving the chemistry of cement in the 21st century. Various concepts and ideas of industrial ecology central to the research, development and application of sustainable cement on the global scale have been discussed. Three alternative cements were investigated, and their relative position to Portland cement compared.

Further developments and new techniques must continue to be introduced into the cement and concrete industry. Green chemistry will play a significant role in facilitating a holistic industrial ecological approach to cement from a fundamental level. This will provide distinct alternatives to an OPC dominated cement market. In the short-term, advanced experimental methods and fundamental science are required to develop the necessary understanding of alternative binders before sufficient know-how develops for wide-scale application. Ultimately, alternative cements should provide a relatively simple and straightforward solution for replacing

OPC and must be cost-competitive for large-volume use. But it is only through additional investigation and characterisation of novel binders, with the help of advanced techniques and methods, that the full potential of novel cements can be realised.

Growth in the codes, standards, guidelines, training and certification programs will play a significant role in the development and acceptance of alternative cements. An emphasis-shift to long-term cost-benefit analyses and performance-based criteria for designing concrete will result in the selection of a cement for a particular application and promote the selection and familiarity of alternative binders. Ultimately, the realisation of the potential of alternative cements will depend upon on strategic planning and vision from industry leaders, government and academia alike. Organisations such as the World Business Council for Sustainable Development (WBCSD) have already provided good leadership, but more is required. Alternative cements offer vastly more potential for reducing the energy wastage and greenhouse gases associated with the production of cement, and can greatly improve durability. Promoting green chemistry within the cement industry will attract more interest to cement alternatives based on different binding chemistry and new processing technology, as this offers the greatest avenue for addressing the environmental challenges of cement into the future.

References

- 1 J. Gebauer, in *Calcium Hydroxide in Concrete*, ed. J. Skalny, J. Gebauer, I. Odler, The American Ceramic Society, Westerville, OH, USA, 2001, special volume, pp. 1–10.
- 2 P.-C. Aitcin, *Cem. Concr. Res.*, 2000, **30**, 1349.
- 3 A. M. Neville, *Concr. Int.*, 1997, **19**, 52.
- 4 V. Penttala, *ACI Mater. J.*, 1997, Sept–Oct, 409.
- 5 G. Matos and L. Wagner, *Annu. Rev. Energy Environ.*, 1998, **23**, 107.
- 6 Batelle, *Toward a sustainable cement industry. Battelle study for the world business council for sustainable development.*, Batelle, Columbus, OH, USA, 2002.
- 7 R. K. Mehta and R. W. Burrows, *Concr. Int.*, 2001, 57–63.
- 8 J. S. Damtoft, D. Herfort and E. Yde, *Concrete binders, mineral additions and chemical admixtures: State of the art and challenges for the 21st Century*, International Conference held at the University of Dundee, 2006.
- 9 S. P. Shah, *Schweiz. Arch.*, 1971, **37**, 405.
- 10 B. F. Johannesson, *Adv. Cem. Based Mater.*, 1997, **6**, 71.
- 11 A. M. Neville, in *Properties of concrete*, Longmann, Harlow, UK, 4th edn, 1995, pp. 844.
- 12 I. Klur, J.-F. Jacquinet, F. Brunet, T. Charpentier, J. Virlet, C. Schneider and P. Tekely, *J. Phys. Chem. B*, 2000, **104**, 10162.
- 13 K. Kuhlmann and H. Paschmann, *ZKG Int.*, 1997, **50**, 1.
- 14 D. T. Allen and R. S. Butner, *Chem. Eng. Prog.*, 2002, **98**, 40.
- 15 T. E. Graedel and B. R. Allenby, in *Industrial Ecology*, Prentice Hall, Englewood Cliffs, NJ, USA, 1995.
- 16 P. T. Anastas and J. J. Breen, *J. Clean. Prod.*, 1997, **4**, 97.
- 17 B. R. Allenby, *Int. Environ. Affair.*, 1992, **4**, 56.
- 18 M. Nehdi, R. Rehan and S. P. Simonovic, *ACI Mater. J.*, 2004, **101**, 216.
- 19 J. K. Stolaroff, G. V. Lowry and D. W. Keith, *Energ. Convers. Manage.*, 2005, **46**, 687.
- 20 S. L. Huang and W. L. Hsu, *Landscape Urban Plan.*, 2003, **63**, 61.
- 21 M. T. Brown and V. Buranakarn, *Resour. Conserv. Recycl.*, 2003, **38**, 1.
- 22 J. R. Mihelcic, J. C. Crittenden, M. J. Small, D. R. Shonnard, D. R. Hokanson, Q. Zhang, H. Chen, S. A. Sorby, V. U. James, J. W. Sutherland and J. L. Schnoor, *Environ. Sci. Technol.*, 2003, **37**, 5314.

- 23 R. Clift, A. Doig and G. Finnveden, *Process Saf. Environ. Prot.*, 2000, **78**, 279.
- 24 K. Gabel, P. Forsberg and A.-M. Tillman, *J. Clean. Prod.*, 2004, **12**, 77.
- 25 D. Rosignoli, G. Martinola and M. Bauml, *Environmental Ecology and Technology of Concrete*, 2006, **302–303**, 35.
- 26 P. C. Kreijger, *Mater. Struct.*, 1987, **20**, 248.
- 27 K. Krass, *Betonwerk+Fertigteil-Tech.*, 1994, **1**, 103.
- 28 G. Wischers, *Betonwerk+Fertigteil-Tech.*, 1992, **4**, 50.
- 29 E. Gartner, *Cem. Concr. Res.*, 2004, **34**, 1489.
- 30 S. Teramura, N. Isu and K. Inagaki, *J. Mater. Civ. Eng.*, 2000, **12**, 288.
- 31 M. R. Chertow, *Annu. Rev. Energy Environ.*, 2000, **25**, 313.
- 32 J. Ehrenfeld and N. Gertler, *J. Ind. Ecol.*, 1997, **1**, 67.
- 33 H. G. van Oss and A. C. Padovani, *J. Ind. Ecol.*, 2002, **6**, 89.
- 34 E. Worrell, N. Martin and L. Price, *Energy*, 2000, **25**, 1189.
- 35 J. P. Degré, *Proceedings of the 34th International Cement Seminar*, Salt Lake City Utah, 1998, 125.
- 36 B. G. Jenkins and S. B. Mather, in *Cement Environmental Yearbook 1997*, Tradeship Publications, Dorking, UK, 1997, pp. 90–97.
- 37 A. Gilling, *Int. Cement Rev.*, 1999, July, 56.
- 38 A. Mishulovich, *Int. Cement Rev.*, 2003, January, 59.
- 39 H. G. van Oss and A. C. Padovani, *J. Ind. Ecol.*, 2003, **7**, 93.
- 40 T. E. Graedel and R. J. Klee, *Environ. Sci. Technol.*, 2002, **36**, 523.
- 41 J. P. Dewulf and H. R. Van Langenhove, *Environ. Sci. Technol.*, 2002, **36**, 1130.
- 42 H. I. Inyang, *J. Environ. Eng.*, 1999, **125**, 1091.
- 43 B. E. Scheetz, D. M. Roy and M. W. Grutzeck, *Mater. Res. Innovations*, 1999, **3**, 55.
- 44 S. Chandra, in *Waste materials used in concrete manufacturing*, Noyes, Westwood, NJ, USA, 1997, pp. 651.
- 45 H. D. Sharma and S. P. Lewis, in *Waste Containment Systems, waste stabilization, and landfills. Design and Evaluation*, Wiley-Interscience, New York, USA, 1st edn, 1994, pp. 590.
- 46 J. R. Conner, in *Chemical Fixation and Solidification of Hazardous Wastes*, Van Nostrand, Reinhold, 1990, pp. 692.
- 47 J. L. Means, L. A. Smith, K. W. Nehring, S. E. Brauning, A. R. Gavaskar, B. M. Sass, C. C. Wiles and C. I. Mashni, in *The application of Solidification/Stabilization to waste materials*, CRC Press, Inc., Boca Raton, 1st edn, 1995, pp. 334.
- 48 M. Arias, T. Barral and F. Diaz-Fierros, *Clays Clay Miner.*, 1995, **43**, 406.
- 49 G. P. J. Dijkema, M. A. Reuter and E. V. Verhoef, *Waste Manage. (Oxford, UK)*, 2000, **20**, 633.
- 50 J. Grimes, C. Haycocks and M. Karmis, Integrated mining and waste disposal systems, *Pollut. Prev. Process Eng., Proc. Tech. Solutions Pollut. Prev. Min. Miner. Process. Ind., Eng. Found. Conf.*, 1996, 249.
- 51 H. Uchikawa, *J. Mater. Civ. Eng.*, 2000, **12**, 320.
- 52 A. Bentur, *J. Mater. Civ. Eng.*, 2002, **14**, 2.
- 53 K. Ishikawa, H. Kitajo, H. Ino, K. Nakajima and K. Halada, *J. Jpn. Inst. Met.*, 2003, **67**, 428.
- 54 N. Takeda, *Haikibutsu Gakkaiishi*, 1999, **10**, 306.
- 55 M. S. Finstein, *Soil Sci.*, 1996, **161**, 343.
- 56 V. Camobreco, R. Ham, M. Barlaz, E. Repa, M. Felker, C. Rousseau and J. Rathle, *Waste Manage. Res.*, 1999, **17**, 394.
- 57 R. A. Bloomfield, *J. Test. Eval.*, 1984, **12**, 119.
- 58 A. Fernandez-Jimenez, J. G. Palamo and F. Puertas, *Cem. Concr. Res.*, 1999, **29**, 1313.
- 59 R. N. Swamy, *Proc. Inst. Civ. Eng. – Structures and Buildings*, 2001, **146**, 371.
- 60 B. Allenby, *IEEE Technol. Soc. Mag.*, 2000, Winter 2000/2001, 10.
- 61 D. M. Roy, *Science*, 1987, **235**, 651.
- 62 D. Singh, A. S. Wagh, J. C. Cunnane and J. L. Mayberry, *J. Environ. Sci. Health, Part A*, 1997, **32**, 527.
- 63 J. S. Popovics, *J. Mater. Civ. Eng.*, 2003, **15**, 211.
- 64 J. S. Popovics, *Mater. Eval.*, 2005, **63**, 50.
- 65 M. Scott, J. C. Duke, N. Davidson, G. Washer and R. Weyers, *Mater. Eval.*, 2000, **58**, 1305.
- 66 N. V. Y. Scarlett, I. C. Madsen, C. Manias and D. Retallack, *Powder Diffraction*, 2001, **16**, 71.
- 67 A. J. Allen and R. A. Livingston, *Adv. Cem. Based Mater.*, 1998, **8**, 118.
- 68 R. A. Livingston, D. A. Neumann, A. J. Allen and J. J. Rush, *Mater. Res. Soc. Symp. Proc.*, 1995, **376**, 459.
- 69 J. W. Phair, J. C. Schulz, W. Bertram and L. P. Aldridge, *Cem. Concr. Res.*, 2003, **33**, 1811.
- 70 J. W. Phair, J. C. Schulz, L. P. Aldridge and J. D. Smith, *J. Am. Ceram. Soc.*, 2004, **87**, 129.
- 71 J. W. Phair, R. A. Livingston, C. M. Brown and A. J. Benesi, *Chem. Mater.*, 2004, **16**, 5042.
- 72 J. S. Schweitzer, R. A. Livingston, C. Rolfs, H. W. Becker, S. Kubsy, T. Spillane, M. Castellote and P. G. de Viedma, *Nucl. Instrum. Methods Phys. Res., Sect. B*, 2005, **241**, 441.
- 73 J. S. Schweitzer, R. A. Livingston, C. Rolfs, H. W. Becker and S. Kubsy, *Nucl. Instrum. Methods Phys. Res., Sect. B*, 2003, **207**, 80.
- 74 A. J. Benesi, M. W. Grutzeck, B. O'Hare and J. W. Phair, *J. Phys. Chem. B*, 2004, **108**, 17783.
- 75 J. Skibsted, E. Henderson and H. J. Jakobsen, *Inorg. Chem.*, 1993, **32**, 1013.
- 76 A. J. Benesi, M. W. Grutzeck, B. O'Hare and J. W. Phair, *Langmuir*, 2005, **21**, 527.
- 77 J. W. Phair, S. N. Tkachev, M. H. Manghnani and R. A. Livingston, *J. Mater. Res.*, 2005, **20**, 344.
- 78 R. A. Livingston, M. Manghnani and M. Prasad, *Cem. Concr. Res.*, 1999, **29**, 287.
- 79 C. Alonso, C. Andrade, M. Keddama, X. R. Novoa and H. Takenouti, *Mater. Sci. Forum*, 1998, **289–2**, 15.
- 80 C. Andrade, V. M. Blanco, A. Collazo, M. Keddama, X. R. Novoa and H. Takenouti, *Electrochim. Acta*, 1999, **44**, 4313.
- 81 M. Keddama, H. Takenouti, X. R. Novoa, C. Andrade and C. Alonso, *Cem. Concr. Res.*, 1997, **27**, 1191.
- 82 D. P. Bentz, *J. Am. Ceram. Soc.*, 1997, **80**, 3.
- 83 D. P. Bentz and P. E. Stutzman, *ASTM Spec. Tech. Publ.*, 1994, **STP 1215**, 60.
- 84 K. van Breugel, *Cem. Concr. Res.*, 2004, **34**, 1661.
- 85 G. Ye, J. Hu, K. van Breugel and P. Stroeven, *Mater. Struct.*, 2002, **35**, 603.
- 86 E. J. Garboczi and D. P. Bentz, *Constr. Build. Mater.*, 1996, **10**, 293.
- 87 G. Constantinides and F. J. Ulm, *Cem. Concr. Res.*, 2004, **34**, 67.
- 88 F. J. Ulm, G. Constantinides and F. H. Heukamp, *Mater. Struct.*, 2004, **37**, 43.
- 89 F. J. Ulm, *Mater. Struct.*, 2003, **36**, 426.
- 90 G. Constantinides, F. Ulm and K. Van Vliet, *Mater. Struct.*, 2003, **36**, 191.
- 91 V. D. Glukhovskiy, G. S. Rostovskaja and G. V. Rumyna, *Communications of the 7th International Congress on the Chemistry of Cement*, 1980, **3**, 164.
- 92 P. Krivenko, *Proceedings of the 10th International Congress on the Chemistry of Cement in Gothenburg, Sweden*, ed. H. Justnes, Amarkai and Congrex Göteborg, Gothenburg, Sweden, 1997, pp. 9–18.
- 93 A. O. Purdon, *J. Soc. Chem. Ind.*, 1940, **59**, 191.
- 94 S. Jahanian and H. Rostami, *Eng. Struct.*, 2001, **23**, 736.
- 95 J. Davidovits, D. C. Comrie, J. H. Paterson and D. J. Ritcey, *Concr. Int.*, 1990, 30.
- 96 J. Davidovits, *Proceedings from the First International Conference on Alkaline Cements and Concretes*, Scientific Research Institute on Binders and Materials, Kiev State Technical University, Kiev, Ukraine, 1994, 131.
- 97 E. M. Gartner and D. F. Myers, *Ceram. Trans.*, 1991, **16**, 621.
- 98 H. G. Wheat, *Cem. Concr. Res.*, **22**, 103.
- 99 J. Davidovits, Mineral polymers and methods of making them, *US Pat. 4 349 386*1982.
- 100 J. Davidovits, *J. Therm. Anal.*, 1991, **37**, 1633.
- 101 H. Knicker, J. C. del Rio, P. G. Hatcher and R. D. Minard, *Org. Geochem.*, 2002, **32**, 397.
- 102 M. A. Kruge, P. Landais, D. F. Bensley, B. A. Stankiewicz, M. Elie and O. Ruau, *Energy Fuels*, 1997, **11**, 503.
- 103 G. D. Cody, R. E. Botto, H. Ade and S. Wirick, *Int. J. Coal Geol.*, 1996, **32**, 69.
- 104 E. A. Razvozhayeva, V. Y. Prokof'ev, A. M. Spiridonov, D. K. Martikhaev and S. I. Prokopchuk, *Geol. Ore Deposit.*, 2002, **44**, 103.
- 105 V. F. F. Barbosa, K. J. D. MacKenzie and C. Thaumaturgo, *Int. J. Inorg. Mater.*, 2000, **2**, 309.

- 106 H. Xu and J. S. J. Van Deventer, *Int. J. Miner. Process.*, 2000, **59**, 247.
- 107 A. Palomo, M. W. Grutzeck and M. T. Blanco, *Cem. Concr. Res.*, 1999, **29**, 1323.
- 108 Z. Pan, L. Cheng, Y. Lu and N. Yang, *Cem. Concr. Res.*, 2002, **32**, 357.
- 109 H. Rostami and W. Brendley, *Environ. Sci. Technol.*, 2003, **37**, 3454.
- 110 J. W. Phair, J. D. Smith and J. S. J. Van Deventer, *Mater. Lett.*, 2003, **57**, 4356.
- 111 J. W. Phair and J. S. J. Van Deventer, *Ind. Eng. Chem. Res.*, 2002, **41**, 4242.
- 112 J. W. Phair and J. S. J. Van Deventer, *Miner. Eng.*, 2001, **14**, 289.
- 113 J. W. Phair, J. S. J. Van Deventer and J. D. Smith, *Appl. Geochem.*, 2004, **19**, 423.
- 114 J. W. Phair and J. S. J. Van Deventer, *Int. J. Miner. Process.*, 2002, **66**, 121.
- 115 R. E. Lyon, P. N. Balaguru, A. Foden, S. Usman and J. Davidovits, *Fire Mater.*, 1997, **21**, 67.
- 116 C. A. Langton and D. M. Roy, in *Mater. Res. Soc. Symp. Proc.*, 1984, 26, 543.
- 117 J. Davidovits and J. L. Sawyer, Early high-strength mineral polymer., *US Pat.* 4 509 985, 1985.
- 118 A. K. Chatterjee, in *Concrete Technology for Sustainable Development*, ed. P. K. Mehta, CMA, India, 1999, pp. 556–89.
- 119 T. Bakharev, J. G. Sanjayan and Y.-B. Cheng, *Cem. Concr. Res.*, 2001, **31**, 331.
- 120 A. Fernandez-Jimenez and F. Puertas, *Cem. Concr. Res.*, 2002, **32**, 1019.
- 121 Z. Xie, W. Xiang and Y. Xi, *J. Mater. Civ. Eng.*, 2003, **15**, 67.
- 122 J. W. Phair, J. S. J. Van Deventer and J. D. Smith, *Colloids Surf., A*, 2001, **182**, 143.
- 123 J. W. Phair, J. S. J. Van Deventer and J. D. Smith, *Ind. Eng. Chem. Res.*, 2000, **39**, 2925.
- 124 S. Sorel, *C. R. Hebd. Seances Acad. Sci.*, 1867, **65**, 102.
- 125 P. Maravelaki-Kalaitzaki and G. Moraitou, *Cem. Concr. Res.*, 1999, **29**, 1929.
- 126 K. Dasgopodar, B. N. Chowdhury and R. Basu, *J. Indian Chem. Soc.*, 1992, **69**, 550.
- 127 W. Kingery, *J. Am. Ceram. Soc.*, 1950, **33**, 242.
- 128 T. Sugama and L. Kukacka, *Cem. Concr. Res.*, 1983, **13**, 407.
- 129 E. Soudee and J. Pera, *Cem. Concr. Res.*, 2000, **30**, 315.
- 130 T. Kanazawa, in *Inorganic Phosphate Materials*, Elsevier, New York, 1989, pp. 121.
- 131 A. J. W. Harrison, Reactive magnesium oxide cements, *US Pat.* 2003/0041785A1, 2003.
- 132 L. Fernandez, C. Alonso, A. Hidalgo and C. Andrade, *Adv. Cem. Res.*, 2005, **17**, 9.
- 133 J. Paya, M. V. Borrachero, J. Monzo and M. Bonilla, *Waste Manage.*, 1999, **19**, 1.
- 134 C. D. Popescu, M. Muntean and J. H. Sharp, *Cem. Concr. Compos.*, 2003, **25**, 689.
- 135 J. H. Sharp, C. D. Lawrence and R. Yang, *Adv. Cem. Res.*, 1999, **11**, 23.
- 136 F. P. Glasser and L. Zhang, *Cem. Concr. Res.*, 2001, **31**, 1881.
- 137 Q. Zhou and F. P. Glasser, *Adv. Cem. Res.*, 2000, **12**, 131.
- 138 K. Quillin, *Cem. Concr. Res.*, 2001, **31**, 1341.
- 139 X. Fu, C. Yang, Z. Liu, W. Tao, W. Hou and X. Wu, *Cem. Concr. Res.*, 2003, **33**, 317.
- 140 T. Grounds, D. V. Nowell and F. W. Wilburn, *J. Therm. Anal. Calorim.*, 2003, **72**, 181.
- 141 J. Majling and D. M. Roy, *Am. Ceram. Soc. Bull.*, 1993, **72**, 77.
- 142 P. Arjunan, M. R. Silsbee and D. M. Roy, *Cem. Concr. Res.*, 1999, 29.
- 143 V. G. Papadakis, M. N. Fardis and C. G. Vayenas, *ACI Mater. J.*, 1992, **89**, 119.
- 144 B. Uzal and L. Turanli, *Cem. Concr. Res.*, 2003, **33**, 1777.
- 145 B. K. Marsh and R. L. Day, *Cem. Concr. Res.*, 1988, **18**, 301.
- 146 A. R. Brough, C. M. Dobson, I. G. Richardson and G. W. Groves, *J. Mater. Sci.*, 1995, **30**, 1671.
- 147 M. Atkins, D. G. Bennett, A. C. Dawes, F. P. Glasser, A. Kindness and D. Read, *Cem. Concr. Res.*, 1992, **22**, 497.
- 148 J. A. Larbi, A. L. A. Fraay and J. M. Bijen, *Cem. Concr. Res.*, 1990, **20**, 506.
- 149 M. Cheriaf, J. C. Rocha and J. Pera, *Cem. Concr. Res.*, 1999, **29**, 1387.
- 150 L. P. Aldridge, W. K. Bertram, T. M. Sabine, J. Bukowski, J. F. Young and R. K. Heenan, *Mater. Res. Soc. Symp. Proc.*, 1995, 376.
- 151 M. H. Zhang and V. M. Malhotra, *Cem. Concr. Res.*, 1995, **25**, 1713.
- 152 K. Sobolev and M. Arikan, *Am. Ceram. Soc. Bull.*, 2002, **81**, 39.
- 153 K. O. Ampadu and K. Torii, *Cem. Concr. Res.*, 2001, **31**, 431.
- 154 G. Marchal, *Cem. Build. Mater. Rev.*, 2001, **3**, 12.
- 155 World Council for Sustainable Business Development, *The cement sustainability initiative: Our agenda for action*, <http://www.wbcscement.org/pdf/agenda.pdf>.
- 156 R. K. Mehta, *Concr. Int.*, 2002, 23–28.
- 157 J. F. Young and S. Mindess, *Concrete*, Prentice Hall, Upper Saddle River, NJ, USA, 2nd edn, 2003.
- 158 H. W. Reinhardt, *Betonwerk+Fertigteile-Tech.*, 1992, **2**, 61.
- 159 Energy Information Association, *Emissions of Greenhouse Gases in the United States*, DOE/EIA-0573(2002), Washington, DC, 2003.
- 160 C. R. Rhyner, *Waste management and resource recovery*, Lewis Publishers, Boca Raton, LA, USA, 1995, pp. 524.
- 161 C. Thaulow, *The Evolving Materials Paradigm*, NTNU TMM4140 course notes, 2005, website: http://www.immtek.ntnu.no/und/fag/TMM4140/materials_paradigm.html.

Reductive degradation of tetrabromobisphenol A (TBBPA) in aqueous medium

Guo-Bin Liu,^{*a} Lu Dai,^a Xiang Gao,^a Miao-Kui Li^a and Thies Thiemann^b

Received 11th April 2006, Accepted 26th June 2006

First published as an Advance Article on the web 5th July 2006

DOI: 10.1039/b605261d

Raney Ni–Al alloy in a dilute alkaline aqueous solution has shown to be a powerful reducing agent and is highly effective for the hydrodebromination of tetrabromobisphenol A (TBBPA) to bisphenol A (BPA) and other debrominated alicyclic compounds. The C–C bond of bisphenol A is cleaved easily under the reaction conditions. An almost quantitative removal of TBBPA can be attained at 90 °C.

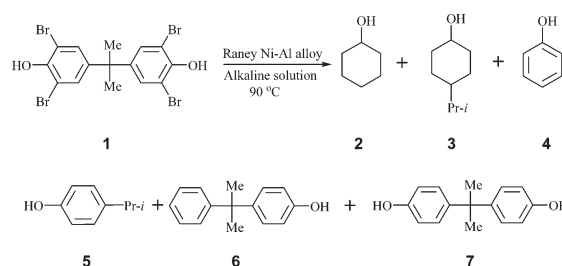
Over the years, brominated flame retardants (BFRs) have been widely used in polymeric substrates in order to improve their flame resistance. In this respect, tetrabromobisphenol A [4,4'-isopropylidenebis(2,6-dibromophenol), TBBPA, **1**] can be found as an additive in epoxy resins¹ utilized by the electronic industry in the production of printed circuit boards. It is believed that TBBPA holds about 50% of the market in brominated flame retardants.² While much of the earlier concern regarding persistent organic pollutants (POPs) has focused on polychlorinated compounds, recently, attention has turned to their brominated cousins. TBBPA is among those brominated man-made compounds that can be classified as ubiquitous, having been detected in sewage sludge,³ thus finding its way into the natural environment. TBBPA has been found as contaminant in the eggs of Norwegian predatory birds,⁴ but has also been detected in human serum.⁵ While the *in vivo* properties of TBBPA are hard to quantify,^{3,6} TBBPA has shown biological activity in *in vitro* studies.^{3,6} Thus, *in vitro*, TBBPA exhibits a high competitive binding to human transthyretin (TTR),⁷ the transport protein of thyroid hormones in the plasma. *In vitro* studies have indicated that TBBPA can alter the permeability of biological membranes.⁸ As with bisphenol A (BPA) itself, TBBPA has been attributed estrogen-like properties, although the binding affinity to the estrogen receptor ER α of TBBPA is lower than that of BPA.⁹ The impact of TBBPA on the environment is far from clear, but its potential harmfulness has led to some calls for an urgent substitution of TBBPA and related brominated compounds in commercial products.¹⁰

Needless to say, even a rapid and comprehensive substitution of TBBPA leaves the problem of waste elimination of existing materials in which TBBPA has been used. A viable elimination of TBBPA wastes in spent products as well as in waste sludge may well be where the more serious problem of TBBPA resides. It has been shown that thermal decomposition of TBBPA at

temperatures above 210 °C leads to a host of brominated phenols and brominated bisphenols.¹¹ It is known that upon incineration of municipal waste, TBBPA can also give rise to highly toxic polybrominated dibenzo-*p*-dioxins and dibenzofurans.¹² In one report, the addition of polypropylene and polyethylene to TBBPA in a pyrolysis experiment in an encapsulated ampoule under inert atmosphere has been shown to reduce significantly the amount of brominated phenols formed.¹³ Debromination of tetrabromobisphenol A in epoxy resins has also been achieved with Na/NH₃ in an autoclave at 100 °C and 6 MPa,¹⁴ and also debromination has been carried out with ethyl acetate at 280 °C and 15 MPa.¹⁵ At lower temperatures and at normal pressure, only partial dehalonitration has been reported, in which TBBPA is converted to a dinitro-dibromobisphenol after treatment with nitric acid in an organic solvent.¹⁶ As a part of our program to develop new ways of degrading hazardous wastes,¹⁷ and in order to look for new reaction conditions for a simpler degradation of TBBPA, the authors have studied the reductive debromination of TBBPA in water at comparatively low temperature. A convenient and practical method for the degradation of TBBPA using a Raney Ni–Al alloy in aqueous media will be discussed.

As shown in Scheme 1 and Table 1, tetrabromobisphenol A (TBBPA, **1**) was easily debrominated by using Raney Ni–Al alloy in a dilute aqueous alkaline solution. Manipulation is easy and organic solvents are not necessary for the reaction to proceed.

The debromination was carried out by slowly adding an aqueous alkaline solution to a mixture of tetrabromobisphenol A (**1**), Raney Ni–Al alloy and water and then heating the resulting mixture at 90 °C. Initially, as inorganic bases, KOH, CsOH and NaOH were employed, all at 1 wt%. Compound **1** was easily reduced to give bisphenol A (**7**) as the major product, together with small amounts of cyclohexanol (**2**), 4-isopropylcyclohexanol (**3**), phenol (**4**), 4-isopropylphenol (**5**) and 2-hydroxyphenyl-2-phenylpropane (**6**) (Table 1, runs 1–4). Compound **4** is formed *via* C–C bond cleavage of compound **6**. Compounds **2** and **3** are produced by hydrogenation of phenols **4** and **5** under the reaction



Scheme 1

^aDepartment of Chemistry, Fudan University, 220 Handan Road, Shanghai, 200433, P. R. China. E-mail: liuguobin@fudan.edu.cn; Fax: +86-21-65642261; Tel: +86-21-65642261

^bInstitute of Materials Chemistry and Engineering, Kyushu University 6-1, Kasuga-kohen, Kasuga, Fukuoka, 816-8580, Japan. E-mail: thies@cm.kyushu-u.ac.jp; Fax: +81-92-5837894

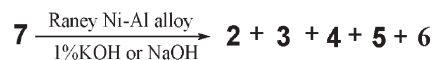
Table 1 Hydrodebromination of tetrabromobisphenol (**1**)^a

Run	Ni–Al/g	Alkaline solution ^b (volume/ml)	Time/h	Ratio (%) ^{c,d}					
				2	3	4	5	6	7
1	5	1% KOH (100)/H ₂ O (100)	5	8.3 (5.4)	9.3 (6.2)	0	27.2 (22.7)	6.3 (4.1)	48.9 (44.2)
2	5	1% NaOH (100)/H ₂ O (100)	6	7.5	8.1	0	23.4	6.0	55.0
3	2.5	1% NaOH (100)/H ₂ O (100)	8	2.8	3.1	0	14.4	2.2	77.5
4	5	1% CsOH (100)/H ₂ O (100)	5	9.3 (5.9)	10.3 (7.1)	0	24.1 (20.6)	6.6 (4.7)	49.7 (44.9)
5	5	1% Ca(OH) ₂ (100)/H ₂ O (100)	5	5.7	8.4	0	22.4	6.1	57.4
6	5	1% LiOH (100)/H ₂ O (100)	6	4.0	7.8	0	20.6	5.6	62.0
7	5	1% Ba(OH) ₂ (100)/H ₂ O (100)	6	3.4	7.1	0	18.0	4.8	66.7
8	2	0.2% KOH (100)/H ₂ O (100)	4	0.6	0.6	0	1.9	7.9	89.0
9	2	0.2% NaOH (100)/H ₂ O (100)	4	0.4	0.4	0	1.6	6.9	90.7
10	2	0.2% CsOH (100)/H ₂ O (100)	5	0.8	0.4	0	2.3	8.5	88.0
11	2	0.2% Ca(OH) ₂ (100)/H ₂ O (100)	5	0.8	0.5	0.6	2.3	4.7	91.1
12	2	0.2% LiOH (100)/H ₂ O (100)	5	0.1	0.3	0.5	1.0	5.5	92.6
13	2	0.2% Ba(OH) ₂ (100)/H ₂ O (100)	5	0.1	0.2	0.4	0.9	3.7	94.7

^a **1** (2.0 mmol, 1.09 g). ^b Added dropwise over 1.0 h. ^c GC ratio. ^d Isolated yields in parentheses.

conditions. While bond cleavage in BPA is known to occur under a number of conditions, such as by enzymatic reaction,¹⁸ thermolysis at above 150 °C¹⁹ and photodegradation,²⁰ this is the first finding that cleavage can also take place under reductive conditions at relatively low temperature in very dilute aqueous alkaline solution, when using Raney Ni alloy. Other alkali and alkali earth hydroxides, such as Ca(OH)₂, LiOH, and Ba(OH)₂, when employed as a 1 wt% aqueous solution, gave a similar mixture of reduction products of **2**, **3**, **5**, **6** and **7** (Table 1, runs 5–8).

Interestingly, compound **7** was afforded in much higher yield (Table 1, runs 8 and 9 vs. runs 1 and 2) when using a 0.2 wt% KOH aqueous solution. This result indicates that the concentration of the base affects the ratio of the debromination products greatly. Thus, compound **6** was afforded in higher yield in the case of using a 0.2 wt% aqueous CsOH solution. In more dilute alkaline conditions, products stemming from C–C cleavage of the bisphenols, such as phenols **4** and **5**, and cyclohexanols **2** and **3** were found only in trace amounts. A tentative pathway for the formation of compounds **2**, **3**, **4**, **5** and **6** is proposed. TBBPA is debrominated to compound **7**. The C–C bond of **7** is cleaved to afford phenols **4** and **5**, under the reductive conditions, which are further hydrogenated to give the corresponding cyclohexanols **2** and **3**. A contribution of a competing pathway *via* the direct cleavage of TBBPA to brominated phenols, which then are hydrodebrominated, cannot be excluded. Brominated phenols as potential intermediates cannot be detected in the product mixture since they are easily reduced to give the corresponding phenols and cyclohexanols under the reaction conditions. Indeed, Tashiro *et al.* had reported that the reduction of 2,4,6-tribromophenol with Raney Ni–Al alloy in 10% NaOH aqueous solution afforded the corresponding phenol and cyclohexanol.²¹ The occurrence of **6**, as deoxygenated **7**, is more interesting. Generally, the deoxygenation

**Scheme 2**

of non-activated phenols is not easy²² and mostly occurs under conditions found in hydroprocessing.²³

To ascertain that bisphenol (BPA, **7**) can function as a common intermediate for the side products under the reaction conditions employed, compound **7** was subjected to the reaction with Raney Ni–Al alloy under the same reaction conditions (Scheme 2 and Table 2). Treatment of **7** with Raney Ni–Al alloy (5.0 g) by addition of a 1 wt% aqueous KOH solution did indeed give a mixture of **2**, **3**, **4**, **5** and **6** in a ratio of 21.6 : 27.0 : 0.8 : 44.4 : 6.2 along with recovered starting material **7** (Table 2, run 1). A similar mixture of **2**, **3**, **4**, **5**, and **6** was formed when the reaction was performed in an aqueous 1 wt% NaOH solution, where some amount of **7** was also recovered (run 2). These results indicate that **7** is most likely the common intermediate of a pathway leading to the side products found in the dehydrobromination of TBBPA. Moreover, Guo and Ding²⁴ had reported the reduction of 1,1'-binaphthyls to 1,1'-bis(decallyl) derivatives with Raney Ni–Al alloy in an aqueous solution in the presence of isopropanol as an organic co-solvent.

In conclusion, we have developed a new and efficient method for the dehydrobromination of TBBPA using commercially available Raney Ni–Al alloy in a dilute alkaline solution. TBBPA was easily dehydrobrominated to afford cyclohexanol (**2**), 4-isopropylcyclohexanol (**3**), phenol (**4**), 4-isopropylphenol (**5**), 2-hydroxyphenyl-2-phenylpropane (**6**), and bisphenol A (**7**) under mild reaction conditions. The ratio of the debromination products strongly depended on the concentration of alkaline solution and amount of the Raney Ni–Al alloy used. The advantages of the

Table 2 Reduction of bisphenol (**7**)^a

Run	Ni–Al/g	Alkaline solution ^b (volume/ml)	Time/h	Ratio (%) ^{c,d}				
				2	3	4	5	6
1 ^e	5	1% KOH (100)/H ₂ O (100)	6	21.6 (9.1)	27.0 (11.2)	0.8	44.4 (21.1)	6.2 (2.9)
2 ^f	5	1% NaOH (100)/H ₂ O (100)	6	20.6 (8.4)	24.5 (10.6)	0.5	46.8(22.5)	7.6 (3.0)

^a **7** (2.0 mmol, 0.446 g). ^b Added dropwise over 1.0 h. ^c GC ratio. ^d Isolated yields in parentheses. ^e 48.6% of **7** was recovered. ^f 50.9% of **7** was recovered.

present approach lie in terms of the ease of manipulation, quickness of the reaction, and mildness of reaction conditions. The different conditions used for the degradation of TBBPA as compared to existing methods, especially in regard to temperature and reaction medium, should make this protocol a valuable alternative. Raney Ni–Al alloy is commercially readily available and is, of course, cheaper than the Raney Ni catalyst made from it. Further work on the hydrodebromination of TBBA and related brominated flame retardant is currently being undertaken in our laboratory.†

References

† A typical procedure is described as follows: An aqueous 1 wt% KOH solution (100 ml) was added to a mixture of **1** (2.0 mmol, 1.09 g), Raney Ni–Al alloy (5.0 g) and water (100 ml) within 1.0 h and at 90 °C. After the mixture was heated for an additional 5 h at 90 °C, it was cooled to rt and filtered over Celite. The residue was washed with ethyl acetate. After being neutralized with hydrochloric acid, the filtrate was extracted with ethyl acetate (3 × 15 ml) and the organic layer was dried over anhydrous magnesium sulfate. After removal of the solvent, a mixture of cyclohexanol (**2**), 4-isopropylcyclohexanol (**3**), 4-isopropylphenol (**5**), 2-hydroxyphenyl-2-phenylpropane (**6**), and bisphenol A (**7**) in the ratio of 8.3 : 9.3 : 27.2 : 6.3 : 48.9 was obtained (Table 1, run 1). Compounds **2**, **3**, **4**, **5**, **6** and **7** were separated by column chromatography on silica gel, when mixtures of structures were obtained from the reactions. All of the compounds, **2**, **3**, **4**, **5**, **6** and **7** were compared with authentic samples and their structures were also assigned on the basis of IR, ¹H NMR and GC-MS spectroscopic data.

- I. Watanabe, T. Kashimoto and R. Tatsukawa, *Bull. Environ. Contam. Toxicol.*, 1983, **31**, 48; U. Sellström and B. Jansson, *Chemosphere*, 1995, **31**, 3085.
- A. Hornung, A. I. Balabanovich, S. Donner and H. Seifert, *J. Anal. Appl. Pyrolysis*, 2003, **70**, 723 and ref. cited therein.
- C. A. de Wit, *Chemosphere*, 2002, **46**, 583.
- D. Herzke, U. Berger, R. Kallenborn, T. Nygard and W. Vetter, *Chemosphere*, 2005, **61**, 441.
- (a) C. Thomson, E. Lundanes and G. Becher, *J. Environ. Monit.*, 2001, **3**, 366; (b) C. Thomsen, E. Lundanes and G. Becher, *Environ. Sci. Technol.*, 2002, **36**, 1414.
- For an overview of toxic effects of brominated flame retardants, see: P. O. Darnerud, *Environ. Int.*, 2003, **29**, 841.
- For *in vitro* studies, see: (a) I. A. T. M. Meerts, J. J. van Zanden, E. A. C. Luijckx, I. van Leewen-Bol, G. Marsh, E. Jakobsson, A. Bergman and A. Brouwer, *Toxicol. Sci.*, 2000, **56**, 95; (b) *in vivo* studies in pregnant rats have not shown any formation of TBBPA–TTR complexes. This may be due to a rapid excretion of TBBPA, see: A. T. M. Meerts, Y. Assink, P. H. Cenjin, B. M. Weijers, H. H. J. van den Berg and A. Bergman, *Organohalogen Compd.*, 1999, **40**, 375.

- B. Inouye, Y. Katayama, T. Ishida, M. Ogata and K. Utsumi, *Toxicol. Appl. Pharmacol.*, 1979, **48**, 467.
- For studies in the MCF-7 human breast cancer cell line: M. Samuelson, C. Olsen, J. A. Holme, E. Meussen-Elholm, A. Bergmann and J. K. Hongso, *Cell Biol. Toxicol.*, 2001, **17**, 139; on the other hand, TBBPA showed no estrogenic activity in bird embryos: C. Berg, K. Hallidin and B. Brunström, *Environ. Toxicol. Chem.*, 2001, **20**, 2836.
- D. Santillo and P. Johnston, *Environ. Int.*, 2003, **29**, 725.
- F. Barontini, V. Cozzani, K. Marsanich, V. Raffa and L. Petarca, *J. Anal. Appl. Pyrolysis*, 2004, **72**, 41; K. Marsanich, S. Zanelli, F. Barontini and V. Cazzoni, *Thermochim. Acta*, 2004, **421**, 95.
- (a) G. Söderström and S. Marklund, *Environ. Sci. Technol.*, 2002, **36**, 1959; H. Wichmann, F. T. Dettmer and M. Bahadir, *Chemosphere*, 2002, **47**, 349; (b) H. Thoma, S. Rist, G. Hauschulz and O. Hutzinger, *Chemosphere*, 1986, **15**, 649; (c) H. R. Buse, *Environ. Sci. Technol.*, 1986, **20**, 404; (d) H. Thoma and O. Hutzinger, *Chemosphere*, 1987, **16**, 1353; (e) D. Bienek, M. Bahadir and F. Koret, *Heterocycles*, 1989, **28**, 719; (f) R. Dumler, H. Thomas, D. Lenoir and O. Hutzinger, *Chemosphere*, 1989, **19**, 2023; (g) R. Dumler, H. Thomas, D. Lenoir and O. Hutzinger, *Chemosphere*, 1990, **20**, 1867; (h) J. Thies, M. Neupert and W. Pump, *Chemosphere*, 1990, **20**, 1921; (i) R. Lujik, H. Wever, K. Olie, H. A. J. Govers and J. J. Boon, *Chemosphere*, 1991, **23**, 1173; (j) R. C. Striebich, W. A. Rubey, D. A. Tierney and B. Dellinger, *Chemosphere*, 1991, **23**, 1197; (k) R. Lujik and H. A. J. Govers, *Chemosphere*, 1992, **25**, 361; (l) M. Riess, T. Ernst, R. Popp, B. Müller, H. Thomas, O. Vierle, M. Wolf and R. van Eldik, *Chemosphere*, 2000, **40**, 937; (m) S. Sakai, J. Watanabe, Y. Honda, H. Takatsuki and I. Aoki, *Chemosphere*, 2001, **42**, 519; (n) H. Wichmann and F. T. Dettmer, *Chemosphere*, 2002, **47**, 349; (o) F. Barontini and V. Cozzani, *J. Anal. Appl. Pyrolysis*, 2006, **77**, 41.
- A. Hornung, S. Donner, A. Balabanovich and H. Seifert, *J. Cleaner Prod.*, 2005, **13**, 525 see also ref. 2.
- K. Mackenzie and F.-D. Kopinke, *Chemosphere*, 1996, **33**, 2423.
- K. Brodersen, D. Tartler and B. Danzer, Wertstoffrückgewinnung aus Vielstoffgemischen am Beispiel Computerschrott, in *BayFORREST (Bayrischer Forschungsverbund Abfallforschung und Reststoffverwertung)*, Berichtsheft 4, ed. P. A. Wilderer and R. Koralewska, BayFORREST, München, 1995, 227.
- S. Adimurthy, S. S. Vaghela, P. V. Vyas, A. K. Bhatt, G. Ramachandraiah and A. V. Bedekar, *Tetrahedron Lett.*, 2003, **44**, 6393.
- G.-B. Liu, T. Tsukinoki, T. Kanda, Y. Mitoma and M. Tashiro, *Tetrahedron Lett.*, 1998, **39**, 5991.
- T. Fukuda, H. Uchida, M. Suzuki, H. Miyamoto, H. Morinaga, H. Nawata and T. Uwajima, *J. Chem. Technol. Biotechnol.*, 2004, **79**, 1212.
- S. E. Hunter and P. E. Savage, *J. Org. Chem.*, 2004, **69**, 4724.
- H. Watanabe, S. Horikoshi, H. Kawabe, Y. Sugie, J. C. Zhao and H. Hidaka, *Chemosphere*, 2003, **52**, 851.
- M. Tashiro, A. Iwasaki and G. Fukuta, *J. Org. Chem.*, 1978, **43**, 196.
- Y. Pan and C. P. Holmes, *Org. Lett.*, 2001, **3**, 2769.
- F. P. Petrocelli and M. T. Klein, *Fuel Sci. Technol.*, 1987, **5**, 25.
- H. Guo and K. Ding, *Tetrahedron Lett.*, 2000, **41**, 10061.

Cationic functionalisation of cellulose using a choline based ionic liquid analogue†

Andrew P. Abbott,*^a Thomas J. Bell,^a Sandeep Handa^a and Barry Stoddart^b

Received 11th April 2006, Accepted 26th June 2006

First published as an Advance Article on the web 4th July 2006

DOI: 10.1039/b605258d

The efficient cationic functionalisation of cellulose is demonstrated using an ionic liquid analogue, based on a eutectic mixture of a choline chloride derivative and urea, which acts as both solvent and reagent. It was determined that all the available hydroxyl groups on cellulose had been modified.

Introduction

The cationic functionalisation of cellulose is of considerable industrial importance and has found applications in the paper industry, cosmetics, textiles, in flotation and flocculation and in drilling fluids.¹ In particular, it is used in the removal of acidic dyes from aqueous effluent produced by the textile industry, which significantly reduces the environmental impact of such processes.² These dyes are of an anionic nature comprising of groups such as sulfonates, carboxylates or sulfates, and so suit the use of a cationic substrate.³ The form of cellulose often used, cotton, is natural, inexpensive and renewable.³

The preferred route to the formation of these materials is by the etherification of cellulose using glycidyl ammonium salts or alkylene epoxides in the presence of a suitable alkaline catalyst, usually sodium hydroxide. Cationic substitution values between 0.034 and 0.5 moles of quaternary nitrogen per mole of glucose unit have been reported.^{4–6} However, such approaches entail the use of large amounts of organic solvents, and result in low yields and the loss of product as a result of solubility in the reaction mixture.¹ Two other approaches, coupling oligo-ionomers to cellulose fibres and grafting on cationic polymer chains, have also been reported, but again yields tend to be poor.⁷

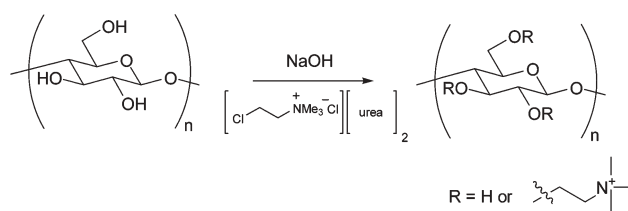
We have previously reported the development of ionic liquids based on a combination of the inexpensive and readily available components choline chloride (ChCl; HOCH₂CH₂N(Me)₃Cl) and zinc chloride as alternatives to the more commonly employed alkyl imidazolium–aluminium chloride mixtures.⁸ These new Lewis acidic solvents have been successfully employed for a variety of reactions.^{9–11} We have also reported a eutectic mixture of choline chloride and urea which forms an ionic liquid analogue with the advantage of being non-toxic and readily biodegradable but has no Lewis acidity.¹² Two uses of this mixture for inorganic applications have recently been reported.^{13,14} In this current study

we report the first successful use for organic synthetic processes of a deep eutectic solvent, consisting of a choline derivative and urea, which can be employed as both a reagent and solvent for the cationic functionalisation of cellulose.

Results and discussion

Cellulose, in the form of cotton wool, was quaternised using sodium hydroxide and a chlorcholine chloride-based (ClChCl; ClCH₂CH₂N(Me)₃Cl) deep eutectic solvent, for 15 h at 90 °C (Scheme 1).† The modified cotton wool was removed from the solvent and copiously washed with water to give the product. A variety of methods for determining the degree of cationic functionalisation of cellulose substituted by conventional means have been reported. Kjeldahl analysis accurately determines the nitrogen content and thus the degree of cationic substitution,¹ although other approaches such as solid-state NMR,¹⁵ elemental analysis¹⁶ and dye adsorption¹⁷ have been reported. Analysis of the product by the Kjeldahl method gave a cationic substitution value of 0.5% of quaternary nitrogen per mole of glucose unit. Cationic functionalisation was also confirmed by the use of a cationic dye, methylene blue. A calibration plot was constructed by using different concentrations of methylene blue and this was used to measure the dye concentration in the supernatant liquid resulting from placing 0.05 g of substituted cotton wool in 3 ml of dye solution for 3 hours (see ESI†). This was repeated with unmodified cotton wool and the concentration of dye repelled due to the functionalisation was determined to be 1.44×10^{-8} moles.

The above analysis assumes that all the quaternised groups become attached to the cellulose by reaction of the chlorcholine chloride with the available OH groups, and that no physisorption onto the cotton wool is occurring. The extent to which physisorption could be occurring was examined by repeating the reaction without the use of sodium hydroxide, thus preventing the chemical reaction from occurring. Dye analysis of the product showed that 8.25×10^{-9} moles of dye were repelled, thus confirming the presence of functionalised material. By reference to



Scheme 1 Derivatisation of cellulose with cationic functionalities.

^aDepartment of Chemistry, University of Leicester, Leicester, UK LE1 7RH. E-mail: apal@le.ac.uk; Fax: +44 (0)116 252 3789;

Tel: +44 (0)116 252 2087

^bP&G Technical Centres, Whitley Road, Longbenton, Newcastle Upon Tyne, UK NE12 9TS

† Electronic supplementary information (ESI) available: Experimental procedures and I.R. calibration plot. See DOI: 10.1039/b605258d

the Kjeldahl analysis and assuming that the repulsion of the cationic dye follows a linear relationship, this equates to 0.28% of quaternary nitrogen per mole of glucose unit.

Samples of the physisorbed material and chemi/physisorbed material were washed with water for varying periods of time (0 to 72 hours) to determine the extent of leaching of quaternised material (Fig. 1). This showed that cellulose containing only physisorbed material progressively loses all its quaternised material whereas the cellulose containing both chemi- and physisorbed material loses around 50%.

Chemisorbed material therefore accounts for around half of the quaternised product. As the cotton wool was washed thoroughly in the work-up procedure the material removed over the period of 72 hours can be assumed to be genuinely physisorbed rather than that merely trapped between the cotton wool fibres.

Secondary Ion Mass Spectrometry (SIMS) showed peaks relating to both chemisorbed and physisorbed material. Taking into account the extent of physisorption, the degree of cationic substitution based only on chemisorbed material was estimated to be 0.22%.

The degree of cationic substitution reported is based on the assumption that all of the hydroxyl groups on the cellulose fibres are available for functionalisation to take place. However, only the hydroxyl groups on the surface of the fibres are likely to be accessible for substitution. The ratio of the surface groups to those in the bulk of the monomer was estimated using the following equation.[†]

$$\text{Ratio} = \frac{\pi(r+2R)^2 - \pi r^2}{\pi(r+2R)^2}$$

Where r is the radius of the cellulose fibre and R is the radius of the glucose monomer on the surface of the fibre. The radius of the cellulose fibre (1×10^{-5} m) was determined by the use of atomic force microscopy, and the radius of a glucose monomer (7.95×10^{-10} m) by a molecular modelling package.¹⁸ The resulting ratio was found to be 3.18×10^{-4} , or 0.0318% of available glucose monomers and hence the available hydroxyl groups present. This figure lies just outside the range of the cationic substitution determined by Kjeldahl analysis. However, the estimation of the

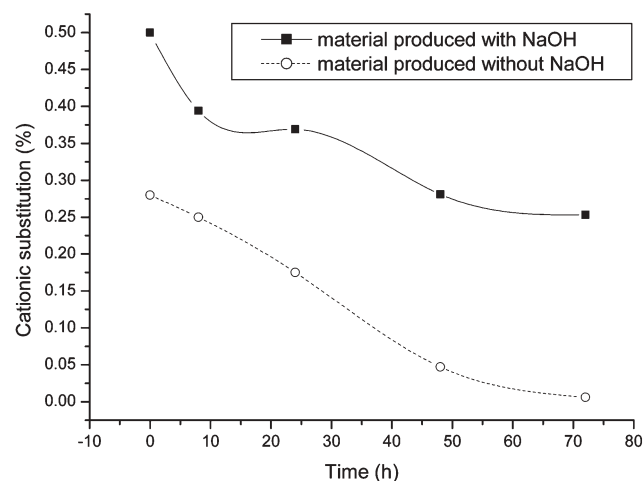


Fig. 1 Comparison of derivatised cellulose produced with and without the use of NaOH.

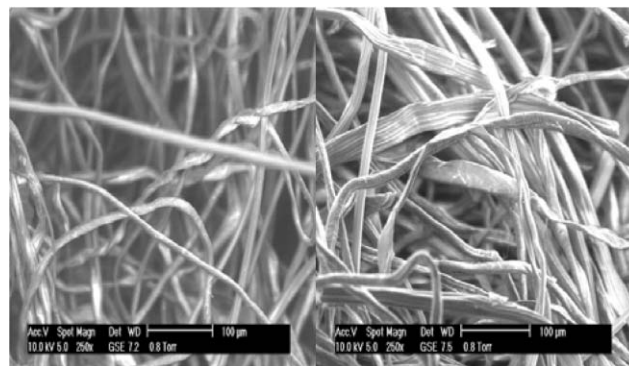


Fig. 2 SEM images of cotton wool (left) and cotton wool after contact with eutectic solvent for 15 hours at 90 °C.

available groups on the surface was based on the assumption that no wetting (opening up) of the cellulose fibres takes place.

Fig. 2 shows scanning electron microscopy (SEM) images of cotton wool before and after being subjected to the deep eutectic solvent. These show that the cotton wool is slightly wetted upon contact with the eutectic solvent presumably resulting in more hydroxyl groups being available for reaction. Taking this into account it is reasonable to assume that the vast majority, if not all, of the available hydroxyl groups on the cellulose have been functionalised.

The cationic functionalisation of the surface leads to a material with increased hydrophilicity. Thermogravimetry showed that the sample was able to absorb an additional 26 wt% of water compared to unmodified cellulose.

The effect of different reaction times (Table 1, entries 1–3) and temperatures (entries 2, 4 and 5) were investigated to discover the optimum conditions for the reaction. The cationic substitution values were calculated using the dye method and are based only on chemisorbed material assuming, as previously, that around 50% of the material was due to physisorption.

From this it was concluded that 15 hours at 90 °C were the most favourable conditions for the cationic functionalisation of cellulose in the deep eutectic solvent, $\text{ClCHCl}(\text{urea})_2$.

While cellulose derivatised with cationic functionalities repels cationic dyes it is very effective at adsorbing anionic dyes, which are the main branch of water soluble dyes used in printing. The efficacy of using cationic functionalised cellulose for dye adsorption was determined using orange II. It was found that the modified cellulose produced in entry 2 of Table 1 was capable of extracting 0.06 wt% orange II dye, which suggests that these materials may be suitable alternatives for cleaning dyes from aqueous waste streams.

Table 1 Determination of the optimum conditions for the cationic functionalisation of cellulose in a deep eutectic solvent

Entry	Time/h	Temperature/°C	Cationic substitution (%)
1	3	90	0.09
2	15	90	0.22
3	60	90	0.19
4	15	60	0.06
5	15	120	0.19

Conclusion

This work has shown that an ionic liquid analogue based on ClChCl and urea acts as both reagent and solvent in the effective cationic functionalisation of cellulose. It was determined that all the available hydroxyl groups on cellulose had been modified and that this material is significantly more hydrophilic than cellulose. We have demonstrated the potential to produce a material with a green application from renewable sources using a green synthetic methodology.

Acknowledgements

The authors would like to acknowledge EPSRC, Crystal Faraday and Procter and Gamble for funding this work.

Notes and references

- 1 R. S. Hasselroth, D. B. Marktbreit and M. H. Eschborn, *U.S. Pat.* 4,940,785, 1990.
- 2 J. A. Laszlo, *Am. Dyest. Rep.*, 1994, 17.

- 3 I. Bouzaida and M. B. Rammah, *Mater. Sci. Eng.*, 2002, **21**, 151.
- 4 F. W. Stone and J. M. Rutherford, *U.S. Pat.* 3,472,840, 1969.
- 5 R. L. Kreeger and S. Zhou, *Int. Pat.* WO 2005/000903 A1, 2005.
- 6 P. M. Van der Horst, *Int. Pat.* WO2005/061792 A1, 2005.
- 7 E. Gruber, C. Ganzow and T. Ott, *ACS Symp. Ser.*, 1998.
- 8 A. P. Abbott, G. Capper, D. L. Davies and R. K. Rasheed, *Inorg. Chem.*, 2004, **43**, 3447.
- 9 A. P. Abbott, G. Capper, D. L. Davies, R. Rasheed and V. Tambyrajah, *Green Chem.*, 2002, **4**, 24.
- 10 R. C. Morales, V. Tambyrajah, P. R. Jenkins, D. L. Davies and A. P. Abbott, *Chem. Commun.*, 2004, 158.
- 11 A. P. Abbott, T. J. Bell, S. Handa and B. Stoddart, *Green Chem.*, 2005, **7**, 705.
- 12 A. P. Abbott, G. Capper, D. L. Davies, R. K. Rasheed and V. Tambyrajah, *Chem. Commun.*, 2003, 70.
- 13 J.-H. Liao, P.-C. Wu and Y.-H. Bai, *Inorg. Chem. Commun.*, 2005, **8**, 4, 390.
- 14 E. R. Cooper, C. D. Andrews, P. S. Wheatley, P. B. Webb, P. Wormald and R. E. Morris, *Nature*, 2004, **430**, 7003, 1012.
- 15 P. Aggarwal and D. Dollimore, *Thermochim. Acta*, 1997, **291**, 65.
- 16 G. S. Chouhan, B. Singh and S. K. Dhiman, *J. Appl. Polym. Sci.*, 2004, **91**, 2454.
- 17 A. Hashem and R. M. El-Shishtawy, *Adsorpt. Sci. and Technol.*, 2001, **19**, 3, 197.
- 18 Spartan Pro, Wavefunction Inc., Irvine, CA, USA.

Zinc catalysed ester solvolysis. Application to the synthesis of tartronic acid derivatives†

Rosa M. Carrillo,^a Ana G. Neo,^{*a} Lucía López-García,^a Stefano Marcaccini^b and Carlos F. Marcos^{*a}

Received 24th May 2006, Accepted 19th July 2006

First published as an Advance Article on the web 28th July 2006

DOI: 10.1039/b607358a

A novel synthesis of hydroxyglycine retropeptidic derivatives was achieved through a Passerini 3-component reaction of glyoxyl amides or esters, followed by an unprecedented environmentally benign zinc catalysed solvolysis.

The synthesis of retro- and retro-inverso peptides, peptide analogues in which one or more peptidic bonds are inverted, was shown to be an effective strategy for the development of peptidomimetic drugs with improved bioavailability and metabolic stability.¹ Tartronamide can be used as a retropeptidic surrogate of hydroxyglycine, which may be regarded as a stable transition state analogue of amide bond hydrolysis. Hence, non-symmetric tartronamides have been synthesised as inhibitors of matrix proteinases,² important pharmacological targets involved in tumour invasion and joint destruction processes. Peptidomimetic tartronamides have been also proposed as analogues of 15-desoxyspergualin, an immunosuppressive agent used to reduce graft rejection.³

Multicomponent reactions (MCRs) are highly convergent processes that allow the efficient preparation of complex molecules from simple starting materials. MCRs of isocyanides, particularly the Ugi reaction, have been employed for the synthesis of peptide derivatives,⁴ though, as far as we know, they have never been used in the synthesis of retropeptides. We envisaged that glyoxylamides (1), isocyanides (3) and a carboxylic acid, such as acetic acid (4), could be combined in a three component Passerini condensation⁵ to give acylated tartronamide derivatives (5). Acyl hydrolysis would then transform adducts 5 into tartronamides (8; Scheme 1).

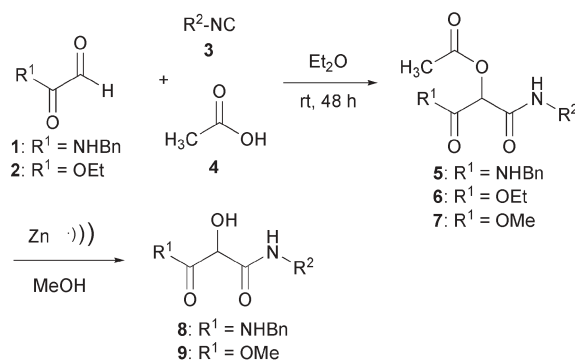
Ester hydrolysis usually requires rather acidic or basic conditions, which involve the use of corrosive reagents, leading to dangerous wastes. By contrast, in living systems many hydrolytic enzymes use Zn²⁺ to catalyse hydrolysis at physiological pH. The role of zinc in these enzymes may be two-fold, enhancing the electrophilic character of the substrate and also facilitating the formation of a nucleophilic hydroxyl anion.⁶ Zn(II) complexes, often containing polydentate ligands, have been prepared as model compounds of hydrolytic metalloenzymes,⁷ although their use in synthesis is generally impractical. We reasoned that cationic centres on the surface of finely divided zinc could be able to coordinate an alcoholic OH or a water molecule, activating them as nucleophiles in a solvolytic process. A heterogeneous catalytic

system using Zn would have evident environmental and practical advantages in ester hydrolysis. We report here the results of the exploration of such catalytic system in the synthesis of tartronic acid derivatives.

In a first experiment we performed a Passerini condensation between benzylglyoxylamide (1),⁸ cyclohexyl isocyanide (3a) and acetic acid (4). An equimolar mixture of the three components was stirred at rt in Et₂O for 3 days. The expected adduct 5a precipitated from the reaction medium and was isolated by filtration, essentially pure, in a 68% yield.⁹ We next attempted the hydrolysis of the ester 5a, using ultrasonically activated Zn, in a mixture of saturated aqueous NH₄Cl and methanol. The reaction was followed by GC-MS until all the starting material was consumed. After 72 h, a single product was isolated from the reaction mixture, which according to its spectroscopic data was identified as the desired tartronamide 8a. Remarkably, conversion was quantitative according to GC-MS data, and no hydrolysis of the amide group, or reduction to the corresponding malonodiamide¹⁰ was detected.

We also investigated the effect of ultrasounds on the solvolysis.¹¹ Irradiation in an ultrasound bath significantly accelerated the reaction, which went to completion in just 6 h, in a methanolic solution with no added water.

Surprisingly, when acetate 5a was treated with ZnCl₂, solvolysis did not take place, and only starting material was recovered, even after 7 days stirring at rt. To rule out cleavage of the ester through reduction of the acyl group, we decided to perform the solvolysis of an ester large enough to allow a convenient analysis of the products by GC-MS. Therefore, aryl ester 10, synthesised by the Passerini reaction of benzylglyoxylamide (1), cyclohexyl isocyanide (3a) and *p*-toluic acid, was subjected to ultrasound irradiation in methanol, in the presence of an excess of Zn. GC-MS monitoring of the reaction revealed only the expected solvolysis products

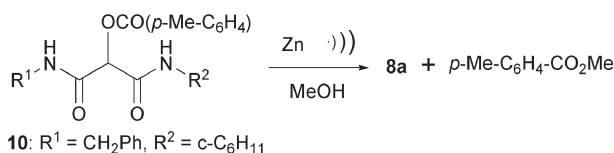


Scheme 1 Synthesis of tartronodiamides and tartronoamidoesters.

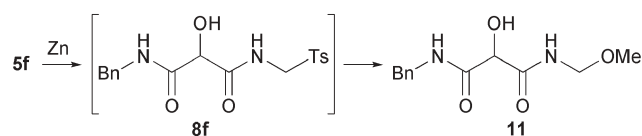
^aLaboratorio de Química Orgánica y Bioorgánica (L.O.B.O.), Dept. Química Orgánica, Facultad de Veterinaria, Universidad de Extremadura, 10071, Cáceres, Spain. E-mail: cfernán@unex.es

^bDipartimento di Chimica Organica 'Ugo Schiff', Università di Firenze, 50019, Sesto Fiorentino (FI), Italy

† Electronic supplementary information (ESI) available: Spectroscopic data of all new compounds. See DOI: 10.1039/b607358a



Scheme 2 Solvolysis of Passerini adduct 10.



Scheme 3 Tandem solvolysis-β N-H elimination of adduct 5f.

tartronamide **8a** and *p*-toluic acid methyl ester, but no *p*-methylbenzyl alcohol was detected (Scheme 2).

It is interesting to note that cleavage with Zn of acetate **5a** was significantly accelerated when a catalytic amount of ZnCl₂ was added. The reaction took place in methanol, in the presence of an excess of Zn and 10 mol% of ZnCl₂, in 6 h, or in just 3 h when ultrasonic irradiation was applied.¹² Apparently, a synergy between Zn²⁺ and the large surface of zinc metal account for the observed catalytic effect, as ZnCl₂ alone did not promote the solvolysis. In the absence of zinc chloride, Zn²⁺ is probably produced by the ultrasounds facilitated oxidation of the metal.¹³

We applied the optimised solvolysis conditions, using Zn and ZnCl₂ in methanol, to other bis(carbamoyl)methyl acetates (**5b–f**), obtained by the Passerini condensation of different isocyanides (**3b–f**). The results are shown in Table 1 (entries 1–5). Passerini reactions gave moderate to good yields of the adducts, and solvolysis was always quantitative as judged by GC-MS, although isolated yields varied between 77 and 99%.

In the case of the Passerini adduct **5f** (Table 1, entry 6), methanolysis was spontaneously followed by nucleophilic substitution of the tosyl group by a molecule of solvent, leading to methoxymethyl amide **11**. Although similar sulfone substituted amides are usually quite stable towards β N-H elimination,¹⁴ in this case displacement of the tosyl group is probably facilitated by anquimeric assistance of the δ OH on intermediate **8f** (Scheme 3). Interestingly, tartronodiamide **11** contains two orthogonal protecting groups, which would allow, in principle, independent functionalisation of both amide groups.

Finally, amidoesters (**6**) obtained by the Passerini condensation of ethyl glyoxylate (**2**) have also been subjected to methanolysis in the same conditions used for the bisamides **5** (Scheme 1). In this

Table 1 Results of the passerini and solvolysis reactions

Entry	R ¹	R ²	Passerini ^a (%)	Solvolysis ^b (%)
1	PhCH ₂ NH	C ₆ H ₁₁	5a (68)	8a (99)
2	PhCH ₂ NH	^t Bu	5b (70)	8b (97)
3	PhCH ₂ NH	PhCH ₂	5c (55)	8c (77)
4	PhCH ₂ NH	2,6-Me ₂ Ph	5d (61)	8d (99)
5	PhCH ₂ NH	^t BuO ₂ CCH ₂	5e (65)	8e (94)
6	PhCH ₂ NH	4-MePhSO ₂ CH ₂	5f (87)	11 (77)
7	CH ₃ CH ₂ O	C ₆ H ₁₁	6a (45)	9a (12) ^c
8	CH ₃ CH ₂ O	2,6-Me ₂ Ph	6d (61)	9d (51) ^c

^a Representative procedure for the Passerini condensation: 5 mmol of each acetic acid (**4**), *N*-benzyl glyoxylamide (**1**) or ethyl glyoxylate (**2**) and the corresponding isocyanide (**3**) were stirred for 72 h in 5 mL of Et₂O at rt. The precipitate was filtered and washed with *i*-PrOH (5 mL) and *i*-Pr₂O (5 mL). ^b Representative procedure for the solvolysis: A mixture of **5** or **6** (0.3 mmol), Zn dust (3 mmol) and ZnCl₂ (0.03 mmol) in MeOH (12 mL) was irradiated in a sonication bath for 3–4 h. The reaction mixture was decanted from the Zn and concentrated, and the product was purified by column chromatography (15 cm × 2.5 cm Ø, SiO₂, hexane–EtOAc 7 : 3 to 1 : 1). ^c Reaction time: 7 h.

case, the cleavage of the acetate was accompanied by transesterification of the ethyl ester. For the reaction of diester **6a**, a mixture of starting material, tartronoamidoester **9a** and the intermediate **7a** was detected by GC-MS. Longer reaction times led exclusively to **9a**, but significant decomposition was also detected. Nonetheless, tartronoamidoester **9d** was obtained in a moderate yield as the only product of the reaction of diester **6d**.

We also studied the possibility of recycling the catalyst. In five successive runs **5a** was hydrolysed to completion, in identical conditions, reusing the same Zn, which was separated by centrifugation and removal of the supernatant solution.

In conclusion, we have developed a novel and convenient synthesis of tartronic acid derivatives through a sequence of a Passerini 3-component condensation and a mild solvolysis catalysed by Zn. Solvolysis is performed in neutral aqueous or alcoholic solution, conditions that are compatible with many different functional groups and in accordance with the principles of green chemistry. Furthermore, Zn can be recycled and reused in successive hydrolyses with no significant loss of catalytic activity. This procedure may be easily adapted for the preparation of partially modified retropeptides with possible pharmacological interest. Experiments are currently underway in our laboratory.‡

Notes and references

‡ We thank the support from C. Educación Ciencia y Tecnología of Junta de Extremadura and FEDER (2PR04A003 & 3PR05C022).

- (a) M. Chorev, *Biopolymers*, 2005, **80**, 67; (b) M. Chorev and M. Goodman, *Acc. Chem. Res.*, 1993, **26**, 266; (c) M. D. Fletcher and M. M. Campbell, *Chem. Rev.*, 1998, **98**, 763.
- E. G. von Roedern, S. Grams, H. Brandstetter and L. Moroder, *J. Med. Chem.*, 1998, **41**, 339.
- L. Lebreton, J. Annat, P. Derrepas, P. Dutartre and P. Renaut, *J. Med. Chem.*, 1999, **42**, 277.
- I. Ugi, D. Marquarding and R. Urban, in *Chemistry and Biochemistry of Amino Acids, Peptides, and Proteins*, ed. B. Weinstein, Marcel Dekker, New York, 1982, p. 246–289.
- M. Passerini, *Gazz. Chim. Ital.*, 1921, **51**, II, 126.
- J. Chin, *Acc. Chem. Res.*, 1991, **24**, 145.
- J. Huang, D. F. Li, S. A. Li, D. X. Yang, W. Y. Sun and W. X. Tang, *J. Inorg. Biochem.*, 2004, **98**, 502 and references therein.
- P. Xu, W. W. Lin and X. M. Zou, *Synthesis*, 2002, 1017.
- Data for (benzylcarbamoyl)(cyclohexylcarbamoyl)methyl acetate (**5a**): (68%) white solid; mp 175–177 °C; IR (cm⁻¹) 3272, 1747, 1679, 1659, 1543; ¹H-NMR (400 MHz, CDCl₃) δ 7.35–7.20 (m, 5 H), 6.65 (d, 1 H, *J* = 7.8 Hz), 5.59 (s, 1 H), 4.46 (m, 2 H), 3.75 (m, 1 H), 2.25 (s, 3 H), 2.00–1.10 (m, 10 H); ¹³C-NMR (100 MHz, CDCl₃) δ 168.52 (C), 164.62 (C), 163.51 (C), 137.25 (C), 128.69 (CH), 127.55 (CH), 72.20 (CH), 48.68 (CH), 43.53 (CH₂), 32.57 (CH₂), 25.29 (CH₂), 24.60 (CH₂), 20.67 (CH₃); MS (FAB) *m/z* (%) 333 (M⁺ + 1, 100), 291 (11); HRMS calcd for C₁₈H₂₅N₂O₄: 333.1813. Found: 333.1814.
- A. G. Neo, J. Delgado, C. Polo, S. Marcaccini and C. F. Marcos, *Tetrahedron Lett.*, 2005, **46**, 23.
- For examples of the effect of ultrasounds on ester hydrolysis see: (a) A. Tuulmets and S. Saalmar, *Ultrason. Sonochem.*, 2001, **8**, 209; (b) S. Saalmar, G. Cravotto, A. Tuulmets and H. Hagu, *J. Phys. Chem. B*, 2006, **110**, 5817.

- 12 Data for *N*¹-benzyl-*N*³-cyclohexyl-2-hydroxymalonamide (**8a**): (99%) white solid; mp 142–144 °C; IR (cm⁻¹) 3279, 1644, 1542; ¹H-NMR (400 MHz, CDCl₃) δ 7.61 (br s, 1 H), 7.35–7.10 (m, 5 H), 7.13 (br d, 1 H, *J* = 7.6 Hz), 4.64 (br s, 1 H), 4.47 (m, 3 H), 3.75 (m, 1 H), 2.0–1.10 (m, 10 H); ¹³C-NMR (100 MHz, CDCl₃) δ 168.72 (C), 167.30 (C), 137.21 (C), 128.71 (CH), 127.62 (CH), 127.50 (CH), 70.26 (CH), 48.70 (CH), 43.60 (CH₂), 32.65 (CH₂), 25.31 (CH₂), 24.58 (CH₂); MS (EI) *m/z* (%) 290 (M⁺, 7), 209 (2), 165 (41), 106 (35), 91 (100); HRMS calcd for C₁₆H₂₂N₂O₃: 290.1630. Found: 290.1642.
- 13 M. L. Doche, J. Y. Hihn, A. Mandroyan, R. Viennet and F. Touyeras, *Ultrason. Sonochem.*, 2003, **10**, 357.
- 14 B. P. Branchaud and P. Tsai, *J. Org. Chem.*, 1987, **52**, 5475.

Chemical Technology

A well-received news supplement showcasing the latest developments in applied and technological aspects of the chemical sciences



Free online and in print issues of selected RSC journals!*

- **Application Highlights** – newsworthy articles and significant technological advances
- **Essential Elements** – latest developments from RSC publications
- **Free access** to the original research paper from every online article

*A separately issued print subscription is also available

RSC Publishing

www.rsc.org/chemicaltechnology

03005020

Zirconium phosphate supported tungsten oxide solid acid catalysts for the esterification of palmitic acid

Katabathini Narasimha Rao,^{*a} Adapa Sridhar,^b Adam F. Lee,^a Stewart J. Tavener,^a Nigel A. Young^c and Karen Wilson^{*a}

Received 28th April 2006, Accepted 28th June 2006

First published as an Advance Article on the web 12th July 2006

DOI: 10.1039/b606088a

A series of zirconium phosphate supported WO_x solid acid catalysts with W loadings from 1–25 wt% have been prepared on high surface area zirconium phosphate by a surface grafting method. Catalysts were characterized by N_2 adsorption, FTIR, Raman, UV-Vis, ^{31}P MAS NMR, pyridine TPD and X-ray methods. Spectroscopic measurements suggest a Keggin-type structure forms on the surface of zirconium phosphate as a $(\equiv\text{ZrOH}_2^+)(\text{ZrPW}_{11}\text{O}_{40}^{5-})$ species. All catalysts show high activity in palmitic acid esterification with methanol. These materials can be readily separated from the reaction system for re-use, and are resistant to leaching of the active heteropolyacid, suggesting potential industrial applications in biodiesel synthesis.

Introduction

Biodiesel is a clean fuel source which is viewed as a viable alternative for dwindling petroleum-based diesel resources. Biodiesel is generally synthesized by the transesterification of natural oils, or fat of vegetable or animal origin,^{1,2} which is carried out by acid or base catalysis.³ As the rate of the latter reactions are much faster than the former,⁴ base catalysis is normally employed commercially. Some of us have recently reported that Li doped CaO and Mg:Al hydrotalcites are promising solid bases for transesterification of triglycerides.^{5,6} For an alkali catalysed transesterification, the glycerides and alcohol must be free from water and free fatty acids (FFAs).² However, some of the natural oils or fats contain considerable amounts of FFAs which interfere with the transesterification process and must be converted into their corresponding esters before reaction. Thus, esterification forms an essential step in the production of biodiesel.⁷

Esterifications are conventionally carried out homogeneously using mineral acids, which are however corrosive with the excess acid also requiring neutralization post-reaction, leaving large quantities of salts for subsequent environmental disposal.⁸ Heterogeneous catalysts are preferable, offering easy separation from the reactants and products by filtration, and continuous reactor operation, particularly using techniques like reactive distillation.⁹ Though considerable literature exists on the esterification of simple aliphatic and aromatic acids by various solid acid catalysts such as zeolites and resins,^{10–12} there are only a few reports on fatty acid esterification.^{13,14}

Heteropolyacids (HPAs) are well known solid acids which are also active towards liquid phase esterification.¹⁵ The most commonly used heteropolyacid, phosphotungstic acid

$\text{H}_3\text{PW}_{12}\text{O}_{40}$ (HPW), exhibits strong acidity, however the use of pure HPW is not favourable due to their low surface area and high solubility in polar solvents.¹⁶ To overcome these limitations HPWs are usually supported on a carrier such as activated carbon, acidic ion-exchange resin, or SiO_2 or ZrO_2 powders.^{17–19} Supporting HPW on high area solids generally improves its catalytic performance. Literature also reveals that ionic interactions between the support surface and HPW clusters help to generate the active species during the impregnation step. However, because of the weak nature of this interaction it is possible for HPW clusters to leach from the support during reactions in polar solvents.²⁰ Polyoxotungstates of Zr are well known²¹ and are proposed to form *via* interactions between WO_3 and zirconia. Zr-exchanged Keggin structures of formula $\text{H}_5\text{PW}_{11}\text{ZrO}_{40}$ exhibit Lewis acidity due to incorporation of Zr within the cage.²² In an analogous way, the successful growth of a polyoxotungstate cluster about a tethered Zr- PO_4 group, such as those found in the framework of a metal phosphate support (Scheme 1), could be used to form a bound Keggin-like cluster which may be stable under polar solvents.

While there are many investigations of the structural and acidic properties of WO_x/ZrO_2 solid acids,²³ to date there have been no studies of the interaction of WO_x with porous phosphate supports. Here we report on the synthesis, characterisation and application of zirconium phosphate (ZrP) supported WO_x catalysts in the esterification of palmitic acid with methanol, and investigate whether it is possible to form Keggin like structures on the surface of the porous phosphate support.

Experimental

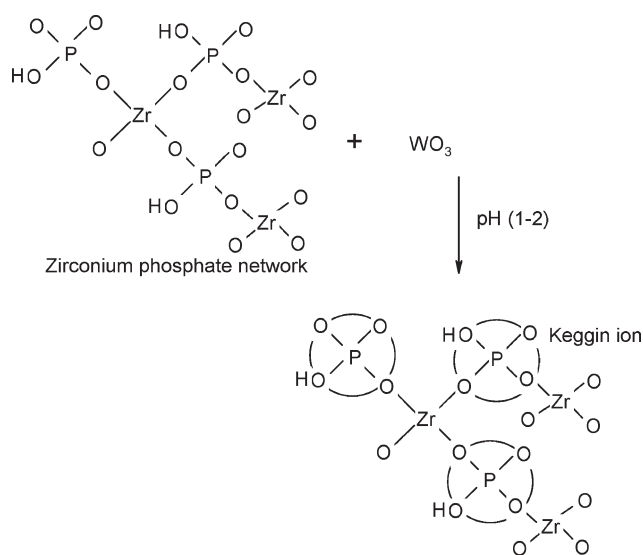
Catalyst preparation

Porous zirconium phosphate. A simple hydrothermal synthesis procedure was used²⁴ during which 0.01 mol of zirconium n-propoxide, (70 wt% solution in 1-propanol, Aldrich) was added drop wise to a 60 mL solution of H_3PO_4 (0.1 mol L^{-1}) under stirring. After a further 2 h stirring at room temperature,

^aDepartment of Chemistry, University of York, Heslington, York, UK YO10 5DD. E-mail: kw13@york.ac.uk; Fax: +44 1904 432516; Tel: +44 1904 432586

^bTechnical Chemistry, University of Kaiserslautern, Erwin-Schrödinger-Straße, 67663, Kaiserslautern, Germany

^cDepartment of Chemistry, University of Hull, Cottingham Road, Hull, UK HU6 7RX



Scheme 1 Possible route to Keggin ion formation *via* grafting of WO_x to the surface of zirconium phosphate.

the obtained mixture was transferred into a Teflon lined autoclave and aged statically at 80 °C for 24 h. The final material was filtered, dried and calcined at 400 °C.

A series of supported WO_x catalysts were prepared with W loadings over the range 1 to 25 wt%. Simple wet impregnation was employed, involving dissolution of the required amount of sodium tungstate (Aldrich 99%) in 20 mL distilled water in a round-bottomed flask, followed by addition of the porous zirconium phosphate support material. The pH of the contents was maintained at ~ 2 *via* addition of dilute HCl. The resulting mixture was left overnight followed by evaporation to a dry, free flowing powder at 60 °C under vacuum. No further pre-treatments were applied to any catalysts, which were stored in air prior to analysis and reaction testing. The following nomenclature was applied for the sample codes: ZrP means “zirconium phosphate”.

WO_3/ZrO_2 . A reference 10 wt% WO_3/ZrO_2 sample was prepared by simple wet impregnation of ZrO_2 (Engelhard) with an aqueous solution of sodium tungstate. The slurry was stirred for 2 h then evaporated to dryness and calcined in air at 400 °C for 4 h.

Catalyst characterization

Nitrogen porosimetry was undertaken on a Micromeritics ASAP 2010 instrument. Surface areas were calculated using a 5–10 point BET plot over the range $P/P_0 = 0.02$ – 0.2 , where a linear relationship was maintained, while pore size distributions were calculated using the Barrett–Joyner–Halenda (BJH) model up to $P/P_0 = 0.6$. DRIFT spectra were obtained using a Bruker Equinox FTIR spectrometer. Samples were diluted in KBr prior to analysis. FT-Raman spectra were collected in 180° scattering geometry from neat samples using a Bruker FRA106/S Raman module mounted on a Bruker Equinox 55 FTIR bench with a cw Nd-YAG 1064 nm laser operating at 100–400 mW, a CaF_2 beamsplitter and liquid nitrogen cooled Ge detector.

Powder X-ray diffraction patterns were collected on a Siemens-AXS D5005 diffractometer using $\text{Cu K}\alpha$ radiation. Zr and P bulk composition of pure support was determined by ICP-OES method at MEDAC LTD analytical and chemical services, Surrey, UK. The bulk chemical composition of W impregnated samples was determined using a Hitachi atomic absorption spectrometer.

XPS measurements were performed using a Kratos AXIS HSi instrument equipped with a charge neutraliser and $\text{Al K}\alpha$ X-ray source. Spectra were recorded at normal emission with an analyser pass energy of 40 eV, and X-ray power of 225 W. Energy referencing was employed using C 1s and the valence band. Spectra were Shirley background-subtracted across the energy region and fitted using CasaXPS Version 2.1.9. Due to overlap of the W 4f and Zr 4p states, quantification of all samples were performed using the W 4d transition.

^{31}P MAS NMR spectra were obtained in single pulse (‘ZG’) mode (3.5 ms pulse, and 8 s delay between pulses) on a Bruker Avance 400 spectrometer, operating at a frequency of 161.98 MHz. NMR measurements were performed in 4 mm outer-diameter rotors, with a sample spin rate of 10 kHz employed. Spectra were referenced externally to sodium dihydrogen phosphate (0.0 ppm). Line broadening of 10 Hz was applied when processing the spectra.

UV-Vis spectra were recorded using a JASCO-V550 spectrophotometer. The measurement of Hammett acid strength (H_0) was carried out by exposing samples (0.1 g), previously evacuated at 100 °C for 2 h, to a known amount of cyclohexane solution of selected Hammett indicators (4-nitroaniline, $\text{p}K_a = +1.0$; 4-phenylazoaniline, $\text{p}K_a = +2.8$; dicinnamalacetone, $\text{p}K_a = -3.0$). UV-Vis spectra of the air dried samples were recorded to quantify the amount of indicator adsorbed on the surface of the catalyst.

Pyridine TPD measurements were performed to titrate the total number of acid sites, using a 16 channel 200 amu quadrupole mass spectrometer (ESS) coupled to a 1500 °C PID-controlled tube furnace heated flow microreactor. A 250 mg catalyst sample was saturated with pyridine (HPLC grade, Aldrich >99.9%) and then dried under vacuum at 100 °C for 2 h to remove physisorbed pyridine prior to analysis. The desorption pattern was recorded by following the 79 amu MS channel while heating the sample to 625 °C at a rate of 10 °C min^{-1} under a steady flow of helium (80 ml min^{-1}) carrier gas. During the TPD mass channels 18 (H_2O), 28 (CO), 44 (CO_2), 95 (pyridine-*N*-oxide) and 158 (pyridine dimer) amu were also followed to check for any pyridine decomposition or oxidation products. The amount of pyridine evolved was determined by comparing the areas desorbed from the sample with those of known amounts of injected pyridine.

Reactivity

Reactions were performed in a stirred batch reactor with samples withdrawn periodically for analysis using a Shimadzu GC17A Gas Chromatograph fitted with a DB1 capillary column (film thickness 0.25 mm, id 0.32 mm, length 30 m), and AOC 20i auto sampler. Esterification reactions were performed at 60 °C using 0.05 g of catalyst, 5 mmol of palmitic acid (Aldrich 98%), 0.0025 mol (0.587 cm^3) hexyl ether

(Aldrich 97%) as internal standard, and 0.3036 mol (12.5 cm³) methanol (Fisher 98%). Reaction profiles were followed for a period of 6 h and continued for 24 h to assess limiting conversions. Initial rates were determined at <20% conversion, which depending on the activity of the catalyst corresponded to ~1–3 h on stream.

Results and discussion

The composition of the as prepared ZrP support material was first verified by elemental analysis which revealed that the sample contained 48.4 wt% Zr and 12.2 wt% P. This was in good agreement with surface composition determined from XPS of 42.9 wt% Zr and 13 wt% P, suggesting that the support material is homogeneous with negligible surface segregation of P or O. The slightly increased P content in XPS is consistent with attenuation of the Zr 3d signal by surface terminating PO₄ groups. The calculated atomic Zr/P ratio also closely matches the formula (ZrO₄)₃(PO₃H)₃. Powder XRD revealed that the sample was largely amorphous, consistent with previous reports on related zirconium phosphates such as Zr₃(OH)₆(PO₄)₄, following low temperature (400 °C) anneals.²⁵

Fig. 1 shows the N₂ adsorption isotherm of the parent ZrP support calcined at 400 °C. The isotherm exhibits a high uptake of N₂ at low relative pressures (P/P_0) of 0.1–0.4, indicating the presence of pore sizes ranging 1–2 nm (between micropore and mesopore regime). BJH analysis of the pore size distribution on the adsorption isotherm reveals a narrow pore size distribution (Fig. 1 inset) centred around 1.2 nm. The specific surface area, pore volume and surface/bulk W content of the resulting WO₃ impregnated catalysts are presented in Table 1. The high ZrP specific surface area of 409 m² g⁻¹ with pore volume of 0.516 cm³ g⁻¹ is comparable to that of previously reported surfactant-templated mesoporous zirconium dioxide.²⁶ Following impregnation with WO₃, a progressive decrease in surface area and pore volume is observed with increasing W loading (3.6–25 wt%). Although the surface areas and pore volumes decrease with WO₃ loading, a high

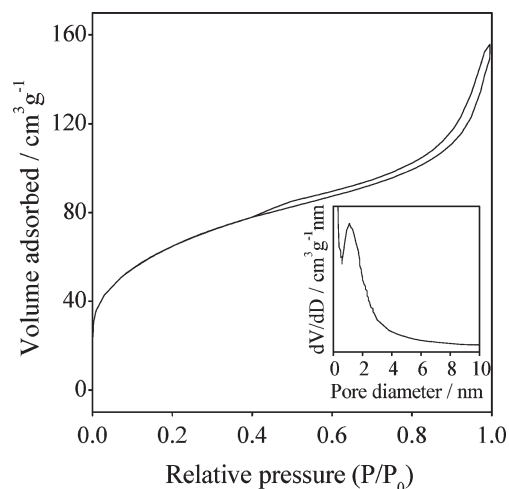


Fig. 1 N₂ adsorption–desorption isotherm for ZrP; inset: BJH pore size distribution.

Table 1 Physical properties of ZrP supported W catalysts

Sample	Bulk W (wt%)	Surface W (wt%)	Surface area/m ² g ⁻¹	Pore volume/cm ³ g ⁻¹
ZrP			409 ± 20	0.516
5 wt% W	3.6	3.7	372 ± 18	0.471
10 wt% W	6.3	5.0	288 ± 14	0.402
15 wt% W	7.8	6.5	201 ± 10	0.384
20 wt% W	13.8	10.7	174 ± 9	0.298
25 wt% W	25.1	12.2	101 ± 5	0.176

surface area 100 m² g⁻¹ can still be obtained even after a 25 wt% W loading. The surface W loading of all the supported samples was less than the bulk value suggesting that in lower loading samples, WO_x species do not completely wet the ZrP surface and preferentially form 3-D clusters.

Fig. 2 shows the variation in surface area and surface W content as a function of bulk tungsten loading. The surface W coverage rose continuously as a function of bulk content, with a slight plateau obtained around ~5 wt% W, followed by a rapid rise for bulk loadings in excess of 10 wt% W. This variation is suggestive of in-pore adsorption of WO_x species for low loadings, with the onset of multilayer/crystalline growth occurring at higher coverages. This observation is consistent with the variation in accessible pore volume which remains high up to 7.8 wt% W, before falling dramatically at higher loadings indicative of micropore blockage.

DRIFT spectra of the supported catalysts are shown in Fig. 3. ZrP exhibits a broad envelope centred at 1080 cm⁻¹, arising from the strong Zr–O–P network, while the band at 1630 cm⁻¹ corresponds to the surface hydroxyl groups.²⁷ An additional peak was observed at 820 cm⁻¹ in all the impregnated samples, attributable to the W–O_c–W vibration of two connecting WO₆ octahedra. With increasing W loading, the broad envelope also sharpens and the peak centre shifts to 1070 cm⁻¹, suggesting either a change in the phosphorus tetrahedron symmetry within the support, or the evolution of an asymmetric W–O–W mode. It is also noteworthy that a band was observed at 640 cm⁻¹ for all impregnated samples which can be assigned to a Zr–O_b vibration. Since this band

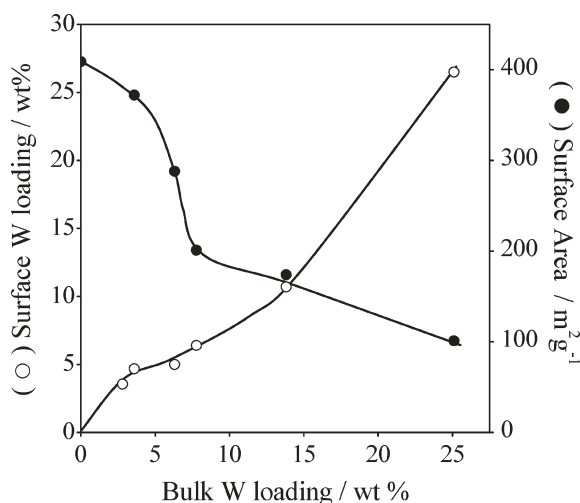


Fig. 2 Surface area and surface W loadings as a function of bulk W content.

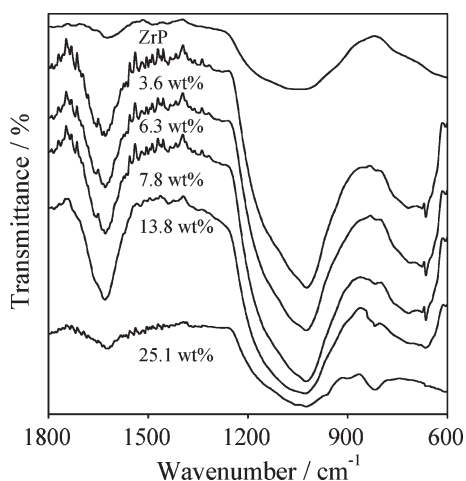


Fig. 3 DRIFT spectra of ZrP and supported WO_x catalysts.

was absent from the ZrP support, it may arise from a Zr–O–W stretching vibration as postulated by Chauveau *et al.*²⁸ It is well known that HPW exhibits characteristic bands at 1070 cm^{-1} , 980 cm^{-1} and 890 cm^{-1} , respectively assigned to (P–O_d), (W–O_t) and (W–O_b–W) asymmetric stretches.²⁹ These frequencies are generally consistent with those observed in the 25 wt% W sample, however their similarity to features also observed in dispersed WO_3/ZrO_2 make conclusive identification of Keggin-like species in our impregnated samples impossible by DRIFTS alone.

Raman spectra are however more sensitive to differences in polyoxotungstate environments. Fig. 4 shows Raman spectra for a series of standard $\text{H}_3\text{PW}_{12}\text{O}_{40}$, Na_2WO_4 and cubic WO_3 samples, along with 3.6 and 25 wt% WO_3/ZrP samples. ZrP exhibits a broad feature at 1026 cm^{-1} attributed to the Zr–PO₄ network.³⁰ Following impregnation with 3.6 wt% W a small band appears at 993 cm^{-1} , which at higher loading evolves into two partially resolved features at 978 and 995 cm^{-1} . Na_2WO_4 and WO_3 exhibit main features at 835 ($\nu_{\text{as}}\text{WO}_4^{2-}$) and 930 ($\nu_{\text{s}}\text{WO}_4^{2-}$) cm^{-1} , and 712 ($\delta\text{W-O}$) and 802 cm^{-1} ($\nu\text{W-O}$) respectively.³¹ None of these correspond to the bands observed for the W-doped ZrP samples, which cannot

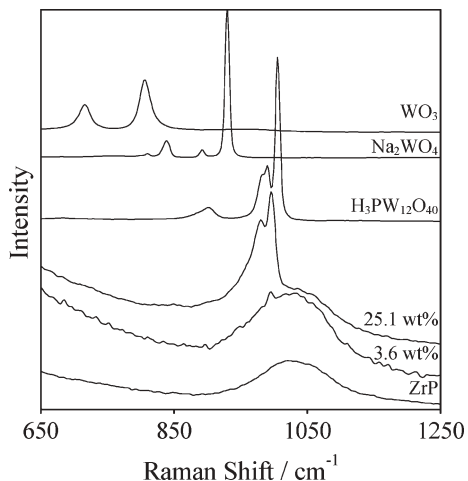
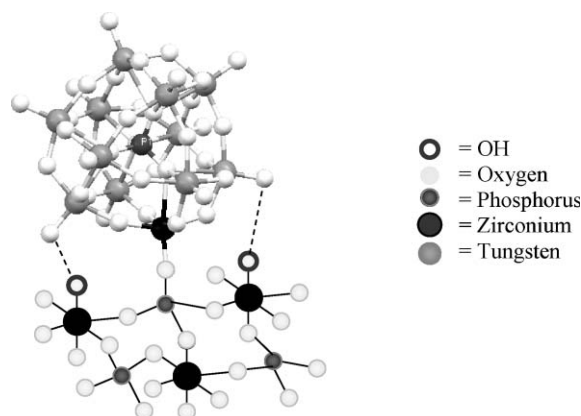


Fig. 4 FT-Raman spectra of ZrP and supported WO_x catalysts.

therefore be attributed to bulk tungstate species. Detailed Raman studies of WO_3/ZrO_2 reveal typical modes for tungstate species occur at either 1019 cm^{-1} , characteristic of terminal $\text{W}=\text{O}_{\text{sym}}$ of dispersed poly and mono tungstate species, or 808 and 720 cm^{-1} , characteristic of crystalline WO_3 which tends to dominate at high loadings,³² which are again inconsistent with our impregnated ZrP materials. In contrast the Raman of bulk HPW exhibits bands at 897 , 980 , 989 and 1005 cm^{-1} for $\nu_{\text{as}}(\text{W-O-W})$, $\nu_{\text{as}}(\text{W-O}_t)$, $\nu_{\text{as}}(\text{W-O}_t)$ and $\nu_{\text{s}}(\text{W-O}_t)$ respectively,³³ which are more consistent with the observed modes for our supported WO_x/ZrP samples. The apparent red shift for the first 2 bands is consistent with Raman measurements of HPW on ZrO_2 where modes at 997 , 981 and 950 cm^{-1} are observed for a 25 wt% HPW/ ZrO_2 loading³⁴ and suggests weakening of the W=O bonds on interaction with ZrO_2 . Together these results suggest that a Keggin-like structure is formed through the interaction of WO_x with ZrP under acidic conditions. However the formation of spherical Keggin cages is not likely on the surface of ZrP without Zr^{4+} coordination to four bridging oxygen atoms of tungstate within the cage as illustrated in Scheme 2. This is not an unreasonable suggestion as in a recent communication Gaunt *et al.*³⁵ reported the synthesis of Zr(IV) coordinated Keggin and lacunary Keggin ions, in which a strong interaction between Zr(IV) and W–O species in the Keggin ion is observed. Formation of such a species would require monodentate surface PO₄ species. Hydrogen bonding to the cage may be observed between adjacent Zr–OH which would be expected to balance the Zr coordination sphere adjacent to monodentate PO₄.

Further support for the formation of a Keggin-like cage can be found from the ³¹P MAS NMR chemical shift which is very sensitive to the nature of Keggin ion present in the phosphate based materials. ³¹P MAS NMR spectra of the catalysts are shown in Fig. 5. ZrP shows a broad peak between -12 ppm and -22 ppm, attributed to a tetrahedral phosphorus environment bound to one hydroxyl group and three ZrO₄ units.³⁶ Comparing this observed chemical shift with that in the literature, we therefore assign this broad signal to phosphorus atoms with two or three P–O–Zr bonds. The higher the chemical shift of the ³¹P signal, the greater the number of



Scheme 2 Possible interaction of an *in situ* constructed Keggin cage with the surface Zr–PO₄.

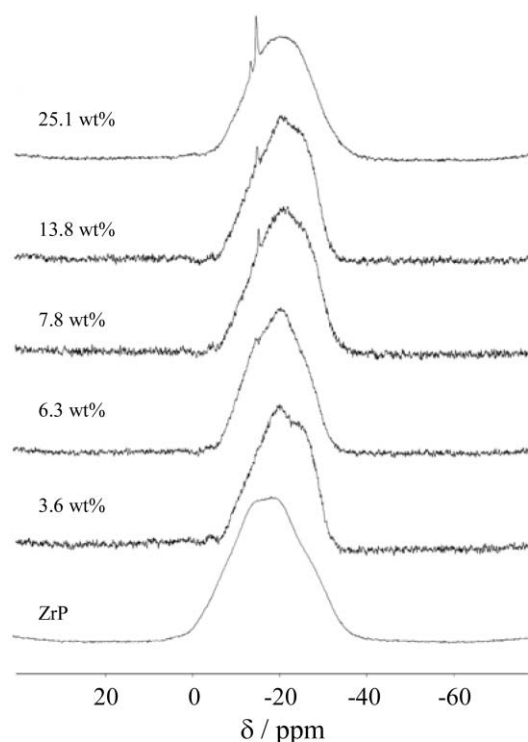


Fig. 5 ^{31}P MAS NMR spectra of WO_x impregnated zirconium phosphate.

Zr–O–P bonds. We did not see any signal at 28 to 30 ppm corresponding to P–O–P bonds, which generally form *via* condensation of phosphate species during calcination. The P environment is clearly perturbed following WO_3 impregnation, with a small, sharp peak at -14.6 ppm emerging with increasing W loading, and an additional peak also visible at -13.3 ppm in the highest loading sample. Bulk HPW (hexahydrate form) normally exhibits a ^{31}P signal at -15.1 ppm.³⁷ Supported heteropolyanion species exhibit peaks which are generally shifted down field due to perturbation of the phosphorus tetrahedron symmetry during immobilisation.³⁸ The peak at -14.6 ppm could thus be attributed to an interfacial species like $(\equiv\text{ZrOH}_2^+)[\text{PW}_{11}\text{O}_{39}]^{5-}$ as suggested in Scheme 2. Such interfacial species could form in acidic media during preparation, through the reaction of WO_3 with phosphorus tetrahedra and protonation of Zr–OH groups leading to ZrOH_2^+ formation; the latter acting as counter ions to the polyanion. The intensity of the peak at -14.6 ppm increases with W loading consistent with an interfacial species on the surface of the support. The peak at -13.3 ppm which emerges for the 25 wt% W loading could be assigned to lacunary-type heteropoly anions, such as $[\text{PW}_{11}\text{O}_{39}]^{7-}$ which may form around polydentate PO_4 species. Indeed, lacunary $[\text{PW}_{11}\text{O}_{39}]^{7-}$ species are expected to give a ^{31}P chemical shift of -10.5 ppm,³⁹ however when bound to SiO_2 surfaces these exhibit a ^{31}P chemical shift of -13.5 ppm⁴⁰ consistent with our observations. However species with a ^{31}P chemical shift of -13.5 ppm have also been attributed to dimeric species⁴¹ such as $[\text{P}_2\text{W}_{21}\text{O}_{71}]^{6-}$ or $\alpha\text{-}[\text{P}_2\text{W}_{21}\text{O}_{62}]^{6-}$, which exhibit peaks at -13 and -13.5 ppm, and their formation cannot therefore be discounted at high loadings.

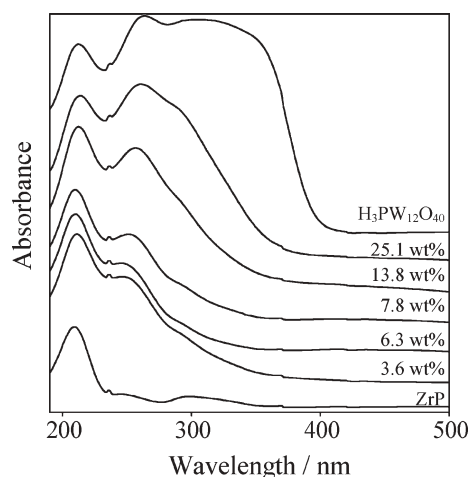


Fig. 6 UV-Vis spectra of ZrP and supported WO_x catalysts.

UV-Vis spectra of all the supported WO_x samples are presented in Fig. 6, along with a spectrum of pure HPW for comparison. The parent ZrP showed a band at 300 nm, which may be due to Zr(IV) cations interacting with the phosphate counter anions in the framework.⁴² HPW shows a band at 260 nm, arising from the oxygen–metal charge-transfer band of the tungstophosphate anion $[\text{PW}_{12}\text{O}_{40}]^{3-}$.⁴³ The lower loading 3.6–7.8 wt% W samples all show a band at ~ 220 nm which grows steadily with loading. Since this wavelength is just below that expected for bulk HPW, it may be indicative of the formation of stable Keggin units such as those reported by Vazquez *et al.*⁴³ who made similar observations in supported HPW catalysts. However UV-Vis cannot differentiate WO_6 clusters in a polyoxotungstate from those in a Keggin structure, and assignments of the latter should be treated with caution. The spectra for the 13.8 and 25.1 wt% W catalysts broaden and shift to 260 nm, resembling the spectrum of bulk HPW. Similar shifts are observed for SiO_2 supported HPW and this peak broadening maybe reflect interactions between neighbouring Keggin units, or the presence of crystalline H_2O .

Powder XRD showed no evidence of crystallized ZrPO_4 or ZrO_2 phases for any sample, except for pure ZrP calcined at 900°C which showed diffraction peaks corresponding to ZrO_2 phase likely due to the break up of the Zr–O–P network (Scheme 1). The absence of HPW reflections for the supported samples confirms grafted tungstate species do not form aggregates with characteristics of the Keggin extended secondary structure. Previous studies support that HPW dispersed over porous solids such as carbon, SiO_2 and alumina does not give rise to diffraction features for loadings below ~ 40 wt% HPW.

The surface tungsten chemical environment was followed by XPS as a function of W loading (Fig. 7). The pure parent HPW shows a spin orbit split doublet (spin orbit splitting = 2.1 eV) with the $4f_{7/2}$ component centred at 35.2 eV. The W $4f_{7/2}$ core level binding energy (BE) for the pure HPW corresponds to a W(VI) species.⁴⁴ At low WO_x coverages the W $4f_{7/2}$ lies at lower BE around 34.8 eV. Given the Raman spectra indicate bulk WO_3 and Na_2WO_4 species are not present in this regime, we tentatively assign this perturbed state to the interfacial Keggin-like species. Indeed we recently

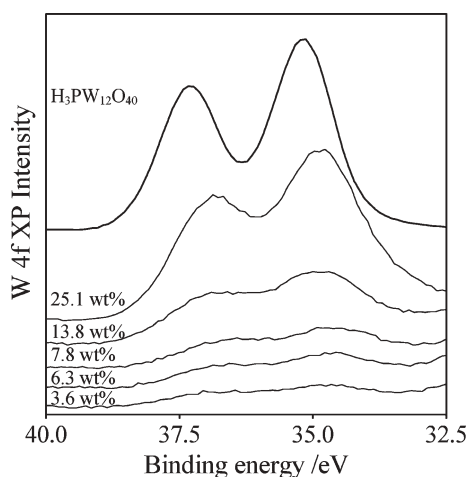


Fig. 7 W 4f XP spectra of ZrP and supported WO_x catalysts.

observed a similar low BE shift for $\text{W}=\text{O}$ species within $\text{H}_3\text{PW}_{12}\text{O}_{40}$ monolayers over a SiO_2 support.⁴⁵

The acidic properties of these supported WO_x materials were subsequently studied by pyridine TPD and Hammett indicator methods. The acid strength of the parent ZrP lies between $H_0 = +1.0$ and $+2.8$, while the WO_x grafted materials exhibit stronger acidities ranging from $H_0 = -3.0$ and $+2.8$. These values all significantly lower than that of pure HPW which lies below $H_0 = -8.2$. The UV-Vis spectra from samples treated with 4-phenylazoaniline indicator ($\text{p}K_a = +2.8$), which gives rise to a strong absorbance at 510 nm, are shown in Fig. 8. It is clear that the intensity of the 510 nm band, and thus concentration of adsorbed indicator and acid site density, increases following tungstate impregnation of ZrP, and with increasing W loading. In contrast a 10 wt% WO_3/ZrO_2 sample exhibits only weak surface acidity, showing negligible change upon 4-phenylazoaniline adsorption.

Pyridine thermal desorption from both pure and 25 wt% W-doped ZrP are shown in Fig. 9. A small increase in the total surface pyridine concentration (number of acid sites) is seen with increasing WO_x content. ZrP exhibited a broad low temperature desorption peak at 110 °C, with a small high

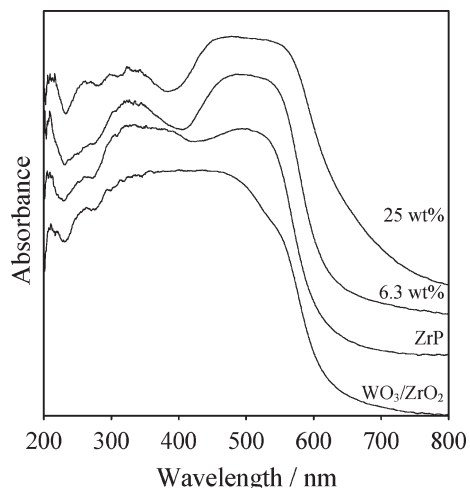


Fig. 8 DRUV spectra of 4-phenylazoaniline adsorbed catalysts.

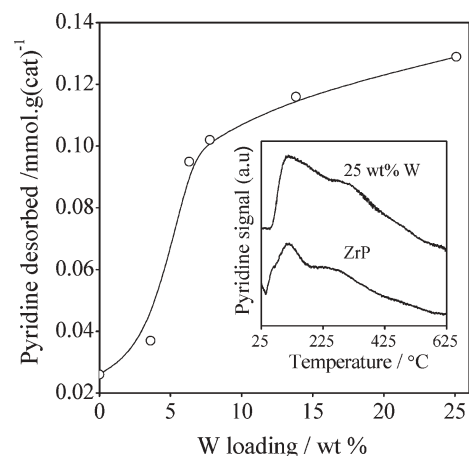


Fig. 9 Integrated pyridine desorption area. (Inset shows raw desorption data).

temperature state at 250 °C. The moderate acid strength of the parent ZrP can be attributed due to the presence of surface $\text{Zr}-\text{OH}$ and $\text{P}-\text{OH}$ groups. Upon impregnation with 25 wt% W, the high temperature desorption peak shifts up to 310 °C. This temperature increase indicates a rise in the Brønsted acidity of the materials, and suggests that both the acid strength, and surface density, increase upon addition of WO_x ions to the ZrP support in line with the Hammett indicator measurements.

The catalyst series were tested in the esterification of palmitic acid with methanol. Fig. 10 shows the resulting reaction profiles which demonstrate that the weakly acidic pure ZrP shows poor activity, reaching only 20% conversion after 6 h.²⁴ Catalyst performance improved dramatically following W impregnation, with activity rising with loading up to a maximum around 6.3–7.8 wt% W, before falling off at higher loadings. These results compare favourably with SBA-15- SO_3H systems, wherein 85% palmitic acid conversion was only attained after 3 h reaction at 85 °C with twice the mass of catalyst.⁹ The variation in catalyst turn over frequency (TOF) with W loading is shown in Fig. 11. The maximum TOF

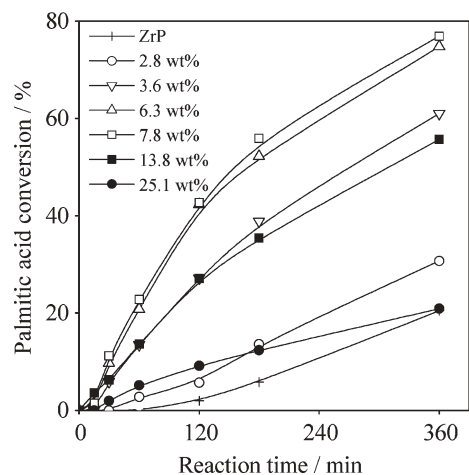


Fig. 10 Palmitic acid conversion during esterification with methanol using W-doped ZrP catalysts.

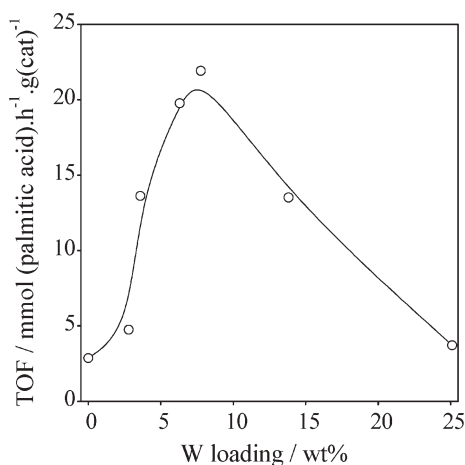


Fig. 11 TOF of W-doped ZrP catalysts in palmitic acid esterification as a function of W content.

of 21.9 mmol h⁻¹ g(cat)⁻¹ was attained at 7.8 wt% W. The limiting 24 h conversion levels are shown in Table 2; all the catalysts approach complete conversion. In all cases the selectivity to methyl palmitate was observed to be >98%.

Even though pyridine TPD suggest that the 13.8 wt% W and 25.1 wt% W catalysts possess more acid sites than their lower loading counterparts, they show much reduced esterification activity. This poorer performance may be attributed to the formation of undesirable species such as lacunary or dimeric Keggin ions on the surface of the support as suggested by MAS NMR, or more likely pore blockage at these higher loadings which prevent the bulky fatty acid from accessing the acid sites. In contrast smaller molecules such as pyridine remain able to diffuse through these constricted pores and titrate a greater number of acid sites. Similar observations have been reported for WO₃/ZrO₂ systems⁴⁶ where a decrease in catalyst activity at high WO₃ loading has been attributed to condensation of W–OH groups and formation of 3-D WO_x clusters which reduce acidity.

The stability and reusability of the optimum 7.8 wt% W supported catalyst was explored *via* hot filtration post-reaction, methanol washes and a final 110 °C drying step. Fig. 12 shows palmitic acid conversion over two consecutive runs, from which it is clear that there is negligible deactivation following one recycle. UV-Vis spectra of the spent catalysts (not shown) were also recorded with the spectra of both fresh and spent catalysts indistinguishable. Simple immobilisation of HPW would not be expected to generate a catalyst capable of withstanding such treatments in polar media. These

Table 2 Conversion of palmitic acid after 24 h reaction with methanol

Catalyst	Palmitic acid conversion (%)
ZrP	78
2.8 wt% W	83
3.6 wt% W	85
6.3 wt% W	95
7.8 wt% W	100
13.8 wt% W	95
25.1 wt% W	75

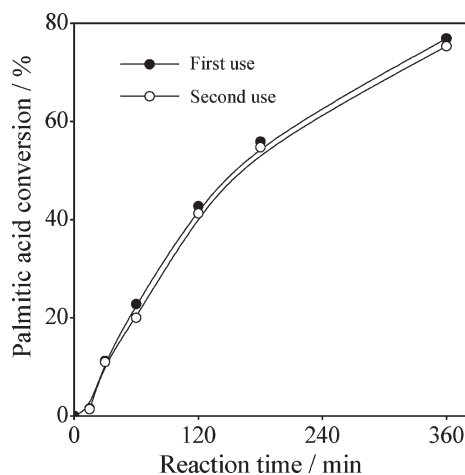


Fig. 12 Reuse of 7.8 wt% W-doped ZrP in palmitic acid esterification.

observations demonstrate that ZrP is an excellent support for stabilising high activity tungstate species for esterification and biodiesel synthesis.

Conclusions

Porous, zirconium phosphate supported WO_x materials, with W loadings ranging between 1 and 25 wt% have been investigated for solid acid catalysed esterification. Raman and ³¹P MAS NMR indicate the formation of a Keggin-like surface structure from the reaction of tungstate with exposed Zr–PO₄ groups. Pyridine TPD and Hammett indicator measurements reveal the WO_x impregnated catalysts possess stronger acidity and more acid sites than the porous phosphate support, and that acid site density scales with WO_x loading. All supported WO_x catalysts showed high activity in the esterification of palmitic acid with methanol, with the highest activity observed around 7.8 wt% W. These catalysts are resistant to leaching, readily recovered, and can be recycled without major activity loss.

Acknowledgements

K. N. Rao thanks the Royal Society, London, UK for the award of a Royal Society Indian Fellowship.

References

- H. Fukuda, A. Kondo and H. Noda, *J. Biosci. Bioeng.*, 2001, **92**, 405.
- F. Ma and M. A. Hanna, *Bioresour. Technol.*, 1999, **70**, 1.
- B. Freedman, R. O. Butterfield and E. H. Pryde, *J. Am. Oil Chem. Soc.*, 1986, **63**, 1375.
- H. Nouredini and D. Zhu, *J. Am. Oil Chem. Soc.*, 1997, **74**, 1457.
- R. S. Watkins, A. F. Lee and K. Wilson, *Green Chem.*, 2004, **6**, 335.
- D. G. Cantrell, L. J. Gillie, A. F. Lee and K. Wilson, *Appl. Catal., A*, 2005, **287**, 183.
- M. Canakci and J. Van Gerpen, *Trans. ASAE*, 2003, **46**, 945.
- A. Corma and H. Garcia, *Catal. Today*, 1997, **38**, 257.
- I. K. Mbaraka, D. R. Radu, V. S. Y. Lin and B. H. Shanks, *J. Catal.*, 2003, **219**, 329.
- A. Corma, H. Garcia, S. Iborra and J. Primo, *J. Catal.*, 1989, **120**, 78.
- H. B. Zhang, B.-Z. Zhang and H.-X. Li, *J. Nat. Gas Chem.*, 1992, **49**.

- 12 F. S. Guner, A. Srikecioglu, S. Yilmaz, A. T. Erciyes and A. Erdem, *J. Am. Oil Chem. Soc.*, 1996, **73**, 347.
- 13 M. Saroja and T. N. B. Kaimal, *Synth. Commun.*, 1986, **16**, 1423.
- 14 K. Ramalinga, P. Vijayalakshmi and T. N. B. Kaimal, *Tetrahedron Lett.*, 2002, **43**, 879.
- 15 W. Chu, X. Yang, X. Ye and Y. Wu, *Appl. Catal., A*, 1996, **145**, 125.
- 16 N. Mizuno and M. Misono, *Chem. Rev.*, 1998, **98**, 199.
- 17 R. T. Sebulsty and A. M. Henke, *Ind. Eng. Chem. Proc. Des. Dev.*, 1971, **10**, 272.
- 18 Y. Izumi and K. Urabe, *Chem. Lett.*, 1981, 663.
- 19 A. Concellon, P. Vazquez, M. Blanco and C. Caceres, *J. Colloid Interface Sci.*, 1998, **204**, 256.
- 20 J. B. Moffat and S. Kasztelan, *J. Catal.*, 1988, **109**, 206.
- 21 R. Villanneau, H. Carabineiro, X. Carrier, R. Thouvenot, P. Herson, F. Lemos, F. Ramo Ribeiro and M. Che, *J. Phys. Chem. B*, 2004, **108**, 12465.
- 22 M. N. Timofeeva, *Appl. Catal., A*, 2003, **256**, 19.
- 23 S. Kubaa, P. Lukinskasa, R. K. Grassellia, B. C. Gates and H. Knözinger, *J. Catal.*, 2003, **216**, 353.
- 24 T. Z. Ren, Z. Y. Yuan and B. L. Su, *Chem. Commun.*, 2004, 2730.
- 25 D. Wang, R. Yu, N. Kumada and N. Kinomura, *Chem. Mater.*, 2000, **12**, 956.
- 26 Z. Y. Yuan, A. Vantomme, A. Leonard and B. L. Su, *Chem. Commun.*, 2003, 1558.
- 27 A. Clearfield and D. S. Thakurb, *Appl. Catal.*, 1986, **26**, 1.
- 28 F. Chauveau, J. Eberle and J. Lefebvre, *Nouv. J. Chim.*, 1985, **9**, 315.
- 29 W. Kuang, A. Rives, M. Fournier and R. Hubaut, *Appl. Catal., A*, 2003, **250**, 221.
- 30 D. Spielbauer, G. A. H. Mekhemer, T. Riemer, M. I. Zaki and H. Knotzinger, *J. Phys. Chem. B*, 1997, **101**, 4681.
- 31 S. Loridant, C. Feche, N. Essayem and F. Figueras, *J. Phys. Chem. B*, 2005, **109**, 5631.
- 32 D. G. Barton, M. Shtein, R. D. Wilson, S. L. Soled and E. Iglesia, *J. Phys. Chem. B*, 1999, **103**, 630.
- 33 A. J. Bridgeman, *Chem. Phys.*, 2003, **287**, 55.
- 34 E. López-Salinas, J. G. Hernández-Cortéza, I. Schifitera, E. Torres-García, J. Navarrete, A. Gutiérrez-Carrillo, T. López, P. P. Lotticic and D. Bersani, *Appl. Catal., A*, 2000, **193**, 215.
- 35 A. J. Gaunt, I. May, D. Collison and O. D. Fox, *Inorg. Chem.*, 2003, **42**, 5049.
- 36 A. Sayari, I. Moudrakovski and J. S. Reddy, *Chem. Mater.*, 1996, **8**, 2080.
- 37 I. V. Kozhevnikov, *Catal. Rev. Sci. Eng.*, 1995, **37**, 311.
- 38 F. Lefebvre, *J. Chem. Soc., Chem. Commun.*, 1992, 756.
- 39 M. T. Pope, *Heteropoly and Isopoly Oxometalates*, Springer-Verlag, Berlin, 1983.
- 40 Y. Yanga, Y. Guoa, C. Hu and E. Wanga, *Appl. Catal., A*, 2003, **252**, 305.
- 41 I. V. Kozhevnikov, K. R. Klotzstra, A. Sinnema, H. W. Zandbergen and H. van Bekkum, *J. Mol. Catal. A: Chem.*, 1996, **114**, 287.
- 42 M. Ziyada, M. Rouimia and J. L. Portefaixb, *Appl. Catal., A*, 1999, **183**, 93.
- 43 P. G. Vazquez, M. N. Blanco and C. V. Caceres, *Catal. Lett.*, 1999, **60**, 205.
- 44 C. D. Wagner, W. M. Riggs, L. E. Davis and J. F. Moulder, *Handbook of X-Ray Photoelectron Spectroscopy*, Perkin Elmer, Eden Prairie, MN, 1979.
- 45 A. D. Newman, A. F. Lee and K. Wilson, *Catal. Lett.*, 2005, **102**, 45.
- 46 C. D. Baertsch, K. T. Komala, Y.-H. Chua and E. Iglesia, *J. Catal.*, 2002, **205**, 44.

Long alkyl chain quaternary ammonium-based ionic liquids and potential applications

Juliusz Pernak,^{*e} Marcin Smiglak,^a Scott T. Griffin,^a Whitney L. Hough,^a Timothy B. Wilson,^a Anna Pernak,^b Jadwiga Zabielska-Matejuk,^c Andrzej Fojutowski,^c Kazimierz Kita^d and Robin D. Rogers^{*a}

Received 24th March 2006, Accepted 28th June 2006

First published as an Advance Article on the web 13th July 2006

DOI: 10.1039/b604353d

Due to the high interest in the applications of ionic liquids, new, cheaper, multifunctional ionic liquids which are easy to prepare are highly desired. Here, we present a new group of air- and moisture-stable, hydrophobic ammonium-based ionic liquids and their properties, including the single-crystal X-ray structure of benzethonium nitrate. These salts have utility as anti-bacterial, anti-fungal agents. Additionally, the potential application of these ionic liquids for wood preservation was tested with positive results. The toxicity of benzalkonium and didecylmethylammonium nitrates were studied and are presented herein.

Introduction

Quaternary ammonium salts (quats) are quite well known and have widespread industrial utilization due to their surface activity and other useful properties. In 1890, Menshutkin synthesized quats by the nucleophilic substitution reaction of tertiary amines with an alkyl halide, and the 'Menschutkin reaction' is still regarded as the best method for the preparation of quat salts.¹

Quats are generally known to be bioactive and have high anti-microbial activity, as has been shown for water-soluble compounds that contain alkyl chains of length C₈ to C₁₆. In alkylbenzyltrimethylammonium chloride, for example, the optimum alkyl chain length to kill *Pseudomonas aeruginosa* was found to be 14 carbon atoms.² One of the most thoroughly investigated anti-microbial quat salts is benzalkonium chloride, [BA][Cl], which is a mixture of homologues of alkylbenzyltrimethylammonium chlorides, with alkyl groups ranging between *n*-C₈H₁₇ and *n*-C₁₈H₃₇.

Recently, new applications for quats have been found in forming ionic liquids (ILs, salts that melt below 100 °C).³ The synthesis and properties of a group of hydrophobic ILs, based on relatively small aliphatic quaternary ammonium cations, [Me₃NR]⁺ or [Et₃NR]⁺ (R = C₃H₇, *n*-C₄H₉ or CH₂CH₂OCH₃), and on perfluoroalkyltrifluoroborate anions have been reported.⁴ Here, we report a novel, economic class of quat-based ILs, derived from common, ammonium-based halide cations with nitrate, nitrite, tetrafluoroborate, and bis(trifluoromethylsulfonyl)imide anions, along with their properties and potential applications.

Results and discussion

Synthesis and characterization

Quats, containing large cationic structures, such as didecylmethylammonium [DDA]⁺, benzalkonium [BA]⁺, and Hyamine 1622 (benzethonium) [HA1622]⁺ (Fig. 1), were synthesized by anion exchange reactions (at room temperature, in water) of the commercially inexpensive and broadly used quats: [DDA][Cl], [DDA][Br], [BA][Cl], and [HA1622][Cl], with inorganic and acidic sources of [NO₃]⁻, [NO₂]⁻, [BF₄]⁻, and [Tf₂N]⁻, with an efficiency of over 95%. All of the synthesized salts, [BA][NO₃], [DDA][NO₃], [HA1622][NO₃], [BA][BF₄], [DDA][Tf₂N], [DDA][NO₂], [BA][NO₂], and [BA][Tf₂N], are reported here for the first time. The only known example of a similar product was noted in the patent literature for [DDA][BF₄].^{5–12} That salt showed significant activity against bacteria and fungi^{6,9–12} and can form an emulsion with polyoxyethylene, exhibiting termite repellency comparable to that of pentachlorophenol.⁵

The prepared salts are all hydrophobic, except for the [NO₂]⁻ salts, which were partially water-soluble (which also explains the low efficiency (75–85% yields) of the synthesis of

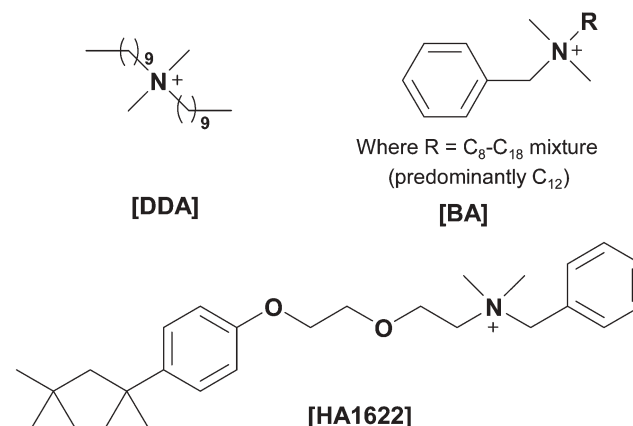


Fig. 1 Structures of the cations

^aDepartment of Chemistry and Center for Green Manufacturing, The University of Alabama, Tuscaloosa, AL, 35487, USA

^bUniversity of Medical Sciences in Poznań, Poznań, Poland

^cInstitute of Wood Technology, Poznań, Poland

^dThe Institute of Industrial Organic Chemistry, Branch Pszczyna, Poland

^ePoznań University of Technology, Faculty of Chemical Technology, Poznań, Poland

the nitrite salts). The concentration of water in the obtained salts was found to be temperature dependant. For example, [DDA][NO₃] at 20 °C was found to contain 0.4 g L⁻¹ water, with a decrease to 0.2 g L⁻¹ at 10 °C.

In the anion exchange reactions we report, both salts and acids can be used to supply the required anion. For example, in the production of [BA][NO₃], we have used NaNO₃, KNO₃, as well as 60% HNO₃. The efficiencies of the reactions proved to be independent of the applied salt or acid. When inorganic salts were used for the ion exchange reaction, the organic phase was washed with water until no chloride ions were detected using AgNO₃. When 60% HNO₃ was used, the product was easily purified by extraction of byproducts with distilled water.

[DDA][NO₃], [BA][Tf₂N], [DDA][Tf₂N], [BA][NO₂] were isolated as room temperature ionic liquids, while [BA][BF₄], [DDA][BF₄], and [DDA][NO₂] were waxes, and [HA1622][NO₃] was a solid. All isolated salts are nonvolatile, nonflammable, soluble in chloroform and ethyl acetate, and insoluble in hexane. Separation of phases using chloroform progressed rapidly and emulsification of the reaction mixture was avoided. After separation, the chloroform phase was transferred to a round-bottomed flask and rotovapped to remove the solvent. The product was dried under vacuum, at 80 °C for 12 h, and then stored over P₄O₁₀. The water content, determined by Karl-Fischer measurements, was found to be less than 500 ppm for all analyzed salts.

The prepared salts were characterized by ¹H and ¹³C NMR and elemental analysis. Only in the case of [BA]⁺ salts were slight shifts in proton spectra observed. These shifts pertained to the benzyl group and were determined to be related to anion interactions. The ¹H NMR spectra of [BA][Cl] showed two multiplets at 7.61 and 7.50 ppm for five aromatic protons and a singlet at 4.68 ppm for the CH₂ group. However, the spectra of the [BA]⁺ salts had a single multiplet at 7.52 and a singlet at 4.54 ppm. Reports indicate that even more distinct shifts in the spectra have been previously observed. In choline derivatives, e.g., for butoxymethyl(2-hydroxyethyl)dimethylammonium, the substitution of a small anion such as [Cl]⁻ for a large one [Tf₂N]⁻ resulted in proton signal shifts as much as 0.53 ppm.¹³

The thermal properties for the reported compounds were determined using DSC and TGA analyses (Table 1). The salts formed stable super-cooled phases. The best example of this was observed for [DDA][Tf₂N], with a glass transition

temperature (*T_g*) of -85.5 °C and an onset for thermal decomposition temperature (*T_{onset}*) of 376 °C. Melting points for [BA][NO₃] and [DDA][NO₃] were observed to be 36.3 °C and 18.8 °C, respectively.

The least thermally stable compounds proved to be the [NO₂]⁻-based salts, with *T_{onset}* of 160–190 °C. The decomposition temperatures of [NO₃]⁻ salts were higher and ranged between 215–230 °C. As compared to [BA][BF₄], which was stable up to 300 °C, [DDA][BF₄] underwent decomposition at 200 °C, losing 20% of its mass while the remaining product was stable until *T_{onset}* = 358 °C.

Literature data¹⁴ indicate that compounds based on the [Tf₂N]⁻ anion generally show high thermal stability. Our analyses confirmed this observation. [BA][Tf₂N] was stable up to 298 °C, while [DDA][Tf₂N] was stable up to 330 °C.

Additionally, we found that the melting point for [HA1622][NO₃], which was determined by DSC on heating, to be 85 °C, was lower than the melting point of the crystalline form of the product (92–94 °C) obtained by crystallization from the THF/anhydrous acetone/ethyl ether system.

The crystal structure of [HA1622][NO₃]¹⁵ was determined at -100 °C and is shown in Fig. 2. The [HA1622]⁺ cations pack in 2-dimensional layers which stack in alternating directions. Cations of the same orientation pack head-to-tail along the long (*c*) axis and stack down the short (*a*) axis. These stacks of like-oriented cations form columns of alternating cations and anions which are slightly offset from each other, creating hydrophobic and hydrophilic regimes. Layers of the same orientation of cations alternate with layers of the opposite orientation along the *b* direction. In Fig. 2, layers of the same orientation are seen to overlay, in a canted fashion, layers of the opposite orientation below when viewed in the *bc* plane.

CCDC reference number 602689. For crystallographic data in CIF or other electronic format see DOI: 10.1039/b604353d

As shown in Table 1, all the synthesized salts can be assigned to the class 'ionic liquids' (as defined by a melting point <100 °C). These ILs are stable in air, and while in contact with water and commonly used organic solvents. The densities of [DDA][NO₃] at 20 °C, [DDA][NO₂] at 20 °C, and [BA][BF₄] and [DDA][BF₄] at 80 °C are lower than that of water while all other salts are more dense than water. All of the prepared ILs are viscous, but become significantly less so upon modest heating or with the addition of water or organic solvents. Additionally, it was found that these salts, even

Table 1 Thermal properties of the prepared quaternary ammonium-based ILs

IL	<i>T_g</i> ^a	<i>T_{l-l}</i> ^b	<i>T_c</i> ^c	<i>T_{s-s}</i> ^d	<i>T_m</i> ^e	<i>T_{onset}</i> (5%) ^f	<i>T_{onset}</i> ^g
[BA][NO ₃]	-56.8	—	6.1	—	36.3	173	215
[DDA][NO ₃]	—	-19.8	—	—	18.8	189	234
[HA1622][NO ₃]	—	—	—	—	85.0 ^h	180	216
[BA][NO ₂]	-48.2	—	—	—	—	131	163
[DDA][NO ₂]	-93.3	—	-30.2	37.6; 67.2	-2.4	150	192
[BA][BF ₄]	-43.2	—	-21.8	—	56	251	305
[DDA][BF ₄]	—	-26.4	-3.0	55.5	27.5	183	(197) 358
[BA][Tf ₂ N]	-54.6	36.1; 71.8	—	—	—	298	346
[DDA][Tf ₂ N]	-85.5	—	—	—	—	330	376

^a Glass transition temperature determined by DSC on heating. ^b Liquid-liquid transition temperature determined by DSC on heating. ^c Crystallization temperature determined by DSC on heating. ^d Solid-solid transition temperature determined by DSC on heating. ^e Melting point determined by DSC on heating. ^f *T_{5%}*^{dec}, decomposition temperatures determined from onset to 5 wt% mass loss. ^g *T_{onset}*, decomposition temperatures determined from onset to 50 wt% mass loss. ^h mp 92–94 °C from THF/anhydrous acetone/ethyl ether.

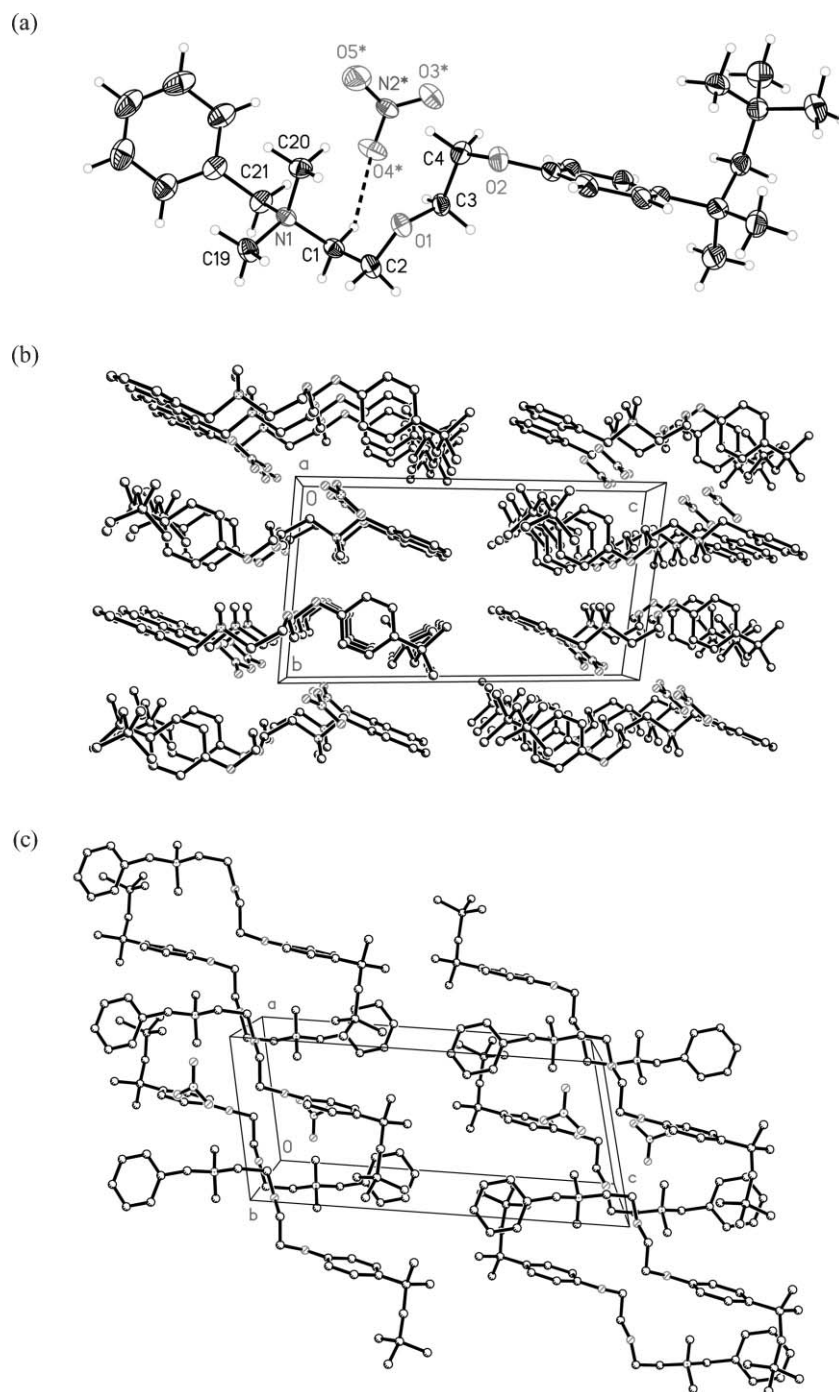


Fig. 2 (a) ORTEP illustration (50% probability ellipsoids) of [HA1622][NO₃] showing connectivity, conformation, and partial atom numbering scheme of the ions present in the asymmetric unit emphasizing the intermolecular contact with the largest negative difference from van der Waals separation (symmetry code for atoms labeled with * is $1 - x, 1 - y, -z$); (b) packing diagram showing alternating orientations of the 2-dimensional layers of [HA1622]⁺ cations packing in the *ac* direction; and (c) the overlay of oppositely orientated cations viewed down the *b* axis.

though highly hydrophobic, absorb small amounts (<2 wt%) of moisture from the atmosphere.

Biological activity

The biological activity of all of the prepared ILs was estimated and the minimum inhibitory concentration (MIC), and minimum bactericidal or fungicidal concentration (MBC)

were established. The studies were conducted on three strains of bacteria and one strain of fungi. MIC and MBC values for 4 strains of the prepared salts and the commercially available [DDA][Cl], [BA][Cl], and [HA1622][Cl] are compared in Tables 2 and 3.

The results demonstrate that the [NO₃]⁻ and [NO₂]⁻ salts are very effective agents against bacteria and fungi. Their activities are comparable to that of the original chlorides.

Table 2 MIC^a values of the studied ILs

Salts	<i>S. aureus</i>	<i>E. faecium</i>	<i>E. coli</i>	<i>C. albicans</i>
[BA][NO ₃]	4	4	16	16
[DDA][NO ₃]	2	4	8	8
[HA1622][NO ₃]	4	8	31.2	8
[BA][NO ₂]	4	8	16	16
[DDA][NO ₂]	4	4	8	16
[BA][BF ₄]	4	8	16	31.2
[DDA][BF ₄]	8	8	16	31.2
[DDA][Tf ₂ N]	31.2	31.2	62.5	62.5
[BA][Cl]	2	4	8	8
[DDA][Cl]	2	4	8	8
[HA1622][Cl]	2	2	16	8

^a MIC in µg mL⁻¹.**Table 3** MBC^a values of the studied ILs

Salts	<i>S. aureus</i>	<i>E. faecium</i>	<i>E. coli</i>	<i>C. albicans</i>
[BA][NO ₃]	16	62.5	62.5	31.2
[DDA][NO ₃]	16	31.2	31.2	16
[HA1622][NO ₃]	31.2	31.2	125	31.2
[BA][NO ₂]	31.2	31.2	31.2	31.2
[DDA][NO ₂]	31.2	31.2	62.5	16
[BA][BF ₄]	125	125	62.5	62.5
[DDA][BF ₄]	31.2	125	62.5	31.2
[DDA][Tf ₂ N]	>1000	>1000	>1000	>1000
[BA][Cl]	62.5	31.2	62.5	16
[DDA][Cl]	31.2	31.2	31.2	16
[HA1622][Cl]	16	62.5	125	31.2

^a MBC in µg mL⁻¹.

The [BF₄]⁻ salts proved to be slightly less effective, while [Tf₂N]⁻ salts exerted no anti-bacterial or anti-fungal effect. The [BA]⁺, [DDA]⁺, and [HA1622]⁺ salts were effective antimicrobial agents at concentrations below 100 µg mL⁻¹, with the solubility of the ILs in water playing a significant role. The [Tf₂N]⁻-based ILs were not soluble in water to concentrations higher than that of the lowest recorded MBC level (16 µg mL⁻¹) and thus, no real values of MBC could be established for these compounds. However, we conclude that all of the other synthesized salts of [NO₃]⁻, [NO₂]⁻, and [BF₄]⁻ anions can be successfully utilized for disinfection. When considering practical application and production costs, the [BA][NO₃] and [DDA][NO₃] salts are the most promising, and they may be regarded as cheap, hydrophobic, multifunctional ILs.

Wood preservation

Recently, ILs have also been studied for wood preservation^{16,17} and as effective anti-electrostatic agents for pine maple.¹⁸ Application of [BA][NO₃] and [DDA][NO₃] as a wood preservative proved to be effective. The effective dose (ED₅₀ and ED₁₀₀) and lethal dose (LD) values were established for the two [NO₃]⁻ salts, targeted for:

1. *Sclerophoma pityophila* fungus, belonging to imperfect fungi (*Deuteromycotina*), which causes blue discoloration of wood (Fig. 3),

2. *Trametes versicolor* fungus, causing white rot,

3. *Coniophora puteana* fungus, causing brown rot (Fig. 5), both belonging to the *Basidiomycotina* class which usually shows higher tolerance to fungicidal chemicals in biological reactions (Fig. 4).

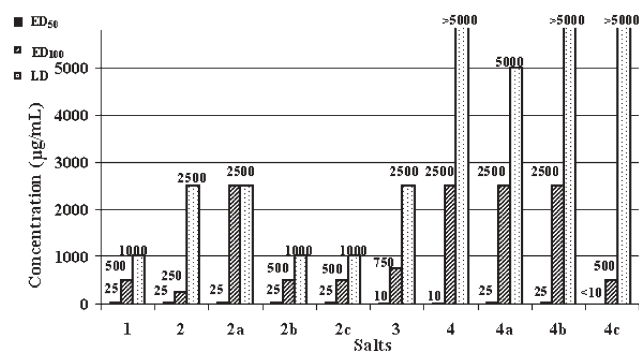


Fig. 3 The effective dose ED and the lethal dose LD of: 1 – [BA][Cl], 2 – [BA][NO₃], 2a – 60% w/w [BA][NO₃] and 40% w/w PEG-400, 2b – 60% w/w [BA][NO₃] and 40% w/w PEG-600, 2c – 60% w/w [BA][NO₃] and 40% w/w PPG-425, 3 – [DDA][Cl], 4 – [DDA][NO₃], 4a – 60% w/w [DDA][NO₃] and 40% w/w PEG-400, 4b – 60% w/w [DDA][NO₃] and 40% w/w PEG-600, 4c – 60% w/w [DDA][NO₃] and 40% w/w PPG-425, tested for *Sclerophoma pityophila*.

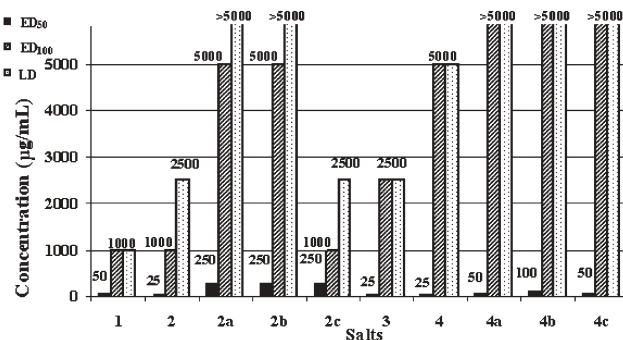


Fig. 4 The effective dose ED and the lethal dose LD of: 1 – [BA][Cl], 2 – [BA][NO₃], 2a – 60% w/w [BA][NO₃] and 40% w/w PEG-400, 2b – 60% w/w [BA][NO₃] and 40% w/w PEG-600, 2c – 60% w/w [BA][NO₃] and 40% w/w PPG-425, 3 – [DDA][Cl], 4 – [DDA][NO₃], 4a – 60% w/w [DDA][NO₃] and 40% w/w PEG-400, 4b – 60% w/w [DDA][NO₃] and 40% w/w PEG-600, 4c – 60% w/w [DDA][NO₃] and 40% w/w PPG-425, tested for *Trametes versicolor*.

The tested nitrate ILs showed the highest anti-fungal–fungistatic action and also exhibited a fungicidal action against wood attacking fungi. The activity of [BA][NO₃] against the fungi tested was more pronounced than that of [DDA][NO₃]. However, the action of the quaternary ammonium [NO₃]⁻ salts was less effective than that of the [Cl]⁻ salts which have been successfully used in wood preservation (Figs. 3–5).¹⁹

The nitrate-based ILs were mixed with polyethylene glycol of average molecular weight 400 (PEG-400) and 600 (PEG-600), as well as, polypropylene glycol of average molecular weight 425 (PPG-425), yielding stable solutions of 60% w/w IL and 40% w/w polyether. Figs. 3–5 show the anti-fungal activities of these mixtures (2a–c and 4a–c). The most effective mixture proved to be 2c (60% w/w [BA][NO₃]/40% w/w PPG-425). The values of ED₅₀, ED₁₀₀, and LD obtained for this salt were comparable to those of [BA][Cl] and were lowered by half in the case of *Sclerophoma pityophila*. In the latter case, addition of PPG-425 improved the effectiveness of [BA][NO₃] in contact with the mycelium. These results show that quaternary ammonium nitrate-based ILs are potentially applicable for wood preservation.

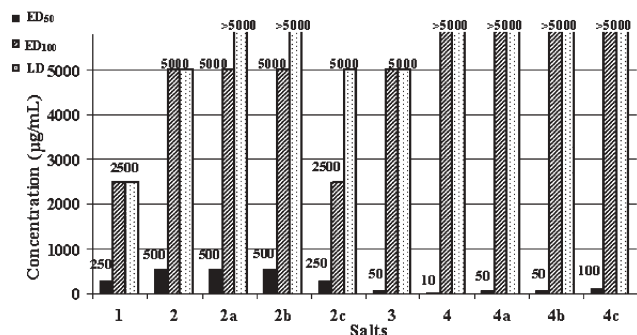


Fig. 5 The effective dose ED and the lethal dose LD of: **1** – [BA][Cl], **2** – [BA][NO₃], **2a** – 60% w/w [BA][NO₃] and 40% w/w PEG-400, **2b** – 60% w/w [BA][NO₃] and 40% w/w PEG-600, **2c** – 60% w/w [BA][NO₃] and 40% w/w PPG-425, **3** – [DDA][Cl], **4** – [DDA][NO₃], **4a** – 60% w/w [DDA][NO₃] and 40% w/w PEG-400, **4b** – 60% w/w [DDA][NO₃] and 40% w/w PEG-600, **4c** – 60% w/w [DDA][NO₃] and 40% w/w PPG-425, tested for *Coniophora puteana*.

Wood penetration

The penetration depth of [DDA][NO₃] and [BA][NO₃] in mixtures with PEG and PPG was tested in Scots pine wood (Fig. 6). In general, it is known that quats poorly penetrate wood, e.g., for [BA][Cl], the penetration depth into dry Scots pine was 3.7 mm and, in the case of wet wood, 2.9 mm.¹⁶ [DDA][NO₃] and [BA][NO₃] penetrated to depths of 3.8 and 3.5 mm, respectively. [BA][NO₃] penetrated faster than [DDA][NO₃], which reflects the different densities of the two salts: [DDA][NO₃] is less dense than water while [BA][NO₃] is more dense than water. Adding PEG or PPG improved the penetration of wood by the ILs to depths of more than 6 mm (**4c** and **2c** in Fig. 6).

Leaching from wood

Resistance to water leaching is significant for wood impregnation agents. To test this aspect of the prepared ILs, the procedures of Zhang and Kamdem²⁰ were used. The results

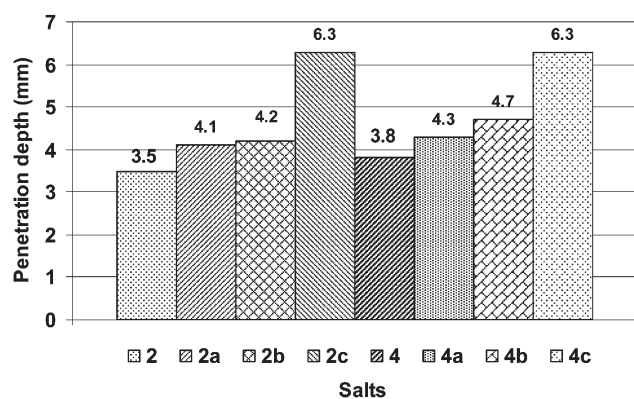


Fig. 6 Penetration depth into Scots pine wood of: **2** – [BA][NO₃], **2a** – 60% w/w [BA][NO₃] and 40% w/w PEG-400, **2b** – 60% w/w [BA][NO₃] and 40% w/w PEG-600, **2c** – 60% w/w [BA][NO₃] and 40% w/w PPG-425, **4** – [DDA][NO₃], **4a** – 60% w/w [DDA][NO₃] and 40% w/w PEG-400, **4b** – 60% w/w [DDA][NO₃] and 40% w/w PEG-600, **4c** – 60% w/w [DDA][NO₃] and 40% w/w PPG-425.

Table 4 Leaching of ILs from treated Scots pine wood after an 8 day shaking cycle

Salts	Treating solution concentration (%)	IL content in treated wood/kg m ⁻³	Degree of leaching (%)
[BA][NO ₃]	1.0	3.87	1.05
	1.6	6.17	2.05
[DDA][NO ₃]	1.0	3.95	0.85
	1.6	6.35	1.00
60% [BA][NO ₃] and 40% PPG-425	1.0	2.34	0.71
	1.6	3.34	1.17
60% [DDA][NO ₃] and 40% PPG-425	1.0	2.11	0.91
	1.6	3.47	1.08
[BA][Cl]	1.0	5.22	5.03
	1.6	8.37	9.66
[DDA][Cl]	1.0	5.25	3.65
	1.6	8.51	7.80

obtained for the [NO₃]⁻ and [Cl]⁻ salts, as well as for the mixtures of ILs with PPG, are listed in Table 4. As compared to the hydrophilic [Cl]⁻ salts, for which the degree of leaching ranged between 3.7 and 9.7%, the hydrophobic [NO₃]⁻ salts might be expected to undergo significantly less leaching. The degrees of leaching for [DDA][NO₃] ranged between 0.9 and 1.0%, and were markedly lower than those for [BA][NO₃] (1.0–2.1%). Mixtures of IL with PPG, which penetrated wood most effectively, showed an insignificant extent of leaching (0.7–1.2%).

These studies indicated that wood was most effectively preserved by the use of the mixture of 60% w/w [BA][NO₃] and 40% w/w PPG-425, which (i) attacked fungi, (ii) penetrated wood to the depth of 6.3 mm, and (iii) was resistant to water leaching (the degree of leaching was approximately 1%). The mixture of 60% w/w [DDA][NO₃] and 40% w/w PPG-425 should be regarded as an effective preparation for wood preservation.

Toxicity

Acute oral toxicity studies of [BA][NO₃] and [DDA][NO₃] were performed with rats, in compliance with the OECD Guideline for Testing of Chemicals No 420 (Fixed Dose Method).²¹ The results reported below allow the conclusion that the oral median lethal dose (LD₅₀) of [BA][NO₃] exceeds 50 mg kg⁻¹ body weight (b.w.) and is lower than 500 mg kg⁻¹ b.w., while for [DDA][NO₃] the dose exceeds 500 mg kg⁻¹ b.w.

Clinical signs. In preliminary experiments [BA][NO₃] was administered at the dose of 2000 mg kg⁻¹ b.w. Ten minutes later the rat developed salivation and the female died after 24 h. The dose of 500 mg kg⁻¹ b.w. induced, after 1–2 h, dejection, restricted motility, staggering gate, and bristled hair in females. None of the females survived six days. On the other hand, administration of [BA][NO₃] at the dose of 50 mg kg⁻¹ b.w. was followed by no toxic symptoms in the course of 14 days observation. Individual results on weight gain in the animals are listed in Table 5.

The dose of 2000 mg [DDA][NO₃] per kg b.w. proved excessively high. Subsequent administration of the [NO₃]⁻ compound to four females at a dose of 500 mg kg⁻¹ b.w. was followed in the same day of application by dejection and

Table 5 Tests of acute oral toxicity of [BA][NO₃] in rats

Dose/ mg kg ⁻¹ b.w.	Rat no.	Animal body weight/g			Difference between day 0 and day 14
		Original	Following 7 days	Following 14 days	
2000	1 ^a	188	—	—	—
	1 ^a	184	—	—	—
	2	176	—	—	—
	3	188	—	—	—
	4	185	—	—	—
500	5	184	—	—	—
	1 ^a	202	231	244	42
	2	194	222	224	30
	3	187	221	226	39
	4	197	222	226	29
	5	191	213	222	31

^a Females in the preliminary experiment.

restricted motility in two females (no. 2 and 5) and by dejection and salivation in a single female (no. 3). The signs developed within 0.5–1 h after administration. The female No. 3 died before the second hour and the female No. 2 before the 24th hour. In the first day after administration, the female No. 5 continued to demonstrate restricted motility, but between the second day and the end of observation period no signs of toxicity were observed and the female survived the observation period. In the female no. 4, no signs of toxicity were observed in the course of the 14 day observation period; the female survived the observation period.

The individual data on body weight in the animals are listed in Table 6. In three females given the studied material at the dose of 500 mg kg⁻¹ b.w., the 14-day observation period was accompanied by less intense growth in body weight (no. 1) or by a decrease in body weight (females no. 4 and 5).

Pathology. In the female which died after being administered the dose of 2000 mg kg⁻¹ b.w., cyanosis was disclosed macroscopically. This was also noted in the four females which died following the dose of 500 mg kg⁻¹ b.w. Moreover, in three of the females, softening of intestinal wall, and in a single one, softening of the gastric wall was disclosed. In five females given the dose of 50 mg kg⁻¹ b.w., which were

Table 6 Tests of acute oral toxicity of [DDA][NO₃] in rats

Dose mg kg ⁻¹ b.w.	Rat no.	Animal body weight/g			Difference between day 0 and day 14
		Original	Following 7 days	Following 14 days	
2000	1 ^a	170	—	—	—
	1 ^a	204	173	209	5
	2	195	—	—	—
	3	195	—	—	—
	4	203	166	192	-11
500	5	202	163	199	-3
	1	205	233	236	31
	2	198	219	217	19
	3	202	229	235	33
	4	198	217	221	23
	5	209	232	235	26

^a Females in the preliminary experiment.

sacrificed following 14 days of observation, no lesions were noted upon macroscopical examination of the internal organs and they did not show any pathological changes in macroscopic study. In control females given dimethylsulfoxide (DMSO), no lesions could be noted upon macroscopic examination.

Experimental

Synthesis

All reagents were purchased from a commercial source (Sigma–Aldrich) and were used as received.

General. NMR spectra were obtained in DMSO-*d*₆ with TMS as the internal standard. Elemental analyses were performed at the A. Mickiewicz University, Poznań. Melting points were determined on a hot-stage apparatus and DSC instrument.

General procedure for preparation of nitrates and nitrites. 0.03 mol of quaternary ammonium halide was dissolved in 40 mL distilled water and then 0.03 mol of nitric acid (60%) was added. The solution was stirred at room temperature for 1 h. Chloroform (40 mL) was added to the reaction mixture and then shaken. The mixture was stirred for an additional 1 h. After separation of the phases, the organic phase was washed with 40 mL distilled, cold water until chloride ion was no longer detected using AgNO₃. Chloroform was removed and the residue was dried at 50 °C in vacuum.

Benzalkonium nitrate ([BA][NO₃]) was obtained in 94% yield (10.3 g, 28.1 mmol). Mp = 36.3 °C. ¹H NMR (360 MHz, DMSO-*d*₆) δ 7.52 (m, 5H), (m, 5H), 4.54 (s, 2H), 3.25 (m, 2H), 2.98 (s, 6H), 1.78 (m, 2H), 1.25 (m, 20H), 0.85 (t, *J* = 7 Hz, 3H); ¹³C NMR 132.8, 130.1, 128.8, 128.1, 66.1, 63.4, 49.0, 31.2, 29.0, 28.96, 28.88, 28.7, 28.65, 28.4, 25.8, 22.0, 21.7, 13.8.

Didecyltrimethylammonium nitrate ([DDA][NO₃]) was obtained in 90% yield (10.5 g, 27.0 mmol). Mp = 18.8 °C. ¹H NMR (360 MHz, DMSO-*d*₆) δ 3.24 (m, 4H), 2.99 (s, 6H), 1.62 (m, 4H), 1.26 (m, 28H), 0.86 (t, *J* = 7 Hz, 6H); ¹³C NMR 62.7, 49.9, 31.2, 28.8, 28.7, 28.6, 28.4, 25.7, 22.0, 21.6, 13.9. Elemental analysis: Found: C 68.12, H 12.71, N 7.03. Calc. for C₂₂H₄₈N₂O₃ (388.6): C 67.99, H 12.45, N 7.21%.

Benzethonium nitrate ([HA1622][NO₃]) was obtained in 93% yield (13.2 g, 27.8 mmol). The wax was obtained from an anhydrous acetone/THF mixture (1 : 1 v/v). The final product was obtained as white crystals with mp = 92–94 °C. ¹H NMR (360 MHz, DMSO-*d*₆) δ 7.53 (m, 5H), 7.25 (d, *J* = 9 Hz, 2H), 6.83 (d, *J* = 9 Hz, 2H), 4.61 (s, 2H), 4.12 (d, *J* = 5 Hz, 2H), 4.00 (s, 2H), 3.83 (t, *J* = 5 Hz, 2H), 3.55 (t, *J* = 4 Hz, 2H), 3.02 (s, 6H), 1.67 (s, 2H), 1.28 (s, 6H), 0.66 (s, 9H); ¹³C NMR 155.8, 141.4, 133.0, 130.1, 128.7, 127.9, 126.8, 113.5, 68.7, 67.4, 66.5, 63.8, 62.5, 56.2, 49.7, 37.4, 31.9, 31.41, 31.38. Elemental analysis: Found: C 73.57, H 9.71, N 6.03. Calc. for C₂₇H₄₂N₂O₅ (474.63): C 68.33, H 8.91, N 5.90%.

Benzalkonium nitrite ([BA][NO₂]) was obtained as a yellow oil in 75% yield (7.9 g, 22.5 mmol). ¹H NMR (360 MHz, DMSO-*d*₆) δ 7.52 (m, 5H), 4.58 (s, 2H), 3.27 (m, 2H), 2.97 (s, 6H), 1.78 (m, 2H), 1.25 (m, 20H), 0.85 (t, *J* = 7 Hz, 3H); ¹³C

NMR 132.9, 130.1, 128.8, 128.2, 65.9, 63.3, 48.9, 31.2, 28.95, 28.87, 28.7, 28.6, 28.5, 25.8, 22.0, 21.7, 13.9.

Didecyldimethylammonium nitrite ([DDA][NO₂]) was obtained as a yellow wax in 85% yield (9.5 g, 25.5 mmol). *M_p* = −2.4 °C. ¹H NMR (360 MHz, DMSO-*d*₆) δ 3.25 (m, 4H), 3.00 (s, 6H), 1.62 (m, 4H), 1.26 (m, 28H), 0.85 (t, *J* = 7 Hz, 6H); ¹³C NMR 62.6, 49.8, 31.2, 28.8, 28.7, 28.6, 28.4, 25.7, 22.0, 21.6, 13.8. Elemental analysis: Found: C 71.12 H 13.15, N 7.43. Calc. for C₂₂H₄₈N₂O₂ (372.6): C 70.91, H 12.98, N 7.52%.

Preparation of benzalkonium tetrafluoroborate ([BA][BF₄]). Equal molar amounts (0.03 mol) of [BA][Cl] and NaBF₄ were dissolved in distilled water and stirred at room temperature for 0.5 h. The addition of chloroform was followed by thorough mixing and then the solution was transferred to a separating funnel where the organic phase was the lower phase. The organic phase was extracted by distilled water until chloride ions were no longer detected using AgNO₃. The chloroform phase was then transferred in a round-bottomed flask to a rotovap at 80 °C under a vacuum to remove any residual chloroform. The wax, prepared in 90% yield (10.6 g, 27.1 mmol), was dried for several hours in vacuum. *M_p* = 56.0 °C. ¹H NMR (360 MHz, DMSO-*d*₆) δ 7.53 (m, 5H), 4.52 (s, 2H), 3.24 (m, 2H), 2.95 (s, 6H), 1.78 (m, 2H), 1.25 (m, 20H), 0.86 (t, *J* = 7 Hz, 3H); ¹³C NMR 132.8, 130.1, 128.8, 128.0, 66.1, 63.4, 49.0, 31.2, 29.0, 28.89, 28.74, 28.67, 28.5, 25.8, 22.0, 21.7, 13.9.

Preparation of didecyldimethylammonium tetrafluoroborate ([DDA][BF₄]). A saturated aqueous solution of NaBF₄ was added to a stoichiometric amount (0.03 mol) of a hot 75% [DDA][Br] aqueous gel. The reaction mixture was stirred at room temperature for 0.5 h affording a heterogeneous mixture. Chloroform (50 mL) was added and the organic phase was washed with distilled water until bromide ions were no longer detected using AgNO₃. The volatile materials were removed under reduced pressure. The liquid product was prepared in 95% yield (11.8 g, 28.6 mmol), and dried at 80 °C in vacuum. *M_p* = 27.5 °C. ¹H NMR (360 MHz, DMSO-*d*₆) δ 3.22 (m, 4H), 2.98 (s, 6H), 1.63 (m, 4H), 1.26 (m, 28H), 0.86 (t, *J* = 7 Hz, 6H); ¹³C NMR 62.7, 49.9, 31.2, 28.8, 28.7, 28.6, 28.4, 25.7, 22.0, 21.5, 13.8. Elemental analysis: Found: C 64.15, H 12.07, N 3.13. Calc. for C₂₂H₄₈BF₄N (413.4): C 63.91, H 11.70, N 3.39%.

Preparation of benzalkonium bis(trifluoromethylsulfonyl) imide ([BA][TF₂N]). (CF₃SO₂)NH as a 55.5% solution in water was added to a stoichiometric amount (0.03 mol) of a saturated, warm aqueous solution of [BA][Cl]. The reaction mixture was stirred at room temperature for 1 h and 50 mL of chloroform was added. The organic phase was separated and extracted with distilled water. The volatile materials were removed under reduced pressure and the liquid obtained was dried at 80 °C in vacuum to give the product in 95% yield (16.6 g, 28.5 mmol). ¹H NMR (360 MHz, DMSO-*d*₆) δ 7.52 (m, 5H), 4.51 (s, 2H), 3.24 (m, 2H), 2.95 (s, 6H), 1.79 (m, 2H), 1.25 (m, 20H), 0.86 (t, *J* = 7 Hz, 3H); ¹³C NMR cation: 132.7, 130.0, 128.7, 127.9, 66.1, 63.4, 48.9, 31.1, 28.91, 28.86, 28.78,

28.63, 28.57, 28.4, 25.7, 21.9, 21.6, 13.7, anion: 121.1–117.6 (d, *J* = 318 Hz).

Preparation of didecyldimethylammonium bis(trifluoromethylsulfonyl)imide ([DDA][TF₂N]). (CF₃SO₂)NH as a 55% solution in water was added to a stoichiometric amount (0.03 mol) of [DDA][Br] (tech., 75% gel in water). The solution was stirred at room temperature for 1 h and 50 mL of chloroform was added. The organic phase was separated and extracted with distilled water. The volatile materials were removed under reduced pressure and the liquid was dried at 80 °C in vacuum to give the product in 99% yield (18.0 g, 29.7 mmol). ¹H NMR (360 MHz, DMSO-*d*₆) δ 3.22 (m, 4H), 2.98 (s, 6H), 1.63 (m, 4H), 1.26 (m, 28H), 0.86 (t, *J* = 7 Hz, 6H); ¹³C NMR 62.8, 49.9, 31.2, 28.8, 28.7, 28.6, 28.4, 25.6, 22.0, 21.6, 13.8, anion 121.2–117.6 (d, *J* = 321 Hz). Elemental analysis: Found: C 47.48, H 7.73, N 4.83. Calc. for C₂₄H₄₈N₂F₆O₄S₂ (606.8): C 47.51, H 7.97, N 4.62%.

Thermal analyses

Melting points were determined using both a hot stage apparatus and a differential scanning calorimeter (DSC), TA Instruments model 2920 Modulated DSC (New Castle, DE) cooled with a liquid nitrogen cryostat. The calorimeter was calibrated for temperature and cell constants using indium (melting point 156.61 °C, Δ*H* 28.71 J g^{−1}). Data were collected at constant atmospheric pressure, using samples between 10–40 mg in aluminum sample pans. Experiments were performed heating at the rate of 5 °C min^{−1}. The DSC was adjusted so that zero heat flow was between 0 and −0.5 mW, and the baseline drift was less than 0.1 mW over the temperature range 0–180 °C. An empty sample pan was used as reference.

Thermal decomposition temperatures were measured in the dynamic heating regime using a TGA (TA Instruments 2950) under air atmosphere. Samples between 2–10 mg were heated from 40–500 °C under constant heating at 5 °C min^{−1}. Decomposition temperatures (*T*_{5%*dec*}) were determined from onset to 5 wt% mass loss, under air; which provides a more realistic representation of thermal stability at elevated temperatures.

X-Ray crystallography

Data was collected on a Bruker CCD area detector-equipped diffractometer with graphite monochromated MoKα (*λ* = 0.71073 Å) radiation and the structure solved using the SHELXTL software package.²² Absorption corrections were made with SADABS.²³ All non-hydrogen atoms were readily located and refined anisotropically and all hydrogen atoms were placed in calculated positions 0.95 Å from the bonded carbon atom unless otherwise noted. The structure was refined by full-matrix least-squares on *F*².

Initial structure solution refined to *R*₁ = 0.1748, *wR*₂ = 0.4824 [*I* > 2σ(*I*)] and *R*₁ = 0.2130, *wR*₂ = 0.4980 (for all data). Analysis of the Fo/*F*_c data using the program TwinRotLat in PLATON²⁴ indicated the possibility for a non-merohedrally twinned structure. The twin law was determined to be [−1 0 0 0 −1 0 1.075 0.355 1]. After inclusion of the BASF parameter and HKLF5 data file, the

twinned structure refined to [R1 = 0.1127, wR2 = 0.3204 and R1 = 0.1507, wR2 = 0.3400] with BASF = 0.27.

Bioactivity tests

Test microorganisms. The microorganisms used included *Staphylococcus aureus* NCTC 6538, *Enterococcus faecium* ATCC 49474, *Escherichia coli* ATCC 25922, and *Candida albicans* ATCC 10231. Standard strains were supplied by the American Type Culture Collection (ATCC).

Anti-microbial activity test procedure. Anti-microbial activity was determined by the tube dilution method. Bacteria strains were cultured on a Müller-Hinton broth for 24 h, and fungi on Sabouraud agar for 48 h. A suspension of the microorganisms at a concentration of 10^6 cfu mL⁻¹ was prepared from each culture. This suspension was then used to inoculate each dilution of the broth medium at a 1 : 1 ratio. Growth of the microorganisms (or lack thereof) was determined visually after incubation for 24 h at 35 °C (bacteria) or 48 h at 22 °C (fungi). The lowest concentration at which there was no visible growth (turbidity) was taken as the MIC (minimal inhibitory concentration). Then, an aliquot taken from each tube in a sample loop was cultured in an agar medium with inactivates (0.3% lecithin, 3% polysorbate 80, and 0.1% cysteine L) and incubated for 48 h at 35 °C (bacteria) or for 5 d at 22 °C (fungi). The lowest concentration of the studied salt supporting no colony formation was defined as the MBC (minimum bactericidal or fungicidal concentration).

The determinations of anti-fungal efficacy. The fungal growth rates were measured in 90 mm Petri dishes using the agar dilution test. Ten concentrations of the compounds were studied in a geometric progression from 10 to 5000 µg mL⁻¹. Stock solutions of each concentration of the studied chemicals were produced in sterile malt agar (1.5% agar and 4% malt-extract), 20 mL of which was added to each Petri dish. Three replicate plates of each concentration of each compound were centrally inoculated with a 5 mm diameter disc taken from the submargin of 10-day-old cultures of the desired test fungus grown on malt agar. The plates were incubated at 22 ± 1 °C in darkness. The duration of the test was either determined by waiting for complete plate coverage by growing mycelium or 12 days for *Sclerophoma ptyophila* and *Coniophora puteana* fungi and 6 days for *Trametes versicolor* fungus (for which growth rates were higher than for the two earlier mentioned fungi). If growth on the preservative-containing agar had not begun after 12 days or 6 days, respectively, the inoculum was removed and transferred to a fresh malt agar plate for determination of the fungal viability.

The results were used to calculate ED₅₀ (preservative concentrations retarding the fungal growth rate by 50 percent in comparison with plates where the toxic agent was omitted), the effective dose ED₁₀₀ (preservative concentrations retarding the fungal growth rate by 100 percent in comparison with plates where the toxic agent was omitted), and LD (concentrations causing death of fungus inoculum) of the examined salts. The strains used for the tests, *Sclerophoma ptyophila* (Corda) v.Höhn, strain S 231, *Coniophora puteana* (Schum.:Fr.) Karst.

strain BAM 15, and *Trametes versicolor* (L.:Fr.) Pilát strain CTB, were obtained from the collection of the Institute of Wood Technology, Poznań, Poland.

Acute oral toxicity study

Wistar rats (outbred, symbol Imp: WIST) used in these studies originated from a culture in the Instytut Medycyny Pracy w Łodzi/Poland (Medical Institute of Work in Lodz/Poland) and were kept in cages of the conventional type. Before the study, the animals were quarantined for a minimum 5 days and observed daily during this period. The animals were marked individually. During quarantine and the experiments, the animals were kept in a conditioned room of the following parameters: temperature 20–23 °C, relative air humidity 30–40%, and artificial illumination 12 h light/12 h darkness. Rats were kept in cages with plastic bottom and wired superstructure, with the dimensions of 58 × 37 × 21 cm (length × width × height). The animals were kept in cages individually (in the observation study – the dose of 2000 or 500 mg kg⁻¹ b.w.) or 4 rats per cage (in the main study – the dose of 500 and 50 mg kg⁻¹ b.w.). UV-sterilized wooden shavings were used as litter. Each cage was equipped with a label containing information on name of test material, study code, used dose, start date and planned ending date of the experiment, sex, and animal numbers. The rats were given standard granulated GLM fodder and tap water *ad libitum*.

The day before the start of the experiment, about 18–19 h before administration of the test material, the animals were left with no food, but water was still available. The food was given again 3 h following administration of the material.

In the preliminary experiment, one female was given the tested material in the form of a solution in dimethylsulfoxide (DMSO), at the dose of 2000 mg kg⁻¹ b.w. The material was administered as a single dose using a metal intragastric catheter. One mL of the administered solution contained 800 mg of the tested material. The total of 0.25 mL solution was given per 100 g rat body mass.

Subsequently, the tested material was administered to a following female rat, at the dose of 500 mg kg⁻¹ b.w. The preparation for administration, administration procedure, and the administered volume corresponded to those described above. This time, 1 mL of the administered solution contained 200 mg of the tested material.

In the main experiment following the preliminary study, the materials were administered to five female rats (including the one from the preliminary experiment) at the dose of 500 mg kg⁻¹ b.w. and, then, to another five female rats at the dose of 50 mg kg⁻¹ b.w. The preparation for administration, administration procedure, and the administered volume corresponded to those used in the preliminary experiment. One mL of the administered solution contained 20 mg of the tested material. Since the tested material was administered in the form of a solution in DMSO, the five control female rats were administered a single dose of DMSO at 0.25 mL per 100 g b.w.

Wood penetration testing

Samples of Scots pine wood (*Pinus sylvestris* L.) were used. The density of the wood ranged between 480 and 540 kg m⁻³,

with the number of growth rings at 5–8 per 1 cm. Each block measured 50 × 50 × 20 mm (one of the longer edges had to be parallel to the fibers and the annual growth increment rings visible in cross section had to be positioned against the edge at an angle of 45 ± 10°) and was conditioned to a moisture content of 12 ± 1%. The investigated samples were cut out from the middle part of the trunk, the side surface and tight surface of which was smoothly planed.

On the 50 × 50 mm wood surface, 0.5 g of the investigated salts were applied. The samples were then conditioned in the dishes over a saturated solution of ammonium nitrate at 20 ± 2 °C for 7 days. Subsequently, the samples were cut perpendicularly into fibers by means of a cross cut saw, and were sprayed carefully on the cross-section surface with bromphenol blue indicator (giving a typical blue color on contact with the IL). The ranges of blue sections were marked with a sharp pencil, which permitted determination of the penetration depth of each IL. In each of the tests, penetration was recorded in 10 wood samples (2 samples from each of 5 fillets of Scots pine wood).

Wood leach testing

Defect-free sapwood boards of Scots pine (*Pinus sylvestris* L.) were used in this study. Cubes measuring 19 mm were prepared from the boards and stored in a climatic chamber maintained at 65% relative humidity (RH) and 20 °C until they reached an equilibrium moisture content (EMC) of 12 ± 1%. The conditioned cubes were then pressure-treated with the solutions of IL and mixtures of IL with polypropylene glycol (PPG), both dissolved in 2-propanol. The concentrations of the solutions (ILs in 2-propanol) were 1.0 and 1.6% by weight. The treating procedure included an initial –88 kPa vacuum for 30 min and atmospheric pressure for 60 min. The treated samples were a subject to seasoning in the drying vessel at room temperature for 3 weeks before further testing. 2-Propanol was evaporated during the seasoning process.

After the conditioning of the treated cubes, the leach tests were carried out to determine the amount of ILs leaching from treated wood. Three treated wood cubes weighing about 10 g, were placed in Erlenmeyer flasks and immersed in 100 mL of distilled water. The flasks were positioned on a horizontal-shaking tray with continuous mild shaking at 150 rpm for 8 days. After this time the leached cubes were analyzed by a two-phase titration, according to standards for determination of quaternary ammonium compounds in wood by two-phase titration set by the American Wood-Preserver's Association.²⁵

Acknowledgements

The research was supported by Polish grant number 3 TO9B 053 29 and at The University of Alabama by the U.S. Environmental Protection Agency's STAR program through grant number RD-83143201. (Although the research described in this article has been funded in part by EPA, it has not been

subjected to the Agency's required peer and policy review and therefore does not necessarily reflect the views of the Agency and no official endorsement should be inferred.)

References

- N. Menshutkin, *Z. Phys. Chem.*, 1890, **5**, 589–601; N. Menshutkin, *Z. Phys. Chem.*, 1891, **6**, 41.
- E. Tomlinson, M. R. Brown and S. S. Davis, *J. Med. Chem.*, 1977, **20**, 1277–1282.
- P. Wasserscheid and W. Keim, *Angew. Chem., Int. Ed.*, 2000, **39**, 3773–3789.
- Zhi-Bin Zhou, Hajime Matsumoto and Kuniaki Tatsumi, *Chem.—Eur. J.*, 2005, **11**, 752.
- Y. Imamura, K. Shinoda and M. Yosimi, *Jap. Pat.*, JP 231 592, 2004, CA141:190504.
- K. Shinoda, *Jap. Pat.*, JP 285 157, 2004, CA141:332997.
- K. Kawaguchi, Y. Hosaka, M. Mikami, and S. Furukawa, *Jap. Pat.*, JP 149 678, 2004, CA140:425275.
- K. Shinoda, *Jap. Pat.*, JP 321 308, 2003, CA139:347037.
- K. Shinoda, *Jap. Pat.*, JP 306 698, 2003, CA139:351965.
- H. Ogasawara and K. Shinoda, *Jap. Pat.*, JP 292 405, 2003, CA139:303275.
- K. Shinoda, *Jap. Pat.*, JP 292 358, 2003, CA139:326959.
- M. Minaki and K. Shinoda, *Jap. Pat.*, JP 206 206, 2003, CA139:118792.
- J. Pernak, P. Chwała and A. Syguda, *Polish J. Chem.*, 2004, **78**, 539–546.
- J. G. Huddleston, A. E. Visser, M. Reichert, H. D. Willauer, G. A. Broker and R. D. Rogers, *Green Chem.*, 2001, **3**, 156–164.
- Crystal data for [HA1622][NO₃]: formula = C₂₇H₄₂N₂O₅, *M* = 474.63, triclinic, *a* = 7.936(3) Å, *b* = 10.048(4) Å, *c* = 17.864(7) Å, α = 91.753(8)°, β = 102.116(7)°, γ = 106.858(7)°, *V* = 1326.5(10) Å³, *T* = 173(2) K, space group *P*–1 (no. 2), *Z* = 2, *D_c* = 1.188 Mg m^{–3}, μ (Mo–K α) = 0.081 mm^{–1}, *F*(000) = 516, crystal size = 0.56 × 0.12 × 0.03 mm³, $\theta_{\text{min/max}}$ = 2.13, 26.41°, completeness to theta = 25.30°, 97.7%, Reflections collected (all independent) = 5238, Observed reflections = 3333 ($[I > 2\sigma(I)]$), Goodness-of-fit on *F*² = 1.046, Final *R* indices [$[I > 2\sigma(I)]$] *R*1^{*a*} = 0.1127, *wR*2^{*c*} = 0.3204, *R* indices (all data) *R*1 = 0.1507, *wR*2 = 0.3400, Extinction coefficient = 0.25(3). GOF = $\{\sum[w(F_o^2 - F_c^2)^2]/(n - p)\}^{1/2}$, where *n* is the number of data and *p* is the number of parameters refined. *R* = $\sum||F_o| - |F_c||/\sum|F_o|$. ^{*c*} is *wR*2 = $\{\sum[w(F_o^2 - F_c^2)^2]/\sum(w(F_o^2)^2)\}^{1/2}$.
- J. Pernak, J. Zabielska-Matejuk, A. Kropacz and J. Fokszowicz-Flaczyk, *Holzforchung*, 2004, **58**, 286–291.
- J. Pernak, I. Goc and A. Fojutowski, *Holzforchung*, 2005, **59**, 473–475.
- X. Li, Y. Geng, J. Simonsen and K. Li, *Holzforchung*, 2004, **58**, 280–285.
- J. N. R. Ruddick and A. R. H. Sam, *Mater. Org.*, 1982, **17**, 299–313.
- J. Zhang and D. P. Kamdem, *Wood Fiber Sci.*, 2000, **32**, 332–339.
- OECD Guideline for Testing of Chemicals No 420 (Fixed Dose Method) as well as Good Laboratory Principles (GLP, OECD, 1997).
- G. M. Sheldrick, *SHELXTL, Version 5.05*, Siemens Analytical X-Ray Instruments, Inc., 1996.
- G. M. Sheldrick, *Program for Semiempirical Absorption Correlation of Area Detector Data*, University of Göttingen, Germany, 1996.
- A. L. Spek, *Acta Crystallogr., Sect. A: Found. Crystallogr.*, 1990, **46**, C34; A. L. Spek, *PLATON – A multipurpose Crystallographic Tool*, Utrecht University, Utrecht, The Netherlands, 2005.
- American Wood-Preservers' Association (AWPA) Standard A 18-93(1993) Standard for determination of quaternary ammonium compounds in wood by two-phase titration: AWPA Subcommittee T-7.

Liquid polymers as solvents for catalytic reductions

David J. Heldebrant,^{ab} Heather N. Witt,^b Sarah M. Walsh,^a Taryn Ellis,^a Japheth Rauscher^b and Philip G. Jessop^{*ab}

Received 18th April 2006, Accepted 26th June 2006

First published as an Advance Article on the web 13th July 2006

DOI: 10.1039/b605405f

Nonvolatile solvents eliminate the health and environmental risks associated with volatile solvent use, but may pose their own risks and separation problems. Several liquid polymers are compared in terms of environmental risk, solvent polarity, and performance as solvents for homogeneously-catalyzed and whole-cell-catalyzed reductions. Asymmetric catalyst use and recycling was demonstrated using a combination of liquid polymer and supercritical CO₂. A polymeric solvent was also found to protect air-sensitive catalysts from inactivation due to exposure to air.

Introduction

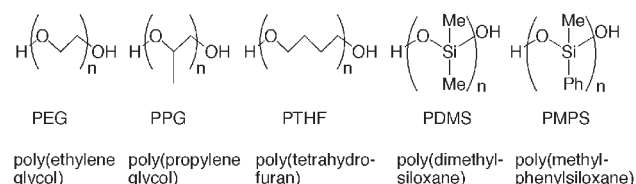
Homogeneous catalysis is traditionally performed in volatile organic solvents, but there are disadvantages associated with those solvents that can be avoided by using nonvolatile organic liquids. Volatile solvents, like other VOC's (volatile organic compounds), are contributors to smog formation, are often flammable and can lead to health problems by inhalation pathways. Additionally, it is very difficult to develop continuous-flow processes based upon homogeneous catalysis in volatile solvents. The use of nonvolatile solvents eliminates these problems but introduces another; it is difficult to separate nonvolatile products from a nonvolatile solvent after the reaction is complete. After the discovery that ionic liquids (ILs) are completely insoluble in supercritical CO₂ (scCO₂),^{1,2} we and others reported methods for performing homogeneous catalysis in ionic liquids, with extraction of the product by scCO₂.^{3–6} In fact, there were reports of continuous-flow methods based upon homogeneous catalysis in an IL with a solution of reactants in scCO₂ coming into the vessel and scCO₂ simultaneously leaving the vessel with dissolved product.^{5,6} This combination of ionic liquids and scCO₂ solved the problems associated with volatile organic solvents without introducing a separation problem. However, the high cost of ionic liquids may slow or in some cases even prevent their industrial adoption. A low-cost nonvolatile organic liquid would be preferable. The authors embarked upon a search for such liquids, followed by testing of them as solvents for catalytic reductions.

In order for a liquid to function as the catalyst-bearing phase in biphasic catalysis, with scCO₂ being the product-bearing phase, then the liquid must meet several requirements: it must be inert, liquid at reaction conditions (we arbitrarily specified 40 °C), able to dissolve homogeneous catalysts, and insoluble in scCO₂. Additionally, one would prefer the liquid to be inexpensive, nontoxic, nonflammable, biodegradable, and, for minimal environmental impact, nonhalogenated.

Many liquids were considered by the authors, but most were rejected because they failed to meet one or more of the criteria. Glycerol, which has very low solubility in scCO₂,⁷ was rejected because it is unable to dissolve many catalysts. Higher alkanes such as eicosane and diols and triols such as 1,2,6-hexanetriol were rejected because they are too soluble in scCO₂. The liquids which remained candidates after the selection process were all liquid polymers (Scheme 1), including poly(ethylene glycol) (PEG), poly(propylene glycol) (PPG), poly(tetrahydrofuran) (PTHF), poly(methylphenylsiloxane) (PMPS) and variations of these with ether or ester end-capping groups. Polydimethylsiloxane (PDMS) was included in some of the experiments, even though it is generally quite soluble in scCO₂, because very high molecular weight fractions of that polymer are known to be insoluble.⁸ In the rest of this article, numbers given after an acronym give the nominal average molar mass of the polymer.

Our first demonstration that the combination of a liquid polymer and scCO₂ can be used for homogeneous catalysis with catalyst recycling was described in a preliminary communication.⁹ We now describe the full study.

Liquid PEG was first used as a solvent for homogeneous catalysis by Naughton and Drago¹⁰ in 1995 but the idea was not developed further until a small flurry of reports starting in 2000.¹¹ Without exception, these reports described the use of traditional (volatile) organic solvents to remove the product from the PEG; this defeats the purpose of using a nonvolatile solvent. In order to rid the process of the volatile organic solvent, and thereby take advantage of the lack of volatile emissions from polymeric solvents, we proposed in the preliminary communication that scCO₂ be used as the extraction solvent.⁹ The previous literature also ignores the



Scheme 1 The structure of selected liquid polymers.

^aDepartment of Chemistry, Queen's University, Kingston, Ontario, Canada K7L 3N6. E-mail: jessop@chem.queensu.ca; Fax: +1-(613) 533-6669; Tel: +1-(613) 533-3212

^bDepartment of Chemistry, University of California, Davis, CA, USA

possibility that other nonvolatile liquid polymers may, for some reactions, be preferable to PEG. One paper by Andrews *et al.*¹² described the use of a volatile fraction of PPG as a solvent for catalysis, with recovery of the product by vacuum distillation of the PPG. The reports have not compared several liquid polymers to determine if they perform equally well for any test reactions. We now describe the full results of our study, along with discussions of whether PEG is always superior and whether polymeric solvents are actually “green” solvents.

Results and discussion

Are liquid polymers green solvents?

Before these liquid polymers can be claimed to be “green”, their credentials in this area must be evaluated. Fortunately, there is some evidence in their favour, especially in the areas of nonvolatility, toxicity, ecotoxicity, and biodegradability. While the nonvolatility is obvious, the other factors need to be examined. The toxicity of PEG is very low (LD50 17 to 76 g kg⁻¹, orally, rat/rabbit/guinea pig),¹³ low enough for PEG to be approved as a food additive for humans.^{14,15} Extremely low ecotoxicity is suggested by the LC50 (*daphnia magna*)¹⁶ of >10,000 mg L⁻¹ (compared to 11 mg L⁻¹ for the ionic liquid [bmim]BF₄).¹⁷ PPG is used in facial cleansers and shampoos. Both PEG¹⁸ and PPG^{19,20} have been found to be nonhazardous to fish. PTHF-1000 in solid form and its aqueous extracts are nontoxic to *daphnia magna* (LC50 >1000 mg L⁻¹ for solid form), but aqueous emulsions of PTHF were toxic with a LC50 (*daphnia*, 48 h) between 10 and 100 mg L⁻¹.²¹ PTHF-1000 had no effect on minnow larvae survival rate but did reduce their size.²² PMPS copolymer was found to have no adverse effects when administered dermally to rabbits,²³ and is “relatively innocuous” to rats (LD50 > 65.5 g kg⁻¹).²⁴ PDMS has very low toxicity for *daphnia*, fish and other tested species,²⁵ and is used as a food additive for humans.²⁶

Biodegradability is also a factor in determining if these solvents can be considered “green”. PEG,^{27,28} and PTHF²⁸ have been found to be biodegradable by bacteria in soil or sewage, but the ability of bacteria to biodegrade PEG decreases with increasing molecular weight.²⁷ A comparison of the extent of biodegradation of many polyethers by activated municipal sewage sludge was performed by Kawai²⁹ (Table 1), showing that PEG, PTHF and to a lesser extent PPG can reasonably be considered biodegradable. However, dialkylether-capped PEG is far less biodegradable,²⁹ and therefore should be avoided. In an earlier study, PDMS was found to be largely non-biodegradable and likely

Table 1 Extent of biodegradation of polyethers by activated municipal sewage sludge after 14 days exposure²⁹

Polymer	<i>M_n</i>	Biodegradation (%)
PEG	390	99.7
PEG	1500	95.9
PEG-DME ^a	1500	9.4
PPG	410	69.7
PTHF	660	99.8

^a PEG-dimethylether, MeO(CH₂CH₂O)_{*n*}Me

persistent but did not accumulate in fish or birds,²⁵ but a more recent study showed that PDMS is biodegradable by some bacteria in soil and sewage.³⁰

In summary, the evidence currently available suggests that these polymers (except PTHF in emulsion form) have low or negligible toxicity to humans and various marine life and some of them (PEG, PTHF and to a lesser extent PDMS and PPG) are biodegradable.

The polarity of liquid polymers and CO₂-expanded liquid polymers

Solvents are traditionally classified in terms of their polarity, and the same parameter can reasonably be used to distinguish the various liquid polymer solvents. The polarities of several liquid polymers have now been measured using the Nile Red solvatochromic dye. The more commonly used “E₇(30)” dye, also known as Reichardt’s dye, is less appropriate for studies involving CO₂ and protic solvents because it is more susceptible to bleaching or colour-change by the action of acids.³¹ The wavelengths of maximum absorbance of Nile Red dissolved in traditional organic liquids, polymers and ILs are listed in Table 2. Judging from the absorbance wavelength, one can see that the liquid polymers cover a range of polarities from the polar PEG at 538 nm to the nonpolar PMPS at 517 nm. However, the range does not overlap with the range of polarity of ionic liquids (546 to 556 nm), which were, without exception, found to be more polar. This opens up the possibility that liquid polymers may serve as complements to ionic liquids rather than replacements for ionic liquids.

The effect of the presence of elevated pressures of CO₂ (typically above 25 bar) on liquid solvents depends greatly on the nature of the liquid solvent. The liquid solvents can be placed into three categories (Table 3). The first group of liquids (let us call them Category I solvents), such as water, dissolve CO₂ so poorly that there is no significant change in the volume or physical properties of the liquid solvent.

Table 2 Wavelengths of maximum UV absorbance for Nile Red dissolved in selected solvents^a

Solvent	λ_{\max} /nm	H ₂ O/ppm	Ref.
[bmim]NO ₂ ^b	556		35
[P(C ₄ H ₉) ₃ (C ₂ H ₅)] [PO ₄ Et ₂]	553	nd	this work
[bmim]BF ₄ ^b	551		35
Methanol	550		36
[P(C ₆ H ₁₃) ₃ (C ₁₄ H ₂₉)]Cl	549	5	this work
DMSO	549		36
[bmim]NTf ₂ ^b	549		36
[dmpim]NTf ₂ ^c	548	7	this work
[P(C ₆ H ₁₃) ₃ (C ₁₄ H ₂₉)]NTf ₂	547	16	this work
[P(C ₆ H ₁₃) ₃ (C ₁₄ H ₂₉)] [N(CN) ₂]	546	6	this work
PEG-1500	538	1700	this work
PEG-1000	538	1200	this work
CH ₂ Cl ₂	535		36
MeCN	532		36
PTHF	528	310	this work
Toluene	522		36
PPG-3500	520	6	this work
PMPS-710	517	3	this work
Hexane	484		36

^a “nd” = not determined. ^b bmim = 1-butyl-3-methylimidazolium. ^c 2-dimethyl-3-*n*-propylimidazolium bis(trifluoromethylsulfonyl)-imide.

Table 3 A comparison of different classes of solvents and their expansion behaviour^a

Category	Solvent	P/bar	Volumetric expansion (%)	CO ₂ /wt%	Ref.
I	H ₂ O	70	na	4.8	37
II	MeCN	69	387	83	32
	1,4-dioxane	69	954	79	32
III	[bmim]BF ₄	70	17	15	33
	PEG-400	80	25	16	38
	PPG-2700	60	25	12	38

^a Data for 40 °C except PPG at 35 °C. Some of the data is interpolated from the data in the cited reference, or converted from mol% to wt%. ^b NPE = mono(nonylphenylether)

Category II solvents, such as methanol, acetone and most other common organic solvents, dissolve the pressurized CO₂ to such an extent that there is an enormous expansion of the volume of the liquid phase (as high as 2500%)³² and equally impressive changes in the physical properties of the liquid solvent. A third group of liquid (Category III solvents), such as ionic liquids, dissolve a moderate amount of CO₂ and experience large changes in some physical properties such as viscosity, but the volume³³ and other properties, such as polarity,³⁴ do not change greatly. The term “expanded liquid” is applied to the CO₂-modified liquid phase in categories II and III solvents.

Liquid polymers should fall in category III because their ability to dissolve CO₂ is comparable, on a wt% basis, to that of ionic liquids (it is meaningless to discuss mole fractions of CO₂ in the presence of polymeric molecules). If liquid polymers are truly category III solvents, then their polarity changes upon expansion should be small. Measurements of the polarity of CO₂-expanded PEG and PPG have now been made using the wavelength of absorbance of the solvatochromic dye Nile Red (Fig. 1). The polarities of these two polymers clearly decrease, as a function of pressure, far less than the polarity of the category II solvent DMSO, which is included for comparison. Similar measurements with CO₂-expanded PMPS were not performed due to insufficient solubility of the dye in that medium.

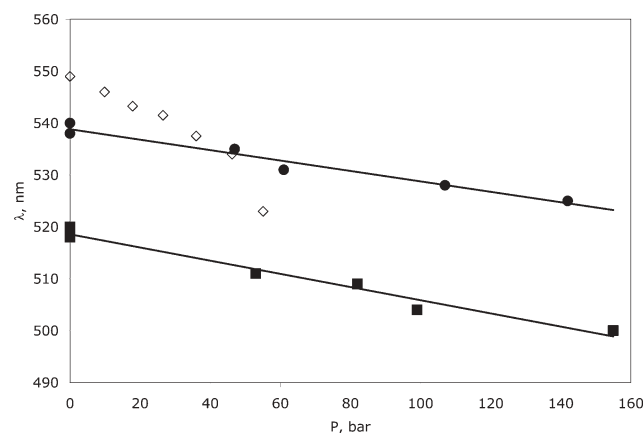
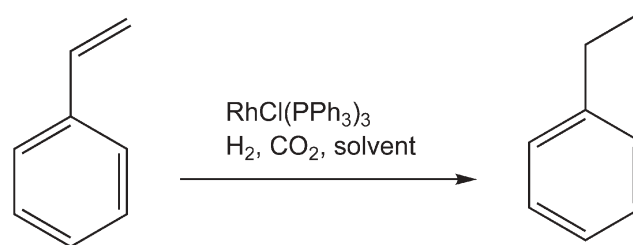


Fig. 1 Wavelength of maximum absorbance of Nile Red as a function of CO₂ pressure in DMSO (◇), PEG-1000 (●), and PPG-3500 (■) at 40 °C. Linear interpolations for the polymeric solvents are shown to guide the eye.

Other observations that have been made about the properties of CO₂-expanded ionic liquids may also be correct for CO₂-expanded liquid polymers. Most importantly, for the present study, is the observation that the solubility of reagent gases (e.g. CO, O₂) in CO₂-expanded ionic liquids is much larger than that in the unexpanded ionic liquid.³⁹ In contrast, the solubility of reagent gases in CO₂-expanded category II solvents is not greatly increased.⁴⁰ These observations suggest that the solubility of reagent gases (possibly including H₂) in CO₂-expanded liquid polymers should be higher than that in the unexpanded liquid polymers. If true, this would have an added benefit for biphasic catalysis in liquid polymer/scCO₂ mixtures. There is, unfortunately, no data yet that confirms or denies this prediction.

The hydrogenation of styrene

Our study of homogeneous catalysis in a liquid polymer, with subsequent scCO₂ extraction of the product, started with the hydrogenation of styrene (reaction 1). Because the styrene hydrogenation work was described in detail in the previous communication,⁹ only the conclusions from that study will be given here. The hydrogenation was performed in PEG-900 for 19 h at 40 °C under 30 bar H₂ and 50 bar CO₂. The presence of CO₂ pressure was required in order to keep the PEG liquid at this temperature; it is normally a waxy solid. After the reaction, the product was extracted from the PEG with scCO₂. Fresh styrene was introduced and the hydrogenation repeated. The single batch of Rh catalyst dissolved in PEG was used a total of five times, without detectable decrease in conversion and without detection of extracted Rh by AA/ICP in the product.



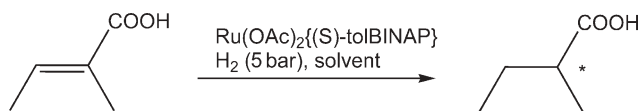
The molecular weight fraction of the PEG makes a significant difference to the performance of the separation. The amount of nonvolatile material (PEG plus water) extracted along with the ethylbenzene product during experiments such as the above was <0.5 wt% if PEG-900 was used, and only 0.1 wt% if PEG-1500 was used.⁹ The higher molecular weights are therefore preferred because they are less readily extracted by CO₂, consistent with their lower solubility.⁴¹ However, these heavier fractions are all solid at room temperature; the melting point increases with increasing molecular weight. The higher melting points are not problematic because applied CO₂ pressure can lower the melting point of solid polymers. The melting point of PEG-1500 under CO₂ pressure has been accurately measured by Weidner,⁴² who found that it dropped from the usual 45 °C to only 29 °C at 70 bar. Similarly, the melting point of PEG-4000 drops from 57 °C to 42 °C at 94 bar. The ability of CO₂ to induce melting makes it possible for PEG fractions to be used as liquid

solvents even at temperatures somewhat below their normal melting points. Overall, the higher molecular weight fractions of these polymers are more desirable as solvents, despite their higher melting points, because they are insoluble in scCO_2 .

The hydrogenation of tiglic acid

Although the experiments with styrene hydrogenation demonstrated that the catalyst could be recycled, they did not conclusively demonstrate that the catalyst was being recycled as an intact homogeneous catalyst rather than a colloidal suspension of over-reduced Rh. They also did not demonstrate that the selectivity of a catalyst could be maintained cycle after cycle with this method of catalyst recycling. For these reasons, we turned to asymmetric hydrogenation. Repeated recycling with maintenance of a satisfactory enantioselectivity would demonstrate both points.

Asymmetric hydrogenation of tiglic acid (reaction 2) using $\text{Ru}(\text{OAc})_2\{(\text{S})\text{-tol-BINAP}\}$ (tolBINAP = 2,2'-bis(di-4-tolylphosphino)-1,1'-binaphthyl) was performed in liquid polymers, and the observed selectivity was compared to that obtained in ionic liquids and methanol (Table 4). Methanol and [bmim]PF₆ gave the best results, with methanol being the better of the two at this temperature (40 °C). The hydrogenations in liquid polymer were achieved in essentially complete conversion and with fair enantioselectivity. While these experiments were being conducted, it became evident that the enantioselectivity of the reaction in liquid polymer was higher if the polymer was washed beforehand with scCO_2 (40 °C, 125 bar, 2 mL min⁻¹ flow rate of scCO_2 for 3 h). This resulted in a 6 to 10% increase in enantiomeric excess (e.e.) of the product 2-methylbutanoic acid regardless of the choice of polymer. The benefit of this washing pretreatment may be to remove air, impurities, stabilizers such as BHT, or light fractions of the polymer. The ee was remarkably independent of the choice of liquid polymer solvent, with PMPS, PEG, PEG-DME, and PTHF giving essentially the same result. The phosphonium ionic liquid, tri(decyl)tetradecylphosphonium dicyanamide, which is significantly less polar than imidazolium ionic liquids such as [bmim]PF₆ and therefore more comparable to the liquid polymers, gave an ee that is essentially identical to that produced in the polymeric solvents.



Catalyst recycling after tiglic acid hydrogenation was attempted with PEG-DME and PEG-1000. After each hydrogenation, the product was extracted with scCO_2 and fresh tiglic acid substrate was then added to the catalyst/polymer mixture in the vessel, following which another hydrogenation was performed. No additional catalyst or polymer was added. Catalyst recycling in PEG-DME showed significant catalyst degradation after three cycles and was therefore discontinued. The results of five cycles of the hydrogenation of tiglic acid in PEG-1000 are shown in Table 5. The ee of the product from the first run was 81%, but the ee of subsequent runs was slightly higher. The

Table 4 Asymmetric hydrogenation of tiglic acid^a

Solvent	ee (%)
Traditional	
MeOH ^b	91
Liquid polymers	
PMPS ^c	83
PEG-DME ^c	82
PEG-1000 ^c	81
PTHF-710 ^c	81
PDMS ^b	76
PPG-3500 ^b	41
Ionic liquids	
[bmim]PF ₆ ^b	87
[(C ₆ H ₁₃) ₃ (C ₁₄ H ₂₉)P][N(CN) ₂] ^b	82

^a Conditions: 40 °C, 5 bar H₂, 24 h, 0.56 to 0.59 mM Ru(OAc)₂(tolBINAP). ^b Concentrations: 23 mM tiglic acid, 2 mL solution. ^c Polymer washed with scCO_2 before use. 100 mM tiglic acid, 10 mL solution.

conversion of each run varied slightly between runs but remained high. These results show that the catalyst remained active, selective, and therefore substantially undegraded over multiple uses.

Catalyst encapsulation in frozen PEG solvent

Encapsulation of air-sensitive homogeneous catalysts in polymers is a strategy for protecting the catalyst from air while the catalyst is not being used. However, physically blocking the access of O₂ molecules to the catalyst also prevents the access of substrate molecules, so the polymer coating must be removed before the catalyst is used.⁴³ A Chinese patent describes the use of paraffin wax to encapsulate a homogeneous catalyst,⁴⁴ which then retained catalytic activity in ethylene oligomerization reactions.

The melting of PEG by CO₂ offers us a new way of protecting the catalyst between runs without preventing catalyst/substrate interactions during runs. We attempted to encapsulate homogeneous catalysts in polyethers such as PEG to generate a superior catalyst recycling method. PEG-1500 and RhCl(PPh₃)₃ were stirred together for 30 min at 50 °C under 50 bar of CO₂. The sample was cooled and bled to atmospheric pressure. The residual puck of solidified PEG-1500 and catalyst (Fig. 2) was exposed to air for 1 month, following which it was tested for catalytic activity for the hydrogenation of styrene at 40 °C under 30 bar H₂ and 50 bar CO₂; the conversion was >99%. For comparison, solid

Table 5 Catalyst recycling runs for hydrogenation of tiglic acid in PEG-1000^a

Cycle	Conversion (%)	ee (%)
1	94	81
2	97	84
3	92	84
4	95	84
5	91	83

^a Reaction conditions: 160 mL vessel, Ru(OAc)₂((S)-tolBINAP) (27.5 μmol), tiglic acid (5 mmol), 40 °C, H₂ (4.9 bar), 24 h, PEG-1000 (10 g, prewashed with scCO_2). Extraction conditions: 40 °C, 125 to 150 bar, 1 mL min⁻¹ CO₂, 12 h. Visual inspection of the PEG layer after each reaction and extraction showed a yellow fluffy solid.

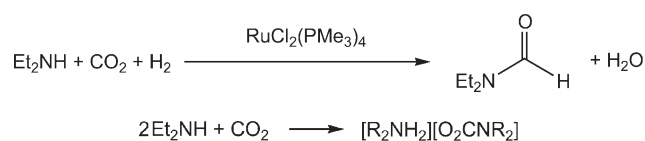


Fig. 2 A sample puck of PEG-1500 containing encapsulated RhCl(PPh₃)₃.

RhCl(PPh₃)₃ and a THF solution of RhCl(PPh₃)₃ were also exposed to air for 1 month and then tested for activity; no hydrogenation to ethylbenzene was observed in either case. This demonstrates that PEG, frozen around the catalyst when the CO₂ pressure is released, protects air-sensitive catalysts from air. However, there is a limit to how far this strategy can be taken. The more air-sensitive complex Ru(OAc)₂[(*S*)-tolBINAP], encapsulated in PEG-1500 and exposed to air for 1 month, was no longer active for the hydrogenation of tiglic acid.

Synthesis of diethylformamide (DEF)

To further evaluate liquid polymers as solvents for catalytic reductions, we investigated the homogeneously catalyzed synthesis of dialkylformamides by hydrogenation of CO₂ in the presence of dialkyl amine (reaction 3). The system reported earlier by one of us^{45,46} used biphasic conditions in which a supercritical CO₂/H₂ mixture lies above a liquid phase consisting primarily of dialkylammonium dialkylcarbamate ionic liquid formed *in situ* by reaction 4. The hydrogenation was studied in detail for the production of dimethylformamide from dimethylamine, and essentially complete conversion of the amine to the formamide was obtained. However, an experiment with diethylamine showed that the conversion was only 38% with that amine (Table 4, entry 1).⁴⁶ Tumas' group⁴ found greatly improved yields for the production of dipropylamine when ionic liquid [bmim]PF₆ was added to the liquid phase and when the catalyst used was RuCl₂(dppe)₂ instead of RuCl₂(PMe₃)₄.



The synthesis of diethylformamide has now been tested in varied liquid polymers (Table 6). All yields were calculated from ¹H NMR spectra using a hexamethylbenzene internal standard. The reaction performance was superior in PPG. Surprisingly, the other polyethers (PEG and PTHF) were inferior for this application.

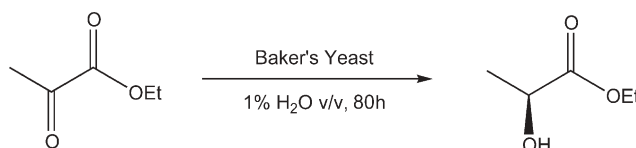
Table 6 Diethylformamide synthesis results^a

Liquid phase	Yield of amide (%)	TON formic acid	TON amide
[Et ₂ NH ₂][O ₂ CNEt ₂]	38 ^b	—	—
PPG-3500	52	78	760
PMPS-710	39	85	570
PTHF	30	37	440
PEG-1000	28	0	410
PEG-DME	15	25	210

^a 5 mmol NHEt₂, 3.4 μmol RuCl₂(PMe₃)₄, 80 bar H₂, 100 °C, 200 bar total pressure with CO₂, 23 h. ^b 2.3 μmol catalyst, 13 h.⁴⁶

Yeast-catalyzed reductions of ethyl pyruvate

Liquid polymers could conceivably find application in other areas of catalysis. Because ionic liquids have been investigated as solvents for cell-catalyzed reactions,⁴⁷ it seemed appropriate to determine whether liquid polymers could be used in such a manner. The Baker's yeast reduction of ethyl pyruvate (reaction 5) was chosen as a test reaction.



Baker's yeast *Saccharomyces cerevisiae* is a highly effective and inexpensive whole-cell catalyst for asymmetric reductions of ketones, aldehydes, keto-acids and keto-esters.^{48,49} Historically these reductions have been performed in water, however noticeable selectivity changes have been reported when Baker's yeast has been used in organic solvents.⁵⁰ Hydrophobic organic solvents such as hexane, toluene and ether gave surprisingly high conversion and with enantioselectivity greater than that observed in water.⁵⁰ Baker's yeast reactions have recently been performed in [bmim]PF₆ but the ee was moderate.⁴⁷ Yeast-catalyzed reactions have been performed in aqueous solutions of PEG,⁵¹ which demonstrates that such polymers are sufficiently biocompatible with yeast.

The Baker's yeast reduction of ethyl pyruvate has now been performed in two liquid polymers and in more ionic liquids. The results of the reductions are compared with corresponding reductions in water and organic media (Table 7). Small amounts of water were added to all reaction mixtures because a minimum of a 1 : 1 mass ratio of water to yeast is required for whole-cell promoted reductions to remain active in organic media.^{47–50,52–55}

Good to excellent conversion was observed in the three ionic liquids tested, but the enantioselectivity was significantly greater than in water only for the phosphonium ionic liquid. Tests with other phosphonium ionic liquids were unsuccessful because we could not identify an effective technique for cleanly extracting the product from the reaction mixture.

The whole-cell reductions in polymers were limited to those that are liquid at room temperature, specifically PPG-3500 and PMPS-710. The reduction in PMPS, with product extraction into water, gave an exceptional 99% ee. The reduction did not proceed in PPG; the starting material was cleanly recovered when extracted from the reaction mixture with scCO₂. The

Table 7 Reductions of ethyl pyruvate with Baker's yeast^a

Solvent	Conversion (%)	ee (%)	Reference
Traditional			
Hexane	100	100	50
Toluene	80	100	50
Diethyl Ether	99	97	50
Ethyl Acetate	97	89	50
Water	100	93	50
Ionic liquid			
[bmim]PF ₆	na	76	47
[bmim]BF ₄	100 ^b	64	This work
[bmp]BF ₄ ^c	100 ^b	94	This work
[P(^t Bu) ₃ Me]O ₃ SC ₆ H ₄ Me	88	99	This work
Liquid polymers			
PMPS-710	62	99	This work
PPG-3500	0	na	This work
PPG-3500	100 ^d	na	This work

^a All conversions are calculated by ¹H NMR spectroscopy. Reactions were performed at 30 °C in traditional solvents and at room temperature for ionic liquids and liquid polymers. Reaction time 23–24 h. ^b 3 days. ^c 1-butyl-3-methylpyridinium tetrafluoroborate. ^d Polymer washed with 0.1 M KOH solution before use. 5 days reaction time.

failure of the reaction in PPG may be a result of the phenolic stabilizer that is present in the liquid polymer supplied by Aldrich. Yeast-catalyzed reactions have been performed in the presence of PEG.⁵¹ The reaction in PPG was repeated in PPG that had been prewashed with 0.1 M KOH solution and then distilled water. This reaction did proceed (product and no starting material was obtained upon post-reaction extraction) but the recovery of product was so poor that it was not possible to determine the enantiomeric excess.

Recovery of the product can be challenging for whole-cell promoted reductions. The enzymes retain a small amount of the product inside the active site and this marginally reduces the recoverable yield. Traditionally organic solvent extractions are used to recover the product from the reaction mixture. Our product extractions from [bmp]BF₄ with hexane gave a very poor isolated yield (3%). The product extraction from [P(^tBu)₃Me]O₃SC₆H₄Me using ether also resulted in poor yields. Since yields were lower than expected, we decided to switch to product distillation due to the negligible vapor pressure of ILs and liquid polymers. This method is effective only if the boiling point of the product is relatively low. Efforts to distill product out of polyether glycols resulted in hydrolysis of the polyethers due to the high water concentration and high temperature. Vacuum distillation of the product from [bmim]BF₄ gave an isolated yield of 7%. Extraction of the product from [P(^tBu)₃Me]O₃SC₆H₄Me with scCO₂ (45 °C, 140 bar, 4 h, 0.3 mL min⁻¹) gave a better yield of product but it was accompanied by large amounts of impurities believed to result from lysing of the yeast. Reducing the extraction pressure to 110 bar greatly reduced both the amount of impurities and the recovered yield of product.

Whole-cell promoted reductions are no longer limited to water and traditional organic solvents. The excellent enantioselectivity of the yeast-catalyzed reaction in triisobutyl(methyl)phosphonium tosylate and in PMPS suggest that, with further work on the separation method, these materials will be promising solvents for such reactions.

Conclusions

Liquid polymers are nonvolatile solvents that can be used in conjunction with scCO₂ as media for homogeneous catalysis with catalyst recovery. The role of the liquid polymer, as reaction medium and catalyst-bearing phase, is similar to that performed by ionic liquids in biphasic catalysis. However, because liquid polymers are less polar than ionic liquids, the polymers should be seen as complementary to, rather than replacements of, ionic liquids. The liquid polymers are tunable over a wide range of polarities by modification of the repeating unit and by expansion of the polymer with dissolved CO₂.

PEG has a reasonable claim to the label “green solvent” because it is nonvolatile, nonflammable, nontoxic to humans, animals and aquatic life, and biodegradable by bacteria in soil and sewage. Each of the other liquid polymers has one less desirable characteristic: PPG is somewhat less biodegradable, PDMS and dialkylether-capped PEG are much less biodegradable and PTHF in the form of an aqueous emulsion is toxic to *daphnia magna*. Not enough is known about PMPS to make a conclusion.

Four different reductions have been successfully performed in liquid polymer solvents, showing that these solvents have the potential to be more widely used as media for reactions and catalysis. The reactions evaluated in various liquid polymers and, for comparison, some ionic liquids, were the hydrogenation of styrene, the asymmetric hydrogenation of tiglic acid, the hydrogenation of CO₂ in the presence of diethylamine to give diethylformamide, and the yeast-catalysed reduction of ethyl pyruvate. The best liquid polymer solvent was different from reaction to reaction; PPG was best for CO₂ hydrogenation, PMPS was superior for yeast-catalyzed reduction, and several polymers performed equally well for tiglic acid hydrogenation. Extraction of the product by scCO₂ followed by recycling of the catalyst was demonstrated for styrene hydrogenation and tiglic acid asymmetric hydrogenation but was difficult for the yeast-catalyzed reduction.

Experimental

The hydrogenation product 2-methylbutanoic acid was purchased from Aldrich. The catalyst precursors Ru(OAc)₂[(*R*)-tolBINAP] and Ru(OAc)₂[(*S*)-tolBINAP] were prepared by the literature method.⁵⁶ Supercritical grade CO₂ (Praxair, SFE grade, 99.999%, H₂O < 0.5 ppm) was used as received. 1,2-Dimethyl-3-*n*-propylimidazolium bis(trifluoromethylsulfonyl)imide was a generous gift from Covalent Associates. Tetraalkylphosphonium ionic liquids were generous gifts of Cytec Industries. Baker's yeast *Saccharomyces cerevisiae* was obtained from Sigma and from Fleischmann's (*via* a grocery store); the Fleischmann's was more active. All other chemicals were obtained from commercial suppliers. Ionic liquids and liquid polymers for use with homogeneous catalysts were dried and degassed by exposure to strong vacuum at 40 °C for two days. The flasks containing the ionic liquids and liquid polymers were back-filled with nitrogen while cooling to room temperature. Traditional organic solvents were degassed with N₂ by repeated freeze–vacuum–thaw cycles.

Solvatochromic measurements

UV/visible spectra of Nile Red dye dissolved in solvents were acquired with a Agilent 8453 spectrophotometer. For atmospheric spectra, a cuvette of 10 mm path length was used. For high pressure spectra, a custom-built high-pressure UV/visible spectroscopy cell with an internal path length of 21 mm was used. The concentration of the dye was adjusted to ensure an absorbance between 0.5 and 1.0 at the peak maximum. UV/visible spectra were taken at room temperature except as indicated.

The high-pressure UV/visible spectroscopy cell was rinsed with acetone and dried by blowing N₂ into the cell for 1 h. All solvents were distilled and dried over 5 Å MS in flame dried flasks. All solvents were deoxygenated and brought into an inert atmosphere where they were tested for water content. The high pressure cell was loaded with 10–20 3 Å molecular sieves, the “Komet” stirbar and then 4 mL of solvent. Nile Red was introduced to the cell and the vessel was sealed.

Hydrogenation of tiglic acid (without pre-washing of the solvent)

Ru(OAc)₂[tolBINAP] (1.0 mg), tiglic acid (4.7 mg), degassed and dried solvent (2 mL) and stir bar were placed into an uncapped 1 dram glass vial which was then placed into a stainless steel vessel under inert atmosphere. The vessel was flushed with H₂ and then warmed to 40 °C and pressurized to 5 bar with H₂ for 24 h. After the hydrogenation, the product was isolated as described below and then dissolved into hexane. The hexane solution was filtered through a Prep Pep[™] silica column to remove any residual catalyst, dried with MgSO₄, filtered, and analysed by GC. 1 µL of the mixture was injected into a Shimadzu GC-17A with Class VP 7.1 software suite with a J&W Scientific Chirasil-Dex CB column, with the following parameters: 240 °C injector temperature, 240 °C detector, 105 °C column, isothermal. The two enantiomers of 2-methylbutyric acid eluted shortly before tiglic acid.

The hexane solutions of the product were prepared using the methods below.

(a) After hydrogenation in MeOH, the solvent was removed by rotary evaporation and the residue was dissolved in 2 mL hexane.

(b) After hydrogenation in PEG, the PEG solution was melted and extracted with five washes of hexane (1.5 mL). The hexane solution was cooled in an ice-bath to precipitate out any dissolved PEG.

(c) After hydrogenation in PMPS-710, the product was extracted with three portions of 1 mL H₂O. The product was then extracted from the combined aqueous layers with three portions of hexane (1.5 mL).

(d) After hydrogenation in triisobutylmethylphosphonium tosylate or PPG-3500, the product was extracted with one portion of 0.1 M KOH (2 mL) and then three 1 mL portions of H₂O. The combined aqueous portions were acidified with 0.1 M HCl and then extracted three times with 1 mL hexane.

Alternatively, the product was extracted from the PEG or PMPS solvent using scCO₂ (40 °C, 125 to 150 bar, 1 mL min⁻¹ CO₂, 12 h).

Hydrogenation of tiglic acid (with pre-washing of the solvent)

Polymer (10 mL) and a 1" Teflon stirbar were loaded into a 160 mL extraction vessel containing a dip tube. The vessel was warmed to 40 °C in a water bath and supercritical CO₂ (40 °C, 150 bar) was passed through the polymer, *via* the dip tube, at a rate of 2 mL min⁻¹ for 3 h. After this time, the vessel was cooled to room temperature and bled to five bar of pressure. The vessel exterior was dried and the remaining CO₂ pressure was released. The vessel was opened under an inert atmosphere revealing the polymer (clear and colourless liquid PMPS or white and fluffy for the other polymers).

Ru(OAc)₂[(*S*)-tolBINAP] (5.3 mg) and tiglic acid (100 mg) were added to the washed sample of polymer in the steel vessel. The vessel was warmed to 40 °C, flushed with H₂, and pressurized to 5 bar with H₂ for 24 h. After the hydrogenation, the product was extracted from the liquid polymer with scCO₂ (150 bar, 40 °C, 8 h, 1 mL min⁻¹) and trapped in ice-cooled acetone. The acetone solution of extracted product was concentrated to dryness, weighed and then dissolved into hexane and analyzed by gas chromatography.

Hydrogenation of tiglic acid in PEG with catalyst recycling

PEG-1000 (10 g) was pre-washed with scCO₂ as described above. The resulting white and fluffy PEG was mixed with Ru(OAc)₂[(*S*)-tolBINAP] (26.5 mg, 27.5 µmol) and tiglic acid (500.0 mg, 5 mmol) and then sealed. The vessel was warmed to 40 °C and pressurized to 4.9 bar with H₂ for 24 h. After the hydrogenation, the product was extracted from the liquid polymer with scCO₂ (125–150 bar, 40 °C, 8 h, 1 mL min⁻¹) and trapped in ice-cooled acetone. Once the extraction was complete, the vessel was cooled to room temperature and bled to five bar. The vessel exterior was dried and then the pressurized vessel was passed into an inert atmosphere glove box, opened and charged again with fresh substrate. After each cycle the PEG was pale yellow and fluffy. This method was performed for a total of five cycles, each time with fresh substrate. Each acetone solution was concentrated to dryness by rotary evaporation, weighed and then dissolved into hexane and analyzed by gas chromatography.

Encapsulation of RhCl(PPh₃)₃ in PEG

PEG-1500 (10 g) and RhCl(PPh₃)₃ (5 mg) were stirred at 50 °C for 30 min under 50 bar of CO₂. The sample was cooled and depressurized. The residual puck of catalyst solidified in PEG-1500 was left open to air for 1 month. The puck and styrene (0.5 mL) were combined in a 160 mL vessel, which was warmed to 40 °C and pressurized to 30 bar with H₂. CO₂ was added to a total pressure of 80 bar, and the solution was stirred for 19 h. The vessel was then heated to 60 °C and the product was extracted with scCO₂ (155 bar, 2 mL min⁻¹, 5 h).

Synthesis of diethylformamide

Diethylamine (5 mmol), RuCl₂(PMe₃)₄ (3.4 µmol), a stir bar, and solvent (2 mL or 2 g) were loaded into a 31 mL stainless steel reactor under nitrogen atmosphere. The vessel was heated to 100 °C in an oil bath for 20 min and then pressurized with H₂ (80 bar) for 1 h. CO₂ was then added to bring the total

pressure to 200 bar. After 23 h with constant stirring at 100 °C, the vessel was cooled in ice water and then in acetone/dry ice until the pressure reached a steady low value. The gas was slowly vented and the vessel then warmed to room temperature and opened. Hexamethylbenzene (0.267 mmol) was added as an internal standard. The contents of the vessel were then transferred into a vial, and any residues in the vessel were washed into the vial with three 0.5 mL aliquots of CDCl₃. A portion of the vial contents were analyzed by ¹H NMR spectroscopy.

Yeast-catalyzed reduction of ethyl pyruvate

Ethyl pyruvate (50 µL), water (50 µL), yeast *Saccharomyces cerevisiae* (50 mg), solvent (5 mL) and a stir bar were placed in an 8 mL glass vial and stirred under air for 23 h. The product and any unreacted ethyl pyruvate was extracted from the reaction mixture with ether or scCO₂ (45 °C, 140 bar, 0.3 mL min⁻¹, 16 h into 50 mL of ice-cold acetone). The extracted material was dissolved in hexane prior to analysis by chiral gas chromatography (70 °C isothermal, injector and detector 225 °C, Supelco Beta DEX-225 (2,3,-di-O-acetyl-6-O-tert-butylidimethylsilyl-β-cyclodextrin) column, 30 m length, 0.25 mm diameter, 0.25 µm thickness). The extent of conversion was determined by ¹H NMR spectroscopy of the extracted material dissolved in CDCl₃.

Racemic ethyl lactate was prepared, in order to determine the GC retention times, by reducing ethyl pyruvate (0.045 moles) with NaBH₄ (0.050 moles) in 20 mL of anhydrous THF stirred for 30 min. The resulting solution was quenched with saturated aqueous NaCl solution, and washed with three 10 mL portions of saturated aqueous NaCl solution. The water layers were extracted with one 10 mL portion of THF. The THF layers were combined and dried over MgSO₄, filtered through filter paper, and concentrated in vacuo to a clear and colourless liquid residue, ethyl lactate, in 66% yield. The identification was confirmed by ¹H NMR spectroscopy.

Before the second experiment with PPG (Table 7, last entry), PPG-3500 (14 mL) was stirred with 0.1 M KOH solution (20 mL) for 30 min, then CHCl₃ was added. Without the CHCl₃, PPG and the KOH solution do not separate cleanly because they have identical densities. The aqueous phase was then discarded and the organic phase was washed with another portion of KOH solution (10 mL) for 30 min. After separation, the organic phase was washed with deionized water three times (70 mL each). The pH of the last aqueous wash was neutral to universal pH paper. The polymer was then heated to 60 °C under vacuum for 1 h. A portion of this washed polymer was used as a solvent for ethyl lactate reduction as described above. The product from the reduction was extracted from the PPG with the following method: hexane (20 mL) was added to the reaction mixture, the product was extracted with water (2 × 20 mL), the combined aqueous fractions were gravity filtered through filter paper and then passed slowly through an SPE column (C18, UCT CUC181M6). The product was removed from the SPE column with CHCl₃ (10 mL), dried with MgSO₄, decanted, and concentrated to the oily product by vacuum evaporation of the solvent.

Acknowledgements

We acknowledge the experimental assistance of David Jessop, Etai Adam, Vanessa Mann, and Andrew Carrier. We thank Cytec Industries and Covalent Associates for gifts of ionic liquid samples. PGJ and DJH acknowledge support from the Division of Chemical Sciences, Office of Basic Energy Sciences, Office of Science, U. S. Department of Energy (grant number DE-FG03-99ER14986) and the Natural Sciences and Engineering Research Council of Canada. PGJ, Canada Research Chair in Green Chemistry, also acknowledges the support of the Canada Research Chair program.

References

- 1 L. A. Blanchard, Z. Gu and J. F. Brennecke, *J. Phys. Chem. B*, 2001, **105**, 2437–2444.
- 2 L. A. Blanchard, D. Hancu, E. J. Beckman and J. F. Brennecke, *Nature*, 1999, **399**, 28–29.
- 3 R. A. Brown, P. Pollet, E. McKoon, C. A. Eckert, C. L. Liotta and P. G. Jessop, *J. Am. Chem. Soc.*, 2001, **123**, 1254–1255.
- 4 F. C. Liu, M. B. Abrams, R. T. Baker and W. Tumas, *Chem. Commun.*, 2001, 433–434.
- 5 M. F. Sellin, P. B. Webb and D. J. Cole-Hamilton, *Chem. Commun.*, 2001, 781–782.
- 6 A. Bösmann, G. Franciò, E. Janssen, M. Solinas, W. Leitner and P. Wasserscheid, *Angew. Chem., Int. Ed.*, 2001, **40**, 2697–2699.
- 7 H. Sovová, J. Jez and M. Khachatryan, *Fluid Phase Equilib.*, 1997, **137**, 185–191.
- 8 A. Garg, E. Gulari and C. W. Manke, *Macromolecules*, 1994, **27**, 5643–5653.
- 9 D. J. Heldebrant and P. G. Jessop, *J. Am. Chem. Soc.*, 2003, **125**, 5600–5601.
- 10 M. J. Naughton and R. S. Drago, *J. Catal.*, 1995, **155**, 383–389.
- 11 (a) R. G. da Rosa, L. Martinelli, L. H. M. da Silva and W. Loh, *Chem. Commun.*, 2000, 33–34; (b) V. V. Namboodiri and R. S. Varma, *Green Chem.*, 2001, **3**, 146–148; (c) A. Haimov and R. Neumann, *Chem. Commun.*, 2002, 876–877; (d) S. Chandrasekhar, C. Narsihmulu, S. S. Sultana and N. R. Reddy, *Org. Lett.*, 2002, **4**, 4399–4401; (e) S. Chandrasekhar, C. Narsihmulu, S. S. Sultana and N. R. Reddy, *Chem. Commun.*, 2003, 1716–1717; (f) J.-H. Li, Q.-M. Zhu, Y. Liang and D. Yang, *J. Org. Chem.*, 2005, **70**, 5347–5349; (g) J.-H. Li, W.-J. Liu and Y.-X. Xie, *J. Org. Chem.*, 2005, **70**, 5409–5412; (h) Z. H. Zhang, L. Yin, Y.-M. Wang, J. Y. Liu and Y. Li, *Green Chem.*, 2004, **6**, 563–565; (i) A. Corma, H. Garcia and A. Leyva, *Tetrahedron*, 2005, **61**, 9848–9854; (j) S. Chandrasekhar, S. J. Prakash and C. L. Rao, *J. Org. Chem.*, in press.
- 12 P. C. Andrews, A. C. Peatt and C. L. Raston, *Green Chem.*, 2004, **6**, 119–122.
- 13 K. Verschueren, *Handbook of environmental data on organic chemicals*, 4th edn, Wiley, New York, 2001.
- 14 *Toxicological Evaluation of Certain Food Additives*, World Health Organization, Food Additives Series 14, Geneva, 1979.
- 15 *Code of Federal Regulations, Title 21*, vol. 3, CITE 21CFR172.820, FDA, Washington, 2001.
- 16 W. Janicke, G. Bringmann and R. Kuehn, *Gesund. Ing.*, 1969, **90**, 133–138.
- 17 R. J. Bernot, M. A. Brueseke, M. A. Evans-White and G. A. Lamberti, *Environ. Toxicol. Chem.*, 2005, **24**, 87–92.
- 18 S. Chemie, *Shell Industrie Chemicalien gids*, Shell Nederland Chemie, Afd. Industriechemicalien, Wassenaarseweg 80, 's-Gravenhage, Nederland, 1975.
- 19 M. Webb, H. Ruber and G. Leduc, *Water Res.*, 1976, **10**, 303–306.
- 20 G. W. Dawson, A. L. Jennings, D. Drozdowski and E. Rider, *J. Hazard. Mater.*, 1977, **1**, 303–318.
- 21 M. R. Britelli and C. F. Muska, *Initial submission: Aquatic toxicity of polytetramethylene glycol and its water soluble extract to daphnia magna with cover letter*, 425656, Doc#: 88-920002793, Haskell Laboratory, U.S. EPA/OPTS Public Files, Fiche #: OTS0539552, 1992.

- 22 B. F. Wilson, G. A. LeBlanc and R. E. Bentley, *Initial submission: Polytetramethylene glycol: The toxicity to Fathead Minnow (*pimephales promelas*) embryos and larvae*, Doc#: 88-920002790, EG&G, Bionomics, Aquatic Toxicology Laboratory, U.S. EPA/OTS, Fiche #: OTS0539549, 1992.
- 23 *28-Day subacute dermal rabbit biological activity study on I.D. No. 130-526 (methylphenylsiloxane copolymer)*, TSCATS/452381, EPA/OTS Doc #86940001642, 1994.
- 24 *Toxicological screening tests with XF-1015 (methylphenylsiloxane copolymer)*, 452400, Doc#: 86940001661, Food and Drug Research Laboratories, U.S. EPA/OTS, Fiche #: OTS0572696, 1994.
- 25 E. J. Hobbs, M. L. Keplinger and J. C. Calandra, *Environ. Res.*, 1975, **10**, 397–406.
- 26 J. L. Friedman and C. G. Greenwald, in *Kirk Othmer Encyclopedia of Chemical Technology*, John Wiley, New York, 1994, vol. 11.
- 27 G. K. Watson and N. Jones, *Water Res.*, 1977, **11**, 95–100.
- 28 F. Kawai and F. Moriya, *J. Fermentation Bioeng.*, 1991, **71**, 1–5.
- 29 F. Kawai, in *Advances in Biochemical Engineering/Biotechnology*, ed. A. Fiechter, Springer-Verlag, Berlin, 1995, vol. 52, pp. 151–194.
- 30 R. G. Lehmann, S. Varaprath, R. B. Annelin and J. L. Arndt, *Environ. Toxicol. Chem.*, 1995, **14**, 1299–1305.
- 31 C. Reichardt, M. Eschner and G. Schäfer, *J. Phys. Org. Chem.*, 2001, **14**, 737–751.
- 32 A. Kordikowski, A. P. Schenk, R. M. Van Nielen and C. J. Peters, *J. Supercrit. Fluids*, 1995, **8**, 205–216.
- 33 S. N. V. K. Aki, B. R. Mellein, E. M. Saurer and J. F. Brennecke, *J. Phys. Chem. B*, 2004, **108**, 20355–20365.
- 34 C. P. Fredlake, M. J. Muldoon, S. N. V. K. Aki, T. Welton and J. F. Brennecke, *Phys. Chem. Chem. Phys.*, 2004, **6**, 3280–3285.
- 35 A. J. Carmichael and K. R. Seddon, *J. Phys. Org. Chem.*, 2000, **V13**, 591–595.
- 36 J. F. Deye, T. A. Berger and A. G. Anderson, *Anal. Chem.*, 1990, **62**, 615–622.
- 37 L. W. Diamond and N. N. Akinfiev, *Fluid Phase Equilib.*, 2003, **208**, 265–290.
- 38 T. Guadagno and S. G. Kazarian, *J. Phys. Chem. B*, 2004, **108**, 13995–13999.
- 39 D. G. Hert, J. L. Anderson, S. N. V. K. Aki and J. F. Brennecke, *Chem. Commun.*, 2005, 2603–2605.
- 40 Z. K. Lopez-Castillo, S. N. V. K. Aki, M. A. Stadtherr and J. F. Brennecke, *Ind. Eng. Chem. Res.*, 2006, DOI: 10.1021/ie0601091.
- 41 C. Drohmann and E. J. Beckman, *J. Supercrit. Fluids*, 2002, **22**, 103–110.
- 42 E. Weidner, V. Wiesmet, Z. Knez and M. Skerget, *J. Supercrit. Fluids*, 1997, **10**, 139–147.
- 43 This differs from the approach of having a homogeneous catalyst reversibly adsorb onto the surface of a solid polymer, which is useful for catalyst recovery but not necessarily for protection of the catalyst from air. (a) M. Wende and J. A. Gladysz, *J. Am. Chem. Soc.*, 2003, **125**, 5861–5872; (b) L. V. Dinh and J. A. Gladysz, *Angew. Chem., Int. Ed.*, 2005, **44**, 4095–4097.
- 44 Y. Fang, Y. Liu and Y. Hu, *Faming Zhuanli Shenqing Gongkai Shuomingshu Pat.*, CN 1361093 A, 2002.
- 45 P. G. Jessop, Y. Hsiao, T. Ikariya and R. Noyori, *J. Am. Chem. Soc.*, 1994, **116**, 8851–8852.
- 46 P. G. Jessop, Y. Hsiao, T. Ikariya and R. Noyori, *J. Am. Chem. Soc.*, 1996, **118**, 344–355.
- 47 J. Howarth, P. James and J. Dai, *Tetrahedron Lett.*, 2001, **42**, 7517–7519.
- 48 S. Servi, *Synthesis*, 1990, 1–24.
- 49 R. Csuk and B. I. Glänzer, *Chem. Rev.*, 1991, **91**, 49–97.
- 50 O. Rotthaus, D. Krüger, M. Demuth and K. Schaffner, *Tetrahedron*, 1997, **53**, 935–937.
- 51 J. Sinha, P. K. Dey and T. Panda, *Biochem. Eng. J.*, 2000, **6**, 163–175.
- 52 T. Haag, T. Arslan and D. Seebach, *Chimia*, 1989, **43**, 351–353.
- 53 K. Nakamura, K. Inoue, K. Ushio, S. Oka and A. Ohno, *J. Org. Chem.*, 1988, **53**, 2589–2593.
- 54 K. Nakamura, S.-i. Kondo, Y. Kawai and A. Ohno, *Tetrahedron Lett.*, 1991, **32**, 7075–7078.
- 55 M. North, *Tetrahedron Lett.*, 1996, **37**, 1699–1702.
- 56 M. Kitamura, M. Tokunaga and R. Noyori, *J. Org. Chem.*, 1992, **57**, 4053–4054.

Continuous kinetic resolution catalysed by cross-linked enzyme aggregates, 'CLEAs', in supercritical CO₂

Helen R. Hobbs,^a Betti Kondor,^a Phil Stephenson,^a Roger A. Sheldon,^b Neil R. Thomas^c and Martyn Poliakoff^{*a}

Received 3rd April 2006, Accepted 23rd June 2006

First published as an Advance Article on the web 17th July 2006

DOI: 10.1039/b604738f

We report the use of cross-linked enzyme aggregates (CLEAs[®]) to catalyse the kinetic resolution of tetralol and 1-phenylethanol in a continuous supercritical carbon dioxide (scCO₂) system. We describe the performance of the CLEA from *Candida antarctica* lipase B (CALB) and compare this to the catalytic activity of Novozym 435 (CALB immobilised on a macroporous acrylic resin). In addition, we report a two-stage reaction with the kinetic resolution of 1-phenylethanol performed in series with the metal (Pd) catalysed hydrogenation of acetophenone. Reactions performed in series have a potential economic advantage as the second, and subsequent reactions do not require additional expenditure of energy for re-pressurization of solvent.

Introduction

Enzymes are increasingly used as catalysts for reactions on an industrial scale due to their high turnover numbers, enantioselectivity, substrate specificity, and ability to promote reactions at acceptable rates under mild conditions. In order to minimise the environmental impact of a chemical transformation, a number of groups have explored the use of enzymes in supercritical carbon dioxide (scCO₂)^{1–5} especially in recent years, Matsuda and co-workers.^{6–10} scCO₂ has been identified as a 'green' solvent with significant potential for industrial use as it provides a clean, non-toxic, non-flammable and tunable solvent system which is easily removed to leave reaction products free from undesirable organic residues; hence the combination of biocatalysis and scCO₂ is extremely attractive.^{11,12}

The use of enzymes in scCO₂ was pioneered by Randolph *et al.* and Hammond *et al.* in 1985.^{13,14} However, it was later reported that native enzymes were deactivated in this medium by CO₂ reacting with lysine residues on the surface of enzymes to form inhibitory carbamates.^{15–18} Several attempts have since been made to combat this phenomenon by using microemulsions or reverse micelles^{19–21} to stabilise the enzyme in a water pool whilst maintaining the benefit of the high diffusivity of scCO₂. Adverse effects on the catalytic activity of the enzyme were still reported, probably due to the reduction in pH of the local microenvironment in the water pool to *ca.* pH 3.5 by dissolution of CO₂.²⁰

Other approaches have been made to stabilise the enzyme by immobilisation. One example is cross-linked enzyme crystals (CLECs[®]) which have been successfully used as commercial biocatalysts^{22–26} and have been shown to be active in scCO₂.^{27,28} The main advantage of using CLECs is that the biocatalyst is almost entirely made up of protein, but the major limitation is the need to crystallise the enzyme, a lengthy procedure requiring high enzyme purity which can often be difficult to obtain and makes CLECs expensive.

Novozym 435 presents another approach which has also been widely investigated for use in scCO₂.^{29–32} It is a commercially available *Candida antarctica* lipase B (CALB) preparation, with the enzyme immobilised on a macroporous acrylic resin which results in some dilution of catalytic activity due to the introduction of a large proportion of non-catalytic matrix; in the case of Novozym 435, the matrix is *ca.* 90% of the total mass. Despite this disadvantage, Novozym 435 has become the biocatalyst most often investigated in scCO₂ because of its proven activity and stability.^{29,33,34} Applications include kinetic resolutions with excellent yields and selectivities, and the ability to scale up from batch to continuous supercritical flow systems.⁷

More recently, cross-linked enzyme aggregates (CLEAs)[†] have been prepared by Sheldon *et al.*³⁵ In a CLEA, the enzyme is precipitated from aqueous solution by adding a salt or a water-miscible organic solvent to form aggregates which are subsequently cross-linked with a bi-functional agent, such as glutaraldehyde^{36,37} or dextran polyaldehyde.³⁸ This procedure removes the need for the laborious crystallisation procedure for the protein, required for CLECs, yet provides an immobilised enzyme which is composed almost entirely of protein with only a minimal amount of cross-linking agent. Catalytic activities of CLEAs have been observed to exceed those of the native lipases due to conformational changes of the protein induced by the aggregated state.³⁹ The CLEA

^aSchool of Chemistry, University of Nottingham, University Park, Nottingham, UK NG7 2RD.

E-mail: martyn.poliakoff@nottingham.ac.uk; Fax: +44 115 9513058; Tel: +44 115 9513520

^bBiocatalysis and Organic Chemistry, Department of Biotechnology, Delft University of Technology, Julianalaan 136, 2628 BL, Delft, The Netherlands. E-mail: R.A.Sheldon@tmw.tudelft.nl; Tel: +31 15 2782675

^cCentre for Biomolecular Sciences, University of Nottingham, University Park, Nottingham, UK NG7 2RD.

E-mail: neil.thomas@nottingham.ac.uk; Tel: +44 115 9513565

[†] CLEAs[®] are a registered trade mark of Clear Technologies, Delft, The Netherlands.

technique is attractive in both its simplicity and its robustness, combining purification with immobilisation in one step. There is also the opportunity to co-immobilise different enzymes for use in one-pot, multi-step syntheses.³⁵

Previously, the majority of biocatalytic reactions in $scCO_2$ have been carried out under batch conditions, but now reactions are increasingly being performed under continuous flow conditions to remove the problems associated with scale-up.^{7,32,40} The application of immobilised biocatalysts in combination with $scCO_2$ facilitates the change from batch to continuous processes. Matsuda and co-workers have reported a most efficient example of continuous biocatalysis using $scCO_2$; the kinetic resolution of 1-arylethanol catalysed by Novozym 435. Matsuda *et al.*⁹ briefly reported the use of a CALB CLEA in combination with $scCO_2$ resulting in high enantioselectivities albeit in a batch process. Interestingly, when $scCO_2$ was used as the reaction medium, a rate enhancement was observed for the CLEA preparation over Novozym 435.

In this paper, we develop further the concept of combining CLEAs and $scCO_2$ in continuous reactions. In addition we demonstrate that the enzyme reaction can be incorporated into a sequential two-stage process (hydrogenation followed by kinetic resolution) with the potential for significant energy saving by removing the requirement to depressurise between reactions.

Experimental

Safety note: All supercritical experiments involve high pressures and must be conducted in appropriate equipment.

Materials

CLEA CALB 301 (28000 U g^{-1}) was kindly donated by Dr Rob Schoevaart of CLEA Technologies (Delft, The Netherlands). Novozym 435 (3500 U g^{-1}) was obtained from Novozymes (Denmark). 1-Phenylethanol, α -tetralol and hexane were purchased from Aldrich, vinyl acetate from Lancaster. SCF grade carbon dioxide (99.99% purity) was obtained from BOC gases.

Batch reactions

Batch reactions in hexane were carried out in a 5 mL glass vial with a rubber septum (Supelco). 1-Phenylethanol (0.08 M) and vinyl acetate (0.54 M) in hexane (5 mL) were added to the CALB preparation (0.12 μ M) and gently stirred with a magnetic stirrer bar at 40 °C. After completion of the reaction time, an aliquot (1 mL) was taken, centrifuged to remove the enzyme and the products were analysed on a Shimadzu GC-2010 GLC equipped with a β -DEX 225 chiral column.

Supercritical batch reactions were conducted in a purpose built autoclave⁴¹ (8.5 mL) containing a magnetic stirrer bar. The CALB preparation (0.12 μ M), 1-phenylethanol (0.08 M) and vinyl acetate (0.54 M) were added to the autoclave which was sealed and heated to the desired temperature. The autoclave was then pressurised with CO_2 and the contents magnetically stirred. At the end of the reaction, the heating and stirring were stopped and the autoclave was placed in a

dry ice–acetone bath. Once the pressure inside the autoclave had fallen to approximately atmospheric pressure, the autoclave was opened and the solid CO_2 was allowed to sublime. The reaction products remaining in the autoclave were collected in acetone (1 mL) and analysed by chiral GLC. This procedure avoided the possibility of losing product if the autoclave was vented at room temperature.

Continuous flow reactions

The apparatus for small scale continuous flow reactions has been described previously.⁴² The system is essentially modular, made from commercially available components. The layouts of the two systems used in this paper are illustrated in Fig. 1 and 2.

Results and discussion

Batch kinetic resolution

The first reaction studied was the kinetic resolution of 1-phenylethanol (**1**) with vinyl acetate (**2**) as the acyl donor (Scheme 1). CALB selectively catalyses the acetylation of (*R*)-**1** forming (*R*)-**3** and acetaldehyde **4** whilst leaving the (*S*)-**1** alcohol unreacted.

Initially, we established that our sample of CALB CLEA was active in batch reactions in both hexane and $scCO_2$ and compared its activity with both native CALB and Novozym 435. The results are summarized in Table 1.

It can be seen that, as expected, Novozym 435 displays excellent activity and selectivity in hexane (entry 1). The same reaction in $scCO_2$ results in a drop in both conversion and enantioselectivity (entry 2). Native CALB displays a much lower activity than Novozym 435 in both hexane and $scCO_2$. CALB CLEA gives excellent enantioselectivity in hexane

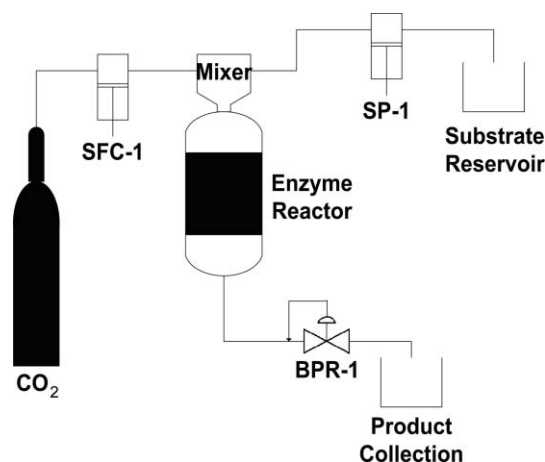


Fig. 1 Schematic diagram of the continuous $scCO_2$ reaction system. The CO_2 is pressurised and delivered by SFC-1 [Jasco PU-1580-CO2]. The organic substrates are delivered at a constant rate *via* a standard HPLC pump, SP-1 [Jasco PU-980]. The feed streams are mixed in a heated, static mixer before being passed through the enzyme reactor (0.5 cm^3 in volume). Products are collected after depressurization of the reaction mixture by an electronic backpressure regulator, BPR-1 [Jasco BP-1580-81], and analysed off-line by chiral GLC.

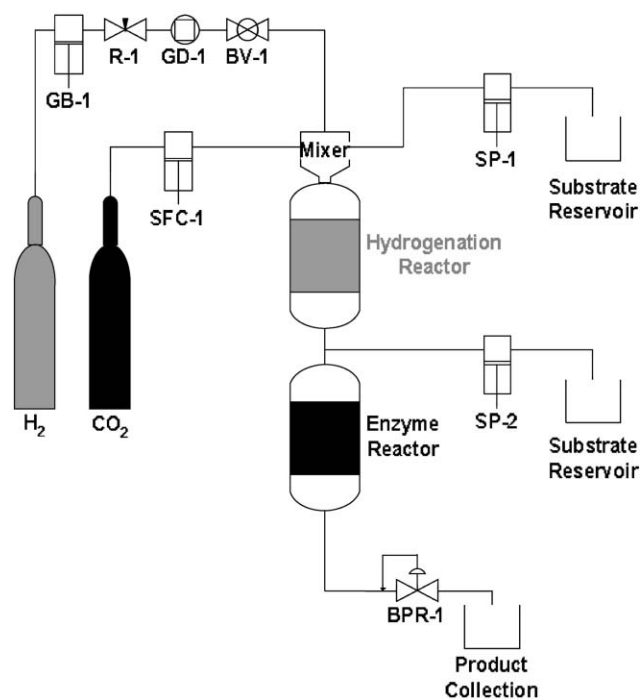
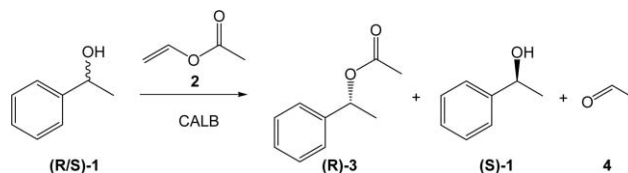
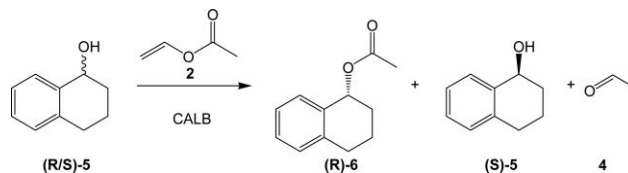


Fig. 2 Schematic diagram of hydrogenation and enzymatic reaction apparatus. Hydrogen gas is pressurised to a constant pressure using a gas booster, GB-1 [NWA CU-105], and regulator, R-1, before being dosed into the reactor by a gas dosage unit, GD-1 [Rheodyne 7000L]; the supply is isolable using the ball valve (BV-1). The CO₂ is pressurised and delivered by SFC-1 [Jasco PU-1580-CO₂], as in the original single reactor set up, Fig. 1. The organic substrate is delivered via a standard HPLC pump, SP-1 [Jasco PU-980]. The reaction mixture is passed over 2% Pd catalyst supported on silica/alumina (Johnson Matthey plc) in the hydrogenation reactor (1.5 mL). A second substrate feed after the first reactor supplies the vinyl acetate. The substrates are immediately passed through the enzyme reactor (1.5 mL) which is filled with either Novozym 435 or CALB CLEA as required.

(entry 5), but both conversion and enantioselectivity are even better in scCO₂ (entry 6). Furthermore, pressures up to 200 bar do not appear to affect the CLEA catalytic activity (entry 7). Thus, CALB CLEA is a superior catalyst for this kinetic resolution in scCO₂ compared to native CALB and Novozym 435 in scCO₂. Novozym 435, however, is the better catalyst for this kinetic resolution in hexane.



Scheme 1 Kinetic resolution of 1-phenylethanol with vinyl acetate as the acyl donor catalysed by CALB enzyme preparation.



Scheme 2 Kinetic resolution of α -tetralol (5) with vinyl acetate (2) using CALB enzyme preparation.

Continuous kinetic resolution

We studied kinetic resolution under continuous supercritical conditions using two alcohols: α -tetralol (5) (Scheme 2) and 1-phenylethanol (1) (Scheme 1).

The kinetic resolution of 5 was investigated using both Novozym 435 and CALB CLEA, see Table 2.

The results in Table 2 show that 5 can be kinetically resolved in a continuous flow scCO₂ reactor under a variety of conditions. For the reaction catalysed by Novozym 435, conversions remain reasonably high for all of the temperatures and pressures studied with *E*-values > 100 indicating good enantioselectivity (entries 1–4). The kinetic resolution of 5 using CALB CLEA was less successful. Conversions and enantioselectivity are lower than for Novozym 435 which may be due to the poor solubility of α -tetralol in scCO₂⁴⁴ which may limit mass transport in this case. For Novozym 435, the CALB enzyme is immobilised on the surface of a macroporous acrylic resin and so all the enzyme active sites are available to 5 as it is pumped over the catalyst bed. But for CALB CLEA active sites can be found both on the enzyme surface and within the aggregate; where this usually is not a problem for substrates fully soluble in scCO₂, it may well be a limitation for 5 due to poor solubility in scCO₂ and hence reduced transport of the substrate to all available active sites. To test this, the experiment was repeated using 60 mg CALB CLEA. Higher

Table 1 Kinetic resolution of 1-phenylethanol (1) catalysed by three different preparations of CALB in both hexane and scCO₂ batch reactions^a

Entry	CALB	Reaction medium	Pressure/bar	<i>ee</i> _s ^b (%)	<i>ee</i> _p ^b (%)	<i>c</i> ^c (%)	<i>E</i> -value ^c
1	Novozym 435	Hexane	—	99	99	50	>1000
2	Novozym 435	scCO ₂	90	20	>99	17	240
3	Native	Hexane	—	3	80	4	N.d. ^d
4	Native	scCO ₂	90	2	>99	<1	N.d. ^d
5	CLEA	Hexane	—	35	>99	26	280
6	CLEA	scCO ₂	90	91	>99	48	640
7	CLEA	scCO ₂	200	93	>99	48	680

^a Reaction conditions: Temperature 40 °C, magnetic stirring for 2.5 hours, 0.08 M 1-phenylethanol, 0.54 M vinyl acetate and 0.12 μ M CALB enzyme (CLEA, native or Novozym 435). ^b Products were analysed on a Shimadzu GC-2010 GLC equipped with a β -DEX 225 chiral column. No side reactions were detected. ^c Enantiomeric excess for substrates (*ee*_s) and products (*ee*_p) were used to determine the *E*-value which evaluates enantioselectivity.⁴³ Conversion (*c*) = $ee_s/(ee_s + ee_p) \times 100$. $E = \ln[(1 - c/100)/(1 + ee_p/100)]/\ln[(1 - c/100)(1 - ee_p/100)]$; *E*-values > 100 indicate a highly enantioselective reaction. ^d N.d.: not determined due to low conversion observed.

Table 2 Continuous kinetic resolution of α -tetralol (**5**) catalysed by Novozym 435 and CALB CLEA under supercritical conditions^a

Novozym 435				CALB CLEA				Entry	<i>ee</i> _s (%)	<i>ee</i> _p (%)	<i>c</i> (%)	<i>E</i> -value	Conditions
Entry	<i>ee</i> _s (%)	<i>ee</i> _p (%)	<i>c</i> (%)	Entry	<i>ee</i> _s (%)	<i>ee</i> _p (%)	<i>c</i> (%)						
1	59	97	30	>100	5	3	88	4	N.d.	100 bar, 30 °C			
2	61	97	39	>100	6	4	91	4	N.d.	200 bar, 30 °C			
3	67	97	41	>100	7	6	93	6	N.d.	100 bar, 40 °C			
4	75	97	44	>100	8	8	95	8	N.d.	100 bar, 50 °C			

^a Reaction conditions: CO₂ flow rate 1 mL min⁻¹, substrate flow rate = 0.2 mL min⁻¹ (1 : 1 volume ratio of α -tetralol : vinyl acetate). The enzyme reactor was filled with Novozym 435 (250 mg, 0.8 nmol CALB) or CALB CLEA (25 mg, 0.8 nmol CALB).

conversion was observed (13%) with *E*-value > 100 at 100 bar and 50 °C. In both cases, the conversion was improved at high temperatures due to the enhanced activity of the enzyme at 50 °C. The resolution of α -tetralol by CALB catalysed transesterification has previously been reported to proceed with an *E*-value of 29, in diisopropyl ether as a solvent at room temperature.⁴⁵

Kinetic resolution of 1-phenylethanol (**1**) was also studied under continuous supercritical conditions and the results are summarized in Fig. 3 and Table 3.

It is clear from Table 3 that increasing pressure decreases the conversion and the *ee* of (*S*)-**1**, although the *ee* and *E*-values of (*R*)-**3** remain very high. This decrease contrasts to the behaviour in the batch reactions (Table 1) and may be due

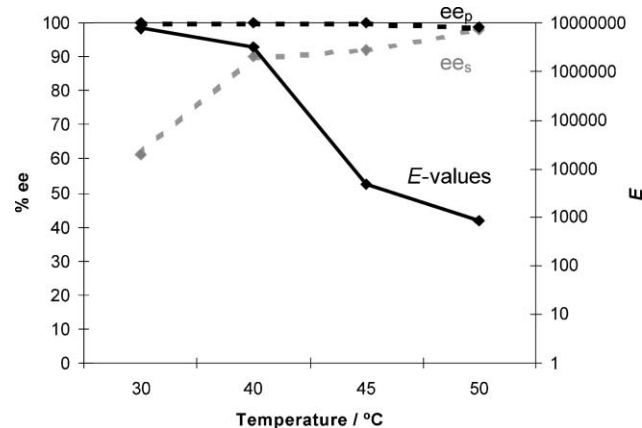


Fig. 3 Kinetic resolution of 1-phenylethanol (**1**) with vinyl acetate (**2**) using CALB CLEA in scCO₂. *ee*_s increases with temperature whereas *ee*_p is high for all temperatures. The *E*-values decrease with temperature but remain relatively high (>100) throughout the experiment. This is a highly efficient reaction as only 60 mg of CLEA was used. Reaction conditions: pressure 110 bar, CO₂ flow rate 0.25 mL min⁻¹, substrate flow rate = 0.05 mL min⁻¹ (1-phenylethanol).

Table 3 Continuous kinetic resolution of 1-phenylethanol (**1**) using CALB CLEA at 50 °C and various pressures in scCO₂^a

Pressure/bar	<i>ee</i> _s (%)	<i>ee</i> _p (%)	<i>c</i> (%)	<i>E</i> -value
110	98	99	50	>100
160	47	99	32	>100
200	37	99	27	>100

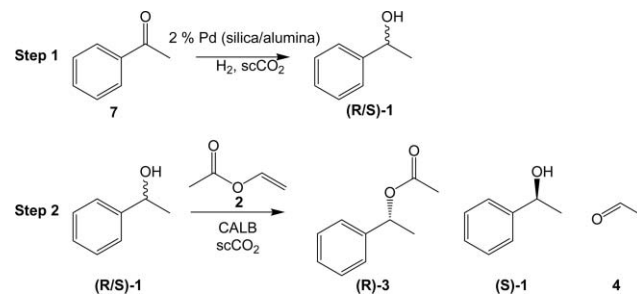
^a Reaction conditions: CO₂ flow rate 0.25 mL min⁻¹, substrate flow rate = 0.05 mL min⁻¹ (1-phenylethanol), 60 mg CALB CLEA (1.8 nmol).

to compaction of the CLEA in the reactor; probably a simple design change of the reactor could prevent this. The batch reaction was carried out at 200 bar with magnetic stirring to agitate the CLEA to ensure no compaction occurred. Under these conditions, *ee* for (*S*)-**1** remains high due to a high conversion (41%, Table 1). Conversions obtained for the kinetic resolution of **1** (Table 3) are much higher than for **5** (Table 2) when CALB CLEA is used as the catalyst. Presumably, this is due to the poor solubility of tetralol in scCO₂⁴⁴ in contrast to the complete miscibility of 1-phenylethanol (1.9 wt%) with scCO₂ under these conditions as determined by observation in a view cell.

Continuous hydrogenation of acetophenone and kinetic resolution of the product

Previous work at Nottingham,⁴² has shown that the hydrogenation of acetophenone over a Pd catalyst will generate 1-phenylethanol (Scheme 3). We have therefore combined this reaction with kinetic resolution with CALB in a single process. The configuration of the reactors and substrate feeds required careful planning, the set up can be seen in Fig. 2 and the results are collected in Table 4.

It can be seen from Table 4 that the sequential reactions work successfully. Even without optimization the conversion of **7** reached a maximum of 82%. The subsequent kinetic resolution catalysed by Novozym 435 proceeded well resulting in reasonable conversions and excellent enantioselectivity. The same reaction with CALB CLEA resulted in somewhat lower conversions but retained excellent enantioselectivity. To the best of our knowledge, this is the first example of a metal catalysed reaction and a biocatalytic reaction being conducted in series in continuous flow scCO₂.



Scheme 3 Hydrogenation of acetophenone (**7**) over an achiral Pd catalyst to produce (*R/S*)-**1**. The second step is the kinetic resolution of (*R/S*)-**1** to produce (*R*)-**3** and (*S*)-**1**.

Table 4 Hydrogenation of acetophenone (**7**) followed by the kinetic resolution of the product (*R/S*)-**1** catalysed by Novozym 435 or CALB CLEA; all *E*-values > 100^a

Pd temperature/°C	Novozym 435			CALB CLEA				
	<i>c</i> of 7 (%)	<i>ee</i> _s (%)	<i>ee</i> _p (%)	<i>c</i> (%)	<i>c</i> of 7 (%)	<i>ee</i> _s (%)	<i>ee</i> _p (%)	<i>c</i> (%)
150	68	41	>99	29	71	19	98	16
200	72	32	>99	24	74	17	>99	14
150 ^b	71	54	>99	35	76	28	98	22
150 ^c	74	44	>99	30	82	21	99	17

^a Reaction conditions: pressure 100 bar, CO₂ flow rate 1 mL min⁻¹, substrate flow rate = 0.1 mL min⁻¹ (acetophenone), H₂ : substrate ratio = 1 : 4, enzyme catalyst bed 40 °C unless otherwise stated, 250 mg Novozym 435 (0.8 nmol CALB) or 55 mg CALB CLEA (1.7 nmol CALB).

^b CO₂ flow rate 0.5 mL min⁻¹, substrate flow rate = 0.05 mL min⁻¹. ^c Enzyme catalyst bed 50 °C.

Conclusions

We have demonstrated that CLEAs from CALB have significant activity and stability in scCO₂. By contrast, native enzymes are often poorly active in scCO₂, probably due to inactivation by the formation of carbamates with lysine residues on the enzyme surface,^{12,15–18} and decrease in local pH due to the formation of carbonic acid.²⁰ However, immobilisation of the enzyme by CLEA methodology apparently prevents or reduces the adverse effects of scCO₂. This can probably be attributed to the fact that the cross-linking process involves the reaction of the amino groups of surface lysine residues in the enzyme thus making them unavailable for reaction with CO₂. For the kinetic resolution of 1-phenylethanol, scCO₂ appears to enhance mass transport, as shown by an increased reaction rate, compared to the same reaction performed in hexane. CALB CLEA has a comparable activity to the same reaction catalysed by Novozym 435. Temperature (30–50 °C) and pressure (90–200 bar) have a minimal effect on the specific activity of the CALB CLEA in scCO₂. For the kinetic resolution of α -tetralol, Novozym 435 is the better catalyst possibly due to the larger number of active sites available on the surface of this enzyme preparation in combination with the limited solubility of the substrate in scCO₂.

Both α -tetralol and 1-phenylethanol have been studied as substrates for kinetic resolution with vinyl acetate and resulted in good enantioselectivities and *E*-values for both Novozym 435 and CALB CLEA in a continuous flow regime. Compression of CO₂ is the single largest energy factor contributing to the cost of a scCO₂ process. Performing reactions in series has a considerable advantage over performing the reactions separately because there is no requirement for the SCF to be depressurized between reactions. Therefore, the economic productivity of the overall process should be increased.

Thus we have successfully expanded the use of a continuous flow system by the incorporation of two reactors linked in series. The first reactor was used for the metal catalysed hydrogenation of acetophenone and the second reactor for immobilised lipase (Novozym 435 or CALB CLEA) to catalyse the kinetic resolution of the resulting 1-phenylethanol. Both the series reactions performed with Novozym 435 and CALB CLEA were successful, with good conversions and excellent enantioselectivities. This demonstration opens up the possibility of exploiting highly selective biocatalytic reactions

in combination with metal catalysed reactions for multi-step chemistry in scCO₂.

Acknowledgements

We would like to thank our colleagues in the Clean Technology Group at The University of Nottingham, in particular to Messrs M. Guyler, M. Dellar, P. Fields, R. Wilson for their invaluable technical assistance. We are also grateful to Drs P. Licence, J. R. Hyde and B. Walsh for helpful discussions. We thank Thomas Swan & Co. Ltd., the CRYSTAL Faraday Partnership, the BBSRC (Grant No. BBSSP200310406) and EPSRC (Grant No. GR/R02863) and the EU Marie Curie EST network, SubClean Probiomat (Grant No. MEST-CT-2004-007767) for financial support.

References

- J. F. Martins, I. B. Decarvalho, T. C. Desampaio and S. Barreiros, *Enzyme Microb. Technol.*, 1994, **16**, 785–790.
- A. Ballesteros, U. Bornscheuer, A. Capewell, D. Combes, J. S. Condoret, K. Koenig, F. N. Kolisis, A. Marty, U. Menge, T. Scheper, H. Stamatis and A. Xenakis, *Biocatal. Biotransform.*, 1995, **13**, 1–42.
- Y. Ikushima, N. Saito, M. Arai and H. W. Blanch, *J. Phys. Chem.*, 1995, **99**, 8941–8944.
- Z. Knez, M. Habulin and V. Krmelj, *J. Supercrit. Fluids*, 1998, **14**, 17–29.
- T. Mori and Y. Okahata, *Chem. Commun.*, 1998, 2215–2216.
- T. Matsuda, T. Harada and K. Nakamura, *Chem. Commun.*, 2000, 1367–1368.
- T. Matsuda, K. Watanabe, T. Harada, K. Nakamura, Y. Arita, Y. Misumi, S. Ichikawa and T. Ikariya, *Chem. Commun.*, 2004, 2286–2287.
- T. Matsuda, T. Harada and K. Nakamura, *Green Chem.*, 2004, **6**, 440–444.
- T. Matsuda, K. Tsuji, T. Kamitanaka, T. Harada, K. Nakamura and T. Ikariya, *Chem. Lett.*, 2005, **34**, 1102–1103.
- T. Matsuda, T. Harada and K. Nakamura, *Curr. Org. Chem.*, 2005, **9**, 299–315.
- S. V. Kamat, E. J. Beckman and A. J. Russell, *Crit. Rev. Biotechnol.*, 1995, **15**, 41–71.
- A. J. Mesiano, E. J. Beckman and A. J. Russell, *Chem. Rev.*, 1999, **99**, 623–633.
- T. W. Randolph, H. W. Blanch, J. M. Prausnitz and C. R. Wilke, *Biotechnol. Lett.*, 1985, **7**, 325–328.
- D. A. Hammond, M. Karel, A. M. Klibanov and V. J. Krukonis, *Appl. Biochem. Biotechnol.*, 1985, **11**, 393–400.
- S. Kamat, J. Barrera, E. J. Beckman and A. J. Russell, *Biotechnol. Bioeng.*, 1992, **40**, 158–166.
- S. Kamat, G. Critchley, E. J. Beckman and A. J. Russell, *Biotechnol. Bioeng.*, 1995, **46**, 610–620.
- I. B. de Carvalho, T. C. de Sampaio and S. Barreiros, *Biotechnol. Bioeng.*, 1996, **49**, 399–404.

- 18 N. Mase, T. Sako, Y. Horikawa and K. Takabe, *Tetrahedron Lett.*, 2003, **44**, 5175–5178.
- 19 Y. Ikushima, *Adv. Colloid Interface Sci.*, 1997, **71–2**, 259–280.
- 20 J. D. Holmes, D. C. Steytler, G. D. Rees and B. H. Robinson, *Langmuir*, 1998, **14**, 6371–6376.
- 21 M. A. Kane, G. A. Baker, S. Pandey and F. V. Bright, *Langmuir*, 2000, **16**, 4901–4905.
- 22 N. L. St. Clair and M. A. Navia, *J. Am. Chem. Soc.*, 1992, **114**, 7314–7316.
- 23 A. L. Margolin, *Trends Biotechnol.*, 1996, **14**, 223–230.
- 24 J. Lalonde, *Chem.-Tech (Heidleberg)*, 1997, **27**, 38–45.
- 25 D. Haring and P. Schreier, *Curr. Opin. Chem. Biol.*, 1999, **3**, 35–38.
- 26 A. L. Margolin and M. A. Navia, *Angew. Chem., Int. Ed.*, 2001, **40**, 2205–2222.
- 27 N. Harper and S. Barreiros, *Biotechnol. Prog.*, 2002, **18**, 1451–1454.
- 28 N. Fontes, M. C. Almeida, S. Garcia, C. Peres, J. Partridge, P. J. Halling and S. Barreiros, *Biotechnol. Prog.*, 2001, **17**, 355–358.
- 29 M. C. Almeida, R. Ruivo, C. Maia, L. Freire, T. C. de Sampaio and S. Barreiros, *Enzyme Microb. Technol.*, 1998, **22**, 494–499.
- 30 M. C. Almeida, N. Fontes, E. Nogueiro, S. Garcia, C. Peres, A. Silva, M. de Carvalho and S. Barreiros, *Biotechnol. Prog.*, 1998, **15**, 487–491.
- 31 C. Peres, D. R. G. Da Silva and S. Barreiros, *J. Agric. Food Chem.*, 2003, **51**, 1884–1888.
- 32 M. D. Romero, L. Calvo, C. Alba, M. Habulin, M. Primozić and Z. Knez, *J. Supercrit. Fluids*, 2005, **33**, 77–84.
- 33 A. Overmeyer, S. Schrader-Lippelt, V. Kasche and G. Brunner, *Biotechnol. Lett.*, 1999, **21**, 65–69.
- 34 G. Madras, R. Kumar and J. Modak, *Ind. Eng. Chem. Res.*, 2004, **43**, 7697–7701.
- 35 R. A. Sheldon, R. Schoevaart and L. M. Van Langen, *Biocatal. Biotransform.*, 2005, **23**, 141–147.
- 36 L. Cao, L. M. van Langen, F. van Rantwijk and R. A. Sheldon, *J. Mol. Catal. B: Enzym.*, 2001, **11**, 665–670.
- 37 Y. Q. Cao and B. G. Pei, *Synth. Commun.*, 2000, **30**, 1759–1766.
- 38 C. Mateo, J. M. Palomo, L. M. van Langen, F. van Rantwijk and R. A. Sheldon, *Biotechnol. Bioeng.*, 2004, **86**, 273–276.
- 39 P. Lopez-Serrano, L. Cao, F. van Rantwijk and R. A. Sheldon, *Biotechnol. Lett.*, 2002, **24**, 1379–1383.
- 40 T. Matsuda, K. Watanabe, T. Kamitanaka, T. Harada and K. Nakamura, *Chem. Commun.*, 2003, 1198–1199.
- 41 C. J. Duxbury, *Ph.D. Thesis*, University of Nottingham, Nottingham, 2005.
- 42 J. R. Hyde, P. Licence, D. Carter and M. Poliakov, *Appl. Catal., A*, 2001, **222**, 119–131.
- 43 C. S. Chen, Y. Fujimoto, G. Girdaukas and C. J. Sih, *J. Am. Chem. Soc.*, 1982, **104**, 7294–7299.
- 44 P. Borg, J. N. Jaubert and F. Denet, *Fluid Phase Equilib.*, 2001, **191**, 59–69.
- 45 K. Suginaka, Y. Hayashi and Y. Yamamoto, *Tetrahedron: Asymmetry*, 1996, **7**, 1153–1158.

Short chain glycerol 1-monoethers—a new class of green solvo-surfactants

Sébastien Queste,^a Pierre Bauduin,^b Didier Touraud,^b Werner Kunz^b and Jean-Marie Aubry^{*a}

Received 17th March 2006, Accepted 26th June 2006

First published as an Advance Article on the web 18th July 2006

DOI: 10.1039/b603973a

The synthesis of short eco-friendly amphiphilic compounds derived from glycerol was carried out. These compounds, called solvo-surfactants, are of great interest since they exhibit both properties of solvents, *e.g.* volatility, solubilization of organics, and surfactants, *e.g.* reduction of interfacial tensions, formation of emulsions and microemulsions. Their surface activity was studied, and binary phase diagrams with water were drawn. Their sensitivity to various electrolytes from Hofmeister's series was also investigated. Short chain glycerol 1-monoethers constitute a new class of green solvo-surfactants with excellent properties, that should be seriously considered for the replacement of reprotoxic glycol ethers. They have, moreover, the advantage of helping to solve the problem of an over-production of glycerol, which is a major side-product of the biocarburant industry.

Introduction

The dissolution of inorganic and organic compounds is an essential operation in chemistry. It can be achieved by molecular solubilization in water or organic solvents, but for different reasons (toxicity, biodegradability, simultaneous solubilization of both polar and unpolar compounds, *etc.*), chemists and formulators often prefer solubilization in micellar systems or microemulsions with the help of added surfactants. Today, both processes are well understood and controlled in most applications.

The use of amphiphilic solvents is an attempt to combine the advantages of solvents and surfactants. They are commonly used in the fields of coatings, degreasing, and numerous other applications (perfumery, inks, *etc.*). They exhibit properties both of solvents, such as volatility and solubilization of organics, and of surfactants, *e.g.* surface activity, self aggregation in water, co-micellization with surfactants, *etc.* They are sometimes nicknamed "solvo-surfactants".¹ The term hydro-trope is also commonly used, but it encompasses a broader range of amphiphilic compounds, including low molecular weight aromatic salts.²

The most widespread hydrotropes today are the ethers derived from ethylene glycol, which are commonly called glycol ethers (C_iE_j). They have been studied extensively^{3,4} because they exhibit interesting properties, mainly due to the fact that they are soluble not only in water but also in most organic solvents. However, recent toxicological studies have put forward a possible reprotoxic activity.⁵ Therefore, some of them have been banned from pharmaceuticals, medicines, and domestic products.

Consequently, there is a need for new harmless amphiphilic solvents possessing comparable physico-chemical properties.

Propylene glycol derivatives (C_iP_j) are today the main substitutes. Although less amphiphilic than their ethylene glycol counterparts, their functional properties are found to be satisfying.^{6,7} However, they also derive from petrochemistry, whereas the "green" tendency encourages the development of new environmentally friendly products, bearing at least a natural polar moiety. In the field of surfactants, for example, sugar-based compounds, such as alkylpolyglucosides, have gained some importance within the last decade.⁸ Within this context, we prepared and studied ethers of glycerol (that will be called C_iGly_j to distinguish them from alkylpolyglucosides C_iG_j) as potential substitutes for glycol ethers.

Glycerol is a natural molecule, also available synthetically (from petrochemicals⁹ or by microbial fermentation¹⁰). The development of bio-carburants and particularly biodiesels (fatty acid methyl esters) will generate, until 2010, an annual glycerol over-production of more than 500 000 tons. To prevent a huge decrease of glycerol prices, which could destabilize the free market of oleochemicals, new uses of glycerol have to be found. The development of solvo-surfactants derived from glycerol could constitute a good opportunity to take advantage of this abundant resource, and to replace the more and more controversial glycol ethers.

Although polyglycerol based surfactants are already well known^{11,12} and common, especially in the food and cosmetic industries,^{13,14} low molecular weight glycerol derivatives have been almost totally ignored during the last century. Only a few of them are used, *e.g.* to deliver drugs,¹⁵ or in degreasing and detergency.¹⁶ Very little attention has been paid to them with respect to their physico-chemical properties and phase behaviour.

In the present paper we focus on short chain glycerol 1-monoethers (C_iGly_1 , $4 \leq i \leq 6$) (Fig. 1). First, their synthesis will be described, followed by a presentation of their aqueous phase behaviour, which is compared to those of common ethylene glycol and propylene glycol derivatives. From the surface activity, minimal aggregation concentrations (MACs) will be determined. Next binary water/solvo-surfactants phase diagrams will be given and discussed. Attention

^aLCOM, Equipe Oxydation et Formulation, ENSCL BP 90108, F-59652, Villeneuve d'Ascq Cedex, France.
E-mail: jean-marie.aubry@univ-lille1.fr; Fax: +33 3 20 33 63 64;
Tel: +33 3 20 33 63 64
^bInstitut für Physikalische und Theoretische Chemie, Universität Regensburg, D-93040, Regensburg, Germany

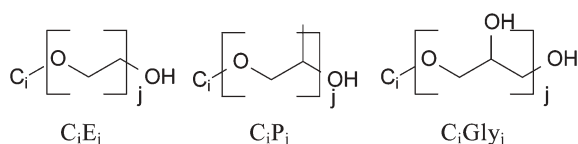


Fig. 1 Molecular structure of the solvo-surfactants studied in this work. Glycerol 1-monoethers (C_iGly_j) are potential substitutes for the controversial ethylene glycol ethers (C_iE_j) and propylene glycol ethers (C_iP_j).

will be paid to the thermodynamics of clouding, which yields information about the influence of temperature on the phase behaviour. In the last part of this paper, salt effects will be studied. A series of salts are chosen and their influence on the cloud points of the solvo-surfactants will be investigated and discussed in terms of the Hofmeister series. Salinity is indeed an important “formulation variable” (a parameter that can be used to balance the hydrophilicity and the lipophilicity of the amphiphile), since these molecules are almost insensitive to temperature, contrary to glycol ethers.

Experimental

Materials

For the synthesis of glycerol 1-monoethers, solketal (98%) was purchased from Aldrich (USA), as well as 1-bromoalkanes (all the highest grade available) and sodium sulfate (99+%). Tetrabutylammonium bromide (>98%) was purchased from Fluka (USA), whereas dichloromethane (99.8%) and cyclohexane (99.8%) were purchased from Acros (USA) and SDS (France) respectively.

All ethylene and propylene glycol ethers were purchased from Sigma–Aldrich (USA) and were the highest grade available (C_3E_1 99.4%, C_4E_1 99+%, C_5E_1 97%, C_4E_2 99+%, C_3P_1 98.5% and C_4P_1 99%). Glycerol 1-monoethers were synthesized according to the procedure described below.

Millipore water with $13 \text{ m}\Omega^{-1} \text{ cm}^{-1}$ conductivity was used for all experiments. Sodium thiocyanate NaSCN 98%, sodium perchlorate NaClO_4 (98+%), sodium iodide NaI (99+%), sodium bromide NaBr (99+%), sodium chloride NaCl (99.5%) and sodium sulfate Na_2SO_4 (99%) were all purchased from Sigma–Aldrich (USA).

Synthesis of short chain glycerol 1-monoethers

0.5 mol (64.3 g) of solketal, 180 mL of KOH 33% and 0.025 mol (8 g) of tetrabutylammonium bromide were successively introduced in a 1 L two-neck round bottom flask, and stirred vigorously for 15 minutes at 25 °C. 0.5 mol of bromoalkane ($C_i\text{H}_{2i+1}\text{Br}$) was then added dropwise. At the end of the addition, the temperature was raised to 100 °C, and the mixture was stirred vigorously for 24 hours. The organic phase was then separated, dried over sodium sulfate, and distilled under reduced pressure to obtain pure alkylsolketal.

The pure alkylsolketal was then added, in a 1 L round bottom flask, to 500 mL HCl (2 M). After 4 hours vigorous stirring at room temperature, the mixture was neutralized with aqueous NaOH, and extracted 3 times with 200 mL of CH_2Cl_2 . CH_2Cl_2 was chosen here because of its high efficiency.

Table 1 Yields^a of the synthesis of glycerol 1-monoethers, and boiling points *E_b* measured during the distillation^b

	C_4Gly_1	iC_5Gly_1	C_5Gly_1	C_6Gly_1
Yield	35	48	52	63
<i>E_b</i>	124/0.23	120/0.40	136/0.31	144/0.77

^a In %; ^b In °C mmHg⁻¹.

However, cyclohexane can also be used, as well as other “greener” solvents. The organic phases were collected, dried over sodium sulfate, and CH_2Cl_2 was removed under reduce pressure. Finally, the residue was distilled under vacuum (Table 1) and under argon to obtain pure 1-*O*-alkylglycerol, which was stored on molecular sieves under argon. Purity was checked by ^1H and ^{13}C NMR, and by gas chromatography.

Yields obtained with different alkyl chain lengths are collected in Table 1. They slowly increase because the aqueous solubility of the final compound decreases with increasing alkyl chain length, resulting in an rise of the CH_2Cl_2 /water partition coefficient.

Chemical shifts of ^1H and ^{13}C NMR spectra are given in Tables 2 and 3.

Surface activity, phase diagrams and salt effects

Solvo-surfactants solutions were obtained by precise dilution of the most concentrated one, prepared by weighing the product. The “rising bubble” mode was chosen to measure

Table 2 ^1H NMR chemical shifts^a of glycerol 1-monoalkyl ethers, compared to TMS in CDCl_3 (δ , multiplicity, coupling constant)

The figure shows two chemical structures of glycerol 1-monoalkyl ethers. The first is a linear alkyl ether with carbons numbered 1 to 5 and protons numbered 1' to 3'. The second is an isopropyl ether with carbons numbered 1 to 5 and protons numbered 1' to 3'.

	C_4Gly_1	iC_5Gly_1	C_5Gly_1	C_6Gly_1
1	0.92, t, 7.0	0.98, m	0.90, t, 6.1	0.89, t, 6.4
2	1.34, m	—	1.31, m	↑
3	1.54, q, 6.8	1.66, m	—	1.29, m
4	3.47, t, 6.7	1.50, m	1.58, q, 6.7	↓
5	—	3.49, t, 6.7	3.47, t, 6.1	1.54, q, 6.4
6	—	—	—	3.48, t, 6.4
1'	3.52, m	3.53, m	3.50, m	3.50, m
2'	3.86, m	3.85, m	3.85, m	3.86, m
3'	3.62, m	3.65, m	3.68, m	3.62, m

^a In ppm.

Table 3 ^{13}C NMR chemical shifts^a of glycerol 1-monoalkyl ethers, compared to TMS in CDCl_3

	C_4Gly_1	iC_5Gly_1	C_5Gly_1	C_6Gly_1
1	13.89	22.62	14.04	14.03
2	19.26	—	22.51	22.63
3	31.64	25.06	28.23	25.77
4	72.34	38.32	29.25	29.56
5	—	70.17	72.40	31.69
6	—	—	—	72.40
1'	71.52	72.44	71.82	71.88
2'	70.74	70.58	70.59	70.71
3'	64.18	64.21	64.21	64.22

^a In ppm.

surface tensions. Surface activity was studied with a drop shape analysis tensiometer (model Tracker from IT Concept, France).

Binary phase diagrams were drawn by visual observation of a series of test tubes closed tightly and placed in a thermostated bath built at the University of Regensburg (Germany) combined with a RT5 multiple places magnetic stirrer from Fisher Bioblock Scientific (USA). Temperature was controlled at $T \pm 0.1$ °C. Samples were prepared by weighing on precision scales.

Salt effects were studied following the same procedure.

Results and discussion

Synthesis of short chain glycerol 1-monoethers

No efficient direct synthesis of glycerol 1-monoethers from glycerol and an alcohol or an alcohol derivative is known today. Two steps are generally required to obtain pure compounds. Usually, an initially “protected” or “modified” glycerol is preferred to the use of glycerol itself, which gives rise to mixtures of various mono- and polyethers that are difficult to purify. Historically, syntheses have been performed from allyl alcohols,¹⁷ glycidol (2,3-epoxy-1-propanol),¹⁸ or epichlorhydrin (2,3-epoxypropyl chloride),^{19–21} but the most common reactant is solketal (1,2-isopropylidenediglycerol).^{17,20–22} In most cases, solketal is firstly etherified by an activated (halogenated, mesylated, tosylated) alcohol, and the resulting acetal is hydrolyzed (boric acid, hydrochloric acid, acid resins *etc.*) to give the target compound. The first step is problematic for several different reasons (use of harmful or expensive organic solvents, reactants that are not commercially available). A promising alternative was formulated by Rivaux *et al.* who used a phase-transfer catalysis²⁰ procedure, which was first introduced by Nougier many years earlier.²³ This method allows the use of solketal and available halogenated alkanes as reactants, and avoids the use of any organic solvent. Solketal is solubilized in a concentrated KOH solution, etherified by an halogenated alcohol using a phase transfer catalyst, and the hydrolysis of the acetal is carried out with an acid resin. We chose to carry out the etherification of solketal on the basis of Rivaux’s work. The subsequent hydrolysis was performed with an aqueous hydrochloric acid solution.

Surface activity of short chain glycerol 1-monoethers

The self-association of surfactants is a well known phenomenon. Hydrophobic interactions are the driving forces which induce the adsorption of the surfactant at the water/air interface. Once this interface is saturated, *i.e.* when the concentration reaches the CMC, the surfactant molecules self-associate to minimize the free energy of the whole system. The size and shape of the aggregates are governed not only by surfactant concentration, but also by other physical parameters such as temperature,²⁴ pH,²⁵ salinity,²⁶ *etc.*

According to their amphiphilic nature, solvo-surfactants or hydrotropes also adsorb at the interface and lower surface tension. However, their self-association is still a matter of debate.²⁷ Historically, the term hydrotrope was coined to describe short chain aromatic salts² that aggregate according

to a stack-type mechanism.²⁸ This stacking phenomenon was assumed to be responsible for their ability to solubilize organic compounds in water. However, molecules without an aromatic ring (*e.g.* sodium alkanoates)²⁹ and even without charge (*e.g.* glycol ethers) turned out to possess similar properties, although stacking cannot occur in this case. A progressive aggregation is more probable, but is hardly detected. Direct visualization by SANS, SAXS, or light scattering^{30,31} has already been carried out but is difficult because aggregates are in general small and polydispersed. The easiest way to detect the onset of aggregation is to follow the evolution of some physico-chemical properties, such as surface tension, with increasing solvo-surfactant concentration. The levelling-off of the corresponding curves is reached at concentrations that are much higher than typical CMC, and may not always correspond to aggregation but only to the saturation of the surface. To distinguish them clearly from CMC, they will be called minimal aggregation concentrations (MACs). The denomination MHC³² (minimal hydrotropic concentration) will not be used here because it usually corresponds to the concentration above which the solubilization of organic solute in water increases dramatically, a concentration which is generally similar but not systematically identical to the one where the surface tension levels-off.

To determine such MACs, surface tension measurements were carried out for a series of solvo-surfactants including ethylene glycol and propylene glycol ethers as references, and short chain glycerol 1-monoethers synthesized in the laboratory. The MAC is best determined, in the case of such low molecular weight compounds, by plotting the surface tension against the logarithm of the mole fraction³³ x (Fig. 2).

Table 4 summarizes the minimal aggregation concentrations deduced from these curves. As Strey *et al.* showed recently,³⁴ the activity should be used for such short amphiphiles instead of the molar concentration because of the extremely high MAC compared to typical CMC (generally 10^{-3} – 10^{-4} mol L⁻¹). With the activity, the levelling-off of the curves is less obvious and can even totally disappear. Consequently, we did not perform calculations of the surface excesses (Γ) and areas at the interface (a_0) because we did not measure activity coefficients. However, the surface tension curves are presented to give, in each case, the surface tension reduction (also collected in Table 4) and the corresponding MAC characteristic of the efficiency of this reduction.

The value of the MAC is clearly dependent on the length of the alkyl chain. The nature of the polar head has less influence but is also relevant; for the same alkyl chain, it can be expected to be responsible for the classification of the MAC. The order found here is $C_4E_2 \geq C_4E_1 > C_4Gly_1$. It is quite surprising that C_4Gly_1 seems to be more hydrophobic than C_4E_1 . On the basis of the molecular structure, the presence of two hydroxyl groups is expected to induce a high hydrophilicity. It seems that strong interactions between the glycerol polar heads exist and lower the global hydrophilicity of the molecule. The presence of one ether function and two hydroxyl groups make the formation of hydrogen bonds probable.

When a carbon atom is added to the alkyl chain, the hydrophilicity and consequently the MAC decrease, *c.f.* C_4Gly_1 and C_5Gly_1 . When the compound becomes too

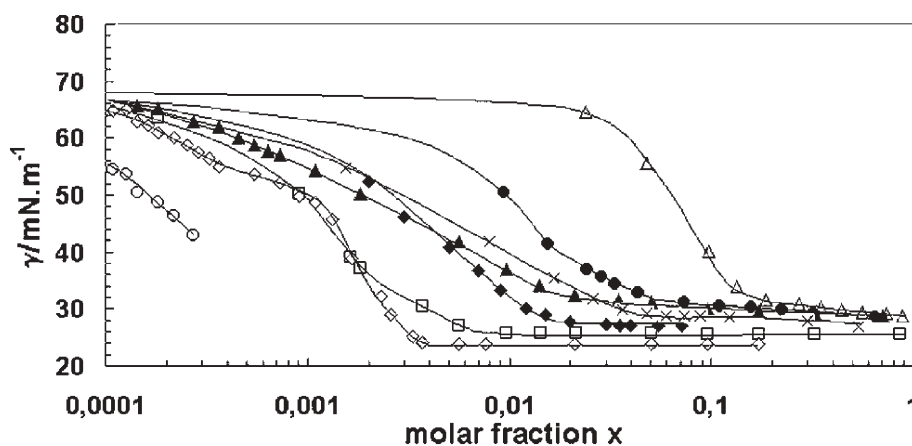


Fig. 2 Surface tension curves for a series of C_jE_j , C_iP_j , and C_jGly_j . ● C_3E_1 , ◆ C_4E_1 , ▲ C_4E_2 , × C_3P_1 , △ C_4Gly_1 , □ iC_5Gly_1 , ◇ C_5Gly_1 , ○ C_6Gly_1 .

Table 4 Minimal aggregation concentrations MAC^a and corresponding surface tensions γ_{MAC}^b for some C_jE_j , C_iP_j , and C_jGly_j

	C_3E_1	C_3P_1	C_4E_1	C_4E_2	C_4Gly_1	iC_5Gly_1	C_5Gly_1
MAC	1.22	1.56	0.83	0.88	0.60	0.36	0.15
γ_{MAC}	33.4	26.5	27.2	28.0	28.6	25.3	23.9

^a In mol L⁻¹. ^b In mN m⁻¹.

hydrophobic, *c.f.* C_6Gly_1 , it reaches its solubility limit before its MAC , and no value can be given. However, solvo-surfactants that are soluble below their MAC reduce γ very efficiently. Glycerol derivatives with C_5 alkyl chains are particularly interesting because their relatively low MAC s allow a very efficient surface tension reduction compared to other solvo-surfactants. The advantage of the glycerol head-group is evident here: its high water solubility allows the use of longer alkyl chains that will aggregate at lower concentrations and will interact more strongly with the organic compounds solubilized for various applications.³⁵

Binary phase diagrams

Binary phase diagrams (water/amphiphile/temperature diagrams) were drawn for several solvo-surfactants. They are less complicated than diagrams involving “true” surfactants, mainly because of the absence of liquid crystals. They are simply composed of two distinct regions, one corresponding to stable, isotropic solutions, and the other corresponding to unstable solutions that unmix into two phases at equilibrium.⁶ In the case of nonionic amphiphiles, the separation curve has the shape of a loop. As the temperature is increased, the molecules become less hydrophilic because of the dehydration of their oxygenated groups. This results in a phase separation, the minimum temperature associated with this unmixing being called the *cloud point* or LCST (lower critical solubility temperature).

Fig. 3 and 4 show the binary phase diagrams of common ethylene and propylene glycol ethers, and of 1-hexylglycerol, respectively. In the case of glycerol ethers bearing C_4 , iC_5 and C_5 alkyl chains, we could not observe any unmixing until the temperature was above 90 °C.

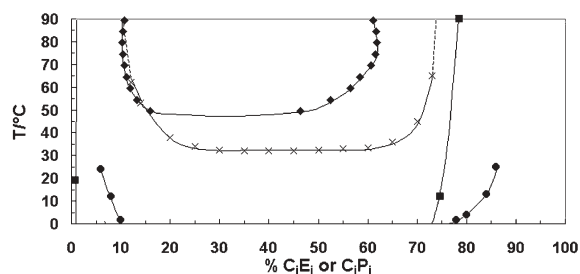


Fig. 3 Binary phase diagrams of common C_jE_j and C_iP_j in water. × C_4E_1 , ■ C_5E_1 , ◆ C_3P_1 , ● C_4P_1 .

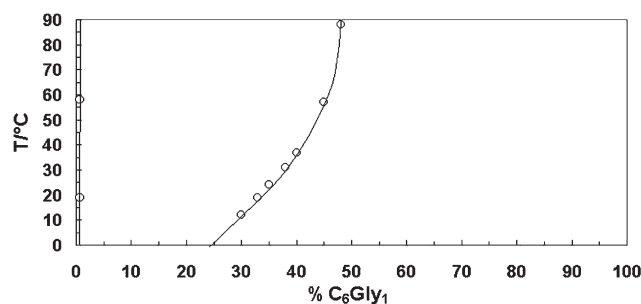


Fig. 4 Binary phase diagram of C_6Gly_1 in water. C_4Gly_1 , iC_5Gly_1 and C_5Gly_1 are miscible with water up to 90 °C.

The shapes of the diagrams are significantly different. They are quite symmetric for glycol ethers, whereas glycerol ethers diagrams are strongly “shifted” to the left. This is obvious in the case of C_6Gly_1 , but also for shorter homologues, whose hypothetical cloud points can be revealed with the addition of salting-out agents (see Fig. 6 and 7). In the case of glycol ethers, the behaviour is typical of solvents, whereas it is more characteristic of nonionic surfactants in the case of glycerol 1-monoethers. The solubility of C_6Gly_1 in water is very poor, but the solubility of water in this solvo-surfactant is huge. Long-chain C_jE_j have similar behaviours.

The phase diagrams confirm that the alkyl chain length has a major influence on the phase behaviour of short amphiphiles. Whereas C_4 , iC_5 and even C_5 glycerol ethers are totally

miscible with water at least from $-20\text{ }^{\circ}\text{C}$ to $95\text{ }^{\circ}\text{C}$, the linear C_6 ether has a very low cloud point. We could not determine it experimentally, even by decreasing the temperature down to $-20\text{ }^{\circ}\text{C}$. The difference in the cloud point is thus larger than $120\text{ }^{\circ}\text{C}$ for a difference of one carbon atom, which is remarkable.

Influence of temperature

The binary phase diagrams show that temperature does not have the same influence on the different molecules. At room temperature, the polar groups of glycol ethers (C_4E_1 , C_3P_1) are hydrated, forming hydrogen bonds with water molecules, and an increase of temperature breaks these bonds, inducing the unmixing. C_4Gly_1 and even C_5Gly_1 , on the contrary, are miscible with water up to more than $90\text{ }^{\circ}\text{C}$. Temperature has little influence on their desolvation. C_6Gly_1 is also not very temperature-sensitive, since the right branch of its phase diagram looks like a small section of a very wide loop. In the first part of this discussion, we suggested the existence of hydrogen bonds between the glycerol polar heads. It is well known that intermolecular hydrogen bonds are dependent on temperature, whereas intramolecular bonds are much more stable.³⁶ In the light of the phase diagrams, it is probable that, in the case of glycerol ethers, hydrogen bonds are essentially intramolecular. Therefore hydrophobicity remains almost constant as the temperature rises, whereas it increases strongly for glycol ethers, a cloud point being detectable in the temperature range between 0 and $100\text{ }^{\circ}\text{C}$.

Thermodynamic parameters associated with the clouding phenomenon can be determined from the shape of the unmixing curve, but have been very seldomly calculated.^{37–40} The micellization process has been much more widely studied.^{41,42} The clouding can be described by eqn 1, allowing the calculation of the standard Gibbs free energy of clouding ΔG_c° :

$$\Delta G_c^\circ(T) = RT \ln(X_c(T)) = \Delta H_c^\circ(T) - T\Delta S_c^\circ(T) \quad (1)$$

where X_c is the mole fraction of solvo-surfactant corresponding to the phase separation at the temperature T . X_c values are calculated from the w/w% of the phase diagrams (Fig. 3 and 4). Eqn 1 is obtained with the hypothetical state of unit mole fraction as reference.

To calculate the enthalpy of clouding ΔH_c° , the Gibbs–Helmholtz equation (eqn 2) has to be considered.

$$[\partial(\Delta G_c^\circ(T)/T)/\partial(1/T)] = -T^2 [\partial(\Delta G_c^\circ(T))/\partial T] = \Delta H_c^\circ(T) \quad (2)$$

Replacing $\Delta G_c^\circ(T)$ in eqn 2 by the expression given in eqn 1 yields

$$\Delta H_c^\circ(T) = -RT^2 [\partial \ln(X_c(T))/\partial T] \quad (3)$$

To calculate numerically ΔH_c° , experimental $(\ln X_c, T)$ values are fitted with a polynomial equation (eqn 4), to give finally eqn 5.

$$\ln(X_c(T)) = a + bT + cT^2 + dT^3 \quad (4)$$

$$\Delta H_c^\circ(T) = -RT^2(b + 2cT + 3dT^2) \quad (5)$$

Once the enthalpy of clouding is known, the entropy $\Delta S_c^\circ(T)$ is simply obtained by eqn 6 to give eqn 7.

$$\Delta S_c^\circ(T) = (\Delta H_c^\circ - \Delta G_c^\circ)/T \quad (6)$$

$$\Delta S_c^\circ(T) = -R(a + 2bT + 3cT^2 + 4dT^3) \quad (7)$$

ΔH_c° , ΔS_c° and ΔG_c° were calculated at different temperatures for C_4E_1 (whose behaviour is also representative of the one of C_3P_1 because of the similarity of their diagrams) and C_6Gly_1 . Due to the insignificant solubility of C_6Gly_1 in water, the calculations were performed only on the right branch of the phase diagram, *i.e.* for the unmixing that occurs when water is progressively added to the pure solvo-surfactant. In the case of C_4E_1 , both branches of the phase diagram were considered. Data are collected in Table 5.

The process is obviously spontaneous, and endothermic at low temperatures. The energy needed to break interactions between the molecules and water surrounding them is higher than the one gained by the creation of interactions between the molecules themselves ($\Delta H_c^\circ > 0$). As the temperature rises, the solvation of headgroups by water decreases and the process becomes progressively exothermic. The entropy of clouding ΔS_c° is also positive at lower temperatures, and drops down to negative values as temperature increases. When it reaches 0,

Table 5 Thermodynamic parameters ΔH_c° , ΔS_c° and ΔG_c° associated to the clouding process in water for C_4E_1 and C_6Gly_1 , as a function of T^d

C_4E_1							C_6Gly_1			
T	Water rich branch			C_4E_1 rich branch			T	C_6Gly_1 rich branch		
	ΔH_c°	ΔS_c°	ΔG_c°	ΔH_c°	ΔS_c°	ΔG_c°		ΔH_c°	ΔS_c°	ΔG_c°
322.5	4.23	46.2	-10.66	5.93	19.4	-0.33	285	4.63	19.2	-0.85
327.5	4.87	48.2	-10.94	4.93	16.4	-0.43	292	4.61	19.1	-0.97
332.5	4.24	46.3	-11.16	3.94	13.4	-0.50	297	4.57	19.0	-1.06
337.5	2.21	40.3	-11.39	2.97	10.4	-0.55	304	4.43	18.6	-1.21
342.5	-1.33	29.7	-11.50	2.01	7.6	-0.61	310	4.26	18.0	-1.32
347.5	-6.51	14.7	-11.61	1.08	4.9	-0.64	330	3.21	14.7	-1.64
352.5	-13.47	-5.2	-11.63	0.19	2.4	-0.65	361	-0.23	4.8	-1.96
357.5	-22.33	-30.0	-11.59	-0.67	0.0	-0.66				
362.5	-33.23	-60.2	-11.40	-1.48	-2.3	-0.65				
367.5	-46.31	-96.4	-10.89	-2.24	-4.4	-0.63				

^a In kJ mol^{-1} . ^b In $\text{J mol}^{-1} \text{K}^{-1}$. ^c In kJ mol^{-1} . ^d In K.

ΔG_c° , which was decreasing before, begins to increase. If measurements had been realized under pressure so that higher temperatures could have been attained, entropy would probably have become so predominant that ΔG_c° would finally have reached 0, so that the clouding would have disappeared. The evolution of ΔS_c° is the consequence of the dehydration of polar headgroups on the one hand and the high motion of the molecules on the other hand that make the disorder more and more important in the homogeneous phase.

The final states being identical, the comparison between the two side branches of the diagram of C_4E_1 provides information about the initial states, *i.e.* the monophasic solutions just before the phase separation. Important differences are observed. First ΔH_c° , which is of the same order of magnitude at lower temperatures, becomes much more negative at higher temperatures for the left branch. This is not surprising given that there are 60 times more water molecules than C_4E_1 ones. The energy of the highly solvated C_4E_1 molecules is very important at high temperature, so they release more energy when they escape from their aqueous environment, breaking their unfavourable interactions with water. In the vicinity of the right branch, C_4E_1 molecules are much more concentrated, which explains the lower enthalpy values. The same explanation can be given concerning the entropy ΔS_c° . It becomes more negative for the left branch, once again because the dehydration of the highly solvated glycol headgroups creates an important disorder. The one induced by the breaking of interactions between water and C_4E_1 on the right branch is lower.

The comparison between C_4E_1 and C_6Gly_1 leads to the conclusion that a similar evolution is observed in both cases, but that C_6Gly_1 is less sensitive to temperature. Indeed values are of the same order of magnitude for each parameter at lower temperatures, but their variations are then clearly less pronounced for C_6Gly_1 . The loop drawn by the demixing curve is wider, the lower critical solubility temperature (LCST) being below -20°C and the upper critical solubility temperature (UCST) being above 100°C , so that the right branch of the diagram looks almost straight.

For many processes involving small molecules in aqueous solution such as solubilization of actives,⁴³ complexation,⁴⁴ oxidation and reduction reactions,⁴⁵ micellization of surfactants⁴⁶ *etc.*, a linear relationship between the entropy change ΔS and the enthalpy change ΔH is observed. This linear relationship is called the compensation phenomenon. According to Lumry and Rajender,⁴⁷ ΔH_c° can be written as shown in eqn 8.

$$\Delta H_c^\circ = \Delta H_c^* + T_{\text{comp}}\Delta S_c^\circ \quad (8)$$

The slope T_{comp} is called the compensation temperature, since it corresponds to the particular temperature, where the process is purely enthalpy-driven ($\Delta G_c^\circ = \Delta H_c^*$). Consequently, the intercept ΔH_c^* is representative of the “chemical” part of the process. The meaning of T_{comp} and the intercept ΔH_c^* have never been investigated in the case of clouding, but T_{comp} is usually assumed to be characteristic of the solute–solute and solute–solvent interactions. In aqueous solution it reflects the desolvation of the polar headgroups of

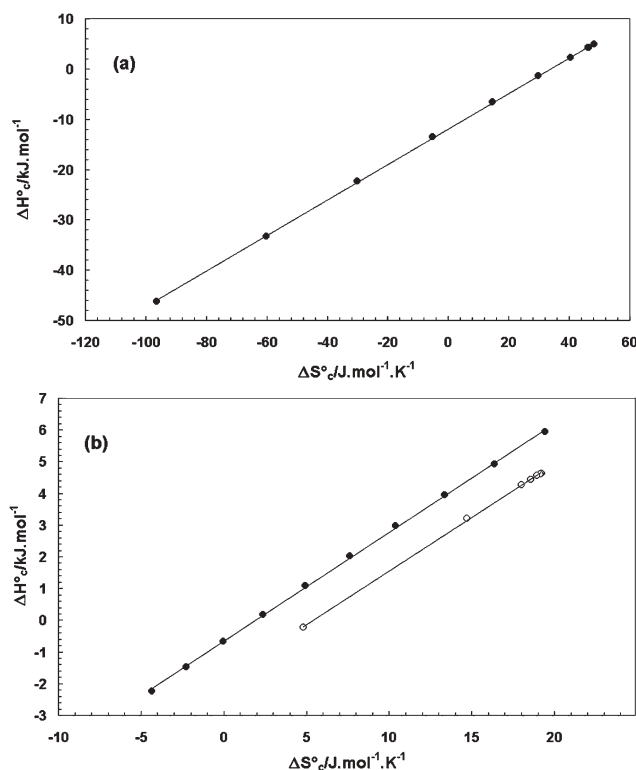


Fig. 5 $\Delta S_c^\circ/\Delta H_c^\circ$ plots for C_6Gly_1 and C_4E_1 . (a) Left branch of the phase diagram for C_4E_1 . (b) Right branches for \bullet C_4E_1 and \circ C_6Gly_1 . The compensation phenomenon is nicely observed.

the solute. The “chemical” term ΔH_c^* represents, for example, in the case of micellization, the strength of the interactions created between the molecules within the micelles, in other words the stability of the micelles. Here it can be assumed to reflect the stability of the biphasic system after the phase separation.

In Fig. 5, ΔH_c° is plotted against ΔS_c° for both molecules. Water-rich and solvo-surfactant-rich sides are presented on separated figures. The compensation phenomenon is nicely observed.

Table 6 gives the compensation temperatures T_{comp} and the intercepts ΔH_c^* , deduced from the plots.

T_{comp} , which is representative of the hydration of the molecules, confirms that, for C_4E_1 , molecules are highly hydrated on the left branch, at lower concentrations. On the right branch, the solvation is lower, and slightly more important for C_4E_1 than C_6Gly_1 . ΔH_c^* is, as expected, much higher on the left branch. It is, on the right side, lower for C_4E_1 than for C_6Gly_1 . This is probably due to the longer alkyl chains

Table 6 T_{comp}^a and $\Delta H_c^*{}^b$ calculated from $\Delta H_c^\circ - \Delta S_c^\circ$ plots for C_4E_1 and C_6Gly_1

Branch	C_4E_1		C_6Gly_1
	Left	Right	Right
T_{comp}	353	343	338
ΔH_c^*	-11.95	-0.66	-1.83

^a In K. ^b In kJ mol^{-1} .

creating stronger interactions in the case of C₆Gly₁, which results in a higher stability of the separated phases.

Influence of electrolytes on the phase behaviour of short chain glycerol 1-monoethers

The role played by ions is essential in many chemical and biological processes. Their influence has been studied extensively, but their mode of action is quite complex, and is still not clearly understood. The work of Hofmeister,⁴⁸ performed at the end of the 19th century, comprises a large amount of information, the main result being the classification of ions either in “salting-in” or in “salting-out” agents. Salting-in agents are able to increase the solubility of proteins in water, whereas salting-out agents decrease it. For anions, Hofmeister’s classification, known as Hofmeister series, is SO₄²⁻ > OH⁻ > F⁻ > CH₃COO⁻ > Cl⁻ > NO₃⁻ > I⁻ > ClO₄⁻ > SCN⁻, the most salting-out agents being on the left and the most salting-in on the right. This classification turned out to be valid for a great number of processes in biology⁴⁹ as well as surface chemistry.^{50,51} But in spite of a huge amount of experimental data, it is still very difficult to explain clearly these specific ion effects, mainly because they result simultaneously from several interactions such as dielectric, steric, and dispersion forces, but also from a specific hydration of ions at interfaces.⁵²

The specific effects of ions on the phase behaviour of short chain amphiphilic compounds were scarcely considered in the last century. Only few results have been published. In 1930, Motoo reported on the influence of various salts on the surface tension of sodium taurocholate solutions.⁵³ In 1942, Reber and coworkers studied their effects on the mutual solubilities of butyl alcohol and water⁵⁴ but these one-off studies were not included in a global approach. More recently, some of us studied Hofmeister effects on water/propylene glycol ethers mixtures.⁵⁵ From the shift of the lower critical solubility temperatures, Bauduin *et al.* calculated a specific coefficient for each salt, and compared these coefficients for two different propylene glycol ethers, namely propylene glycol propyl ether (C₃P₁) and dipropylene glycol propyl ether (C₃P₂). Following their methodology, we measured the evolution of the cloud points and calculated equivalent coefficients for our newly

Table 7 Salt coefficients a^a according to eqn 9 for some glycerol 1-monoethers and other solvo-surfactants. * from ref. 54. LCSTs^b are also given

	C ₅ Gly ₁	C ₆ Gly ₁	C ₄ E ₁	C ₃ P ₁	C ₃ P ₂
NaSCN	—	8.20	8.60	3.42*	3.17*
NaClO ₄	—	5.39	6.26	2.64*	2.38*
NaI	—	0.92	1.31	0.35*	1.74*
NaBr	-1.61	-0.32	-1.18	-2.54	-1.02*
NaCl	-2.57	-2.15	-2.42	-2.80	-2.07*
Na ₂ SO ₄	-12.12	-14.88	-15.32	-11.95	-9.62*
LCST	(158)	<-20 °C	48	35	14

^a In mmol of salt per mole of water in solvo-surfactant mixture.
^b In °C.

synthesized glycerol 1-monoethers, namely 1-pentylglycerol (C₅Gly₁) and 1-hexylglycerol (C₆Gly₁), as well as for a common ethylene glycol ether, 2-butoxyethanol (C₄E₁). We tested 3 salting-in agents (sodium thiocyanate NaSCN, sodium perchlorate NaClO₄ and sodium iodide NaI) and 3 salting-out agents (sodium chloride NaCl, sodium bromide NaBr and sodium sulfate Na₂SO₄). Measurements with C₃P₁ and NaClO₄, NaI and NaBr, that had not been performed previously, were also carried out for the sake of comparison.

The LCST/salt concentration curves appear to be perfectly linear. According to Bauduin’s methodology, they were represented as

$$\text{LCST} = \text{LCST}_0 + a \times c \quad (9)$$

where c is the salt concentration in mmole of salt per total number of moles of solvents (water + solvo-surfactant). The characteristic coefficients a are given for each experiment in Table 7. Note that in the case of C₅Gly₁ and iC₅Gly₁ the LCSTs are above 100 °C. Therefore we chose a composition of 15% solvo-surfactant and 85% water instead of the true composition of the hypothetical LCST, see Fig. 6 and 7. We added only salting-out agents, because salting-in agents would further increase the LCSTs.

Thanks to the salting-out agents, it was possible to evaluate the hypothetical LCST of C₅Gly₁, as shown in Fig. 8. The value of 158 °C was found with an excellent accuracy (± 1 °C). This is obviously an unreachable cloud point at atmospheric

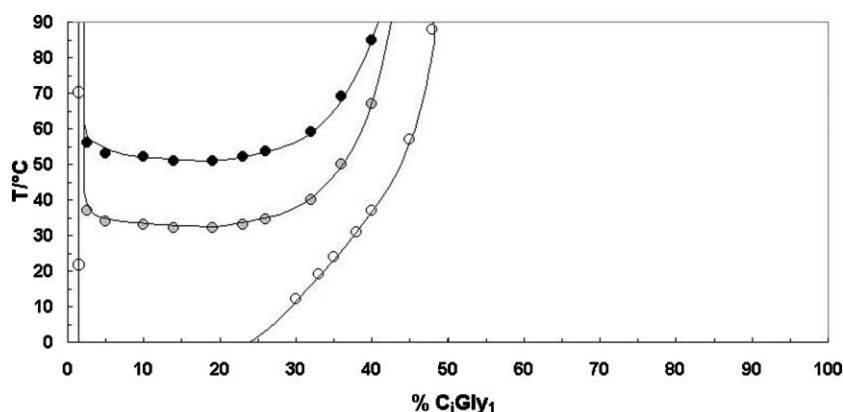


Fig. 6 Binary phase diagrams displaced to the available temperature window by addition of salt for C₆Gly₁. Curve minima are around 15%. The huge increase of the cloud point at very low salt concentrations is remarkable. ○ C₆Gly₁, C₆Gly₁ + NaSCN 1%, ● C₆Gly₁ + NaSCN 2%.

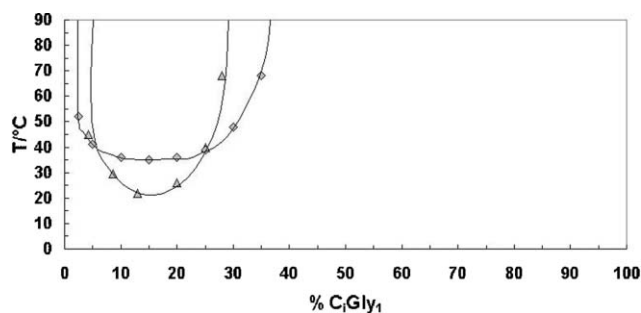


Fig. 7 Phase diagrams displaced to the available temperature window for iC_5Gly_1 and C_5Gly_1 . Curve minima are once more around 15%. Δ $iC_5Gly_1 + Na_2SO_4$ 13.8%, \diamond $C_5Gly_1 + Na_2SO_4$ 7.5%.

pressure, but it can be useful to compare the hydrophilicity of C_5Gly_1 with the one of other compounds.

The same composition, 15% of solvo-surfactant and 85% of water, was chosen for the aqueous mixture of C_6Gly_1 —which has a hypothetical $LCST_0$ below $0\text{ }^\circ\text{C}$ —when salting-in agents were added, whereas a composition of 40% C_6Gly_1 and 60% water was preferred when salting-out agents were added, see also Fig. 6.

As expected salting-in salts increase and salting-out salts decrease the LCST. In the first case, the ions go to the surface or even slightly into the organic component making it more polar or even partially charged. As a result, the compatibility of the two solvents increases. By contrast, salting-out salts, especially sodium sulfate, “salt out” the solvo-surfactant for the usual reason: the highly charged unpolarizable anion, *e.g.* sulfate, withdraws water molecules from the organic component and strongly binds them within its hydration shell. Similarly, and known for a long time, salts can considerably decrease the solubility of small polar but uncharged molecules like methanol.

The effect of the ions (Table 7) strictly follows the Hofmeister series without any exception and for all mixtures studied. However, the sensitivity of each system is quite different. Roughly speaking, the more hydrophilic solvo-surfactants are more sensitive to the addition of ions than the more hydrophobic ones. A notable exception is C_6Gly_1 . According to the very low $LCST_0$, it should be very hydrophobic. Nevertheless, it is highly sensitive to salts. Since this is the case both for salting-in and salting-out agents, which should have very different effects, we currently have no

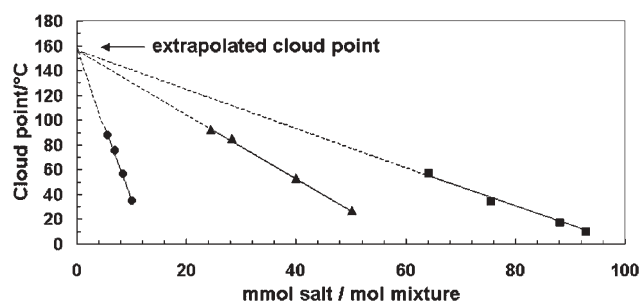


Fig. 8 Effect of salting-out agents on the cloud point of C_5Gly_1 . An extrapolated cloud point is determined to be $158\text{ }^\circ\text{C}$. \bullet Na_2SO_4 , \blacktriangle $NaCl$, \blacksquare $NaBr$.

satisfactory explanation for this exception. Note that ions can have strong interactions with the glycerol headgroup, much as with water⁵⁶ and therefore the ions can efficiently break up intra- and intermolecular hydrogen bonds in glycerol.

Another interesting point is the different relative sensitivity of a given ion towards different solvo-surfactants. For all investigated sodium halides their influence on the $LCSTs$ of mixtures considered here is relatively small and no clear trend among hydrophilic or hydrophobic solvo-surfactant is visible. More subtle hypotheses are difficult to infer from the global thermodynamic results that we present here.

Conclusions

Short chain glycerol 1-monoethers were synthesized and their surface activity was measured. The temperature-dependent phase diagrams of their mixtures with water and salts effects on these diagrams were also studied.

It turns out that this new class of molecules is a promising alternative to commonly used solvo-surfactants such as ethylene or propylene glycol ethers, showing similar properties. However, in contrast to them, glycerol ethers can be synthesized from natural products independently of petrochemistry. Since glycerol is a side product of the increasing biocarburant production, these new solvo-surfactants have the double advantage of being partly “green” products and also provide new uses of glycerol.

References

- 1 K. Lunkenheimer, S. Schroedle and W. Kunz, *Prog. Colloid Polym. Sci.*, 2004, **126**, 14.
- 2 C. Neuberg, *J. Chem. Soc., Trans.*, 1916, **110**, II, 555.
- 3 P. K. Kilpatrick, C. A. Gorman, H. T. Davis, L. E. Scriven and W. G. Miller, *J. Phys. Chem.*, 1986, **90**, 5292.
- 4 M. Kahlweit, E. Lessner and R. Strey, *J. Phys. Chem.*, 1983, **87**, 5032.
- 5 *Technical report no. 64 – European Center for Ecotoxicology and Toxicology of Chemicals*, 1995, **64**, pp. 350.
- 6 P. Bauduin, L. Wattebled, S. Schrödle, D. Touraud and W. Kunz, *J. Mol. Liq.*, 2004, **115**, 23.
- 7 P. Bauduin, A. Basse, D. Touraud and W. Kunz, *Colloids Surf., A*, 2005, **270–71**, 8.
- 8 W. Von Rybinski and K. Hill, *Angew. Chem., Int. Ed.*, 1998, **37**, 1328.
- 9 E. C. Williams, *Trans. Am. Inst. Chem. Eng.*, 1941, **37**, 157.
- 10 Z. Z. J. Wang, J. Zhuge, H. Fang and B. A. Prior, *Biotechnol. Adv.*, 2001, **19**, 3, 201.
- 11 C. Debaig, T. Benvegnu and D. Plusquellec, *OL, Corps Gras, Lipides*, 2002, **9**, 2–3, 155.
- 12 S. Cassel, T. Benvegnu, P. Chaimbault, M. Lafosse, D. Plusquellec and P. Rollin, *J. Org. Chem.*, 2001, **5**, 875.
- 13 D. Cauwet and C. Dubief, *Eur. Pat.*, 400 291, 1993.
- 14 A. Miyamoto and K. Matsushita, *New Food Ind.*, 1988, **30**, 11, 12.
- 15 J. Engel, M. Molliere and I. Szelenyi, *Eur. Pat.*, 100 071, 1990.
- 16 K. Kasuga and T. Miyajima, *US Pat.*, 6 221 816, 2001.
- 17 W. J. Baumann and H. K. Mangold, *J. Org. Chem.*, 1964, **29**, 3055.
- 18 G. Vanlerberghe, *German Pat.*, DE 19 691 209, 1969.
- 19 T. Miyajima and M. Uno, *World Pat.*, 0 043 340, 2000.
- 20 Y. Rivaux, *PhD. Thesis*, Université de Rennes I, France, 1996.
- 21 C. F. Cheng, *US Pat.*, 5 239 093, 1993.
- 22 S. C. Gupta and F. A. Kummerow, *J. Org. Chem.*, 1959, **24**, 409.
- 23 E. Flesia, T. Nougier and J. M. Surzur, *Tetrahedron Lett.*, 1979, **2**, 197.
- 24 M. S. Bakshi, A. Kaura and R. K. Mahajan, *Colloids Surf., A*, 2005, **262**, 1–3, 168.
- 25 G. Sugihara, *J. Phys. Chem.*, 1982, **86**, 14, 2784.

- 26 E. Dutkiewicz and A. Jakubowska, *Colloid Polym. Sci.*, 2002, **280**, 11, 1009.
- 27 S. E. Friberg and C. Brancewicz, *Surf. Sci. Ser.*, 1997, **67**, 21.
- 28 A. M. Saleh and L. K. El-Khordagui, *Int. J. Pharm.*, 1985, **24**, 231.
- 29 I. Danielsson and P. Stenius, *J. Colloid Interface Sci.*, 1971, **37**, 2, 264.
- 30 G. D'Arrigo, J. Teixeira, R. Giordano and F. Mallamace, *J. Chem. Phys.*, 1991, **95**, 4, 2732.
- 31 F. Quirion, L. J. Magid and M. Drifford, *Langmuir*, 1990, **6**, 1, 244.
- 32 V. Srinivas, G. A. Rodley, K. Ravikumar, W. T. Robinson, M. M. Turnbull and D. Balasubramanian, *Langmuir*, 1997, **13**, 12, 3235.
- 33 M. Kahlweit, G. Busse and J. Jen, *J. Phys. Chem.*, 1991, **95**, 5580.
- 34 R. Strey, Y. Viisanen, M. Aratono, J. P. Kratochvil, Q. Yin and S. E. Friberg, *J. Phys. Chem. B*, 1999, **103**, 43, 9112.
- 35 S. Queste, P. Sabre and J. M. Aubry, *Proceedings of the Spanish Committee of Detergents, Surfactants and Related Industries (CED) annual meeting*, Barcelona, 2006.
- 36 *Topics in Current Chemistry*, ed. P. Schuster, Springer-Verlag, Berlin, 1984, vol. 120, pp. 117.
- 37 S. Ghosh and S. P. Moulik, *J. Surf. Sci. Technol.*, 1998, **14**, 1–4, 110.
- 38 M. Prasad, S. P. Moulik, D. Chisholm and R. Palepu, *J. Oleo Sci.*, 2003, **52**, 10, 523.
- 39 A. Van Bommel and R. M. Palepu, *Colloids Surf., A*, 2004, **233**, 109.
- 40 A. Chatterjee, B. K. Roy, S. P. Moulik, N. P. Sahu and N. B. Mondal, *J. Dispersion Sci. Technol.*, 2002, **23**, 6, 747.
- 41 M. Prasad, S. P. Moulik, A. Al Wardian, S. More, A. Van Bommel and R. Palepu, *Colloid Polym. Sci.*, 2005, **283**, 887.
- 42 M. N. Islam and T. Kato, *J. Phys. Chem. B*, 2003, **107**, 965.
- 43 S. Y. Lin, C. C. Huang and L. J. Chen, *J. Phys. Chem. B*, 1998, **102**, 4350.
- 44 P. Bustamante, S. Romero, A. Pena, B. Escalera and A. Reillo, *J. Pharm. Sci.*, 1998, **87**, 12, 1590.
- 45 P. Irwin, J. Brouillette, A. Giampa, K. Hicks, A. Gehring and S. I. Tu, *Carbohydr. Res.*, 1999, **322**, 1–2, 67.
- 46 G. Battistuzzi, M. Bellei, M. Borsari, G. W. Canters, E. de Waal, L. J. C. Jeuken, A. Ranieri and M. Sola, *Biochemistry*, 2003, **42**, 30, 9214.
- 47 R. Lumry and S. Rajender, *Biopolymers*, 1970, **9**, 10, 1125.
- 48 J. L. Abernethy, *J. Chem. Educ.*, 1967, **44**, 3, 177.
- 49 W. Kunz, P. Lo Nostro and B. W. Ninham, *Curr. Opin. Colloid Interface Sci.*, 2004, **9**, 1,2, 1.
- 50 H. Schott and A. E. Royce, *J. Pharm. Sci.*, 1983, **72**, 12, 1427.
- 51 C. Holtzschcher and F. Candau, *J. Colloid Interface Sci.*, 1988, **125**, 1, 97.
- 52 P. Jungwirth and D. J. Tobias, *Chem. Rev.*, 2006, **106**, 83.
- 53 I. Motoo, *J. Biochem.*, 1930, **12**, 83.
- 54 L. A. Reber, W. M. McNabb and W. W. Lucasse, *J. Phys. Chem.*, 1942, **46**, 500.
- 55 P. Bauduin, L. Wattebled, D. Touraud and W. Kunz, *Z. Phys. Chem. (Munich)*, 2004, **218**, 631.
- 56 D. C. Champeney and H. Comert, *Phys. Chem. Liq.*, 1988, **18**, 1, 43.

Green photochemistry: solar-chemical synthesis of Juglone with medium concentrated sunlight

Michael Oelgemöller,*^a Niall Healy,^a Lamark de Oliveira,^b Christian Jung^b and Jochen Mattay^c

Received 25th April 2006, Accepted 28th June 2006

First published as an Advance Article on the web 21st July 2006

DOI: 10.1039/b605906f

Dye sensitized photooxygenations of 1,5-dihydroxynaphthalene were investigated with soluble and solid-supported sensitizers and moderately concentrated sunlight. Moderate to good yields up to 79% of 5-hydroxy-1,4-naphthoquinone (Juglone) were achieved on multiple gram-scales after just 4 h of illumination. The mild and environmentally friendly reaction conditions make this application particularly attractive for 'green photochemistry'.

Introduction

Since light is regarded as a *clean reagent*,¹ photochemistry can contribute efficiently to the growing field of *green chemistry*.² To furthermore overcome the unfavorable energy demand of artificial light sources, photochemical transformations have been subjected to concentrated sunlight using modern solar collectors.^{3,4} We have recently realized a number of large-scale solar-chemical model reactions based on photoacylation⁵ and sensitized photooxygenation reactions.⁶ Due to the favorable absorption of most organic dyes within the visible spectrum,⁷ the latter are especially interesting examples for solar-chemical applications.^{3,6}

For our ongoing study on the photoacylation of quinones,^{5,8} we required larger amounts of 5-hydroxy-1,4-naphthoquinone (Juglone, **1**). Juglone is a versatile building block for the synthesis of biologically active quinonoid compounds,⁹ and is most commonly synthesized from the cheap and commercially available 1,5-dihydroxynaphthalene **2** by oxidation.¹⁰ Many of these thermal pathways suffer from severe disadvantages in terms of yield, selectivity, sustainability, scale-up or reproducibility, respectively. The dye sensitized photooxygenation of **2** can serve as an efficient and versatile alternative and various laboratory examples with artificial light have been described in the literature.¹¹ The reaction proceeds *via* a [4 + 2]-cycloaddition followed by a break-down of the *endoperoxide* intermediate. We have recently reported preliminary results on the solar-chemical synthesis of Juglone using holographic concentrators.⁶

Results and discussion

All experiments described in here were performed in August and September 2005 at the solar-chemical facility of the

German Aerospace Center (DLR) close to Cologne, Germany (latitude 50°51' N, 7°07' E, 70 m above sea level).¹² A parabolic trough collector designed for laboratory-scale applications and equipped with a highly reflecting eloxated aluminum mirror (aperture: 20 × 94 cm = 0.188 m²) was used for the present study (Fig. 1).¹³ This reactor type requires direct sunlight since it can only concentrate the direct part of the global radiation. The reactor offers a geometric concentration factor of about 15, but its efficiency is reduced in practice due to optical losses. Its one-axis design allows automatically tracking of the sun only for the elevation, whereas tracking of the azimuth is performed manually every 15 min.¹⁴ The reaction mixture is continuously pumped (fluid flow: *ca.* 2.5 L min⁻¹) through a Pyrex tube (diameter: 1.2 cm), which is placed in the focal line of the concentrator, and is cooled externally (*ca.* 20 °C). Oxygen gas was fed *via* a T-connector which generated relatively large gas bubbles with a small overall surface and thus limited its homogeneous distribution within the absorber tube.

For the present study, we have selected rose bengal (RB) and methylene blue (MB) as soluble sensitizers. Both dyes show favorable absorptions within the visible spectrum: rose bengal absorbs up to 600 nm with a maximum at 555 nm, methylene

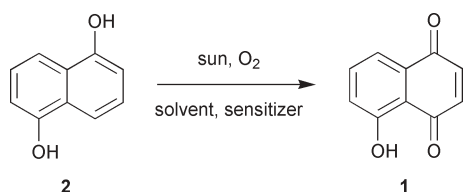


Fig. 1 Small-scale parabolic trough reactor equipped with aluminum mirrors. The storage vessel and O₂-feeding equipment can be seen on the lower left hand-side.

^aDublin City University, School of Chemical Sciences and National Institute for Cellular Biotechnology, Dublin 9, Ireland.
E-mail: michael.oelgemoller@dcu.ie; Fax: +353-1-700-5503;
Tel: +353-1-700-5312

^bDeutsches Zentrum für Luft- und Raumfahrt e.V. (DLR), Solarforschung, Linder Höhe, D-51147, Köln, Germany.
Fax: +49-2203-601-4141; Tel: +49-2203-601-2940

^cOrganische Chemie I, Fakultät für Chemie, Universität Bielefeld, Postfach 10 01 31, D-33501, Bielefeld, Germany.
E-mail: mattay@uni-bielefeld.de; Fax: +49-521-106-6417;
Tel: +49-521-106-2072



Scheme 1 Solar photooxygenation of 1,5-dihydroxynaphthalene **2**.

blue up to 725 nm with a maximum at 685 nm (data in ethanol). The solar sensitizing efficiencies have been reported as 0.54 (RB) and 0.37 (MB), respectively.^{3d} To simplify the work-up procedure, we have furthermore examined solid-supported sensitizers, in particular Sensitox[®] (rose bengal on Merrifield resin; RB_{MF})¹⁵ and methylene blue on ion-exchange resin (MB_{IE}).¹⁶ Both materials can be easily removed by filtration and are reusable. In almost all cases, non-hazardous isopropanol was chosen as solvent, whereas the laboratory procedure most commonly uses acetonitrile or a mixture of methanol and dichloromethane,¹¹ respectively.

Following a standardized procedure, a 0.05 M solution of 1,5-dihydroxynaphthalene **2** was illuminated in the presence of a sensitizer while a stream of oxygen was fed into the solution (Scheme 1). The progress of the reaction was followed by GC vs. tetradecane as internal standard in 15 min intervals. After a fixed illumination time of 4 h, Juglone **1** was isolated *via* continuous extraction with *n*-hexane or column chromatography. Experimental details and results are summarized in Table 1.

The first experiment was performed on August 18th with rose bengal as soluble sensitizer under almost perfect illumination conditions. The reaction mixture significantly darkened from bright red to dark brownish-red during the course of the reaction thus indicating partial decomposition of the sensitizer. GC-analysis showed that the starting material was readily consumed and after 4 h, the conversion reached an almost constant value of 93%. During that time the reactor

collected 2.0 mol of photons in the important absorption range of rose bengal between 500–600 nm.[†] After work-up, the desired product (**1**) was obtained in a high yield of 75% (81% based on conversion of **2**).

Soluble methylene blue was used in the second run with perfect insolation conditions. The color of the reaction mixture turned dark green-blue during the experimental period but this did not significantly affect the progress of the photooxygenation (Fig. 2). At the end of the reaction, the conversion was determined as 83% and Juglone was obtained in a, compared to the rose bengal case, lower yield of 62% (75% based on conversion). This finding is in line with the lower solar sensitizing efficiency of 0.37 for methylene blue (*vs.* 0.54 for rose bengal).[‡] During the illumination the reactor received 2.1 mol of photons between 600–700 nm—the important absorption range of methylene blue.

For the third experiment between August 18th and 19th, Sensitox[®] was applied as solid-supported sensitizer. The weather conditions were less favorable with lots of cloudy periods. After a relatively short illumination time, the characteristic orange color of Juglone became clearly visible within the reactor tube and further deepened with progressing exposure to concentrated sunlight. The reaction remained incomplete after 4 h and GC-analysis showed a conversion of 70% (Fig. 3). Juglone (**1**) was finally obtained in 53% yield which corresponded to 76% based on conversion of the diol **2**. In total, the collector received just 1.3 mol of photons in the range of 500–600 nm. When the amount of Sensitox[®] was reduced to half (Experiment IV), the conversion and yield

[†] The amounts of collected photons were calculated using *SEDES for Windows*.¹⁸

[‡] Esser and co-workers have examined the photooxygenation of furfural and found that methylene blue was superior over rose bengal.^{3d} The authors explained this finding with the weakly acidic reaction conditions and the lower UV-stability of rose bengal. Although we observed partly decomposition of the soluble sensitizers during our studies as well, the excess amounts used and the relatively short illumination times of 4 h did not require additional feeding.

Table 1 Experimental data for the photooxygenation reactions of 1,5-dihydroxynaphthalene **2**

	Experiment I	Experiment II	Experiment III	Experiment IV	Experiment V	Experiment VI	Experiment VII
Date	18.08.2005	29.08.2005	18–19.08.2005	29.08.2005	30.08.2005	31.08.2005	01.09.2005
Scale							
Diol 2 /g	2.0	2.0	2.0	2.0	2.0	2.0	24.0
Sensitizer ^a /g	0.1 (RB)	0.05 (MB)	1.0 (RB _{MF})	0.5 (RB _{MF})	2.0 (MB _{IE})	0.1 (RB)	0.3 (RB)
Solvent/mL	250 (<i>i</i> -PrOH)	250 (<i>i</i> -PrOH)	250 (<i>i</i> -PrOH)	250 (<i>i</i> -PrOH)	250 (<i>i</i> -PrOH)	250 (acetone)	3000 (<i>i</i> -PrOH)
Time (CEST ^b)							
1st day	09:45–13:45	08:55–12:55	15:20–16:45	14:55–18:55	08:30–12:30	13:25–17:25	09:55–17:35 ^c
2nd day	—	—	08:00–09:15	—	—	—	—
Total/h	4	4	4	4	4	4	10 ² / ₃
Photons ^d /mol							
1st day	2.0	2.1	0.9	1.7	2.0	2.1	2.1
2nd day	—	—	0.4	—	—	—	—
Total ^d /mol	2.0	2.1	1.3	1.7	2.0	2.1	2.1
Conversion ^e (%)	93	83	70	46	47	99	48
Isolated yield 1 (%)	75 (81 ^f)	62 (75 ^f)	53 (76 ^f)	33 (72 ^f)	31 (66 ^f)	79 (80 ^f)	N.d. ^g
Isolated yield 1 (lamp ^h) (%)	29	31	7	6	4	23	N.d. ^g

^a Sensitizers: rose bengal (RB), methylene blue (MB), rose bengal on Merrifield resin (Sensitox[®], RB_{MF}) and methylene blue on ion-exchange resin (MB_{IE}). ^b Central European summer time. ^c Stopped due to rainfall. ^d Calculated amount of photons collected between 500–600 nm (RB) or 600–700 nm (MB). ^e Conversion of diol **2** as determined by GC-analysis (*vs.* tetradecane). ^f Yield calculated based on conversion. ^g Not determined. ^h Comparison laboratory experiment with 2 × 500 W Armley halogen lamps.

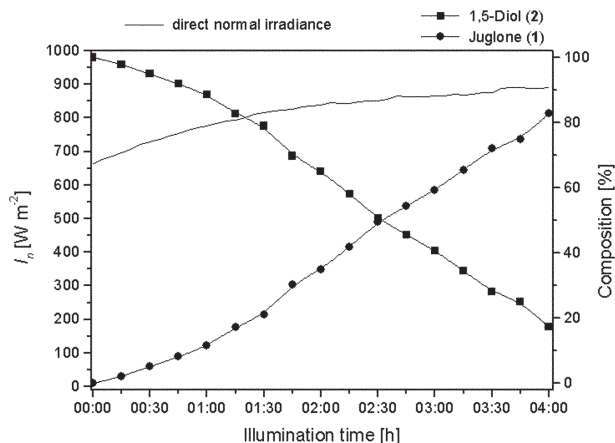


Fig. 2 Direct normal irradiance and product composition vs. illumination time for the methylene blue mediated photooxygenation in isopropanol (Experiment II).

dropped to 46% and 33% (72% based on consumed **2**), respectively. Since the collected amount of photons was notably higher with 1.7 mol, the amount and thus distribution of the solid supported material did significantly affect the outcome of the reaction.

Surprisingly, ion-exchange resin fixed methylene blue gave a low conversion of 47% and an isolated yield of **1** of 31% (66% based on conversion). In contrast to Sensitox[®], the large particle size of the resin did not allow a homogeneous transport and distribution of the sensitizer particles. In particular, the beads stayed on the bottom of the absorber tube and were not directly struck by the focused light. This limitation becomes obvious when comparing the amounts of collected photons. During the 4 h period, the mirror collected 2.0 mol of photons between 600–700 nm and thus more than during the experiments with Sensitox[®]. The sensitizer furthermore showed severe leaching and the reaction mixture turned dark green during the illumination process.

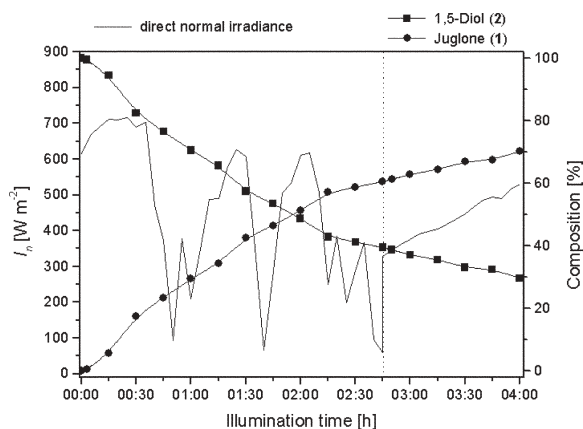


Fig. 3 Direct normal irradiance and product composition vs. illumination time for the Sensitox[®] mediated photooxygenation in isopropanol (Experiment III). The two days are separated by a vertical, dotted line.

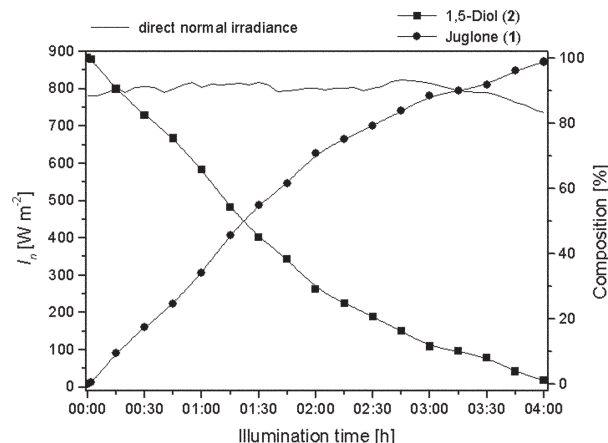


Fig. 4 Direct normal irradiance and product composition vs. illumination time for the rose bengal mediated photooxygenation in acetone (Experiment VI).

In an exemplary run, acetone was used as an alternative solvent (Experiment VI). Its compared to isopropanol higher volatility and flammability makes it less suitable for outdoor applications, but it was found to give higher yields during laboratory experiments with artificial light.^{11a} The solar-chemical reaction proceeded with 99% conversion after 4 h (Fig. 4), and furnished Juglone in the best yield of 79% (80% based on consumed **2**). The weather conditions were optimal and the reactor received 2.1 mol of photons within the 500–600 nm range.

The superiority of the solar-chemical protocol became clear when the results were compared to laboratory experiments with artificial light. Under identical conditions (*i.e.* concentration, solvent and time), irradiations with a set of two 500 W halogen lamps furnished the desired **1** in poor to moderate yields of 4–31% (Table 1). Noteworthy, much higher conversions and yields can be easily obtained upon dilution.^{11a}

For the final solar experiment on September 1st, the reaction was scaled-up to 24 g of the diol **2** and 0.3 g of rose bengal in 3 L of isopropanol. Additionally, the reactor was equipped with a wider absorber tube with a diameter of 3.2 cm. Due to the large amounts and the less favorable weather conditions, a prolonged illumination time was envisaged, but the reaction had to be stopped after *ca.* 11 h of partly sunny conditions due to beginning rainfall. At this stage a conversion of 48% was reached and the reactor collected 2.1 mol of photons between 500–600 nm.

Conclusions

The present study on solar photooxygenations of 1,5-dihydroxynaphthalene (**2**) clearly demonstrates that the solar-chemical production of Juglone (**1**) can serve as a powerful and environmentally friendly alternative to existing thermal processes. All solar transformations proceeded cleanly and no or only minor amounts of side-products could be detected in the GC-spectra. Compared to illuminations with non-concentrated sunlight,^{11a,17} the application of concentrated sunlight furthermore operated more efficiently due to higher space-time yields.

Experimental

General procedure (concentrated sunlight)

2 g (12.5 mmol) of 1,5-dihydroxynaphthalene **2** were dissolved in 250 mL of solvent. The sensitizer was added and the solution was exposed to moderately concentrated sunlight in a parabolic trough reactor for 4 h while feeding with a stream of oxygen. The progress of each reaction was monitored by GC analysis vs. tetradecane as internal standard. The reaction mixture was filtrated and the solvent was removed in vacuum. Juglone **1**^{11a} was isolated *via* continuous extraction in a Soxhlet extractor with *n*-hexane or by column chromatography on silica gel using CHCl₃ as eluent. Experimental details are given in Table 1.

General procedure (halogen lamp)

2 g (12.5 mmol) of 1,5-dihydroxynaphthalene **2** were dissolved in 250 mL of solvent. The sensitizer was added and the solution was irradiated (2 × 500 W Armley halogen lamps) in a Schlenck-flask equipped with a cold finger and a reflux condenser for 4 h at room temperature while purging with oxygen (flow rate: 10 mL min⁻¹). Evaporated solvent was frequently refilled. The progress of the reactions was monitored by TLC analysis (SiO₂, CHCl₃). After 4 h, the reaction mixture was filtrated and the solvent was removed in vacuum. Juglone **1**^{11a} was isolated *via* continuous extraction of the solid residue in a Soxhlet extractor with *n*-hexane or by column chromatography on silica gel using CHCl₃ as eluent. Experimental details are given in Table 1.

Acknowledgements

This research project was financially supported by the Arbeitsgemeinschaft Solar Nordrhein-Westfalen (Themenfeld 3: Solare Chemie und Solare Materialuntersuchungen), the National Institute for Cellular Biotechnology (PRTL1-3) and Dublin City University (Research Alliance Fund). The authors would like to thank Dr Christian Sattler and Damien McGuirk for technical assistance.

References

- (a) A. Albini and M. Fagnoni, *Green Chem.*, 2004, **6**, 1; (b) J. Mattay, *Chem. unserer Zeit*, 2002, **36**, 98; (c) A. Albini, M. Fagnoni and M. Mella, *Pure Appl. Chem.*, 2000, **72**, 1321; (d) K.-H. Funken, *Sol. Energy Mater.*, 1991, **24**, 370.
- (a) P. Tundo, P. Anastas, D. StC. Black, J. Breen, T. Collins, S. Memoli, J. Miyamoto, M. Polyakoff and W. Tumas, *Pure Appl. Chem.*, 2000, **72**, 1207; (b) P. T. Anastas and J. C. Wagner, *Green Chemistry. Theory and Practice*, Oxford University Press, Oxford, 1998.
- (a) M. Oelgemöller, C. Jung, J. Ortner, M. Mattay, C. Schiel and E. Zimmermann, *The Spectrum*, 2005, **18**, 28; (b) M. Oelgemöller, C. Jung, J. Ortner, J. Mattay, C. Schiel and E. Zimmermann, in *Proceedings of the 2004 International Solar Energy Conference - Portland, USA*, ASME, Boulder, CO, 2004, ISEC 2004-65021, ISBN 0-89553-176-3 (CD-ROM); (c) B. Pohlmann, H.-D. Scharf, U. Jarolimek and P. Mauermann, *Sol. Energy*, 1997, **61**, 159; (d) P. Esser, B. Pohlmann and H.-D. Scharf, *Angew. Chem., Int. Ed. Engl.*, 1994, **33**, 2009.
- This concept leads back to the beginnings of organic photochemistry in the late 19th century where sunlight was the only available source of radiation. See: (a) H. D. Roth, *Pure Appl. Chem.*, 2001, **73**, 395; (b) H. D. Roth, *Angew. Chem., Int. Ed. Engl.*, 1989, **28**, 1193; (c) G. Ciamician, *Science*, 1912, **36**, 385.
- (a) C. Schiel, M. Oelgemöller, J. Ortner and J. Mattay, *Green Chem.*, 2001, **3**, 224; (b) M. Oelgemöller, C. Schiel, J. Ortner and J. Mattay, in *AG Solar Nordrhein-Westfalen - Solare Chemie und Solare Materialforschung*, AG-Solar NRW, Jülich, 2002, ch. 2.2, ISBN 3-89336-306-8 (CD-ROM).
- M. Oelgemöller, C. Jung, J. Ortner, M. Mattay and E. Zimmermann, *Green Chem.*, 2005, **7**, 35.
- (a) E. L. Clennan and A. Pace, *Tetrahedron*, 2005, **61**, 6665; (b) A. A. Frimer, *Singlet Oxygen*, CRC Press, Boca Raton, FL, 1985; (c) K. Gollnick, *Chim. Ind. (Milan, Italy)*, 1982, **64**, 156; (d) N. V. Shinkarenko and V. B. Aleskovskii, *Russ. Chem. Rev.*, 1981, **50**, 220.
- (a) P. A. Waske, J. Mattay and M. Oelgemöller, *Tetrahedron Lett.*, 2006, **47**, 1329; (b) M. Oelgemöller, C. Schiel, R. Fröhlich and J. Mattay, *Eur. J. Org. Chem.*, 2002, 2465; (c) C. Schiel, M. Oelgemöller and J. Mattay, *Synthesis*, 2001, 1275; (d) C. Schiel, M. Oelgemöller and J. Mattay, *J. Inf. Rec.*, 1998, **24**, 257.
- For *rac*-Juglomycin A, see: (a) G. A. Kraus and P. Liu, *Synth. Commun.*, 1996, **26**, 4501; (b) for Urdamycinone B, see: G. Matsuo, Y. Miki, M. Nakata, S. Matsumura and K. Toshima, *J. Org. Chem.*, 1999, **64**, 7101; (c) for *rac*-Frenolicin B, see: P. Contant, M. Haess, J. Riegl, M. Scalone and M. Visnick, *Synthesis*, 1999, 821; (d) for (+)-Nocardione A, see: D. L. J. Clive and S. P. Fletcher, *J. Org. Chem.*, 2004, **69**, 3282; (e) for Aloesaponarin I, see: S. J. Bingham and J. H. P. Tyman, *J. Chem. Soc., Perkin Trans. 1*, 1997, 3637; (f) for (+)-Rubiginone B₂, see: J. Motoyoshiya, Y. Masue, G. Iwayama, S. Yoshioka, Y. Nishii and H. Aoyama, *Synthesis*, 2004, 2099; (g) for Angucyclines in general, see: M. C. Carreño and A. Urbano, *Synlett*, 2005, 1.
- For overviews on thermal preparations of Juglone, see: (a) T. Wakamatsu, T. Nishi, T. Ohnuma and Y. Ban, *Synth. Commun.*, 1984, **14**, 1167; (b) D. J. Crouse, M. M. Wheeler, M. Goemann, P. S. Tobin, S. K. Basu and D. M. S. Wheeler, *J. Org. Chem.*, 1981, **46**, 1814; (c) C. Grundmann, *Synthesis*, 1977, 644.
- (a) O. Suchard, R. Kane, B. J. Roe, E. Zimmermann, C. Jung, P. A. Waske, J. Mattay and M. Oelgemöller, *Tetrahedron*, 2006, **62**, 1467; (b) S. Croux, M.-T. Maurette, M. Hocquaux, A. Ananides, A. M. Braun and E. Oliveros, *New J. Chem.*, 1990, **14**, 161; (c) G. Wurm and U. Geres, *Arch. Pharm. (Weinheim, Ger.)*, 1985, **318**, 931; (d) H.-J. Durchstein and G. Wurm, *Arch. Pharm. (Weinheim, Ger.)*, 1984, **317**, 809; (e) V. P. Pathak and R. N. Khanna, *Indian J. Chem., Sect. B: Org. Chem. Incl. Med. Chem.*, 1983, **22**, 412; (f) J. Griffiths, K.-Y. Chu and C. Hawkins, *J. Chem. Soc., Chem. Commun.*, 1976, 676.
- K.-H. Funken and M. Becker, *Renewable Energy*, 2001, **24**, 469.
- (a) J. Ortner, D. Faust, K.-H. Funken, T. Lindner, J. Schulat, C. G. Stojanoff and P. Fröning, *J. Phys. IV*, 1999, **9**, Pr3-379; (b) J. Ortner, D. Faust and K.-H. Funken, in *Solare Chemie und solare Materialforschung*, ed. M. Becker and K.-H. Funken, C. F. Müller Verlag, Heidelberg, 1997, p. 254.
- For overviews on different reactor types, see: (a) S. Malato, J. Blanco, A. Vidal and C. Richter, *Appl. Catal., B*, 2002, **37**, 1; (b) K.-H. Funken and J. Ortner, *Z. Phys. Chem.*, 1999, **213**, 99.
- (a) B. Paczkowska, J. Paczkowski and D. C. Neckers, *Macromolecules*, 1986, **19**, 863; (b) A. P. Schapp, A. L. Thayer, E. C. Blosssey and D. C. Neckers, *J. Am. Chem. Soc.*, 1975, **97**, 3741; (c) E. C. Blosssey, D. C. Neckers, A. L. Thayer and A. P. Schapp, *J. Am. Chem. Soc.*, 1973, **95**, 5820.
- J. R. Williams, G. Orton and L. R. Unger, *Tetrahedron Lett.*, 1973, **14**, 4603.
- For some selected examples, see: (a) A. Itoh, S. Hashimoto, K. Kuwabara, T. Kodama and Y. Masaki, *Green Chem.*, 2005, **7**, 830; (b) R. A. Doohan and N. W. A. Geraghty, *Green Chem.*, 2005, **7**, 91; (c) J.-T. Li, J.-H. Yang, J.-F. Han and T.-S. Li, *Green Chem.*, 2003, **5**, 433; (d) T. Rütther, A. M. Bond and W. R. Jackson, *Green Chem.*, 2003, **5**, 364.
- T. Walsch and K.-J. Riffelmann, *SEDES for Windows v. 2.5*, DLR, Köln, 1997.

A facile, environmentally benign sulfonamide synthesis in water†

Xiaohu Deng* and Neelakandha S. Mani

Received 2nd May 2006, Accepted 30th June 2006

First published as an Advance Article on the web 21st July 2006

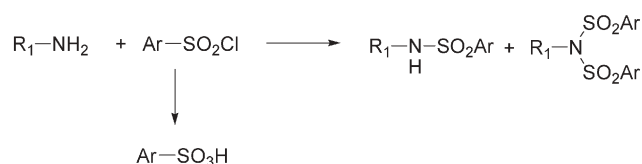
DOI: 10.1039/b606127c

A facile, environmentally benign synthesis of sulfonamides under dynamic pH control in aqueous media is described. This methodology uses equimolar amounts of amino compounds and arylsulfonyl chlorides and omits the use of organic bases. Isolation of products involves only filtration after acidification. Excellent yields and purity were obtained without further purification.

Introduction

Sulfonamides are a very important class of compounds in the pharmaceutical industry, being widely used as anticancer, anti-inflammatory and antiviral agents.¹ The search for general, efficient syntheses of sulfonamides under mild conditions is of continuing interest for organic chemists. Although recently many efforts have been put into the development of novel sulfonamide syntheses,² the conventional synthesis from amino compounds and sulfonyl chlorides is still the method of choice because of the reactivity and simplicity.³ Two general protocols for this synthesis are widely exploited in the literature. One is to perform the reaction in organic solvents and employ organic amine bases to scavenge the acid (HCl) that is generated.⁴ Elevated temperature is often required, especially for the less reactive aniline substrates. For primary amines, bis-sulfonylation is a common side reaction, which makes isolation difficult.⁵ The other protocol uses the modified Schotten–Baumann conditions.⁶ A typical procedure involves adding the sulfonyl chloride slowly into an amine solution in a biphasic system of organic solvents and basic (Na₂CO₃ or NaOH) aqueous solution.⁷ Under these conditions, hydrolysis of sulfonyl chlorides is the major competing reaction, which necessitates the use of excess sulfonyl chloride and results in diminishing yields. Furthermore, in either protocol, the isolation and purification of the sulfonamide products are not always straightforward.

Recently, water has attracted considerable attention as the desired solvent for chemical reactions because of cost, safety and environmental concerns.⁸ Herein we disclose a facile,



Scheme 1

Department of Drug Discovery, Johnson & Johnson Pharmaceutical Research & Development LLC, 3210 Merryfield Row, San Diego, CA, 92121, USA. E-mail: xdeng@prdus.jnj.com

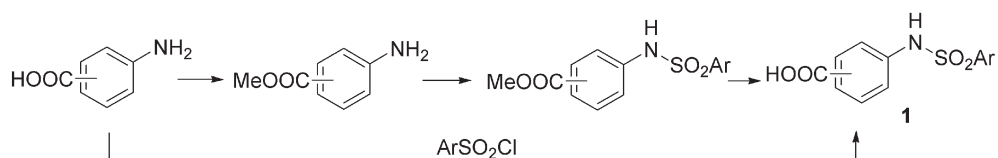
† Electronic supplementary information (ESI) available: Experimental details and characterization of the sulfonamide compounds (Table 1, entries 1–13 and Table 2, entries 1–8). See DOI: 10.1039/b606127c

environmentally benign sulfonamide synthesis at room temperature in *water* under pH control with Na₂CO₃. This method uses equimolar amounts of sulfonyl chlorides and amines. The desired sulfonamides are easily isolated in excellent yields and purity by simple filtration of the precipitated solid after acidification. This method eliminates the use of expensive organic solvents and amine bases; isolation and purification of the sulfonamides involves only filtration; and the procedure generates virtually no waste, which makes it ideal for green chemistry.

Results and discussion

As part of our drug discovery efforts we recently required a practical synthesis of sulfonamide **1** that was amenable to large scale. To avoid the typical, lengthy protection–sulfonamidation–deprotection sequence (Scheme 2), we explored the possibility of direct sulfonamidation of aminobenzoic acids.

The initial attempts were not very encouraging. As expected, the reaction of aminobenzoic acids and tosyl chloride in organic solvents (CH₂Cl₂, THF) with organic amine bases yielded little product. Schotten–Baumann conditions in acetone–aqueous basic (Na₂CO₃ or NaOH) solution afforded incomplete reaction, and hydrolysis of the sulfonyl chloride was a major side reaction. We envisioned that to suppress this competing hydrolysis reaction, minimizing the exposure of the sulfonyl chloride to the base as well as the solvent would be the key. To accomplish this task, we reasoned that eliminating the organic co-solvent typically used in Schotten–Baumann conditions would allow the sulfonyl chloride to slowly get into the reaction system, thus minimizing the occurrence of hydrolysis. Furthermore, pH control would also be crucial to control this side reaction, as demonstrated in other nucleophilic reactions in water.⁹ To test this idea, stoichiometric amounts of tosyl chloride and 4-aminobenzoic acid were suspended in *water*. The initial pH was between 2–3. Under vigorous stirring, aqueous Na₂CO₃ solution was added to adjust the pH. We observed that the optimal pH for the desired reaction was between 8.0 and 9.0. At lower pH (< 7.0), little reaction took place, whereas at higher pH (> 10), the competing hydrolysis reaction accelerated significantly.¹⁰ As the reaction progressed, HCl was generated and additional aqueous Na₂CO₃ solution was added to maintain the pH at 8.0. Over time, the suspension became a clear solution, and the



Scheme 2

Table 1 The reaction between aminobenzoic acids and arylsulfonyl chlorides

Entry	Amino acid	Sulfonyl chloride	Product	Yield
1				98%
2				94%
3				93%
4				83%
5				91%
6				84%
7				85%
8				95%
9				92%
10				93%
11				84%
12				65%
13				96%

Table 2 The reaction of amino compounds with sulfonyl chloride

Entry	Amine	Sulfonyl chloride	Product	Yield
1				92%
2				91%
3				92%
4				81%
5				55%
6				85%
7				90%
8				30% (94%) ^a
9				0%

^a 5% Bu₄N⁺Br⁻ was added.

pH became constant, indicating the completion of the reaction. The reaction usually took several hours to reach completion and approximately 1.4 equivalents of Na₂CO₃ were consumed in the process. Simply acidifying the solution with concentrated HCl to pH = 2.0 allowed the precipitation of the desired sulfonamide in 94% yield and with greater than 95% purity. Furthermore, the reaction was easily scalable to 100 grams.

Excited by these results, we applied this new protocol to a variety of aminobenzoic acids and arylsulfonyl chlorides, as shown in Table 1. Two, three or four-substituted aminobenzoic acid gave virtually identical results. Various functional groups were well tolerated. Primary and secondary anilines worked equally well in the reaction. Various arylsulfonyl chlorides also afforded excellent yields.

In principle, this new protocol should not be limited to aminobenzoic acids as long as the amino compounds have reasonable solubility in water at the reaction pH. With this in mind, we set out to investigate aminophenols, with which the reaction also worked very efficiently (Table 2, entries 1–2). These results were particularly intriguing because under the organic conditions reported in the literature, sulfonylation on phenols was the dominant process.¹¹ We then investigated cases where the amine and the acid functionalities were not attached to the same aromatic ring. Both (4-amino-phenyl)-acetic acid and 4-aminomethyl-benzoic acid reacted with tosyl chloride smoothly to give excellent yields (Table 2, entries 3–4).

However, in the case of 2-phenylglycine, significant hydrolysis of the tosyl chloride was observed (Table 2, entry 5). Fortunately, the sulfonamide product was cleanly isolated after acidification in 55% yield. We then demonstrated that an acidic functional group was not necessary for the reaction to proceed. Both primary and secondary amines gave excellent yields of corresponding sulfonamides (Table 2, entries 6–7). However, simple aniline yielded only 30% of the desired product after 3 days, presumably because of the poor solubility of aniline in water. To solve this problem, 5% Bu₄N⁺Br⁻ was added as a phase transfer catalyst, which greatly accelerated the sulfonamidation reaction. The desired sulfonamide was isolated in 94% yield, and little hydrolysis product was observed. Finally, when the same conditions were applied to methyl sulfonyl chloride, hydrolysis was more rapid than sulfonamide formation (Table 2, entry 9).

In conclusion, we have developed a facile sulfonamide synthesis in *water* under pH control. This method is quite general for various amino compounds and arylsulfonyl chlorides and is easily scalable. The yields are excellent and the product isolation is very straightforward. It appears that, for this reaction to proceed as desired, the amino compounds need to be at least partially soluble in water, and hydrolysis of the arylsulfonyl chloride cannot be too fast under the reaction conditions. In certain cases, a phase transfer reagent is useful to facilitate the reaction.

Experimental

General procedure

The solid mixture of 4-aminobenzoic acid (1.0 g, 7.3 mmol, 1.0 equiv.) and *p*-toluenesulfonyl chloride (1.4 g, 7.3 mmol, 1.0 equiv.) was suspended in 30 mL water. The pH of the suspension was adjusted and was maintained at 8.0 by adding 1 mol L⁻¹ Na₂CO₃ aqueous solution at room temperature, using a syringe pump equipped with a pH controller. It took 2 hours for the reaction to complete. Concentrated HCl was added slowly to adjust the pH to 2.0. The precipitate was collected by filtration, washed with water and dried to afford the title compound as a white solid (2.08 g, 7.1 mmol, 98%). No further purification was needed.

Acknowledgements

We thank Dr Jiejun Wu and Mr. David Tognarelli for analytical support.

References

- (a) C. T. Supuran, A. Casini and A. Scozzafava, *Med. Res. Rev.*, 2003, **5**, 535–558; (b) A. Scozzafava, T. Owa, A. Mastrolorenzo and C. T. Supuran, *Curr. Med. Chem.*, 2003, **10**, 925–953.
- (a) S. W. Wright and K. N. Hallstrom, *J. Org. Chem.*, 2006, **71**, 1080–1084; (b) A. R. Katritzky, A. A. A. Abdel-Fattah, A. V. Vakulenko and H. Tao, *J. Org. Chem.*, 2005, **70**, 9191–9197; (c) S. Caddick, J. D. Wilden and D. B. Judd, *J. Am. Chem. Soc.*, 2004, **126**, 1024–1025; (d) R. Pandya, T. Murashima, L. Tedeschi and A. G. M. Barrett, *J. Org. Chem.*, 2003, **68**, 8274–2876; (e) J. W. Lee, Y. Q. Louie, D. P. Walsh and Y.-T. Chang, *J. Comb. Chem.*, 2003, **5**, 330–335; (f) C. G. Frost, J. P. Hartley and D. Griffin, *Synlett*, 2002, **11**, 1928–1930.
- K. K. Andersen, *Comprehensive Organic Chemistry*, ed. D. N. Jones, Pergamon Press, Oxford, 1979, vol. 3.
- T. J. J. Holmes and R. G. Lawton, *J. Org. Chem.*, 1983, **48**, 3146–3150.
- A. Yasuhara, M. Kameda and T. Sakamoto, *Chem. Pharm. Bull.*, 1999, **47**, 809–812.
- (a) N. O. V. Sonntag, *Chem. Rev.*, 1953, **52**, 272; (b) C. M. R. Low, H. B. Broughton, S. B. Kalindjian and I. M. McDonald, *Bioorg. Med. Chem. Lett.*, 1992, **2**, 325–330.
- (a) M. D. Surman, M. J. Mulvihill and M. J. Miller, *Org. Lett.*, 2002, **4**, 139–141; (b) W. Hu, Z. Guo, F. Chu, A. Bai, X. Yi, G. Cheng and J. Li, *Bioorg. Med. Chem.*, 2003, **11**, 1153–1160; (c) M. Medebielle, O. Onomura, R. Keirouz, E. Okada, H. Yano and T. Terauchi, *Synthesis*, 2002, **17**, 2601–2608; (d) C. Goldenberg, R. Wandestrück and J. Richard, *Eur. J. Med. Chem.*, 1977, **12**, 81–86.
- (a) S. Narayan, J. Muldoon, M. G. Fin, V. V. Folkin, H. C. Kolb and K. B. Sharpless, *Angew. Chem., Int. Ed.*, 2005, **44**, 3275–3279; (b) U. M. Lindstrom, *Chem. Rev.*, 2002, **102**, 2751–2772; (c) C.-J. Li, *Chem. Rev.*, 1993, **93**, 2023–2035.
- (a) J. F. King, M. S. Gill and P. Ciubotaru, *Can. J. Chem.*, 2005, **83**, 1525–1535; (b) J. F. King, R. Rathore, J. Y. L. Lam, Z. R. Guo and D. F. Klassen, *J. Am. Chem. Soc.*, 1992, **114**, 3028–3033.
- J. Morita, H. Nakatsuji, T. Misaki and Y. Tanabe, *Green Chem.*, 2005, **7**, 711–715.
- (a) S. L. Gwaltney, H. M. Imade, Q. Li, L. Gehrke, R. B. Credo, R. B. Warner, J. Y. Lee, P. Kovar, D. Frost, S.-C. Ng and H. L. Sham, *Bioorg. Med. Chem. Lett.*, 2001, **11**, 1671–1673; (b) G. Lin and A. Zhang, *Tetrahedron*, 2000, **56**, 7163–7171.



NJC

New Journal of Chemistry

A prime source of international, cutting-edge research,
encompassing all areas of the chemical sciences

- Impact factor: 2.574
- Fast times to publication
- Multidisciplinary with broad appeal

Read it today!

RSC Publishing



CENTRE NATIONAL
DE LA RECHERCHE
SCIENTIFIQUE

www.rsc.org/njc

One small step for *Soft Matter*...



...one giant leap for interdisciplinary research

Launched: June 2005

Its mission: To provide an interdisciplinary platform for the exchange of ideas on soft matter

The crew: Piloted by Carol Stanier, Editor, and Ullrich Steiner, Chairman of the Editorial Board, bringing together leading international scientists

Flight schedule: Stage I – Launch; Stage II – Separation; Stage III – Exploring new territories

Soft Matter has enjoyed stellar success since launch. The next stage in its journey takes place in January 2007 when *Soft Matter* will separate from its host journal, *Journal of Materials Chemistry*, to take flight as a solo publication.

To ensure that you continue to read the very best in soft matter research recommend *Soft Matter* to your librarian today!